Access to Electronic Thesis

Author:	Kate Louise Thompson
Thesis title:	Covalently Cross-linked Colloidosomes
Qualification:	PhD

Covalently Cross-linked Colloidosomes
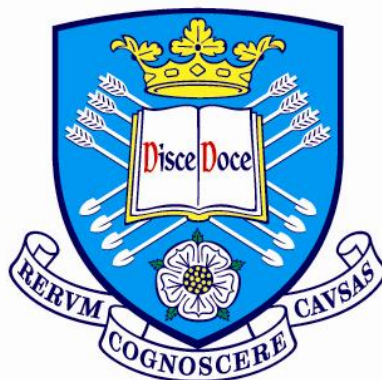
Kate Louise Thompson

Department of Chemistry

The University of Sheffield

Submitted to the University of Sheffield

In fulfilment of the requirements for the award of

Doctor of Philosophy

September 2011

Declaration

The work described in this thesis was carried out at the University of Sheffield between October 2008 and September 2011 and has not been submitted, either wholly or in part, for this or any other degree. All the work is the original work of the author, except where acknowledged by references.

Signature: _____

          K. L. Thompson   September 2011

Acknowledgements

First and foremost, I would like you say a huge thank you to my supervisor Steve Armes, for giving me the opportunity to work in your group and introducing me to the joys of polymer chemistry. Thank you for your support, encouragement and advice over the past three years and for giving me the chance to travel to some great conferences. I would also like to thank Procter and Gamble for sponsoring my project, especially David York. Thank you for all your advice and guidance in every project meeting and throughout my PhD.

Much of the work in this thesis wouldn't be possible without the help of so many people, so I wish to say a big thank you to: Heath Bagshaw for SEM training, Claire Hurley for XPS measurements, Jonathan Howse and Steve Ebbens for fluorescence microscopy, Lee Fielding for the TEM images and Nick and Jeppe for the fluorescent monomer syntheses.

Thank you to all members of the Armes group, past and present, for the supportive working environment and for making my PhD such an amazing experience. Thanks to all of you for helping me hold onto my sanity and sense of humour despite trying to finish a PhD, organise MSc students and plan a wedding. A special thank you goes to Liz, for all her help during my summer and MChem projects. Your support, friendship and shopping skills helped me through my final undergraduate year and opened my eyes to the possibility of doing a PhD, thank you. A big thank you goes to another Armes group lady, Jennifer. Thanks for all your help, advice and friendship. We had some adventures; from the dizzy heights of Hazel Grove all the way to New York, New York. To all the boys; Lee, Andrew, Marksy, Nick, Dam Dam, Ads, Hot Liam R, Ju, Pierre, Dave, Rob, Joe, Daniel, Vincent, Jeppe and Simon – thanks for making me smile and all the 'banter'. And for the times when the testosterone got a bit too much I have to say a big thank you to all the girls; Amy, Michelle, Tiffs, Mona, Grace, Lizzy, Raquel, Amanda and Froso. Also, lunch time in the department wouldn't be the same without Lunch Club and all its members over the years, too many to mention here, but you know who you all are. A special mention goes to Lee and Tracy, our Velocity family. We've had some fun times; San Fran, Skegness, Cleethorpes and many more. Thank you Tracy, for your friendship, Hen party planning and all the White Zinfandel, no one makes me laugh quite like you (bes-i-des!). Oh and Lee, I agree…it was nothing like a Cornetto! A massive thank you goes to Scarlett, for all the dinners out, shopping and generally being an amazing friend. Also, huge thanks to all my family, for your love and support over the past 7 years in Sheffield, especially mum, for believing in me from the very beginning.

My final thanks go to my husband James. Thank you for always being there for me, for making me smile when I really needed it and for all the washing up! Without your love and support none of this would have been possible. You are my hero and this thesis is dedicated to you.

Publications

Primary publications from work carried out for this thesis:

(1) "Synthesis of Sterically-Stabilized Latexes Using Well-Defined Poly(glycerol monomethacrylate) Macromonomers" K. L. Thompson, S. P. Armes, D. W. York and J. A. Burdis, *Macromolecules,* **2010,** *43*, 2169-2177.

(2) "From well-defined macromonomers to sterically-stabilised latexes to covalently cross-linkable colloidosomes: exerting control over multiple length scales" K. L. Thompson and S. P. Armes, *Chem. Commun.,* **2010,** *46*, 5274-6.

(3) "Covalently Cross-Linked Colloidosomes" K. L. Thompson, S. P. Armes, J. R. Howse, S. Ebbens, I. Ahmad, J. H. Zaidi, D. W. York and J. A. Burdis, *Macromolecules,* **2010,** *43*, 10466-10474.

(4) "Preparation of Pickering Emulsions and Colloidosomes with Relatively Narrow Size Distributions by Stirred Cell Membrane Emulsification" K. L. Thompson, S. P. Armes and D. W. York, *Langmuir,* **2011,** *27*, 2357-2363.

Secondary publications from work carried out during other projects:

(1) "Polyamine-Functional Sterically Stabilized latexes for Covalently Cross-linkable Colloidosomes" A. Walsh, K. L. Thompson, S. P. Armes and D. W. York, *Langmuir,* **2010,** *26*, 18039-18048.

(2) "Controlling Deposition and Release of Polyol-Stabilized Latex on Boronic Acid-Derivatized Cellulose" D. Zhang, K. L. Thompson, R. Pelton and S. P. Armes, *Langmuir,* **2010,** *26*, 17237-17241.

(3) "Borate Binding to Polyol-Stabilized Latex" R. Pelton, D. Zhang, K. L. Thompson and S. P. Armes, *Langmuir,* **2011,** *27*, 2118-2123.

(4) "Preparation of stimulus-responsive liquid marbles using a polyacid-stabilised polystyrene latex" D. Dupin, K. L. Thompson and S. P. Armes, *Soft Matter*, **2011**, *7*, 6797-6800.

Oral Presentations at Conferences

(1) "Synthesis of well-defined hydroxy-functionalised macromonomers and their use as steric stabilisers for the preparation of latex particles" K. L. Thompson, S. P. Armes, D. W. York and J. A. Burdis; 239th American Chemical Society Meeting and Exposition: 21st-25th March, **2010**, San Francisco, USA.

(2) "Hydroxy-Functional Sterically-Stabilised Latexes for Cross-linkable Colloidosomes" K. L. Thompson, S. P. Armes, and D. W. York; Macro Group Young Researchers Meeting: 29th-30th April, **2010**, Nottingham, UK.

(3) "Covalently Cross-linked Colloidosomes" K. L. Thompson, S. P. Armes, and D. W. York; UK Colloids 2011: 4th-6th July, **2011**, Canary Wharf, London, UK.

Poster Presentations at Conferences

(1) "Preparation of well-defined biocompatible macromonomers and their use as steric stabilisers in latex syntheses" K. L. Thompson and S. P. Armes: 14th UKPCF Annual Meeting: 14th-16th September, **2009**, University of Hull, Kingston-upon-Hull, UK.

(2) "Covalently Cross-linked Colloidosomes" K. L. Thompson, S. P. Armes, and D. W. York; 239th American Chemical Society Meeting and Exposition: 21st-25th March, **2010**, San Francisco, USA.

(3) "Amine-functional sterically-stabilised latexes to make cross-linkable colloidosomes" K. L. Thompson, A. Walsh, S. P. Armes, D. W. York and J. A. Burdis; Macro 2010: 43rd IUPAC World Polymer Congress: 14th-11th July, **2010**, SECC, Glasgow, UK.

Abstract

A range of well-defined macromonomers based on glycerol monomethacrylate (GMA) has been synthesised by a two-step protocol in alcoholic media. A tertiary amine-functionalised initiator was used to produce six homopolymer precursors with target degrees of polymerisation of 20 to 70 by atom transfer radical polymerisation (ATRP). These polymerisations proceeded to high conversion (> 99 %) and afforded relatively low polydispersities (M_w/M_n < 1.33). The tertiary amine end groups were then quaternised using 4-vinylbenzyl chloride at 20 °C. These styrene-functionalised macromonomers were evaluated as reactive steric stabilisers for latex syntheses. Near-monodisperse submicrometer-sized and micrometer-sized polystyrene latexes were obtained by aqueous emulsion and alcoholic dispersion polymerisation, respectively. In addition poly(2-hydroxypropyl methacrylate) latexes were prepared via aqueous dispersion polymerisation. Latex syntheses conducted in the presence of the $PGMA_{50}$ homopolymer precursor produced particles with significantly larger diameters than those prepared with the corresponding styrene-functionalised macromonomer. Such control experiments confirmed the importance of having a terminal styrene group on the macromonomer chains for successful latex formation. FT-IR spectroscopy indicated the presence of the $PGMA_{50}$ macromonomer within the polystyrene latex and XPS studies indicated that these chains are located at (or very near) the latex surface, as expected.

The $PGMA_{50}$-PS latexes have appropriate surface wettability to stabilise 25-250 μm oil-in water Pickering emulsions. Colloidosomes were formed by covalent cross-linking of the hydroxyl-functional stabiliser chains from within the oil droplets using a polymeric diisocyanate (tolylene 2,4-diisocyanate-terminated poly(propylene glycol). This oil soluble cross-linker was confined within the oil droplets, allowing colloidosomes to be prepared at 50 vol% solids without any aggregation. The resulting microcapsules survive removal of the internal oil phase using excess alcohol, unlike the non cross-linked Pickering emulsion precursor. These observations confirm the robust nature of these colloidosomes. Annealing the capsule shells at temperatures below the latex T_g was investigated by exploiting the solvent properties of binary cyclohexane/n-dodecane oil mixtures. Microcapsule permeability has been explored via dye release experiments. The $PGMA_{50}$-PS particle size had no effect on the release profile of the fluorescein active, nor did the cyclohexane annealing protocol. Release can be retarded to some extent by deposition of polypyrrole onto the colloidosome exterior. However, such capsules do not allow the long-term retention of such small molecules. More success has been achieved when the model active is considerably larger. Thus colloidosomes have successfully encapsulated a series of poly(2-diethylaminoethyl methacrylate)-stabilised polystyrene latexes. Such particles cannot physically fit through the interstices in the colloidosome shell and therefore are retained inside the microcapsules via size exclusion.

More uniform Pickering emulsions stabilised using a 250 nm $PGMA_{50}$-PS latex have been prepared using a stirred cell membrane emulsification technique. Pickering emulsions of 44-269 μm in diameter can be prepared with coefficients of variation as low as 25% by varying the emulsification parameters. The cell membrane consists of 5 μm pores with a pore-to-pore spacing of 200 μm. Significantly more uniform emulsions are produced when these open pores are restricted to a narrow annular ring around the membrane surface. Increasing the oil flux rate through the membrane increases both the size and polydispersity of the resulting emulsion droplets. Increasing the paddle stirrer speed from 500 to 1500 rpm reduces the average droplet diameter from 269 to 51 μm while simultaneously reducing the coefficient of variation from 47% to 25%. Any further increase in surface shear led to droplet break-up and resulted in a significantly more polydisperse emulsion. The Pickering emulsions reported here have much narrower droplet size distributions than those prepared in control experiments by conventional homogenisation (coefficient of variation = 25 %, rather than 75%).

Contents

Contents

List of Tables

List of Figures

List of Abbreviations

ACVA	4,4'-azobis(4-cyanovaleric acid)
AIBA	2,2'-azobis(isobutyramidine) dihydrochloride
AIBN	2,2'-azobisisobutyronitrile
Amide based initiator	N-(dimethylamine)ethyl-2-bromoisobutyrylamide
APS	ammonium persulfate
ATRP	atom transfer radical polymerisation
bpy	2, 2,-bipyridine
CMC	critical micelle concentration
CTA	Chain transfer agent
Cu(I)Cl	copper (I) chloride
DCP	disc centrifuge photosedimentometry
DEA	2-(diethylamino)ethyl methacrylate
DLS	dynamic light scattering
DP	degree of polymerisation
DSC	differential scanning calorimetry
EDL	electric double layer
FE-SEM	field emission scanning electron microscopy
FT-IR	fourier transform infrared
GMA	glycerol monomethacrylate
GPC	gel permeation chromatography
^{1}H-NMR	proton nuclear magnetic resonance spectroscopy
HPMA	2-hydroxypropyl methacrylate
IEP	isoelectric point
IPA	2-propanol (isopropanol)
LCST	lower critical solution temperature
M_n	number-average molecular weight
MPC	2-(methacryloyloxy)ethyl phosphorylcholine
M_w	weight-average molecular weight
NIPAM	*N*-isopropylacrylamide
NMP	nitroxide-mediated polymerisation
PDEA	poly(2-(diethylamino)ethyl methacrylate)
PDI	polydispersity index (PDI=M_w/M_n)
PGMA	poly(glycerol monomethacrylate)

PMPC	poly(2-(methacryloyloxy)ethyl phosphorylcholine)
PPG-TDI	tolylene 2,4-diisocyanate-terminated poly(propylene glycol)
PPy	polypyrrole
PS	polystyrene
RAFT	reversible addition fragmentation chain transfer polymerisation
SEM	scanning electron microscopy
TEM	transmission electron microscopy
THF	tetrahydrofuran
UCST	upper critical solution temperature
4-VBC	4-vinyl benzyl chloride
XPS	x-ray photoelectron spectroscopy

Chapter One

Introduction

INTRODUCTION

Colloidosomes are microcapsules whose shells are composed of colloidal particles that have been fused together to give the shell additional stability.[1] In recent years colloidosomes have received considerable attention due to their potential importance in the area of microencapsulation. Microencapsulation allows the controlled release of active ingredients in industrial sectors such as medicine, food, home and personal care products, agrochemicals and cosmetics, for the delivery of actives such as drugs, pesticides and fragrances.[2-6] Routes to colloidosomes are most commonly based on the self-assembly of colloidal particles at the interface between two immiscible liquids, typically water and oil. The initial self-assembled structures are known as Pickering[7] or Ramsden[8] emulsions and have been recognised for over a century. A large body of work in this area has been conducted using polymeric particles synthesised by various polymerisation techniques. Before continuing with a review of the various routes to colloidosomes, pertinent background information on conventional free radical, emulsion, dispersion and controlled radical polymerisation techniques is presented.

Free radical Polymerisation

Conventional free radical polymerisation is a relatively inexpensive process and is the most widely used method of chain polymerisation.[9] As with other types of chain polymerisation, free radical polymerisation can be divided into three stages; initiation, propagation and termination.

The formation of primary free radicals (R•) is usually achieved via the thermal decomposition of the initiator (I).

$$(1) \qquad I \xrightarrow{\ k_d\ } 2R\bullet$$
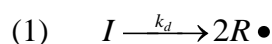
This most commonly occurs via homolytic dissociation of a covalent bond from the initiating species, as shown above where k_d is the rate constant for this dissociation. Common free radical initiators that undergo homolytic scission via thermolysis are those that contain azo (-N=N-) or peroxide (O-O-) groups. Examples of typical free radical initiators are shown in Figure 1.1.
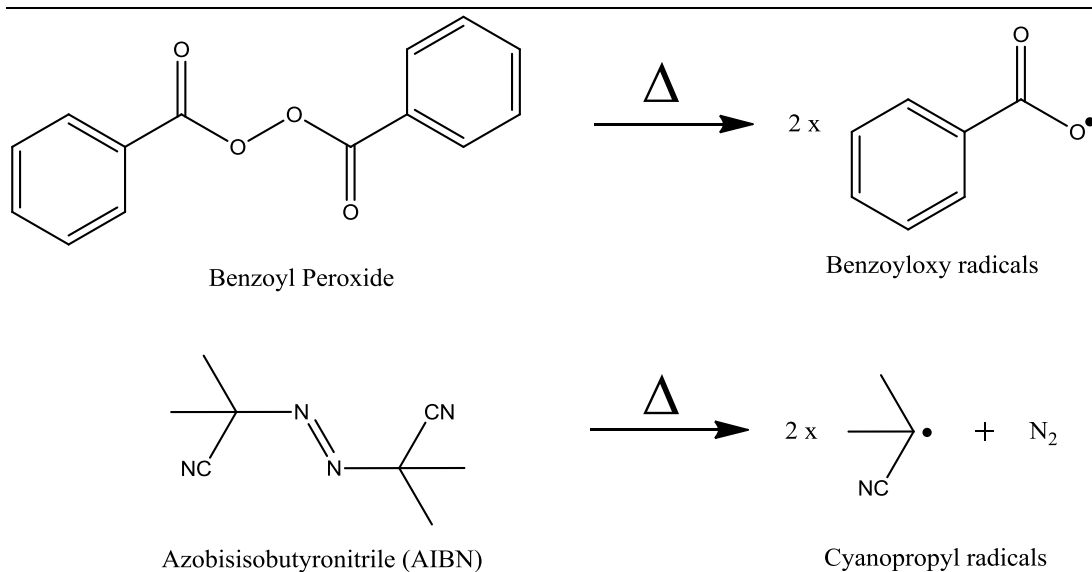
Figure 1.1. Two examples of common free radical initiators containing peroxide and azo functionalities. These undergo homolytic cleavage upon the application of heat to generate primary radical species.

Once generated, these primary free radicals (R•) react with the vinyl group from the monomer to produce a chain-initiating radical (RM$_1$•) in an initiation step that proceeds with a rate constant k$_i$

$$(2) \quad R \bullet + M \xrightarrow{k_i} RM_1 \bullet$$
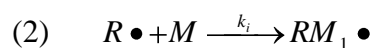
The next step involves the rapid addition of monomer units to the active radical centre in order to grow the polymer chain (propagation), as follows:

$$(3) \quad RM_n \bullet + M \xrightarrow{k_p} RM_{(n+1)} \bullet$$
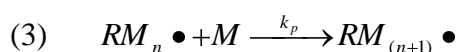
where k$_p$ is the rate constant for propagation. The final stage in the polymerisation is where the growth of the polymer chains is terminated by the bimolecular reaction between two radicals. This can occur by combination, when two polymer radicals react to form one single (dead) polymer chain:

$$(4) \quad RM_n \bullet + R'M_m \bullet \xrightarrow{k_{tc}} RM_{(n+m)}R'$$

where k_{tc} is the rate constant for termination by combination. Termination can also occur by disproportionation, when a hydrogen atom is abstracted from one chain by another; this results in one saturated and one unsaturated chain end

$$(5) \qquad RM_n \bullet + RM_m \bullet \xrightarrow{\ k_{td}\ } RM_n + RM_m(CH = CH_2)$$
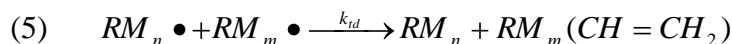
where k_{td} is the rate constant for termination by disproportionation. Monomers such as styrene and acrylates almost exclusively undergo termination by combination, whilst more sterically hindered radicals such as methacrylates undergo termination by both combination and disproportionation.[10] In addition to these termination mechanisms, chain transfer reactions can also occur as shown below:

$$(6) \qquad RM_n \bullet + XY \rightarrow RM_n X + Y \bullet$$

where XY is a hypothetical reactive molecule such as a thiol. The radical chain abstracts X• (commonly a halogen or hydrogen atom) from XY to give a 'dead' polymer chain and a new radical Y•. This radical (Y•) can initiate unreacted monomer to grow a new polymer chain. Although one growing polymer chain has been terminated, the generation of a new radical means the overall concentration of propagating chains is not affected.

Kinetics of Free Radical Polymerisation

The rate of polymerisation is the rate at which monomer is consumed. Monomer consumption occurs in both the initiation and propagation steps. However, the amount of monomer consumed in the initiation stage is negligible compared that used up in the propagation step; therefore the rate of polymerisation can be closely approximated to the rate of propagation:

$$(7) \qquad -\frac{d[M]}{dt} = R_p = k_p [RM_n \bullet][M]$$

where R_p is the rate of propagation, $[RM_n \bullet]$ is the concentration of all radicals of size $RM_1 \bullet$ or larger and $[M]$ is the monomer concentration. It can be assumed that the rate of radical generation (R_i) is equal to the overall rate of termination by both combination and disproportionation ($R_{tc} + R_{td}$). Therefore the concentration of radicals ($[RM_n \bullet]$) is constant throughout the polymerisation and the rate of change of

radical concentration is effectively zero (the so-called steady-state approximation). This can be expressed as:

$$(8) \quad \frac{d[RM_n\bullet]}{dt} = R_i - R_{tc} - R_{td} = 0$$

$$(9) \quad R_i - 2k_{tc}[RM_n\bullet][RM_n\bullet] - 2k_{td}[RM_n\bullet][RM_n\bullet] = 0$$

Equation (9) can be simplified to give equation (10), where termination by combination and disproportionation has been grouped into one rate of overall termination (R_t).

$$(10) \quad R_i = R_t = 2k_t[RM_n\bullet]^2$$

where k_t is the overall rate constant for radical termination (given by $k_t = k_{tc} + k_{td}$). The numerical factor of two arises because two radical chains are lost in any one termination event. Equation (10) can be rearranged in terms of [$RM_n\bullet$] and substituted into equation (7) to give equation (11):

$$(11) \quad R_p = k_p[M]\left(\frac{R_i}{2k_t}\right)^{\frac{1}{2}}$$

Thus the rate of propagation has a square root dependence on the initiation rate, R_i. As discussed earlier, initiation consists of two steps: (i) generation of primary radicals by dissociation of the initiator (commonly by thermolysis), followed by (ii) the addition of one monomer unit to generate the secondary radical adduct. The rate of generation of the primary radicals is much slower than the addition of the first monomer unit, therefore thermal decomposition can be considered the rate-determining step for initiation, see equation (12):

$$(12) \quad R_i = R_d = 2fk_d[I]$$

where R_i is the rate of initiation, R_d is the rate of production of primary radicals (decomposition), k_d is the rate constant for initiator dissociation, [I] is the initiator concentration and f is the initiator efficiency. The initiator efficiency is defined as the fraction of radicals produced that go on to initiate polymer chains. Equation 11

can now be substituted into equation 12 to give the rate equation for the most common case of free radical chain polymerisation.

$$(13) \qquad R_p = k_p[M]\left(\frac{fk_d[I]}{k_t}\right)^{\frac{1}{2}}$$

The above equation shows that the rate of conventional free radical polymerisation is dependent on the square root of the initiator concentration and follows first order kinetics with respect to monomer concentration.

Dispersion Polymerisation

Dispersion polymerisation was developed by researchers at both ICI[11] and Rohm & Haas[12] in the early 1960's as a method of producing near-monodisperse micrometer (or submicrometer) sized latex particles. In such formulations the continuous phase is chosen to be a solvent for the monomer, initiator and stabiliser, but a non-solvent for the growing polymer chains. The reaction mixture is therefore initially homogeneous and, as polymerisation progresses, becomes heterogeneous. Oligomers are formed and grow to a certain critical chain length, at which point the polymer chains precipitate from solution.[9]

A steric stabiliser is used to prevent macroscopic precipitation. Depending on how good the solvent is for the growing polymer, phase separation can occur at an early or later stage. This leads to nucleation and the formation of primary particles. These primary particles are swollen by the polymerisation medium and/or the monomer. As a result, polymerisation continues largely within the individual particles, leading to the formation of colloidally stable spherical polymer latex particles of 0.1-10 μm.[13] In the absence of a suitable stabiliser, the growing polymer chains simply precipitate from solution with no well-defined morphology. The general mechanism for dispersion polymerisation is shown in Figure 1.2.

A suitable stabiliser for dispersion polymerisation must have two distinct properties. It must contain a segment with some affinity for the polymer particle surface and also a segment that is soluble in the chosen solvent. Three types of macromolecule are commonly used as steric stabilisers in dispersion polymerisation: homopolymers, block or graft copolymers and macromonomers.[9]
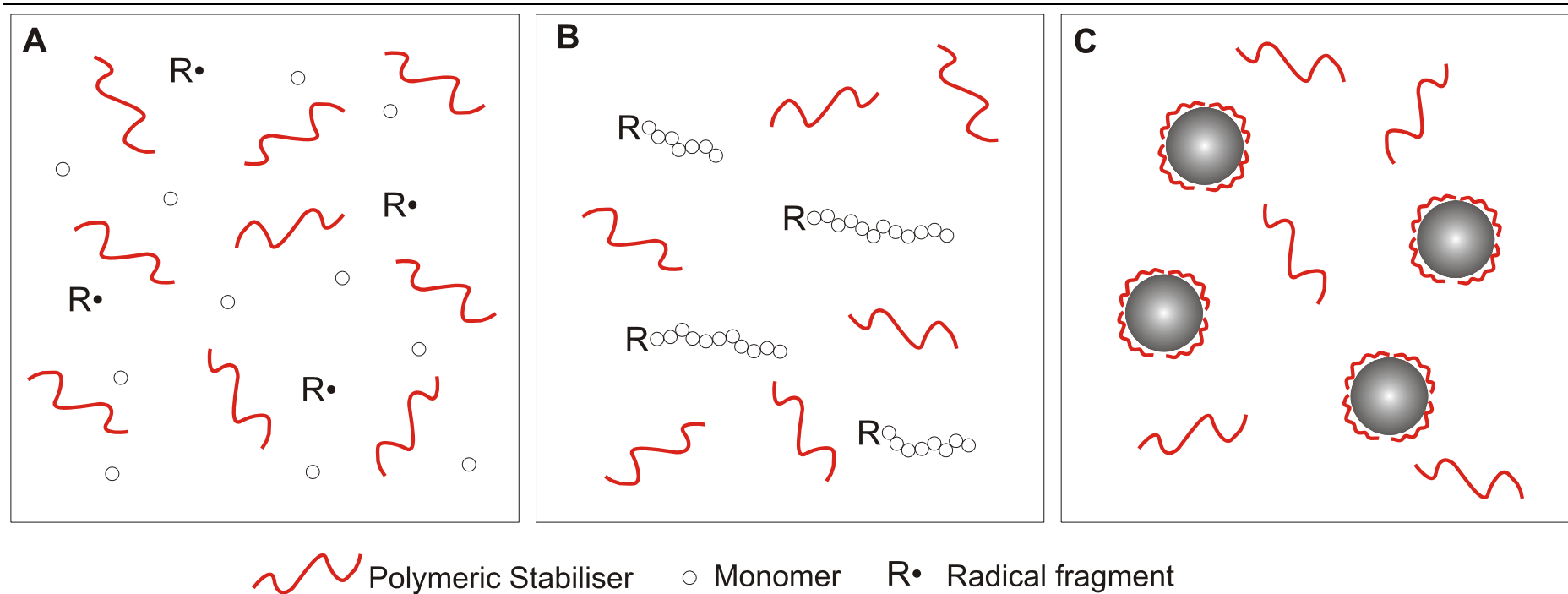
Figure 1.2. Schematic representation of dispersion polymerisation and its three characteristic stages. Stage A - The monomer, initiator and stabiliser are dissolved in the continuous phase. Stage B - Radical fragments initiate homogeneous polymerisation. At some critical chain length, they precipitate from solution to form primary particles. Stage C - Polymerisation continues within these monomer-swollen primary particles, eventually resulting in sterically-stabilised polymer particles.

An example of a homopolymer that has been successfully used in dispersion polymerisation is poly(*N*-vinylpyrrolidone) (PNVP).[14-15] Dawkins *et al.*[16] used AB block copolymers of poly(styrene-block-dimethyl siloxane) to prepare both poly(methyl methacrylate) and polystyrene latex particles in *n*-alkanes. Poly(2-(dimethylaminoethyl methacrylate) (PDMA) macromonomers have been prepared by oxyanionic polymerisation and these in turn have been used to prepare polystyrene latexes by alcoholic dispersion polymerisation.[17]

Dispersion polymerisation has been traditionally carried out in either hydrocarbon or alcoholic media.[18] More recently, aqueous dispersion polymerisation has been investigated, with the polymerisation of 2-hydroxypropyl methacrylate (HPMA) being conducted in the presence of a PNVP homopolymer stabiliser.[19] This formulation is potentially advantageous, since it avoids the use of volatile organic solvents.
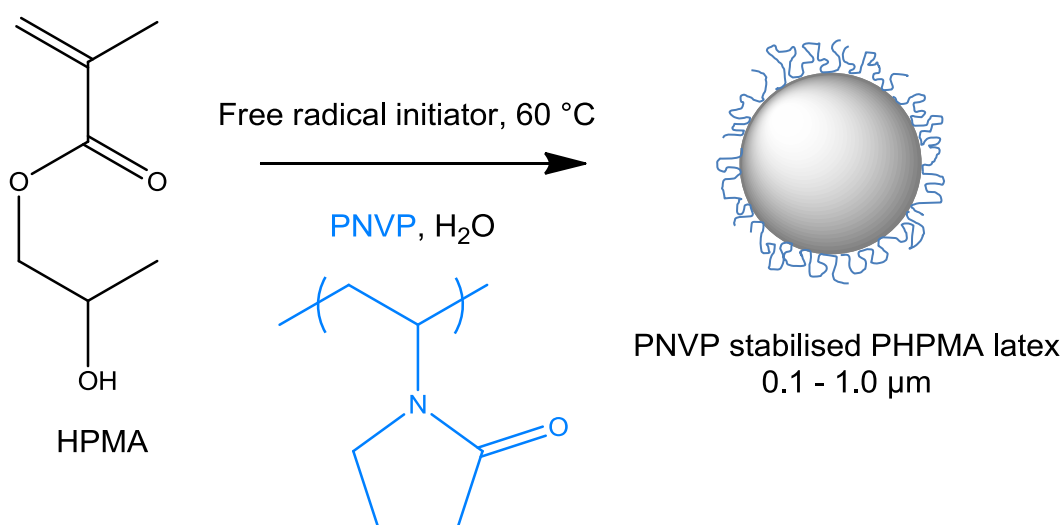
Figure 1.3. Schematic representation of the aqueous dispersion polymerisation of HPMA monomer in the presence of PNVP steric stabiliser.[19]

Emulsion Polymerisation

Emulsion polymerisation was developed at the Goodyear Tyre and Rubber Company in the 1920's.[20] Emulsion polymerisation is used widely in the paints, plastics and construction industries to produce a wide range of products.[21] Emulsion polymerisation produces a free-flowing aqueous dispersion of latex particles from which the polymer can be readily separated if required.[21] One advantage of emulsion over alcoholic dispersion polymerisation is that the solvent is water. Water is an environmentally-friendly, non-toxic and very cheap solvent, and an attractive alternative to alcoholic solvents, which are both flammable and toxic.

Emulsion polymerisation offers many advantages over other polymerisation techniques. The low viscosity and high heat capacity of water leads to efficient stirring and excellent heat dissipation, respectively. It also allows high molecular weight polymers to be generated at high rates and to very high conversions, with the latex products often requiring little or no further processing.

In contrast to dispersion polymerisation, the vinyl monomer is not soluble in the reaction medium, hence emulsion polymerisation is heterogeneous from the outset. The monomer (e.g. styrene) is dispersed in the aqueous phase by an emulsifying agent such as a surfactant. The free radical initiator and stabiliser are soluble in the aqueous phase but the monomer has relatively low aqueous solubility, and is largely confined within the monomer droplets and surfactant micelles. There are three characteristic stages, or intervals, in emulsion polymerisation.

Interval I[22]

At the beginning of emulsion polymerisation, monomer-swollen surfactant micelles (5-15 nm) are present in solution, along with large surfactant-stabilised monomer droplets (1- 10 μm). Despite the monomer being largely water-insoluble, a very small amount is nevertheless present in the aqueous phase. Radicals are generated in the aqueous phase due to the introduction of the initiator. These radicals react with the monomer in the aqueous phase to generate oligoradicals. Such oligomers are initially soluble until they reach a critical chain length by further addition of monomer. At this point, they can either enter a pre-existing micelle (heterogeneous nucleation), or aggregate and adsorb free surfactant to generate a new micelle

(homogeneous nucleation).[10] Heterogeneous nucleation occurs predominantly when the surfactant concentration is above the critical micelle concentration (CMC). Around the CMC heterogeneous nucleation still dominates however homogeneous nucleation occurs also. For syntheses conducted below the surfactant CMC, no micelles are present in solution and therefore homogeneous nucleation occurs exclusively.[10] Entry of these oligoradicals into the bulk monomer droplets is also possible, but is usually not significant due to their low number concentration and low surface area compared to the surfactant micelles. The monomer concentration inside the micelles is much higher than that in the bulk solution, so polymerisation proceeds rapidly to form a latex particle. During this interval both the polymerisation rate and particle number increase as a function of time. Interval I ends when there are no more surfactant micelles in solution and particle nucleation is complete.

Interval II[22]

Interval II begins when particle nucleation is complete. At this stage, only surfactant-stabilised monomer droplets and monomer-swollen latex particles are present in the reaction solution, with no new particles being formed. Polymerisation continues inside the monomer-swollen latex particles with further monomer diffusing in from the monomer droplets. Due to this diffusion-controlled process, the overall monomer concentration inside the particles remains relatively constant. Radicals from the aqueous phase can enter a latex particle and termination occurs if the particle already contains a growing polymer radical. Conversely if the particle does not contain a growing radical, propagation can recommence. Interval II is complete once all the monomer has been consumed from the monomer droplet reservoirs.

Interval III[22]

At this stage of the polymerisation, only monomer-swollen latex particles remain. Now that the monomer droplet reservoirs have been depleted, the monomer concentration inside the particles decreases and so the reaction rate is retarded. Under ideal conditions, polymerisation continues inside these latex particles until all the remaining monomer is consumed and polymerisation ceases. Typical surfactants used in emulsion polymerisation include both ionic and non-ionic surfactants. Anionic surfactants typically consist of a carboxylic sulfate, sulfonate or phosphate group attached to a long alkyl chain, such as sodium dodecylsulfate (Figure 1.4).
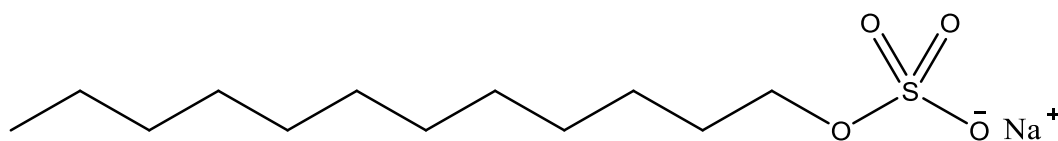
Figure 1.4. An example of an anionic surfactant commonly used in emulsion polymerisation, sodium dodecyl sulphate (SDS).

If a charged initiator (e.g. ammonium persulfate) is used, stable polymer latexes can still be produced in the absence of any surfactant or stabiliser. This is due to the charged initiator fragment (e.g. sulphate) on the end of each growing polymer chain, which creates an 'in situ' surfactant, with the charged end-groups providing the particle with sufficient colloidal stability.[13, 22] This is sometimes referred to as surfactant-free or soap-less emulsion polymerisation and the final latexes are 'charge-stabilised'.
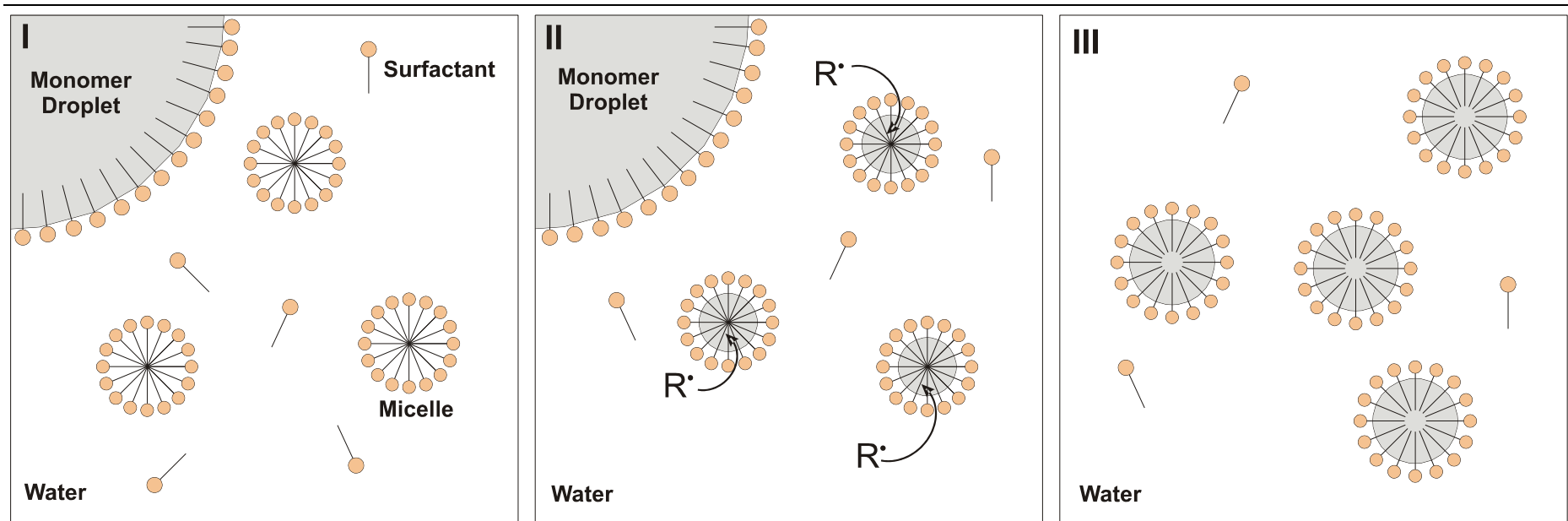
Figure 1.5. The three intervals of emulsion polymerisation. Interval I – the monomer is dispersed in water as surfactant-stabilised monomer droplets and excess surfactant forms micelles. Polymerisation begins when free radicals generated in the aqueous phase reacting with monomer to form oligomers, which then migrate into the monomer-swollen surfactant micelles. Interval II commences when particle nucleation has ceased and article growth continues with the diffusion of monomer from the droplets into the swollen latex particles. This diffusion-controlled transport continues until the monomer droplets are used up and polymerisation continues inside the monomer-swollen particles until the monomer is depleted (interval III).[9, 22]

COLLOID STABILITY

Colloidal particles are constantly undergoing Brownian motion that frequently brings them into close contact.[23] In the absence of a suitable stabilisation mechanism, the particles will aggregate due to attractive Van der Waals forces.[23] Thus a stable colloidal dispersion requires long range repulsive forces acting between particles in order to counteract these Van der Waals interactions.[23] There are two main mechanisms that impart colloidal stability: electrostatic (charge) and steric stabilisation.

Electrostatic Stabilisation

In the case of electrostatic stabilisation, each particle exhibits a surface charge that leads to the build up of a diffuse layer of oppositely charged ions around the colloid surface.[24] This is known as the electric double layer (see Figure 1.6A). It is energetically unfavourable for two electric double layers to overlap. If the ion clouds from two such layers do overlap, the ionic concentration between the particles is increased. This in turn increases the electrochemical potential between the particles causing a driving force for separation.[24]
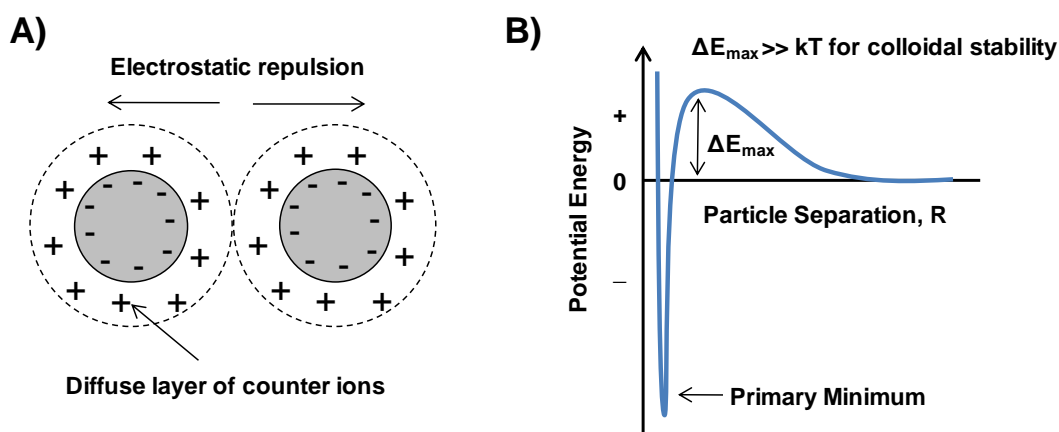
Figure 1.6. (A) Schematic representation of the electric double layer[23] and (B) the potential energy curve with separation distance for two approaching charge-stabilised particles.

This potential energy maximum (ΔE_{max}) leads to mutual repulsion of the particles. A large ΔE_{max} relative to the particle thermal energy (kT, where k is the Boltzmann constant and T is the system temperature) provides an effective kinetic barrier to

aggregation (see Figure 1.6B). However, this ΔE_{max} is reduced in less polar solvents or in the presence of added electrolyte, due to the reduction in the size of the electric double layer. Therefore, such charge stabilised colloids are only kinetically stable, despite long term stability being achieved in some cases.[9]

Steric Stabilisation

Steric stabilisation of colloidal particles is imparted by macromolecules that are either grafted or adsorbed onto the colloid surface. The poly(glycerol monomethacrylate) macromonomer prepared in this thesis is chemically grafted onto the particle surface via copolymerisation with the latex monomer.
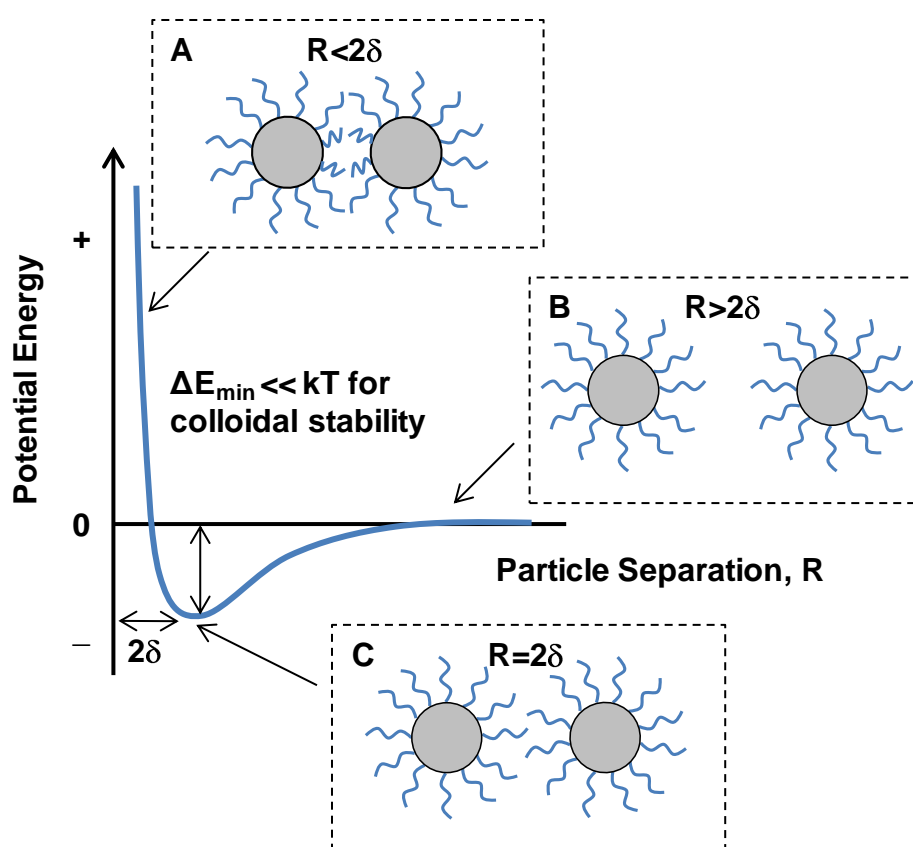
Figure 1.7. Potential energy curve for two sterically stabilised latexes of stabiliser thickness δ with separation distances of (A) less than 2δ, (B) greater than 2δ and (C) equal to 2δ.

These macromolecule chains form a steric barrier to particle aggregation. The steric repulsion arises as it is enthalpically unfavourable for two such sterically stabilised latexes to come into close contact (distance $\leq 2\delta$). This is due to the restriction in conformation that occurs when the polymer chains interpenetrate on close

approach.[9, 25] There is also a mixing component to steric repulsion which depends on how much the polymer chains prefer to be solvated, rather than interpenetrating with other chains.[9, 25] In contrast to electrostatic stabilisation, steric stabilisation is relatively insensitive to the presence of electrolytes and is effective in both aqueous and non-aqueous media.[23] Such particles are thermodynamically stable provided that ΔE_{min} is much smaller than the kinetic energy of the particles (see Figure 1.7). In cases where ΔE_{min} is greater than kT, the particles aggregate as they do not possess enough kinetic energy to escape the potential well after a collision event. This aggregation may be reversible if additional energy is supplied to the system.[23] Aggregation can also occur if a poor solvent for the stabiliser chains is introduced. This reduces the stabiliser thickness (δ) and as a result allows the particles to approach each other more closely. This leads to greater Van der Waals interactions and in turn increases ΔE_{min}.

CONTROLLED/LIVING POLYMERISATION

Conventional free radical polymerisation has been described earlier in this section. It forms the basis of many commercially important processes and offers significant advantages over other polymerisation techniques.[26] For example, this process does not require particularly stringent conditions and can be used to polymerise a wide range of vinyl monomers. However, free radical polymerisation does not offer good control over many aspects of the polymerisation, such as molecular weight and polydispersity. The growing radical species suffer from bimolecular termination by combination and disproportionation, along with numerous chain transfer side reactions.[20]

Controlled synthesis of polymers with narrow molecular weight distributions can be accomplished via various living or pseudo-living polymerisation techniques. These techniques are noted for their lack of (or suppression of) irreversible termination and chain transfer processes. Living polymerisations are characterised by low polydispersities, linear evolution of molecular weight with conversion and the ability to prepare diblock copolymers via sequential monomer addition.[27]

The first example of a living polymerisation was the anionic polymerisation of styrene in tetrahydrofuran (THF), which was reported in 1956 by Szwarc.[28] The propagating species is a carbanion[20] and hence these polymerisations must be carried

out in the absence of protic impurities to avoid any termination of the living chain ends.

For a living polymerisation under ideal conditions the degree of polymerisation (DP) is directly related to the initial monomer concentration $[M]_o$ and the initiator concentration $[I]_o$ according to equation (14):

$$(14) \quad DP = \frac{[M]_o}{[I]_o}$$

This allows molecular weights to be simply targeted by varying the initiator/monomer ratio. A crude measure of the width of the molecular weight distribution is given by the ratio of the weight-average molecular weight (M_w) to the number average molecular weight (M_n). This is known as the polydispersity index. M_n is calculated by counting the *number* of molecules in the sample of each molecular weight[20] according to equation (15):

$$(15) \quad M_n = \frac{\Sigma N_i M_i}{\Sigma N_i}$$

Where N_i is the number of molecules (or number of moles of those molecules) having a molecular weight M_i.[20] In contrast M_w is calculated by the *mass* of molecules of each molecular weight according to equation (16):

$$(16) \quad M_w = \frac{\Sigma W_i M_i}{\Sigma W_i} = \frac{\Sigma N_i M_i^2}{\Sigma N_i M_i}$$

In an ideal case the molecular weight is Poisson-type and the polydispersity of the polymer is given by equation (17):

$$(17) \quad \frac{M_w}{M_n} = 1 + \left(\frac{DP}{\left(DP+1\right)^2} \right)$$

CONTROLLED RADICAL POLYMERISATION

Living ionic polymerisation is extremely intolerant of protic impurities such as water, leading to the need for rigorously dried reagents, solvents and apparatus[28-30].

Such formulations are also only amenable to a limited number of monomers and inert solvents. In particular, living ionic polymerisations are intolerant of protic functional groups (e.g. –OH, -COOH, -NH$_2$) in both the monomer and the solvent. For this reason, controlled radical polymerisation methods[31-32] offer significant advantages over traditional ionic polymerisation techniques[28-30] These may be considered 'pseudo-living' rather than truly living polymerisations, since termination reactions are not completely eliminated but merely suppressed relative to propagation. This is because the rate of propagation (R_p) is proportional to the concentration of propagating radical ([$RM_n\bullet$], (see equation (7)), whereas the rate of termination (R_t) is proportional to [$RM_n\bullet$]^2 (see equation (10)). Therefore by minimising [$RM_n\bullet$], R_t is reduced significantly compared to R_p. In many cases termination is essentially negligible and such controlled radical polymerisations display all the necessary important characteristics of living ionic polymerisations.

Such controlled radical polymerisation techniques include Nitroxide-mediated Polymerisation (NMP),[33] Reversible Addition-Fragmentation Chain Transfer Polymerisation (RAFT)[34] and Atom Transfer Radical Polymerisation (ATRP).[35]

Nitroxide-Mediated Polymerisation

Solomon and Rizzardo first reported the use of nitroxides in the polymerisation of methyl acrylate (MA) in 1986.[36] Here nitroxides were used at low temperatures (40-60 °C) where they acted as spin traps for the polymer radical intermediates.[33] Later Georges *et al.*[37] used 2,2,6,6-tetramethyl-1-piperidinyloxy (TEMPO) at higher temperatures (125-150°C) for the polymerisation of styrene (see Figure 1.9). At these elevated temperatures TEMPO acts as a radical mediator rather than an inhibitor, yielding polystyrene and poly(styrene-co-butadiene) resins with $M_w/M_n <$ 1.36. In contrast, a control copolymer prepared in the absence of TEMPO had a M_w/M_n of 4.29.[37] NMP involves the reversible coupling of a stable free radical (the nitroxide) with the growing polymeric radical. The equilibrium between the capped dormant chains and the propagating radical lies to the left-hand side (see Figure 1.8). This leads to a relatively low concentration of propagating polymer radicals (P•) in solution at any one time, reducing the probability of bimolecular termination reactions that are so prevalent in conventional free radical polymerisation.

Figure 1.8. Reversible capping of the polymer radical by the stable nitroxide radical. The equilibrium lies over to the left hand side in favour of the dormant species.

Ideally, the stable free radical (X•) should only react reversibly with the polymer radicals and not with itself or monomer, nor should it participate in side reactions such as hydrogen abstraction.[38]
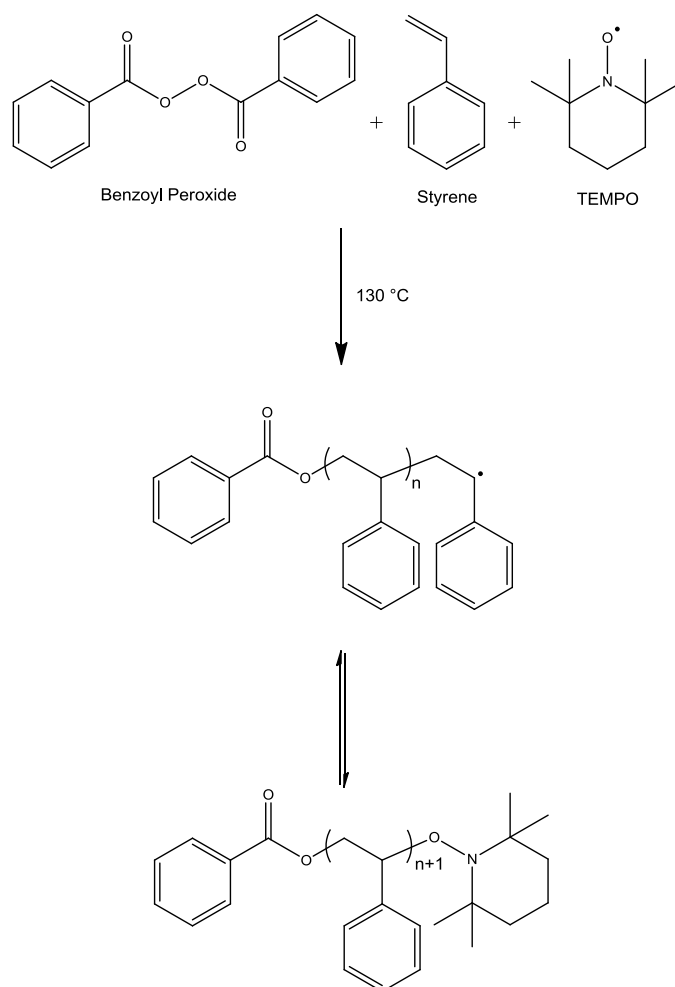
Figure 1.9. TEMPO-mediated radical polymerisation of styrene according to Georges *et al*.[37]

Reversible Addition-Fragmentation Chain Transfer Polymerisation

RAFT polymerisation was reported in 1998 by Rizzardo and coworkers[34] and involves the conventional free radical polymerisation of monomer in the presence of

a dithioester chain transfer agent (CTA). The general mechanism for the RAFT process is shown in Figure 1.10.
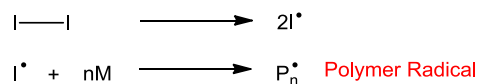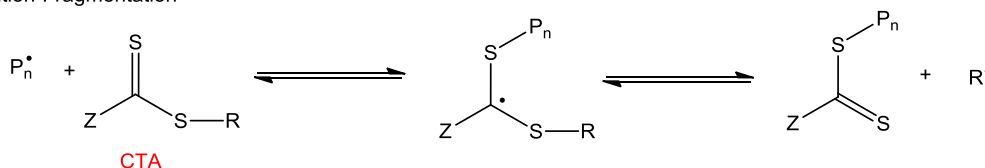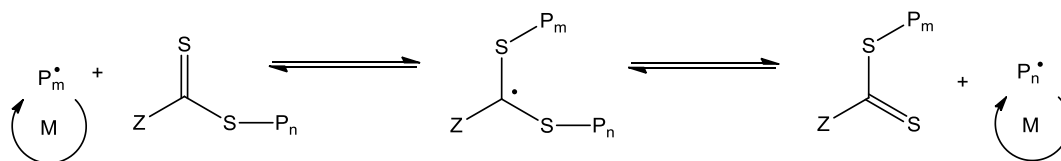
Figure 1.10. The general mechanism for RAFT polymerisation according to Rizzardo *et al.*[34]

Conventional free radical initiators such as azo or peroxide compounds are used as a source of radicals that react with monomer to form a polymer radical. This polymer radical then reacts with the RAFT CTA to create a dormant-capped polymer chain. Living character is achieved through the rapid and reversible transfer of the S=C(Z)S- group between dormant and active chains.

The target molecular weight is controlled by adjusting the monomer/CTA molar ratio rather than the monomer/initiator molar ratio as with anionic polymerisation. The choice of Z and R groups in the CTA is critical for the RAFT process.[34] The Z group should activate the C=S bond towards radical addition and is commonly an aryl or alkyl group. The R group should be a good free radical leaving group,

whereby the eliminated radical has the ability to reinitiate polymerisation; common R groups include cumyl and cyanoisopropyl moieties.[39]

RAFT is considered to be a highly versatile technique enabling polymerisation of a wide range of monomers such as (meth)acrylates,[39] (meth)acrylamides,[40-41] styrene,[34] and 2-vinylpyridine.[42] However, it is worth mentioning that no single CTA can be used to polymerise all of the aforementioned monomer classes. Furthermore, the CTA needs to be carefully selected for a particular monomer class, making some block copolymer synthesis problematic.

Atom Transfer Radical Polymerisation

Atom Transfer Radical Polymerisation was developed independently in 1995 by Wang and Matyjaszewski[31] and Sawamoto and co-workers [32]. ATRP has been utilised in this thesis for the preparation of reactive macromonomers and steric stabilisers (see later chapters). The ATRP formulation comprises monomer, an initiator containing a labile (pseudo)halogen atom and a transition metal catalyst combined with a suitable ligand. In the case of Sawamoto and co-workers, the transition metal complex was dichlorotris(triphenylphosphine)ruthenium(II), $[(RuCl_2(PPh_3)_3)]$ and the initiator was CCl_4.[32] In contrast, Matyjaszewski and co-workers chose a copper(I)-based transition metal (CuCl) with a 2,2'-bipyridine (bpy) ligand and a 1-phenylethyl chloride initiator.[31] ATRP enables many well-defined polymers to be synthesised with narrow molecular weight distributions that were not previously accessible using conventional radical polymerisation techniques. Our current understanding[35] of the mechanism of ATRP is illustrated in Figure 1.11.
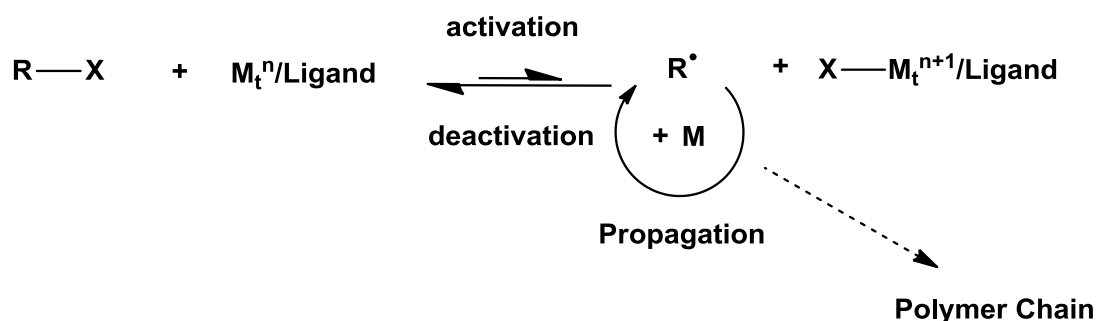
Figure 1.11. Proposed mechanism for transition-metal catalysed ATRP according to Matyjaszewski and co-workers.[35]

Initiation begins with transfer of the halogen atom from the initiator R-X to the metal complex M_t^n/ligand. The metal centre undergoes one-electron oxidation and a radical R˙ is formed. The polymer chain propagates by addition of monomer units to this activated radical species. This halogen atom transfer is both rapid and reversible and one-electron reduction of the metal centre occurs when the halogen ligand is removed by the radical species. The equilibrium for this process lies in favour of the deactivated halogen-capped polymer chain. This rapid reversible chain capping ensures that only a relatively low concentration of polymer radicals exists at any given time. This minimises the bimolecular termination reactions that are so prevalent in conventional free radical polymerisation.[35, 43]

The catalyst is an important component of ATRP because it determines the position of the atom transfer equilibrium. An ATRP catalyst must have two oxidation states accessible by one-electron transfer. It must also have a vacant site capable of coordinating the halogen ligand as well as the chosen ligand. Many different transition metals have been explored as potential ATRP catalysts. Examples include, iron(II),[44] ruthenium(II),[32] lithium molybdate(V)[45] and rhodium(I).[46] However, copper(I) catalysts with polydentate nitrogen-containing ligands such as bpy are the most widely used, perhaps due to the relatively low cost of this metal.[35] Studies of the copper(I)/bpy catalyst confirm that the rate of polymerisation is first order with respect to monomer. The optimum ligand/copper molar ratio has been empirically determined to be 2:1 and CuCl or CuBr catalysts give the best results. The strength of the CuF bond is apparently too strong to make it a useful ATRP catalyst.[35, 43]

Another important aspect of the ATRP formulation is the initiator. Matyjaszewski suggests that the chemical structure of the initiator should ideally resemble the required monomer to achieve a well-controlled polymerisation.[35] The rate of initiation needs to be at least as fast as the rate of propagation. If the former rate is too slow, polymers with higher than expected molecular weights result, coupled with relatively high polydispersities. However, initiation cannot occur too quickly, as this would lead to a large number of radicals present in the reaction mixture and hence undesirable bimolecular termination.
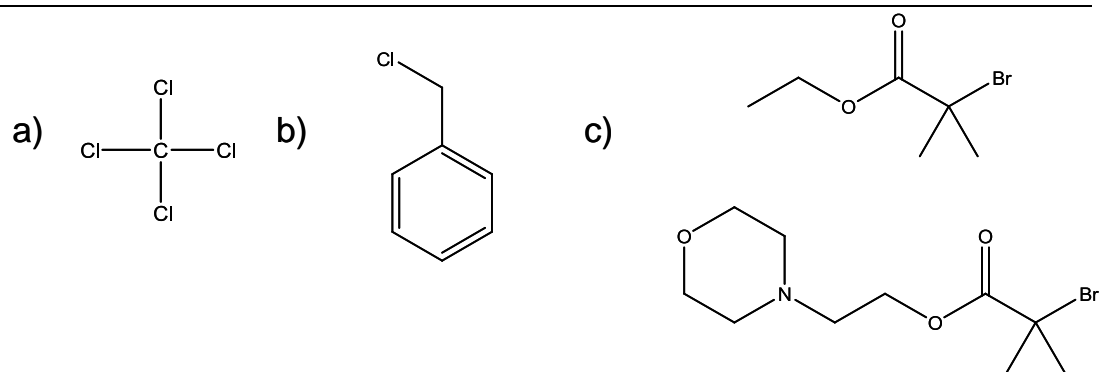
Figure 1.12. Literature examples of ATRP initiators: a) halogenated alkenes[32] b) benzylic halides[45] c) α-haloesters.[47]

ATRP has been used to polymerise a range of monomers with good control, including acrylates,[48] methacrylates[49] and styrene.[50] It is also particularly tolerant of monomer functionality, with methacrylates containing hydroxy, amino and epoxy groups all being successfully polymerised.[51-53] ATRP can be conducted in various solvents depending on the nature of the vinyl monomer being polymerised. Methanol[54], 2-propanol (IPA)[54], DMF[55], carbon dioxide[56] and even water[57] have been used successfully. ATRP for monomers such as styrene has typically been conducted in toluene at relatively high temperatures (e.g. 110 ^{o}C).[58] Polar solvents offer certain advantages for ATRP. Solvents such as 2-propanol are easier to remove than toluene and are less toxic. The activity of the Cu(I)X/bpy catalyst is higher in protic solvents such as water and alcohols,[59-60] which allows polymerisations to be conducted at room temperature with significantly reduced reaction times. The ideal ATRP conditions may vary depending on the monomer, catalyst and target molecular weight and formulations often require some optimisation.

The initial focus of this project was to prepare a series of well-defined macromonomers based on glycerol monomethacrylate (GMA). Poly(glycerol monomethacrylate) (PGMA) is a hydrophilic polymer that has been shown to be biocompatible.[61] GMA is a speciality monomer available from Cognis that is prepared via acetone protection of glycerol, followed by esterification of the remaining alcohol. One consequence of this preparation route is that GMA exists in two isomeric forms (see Figure 1.13).
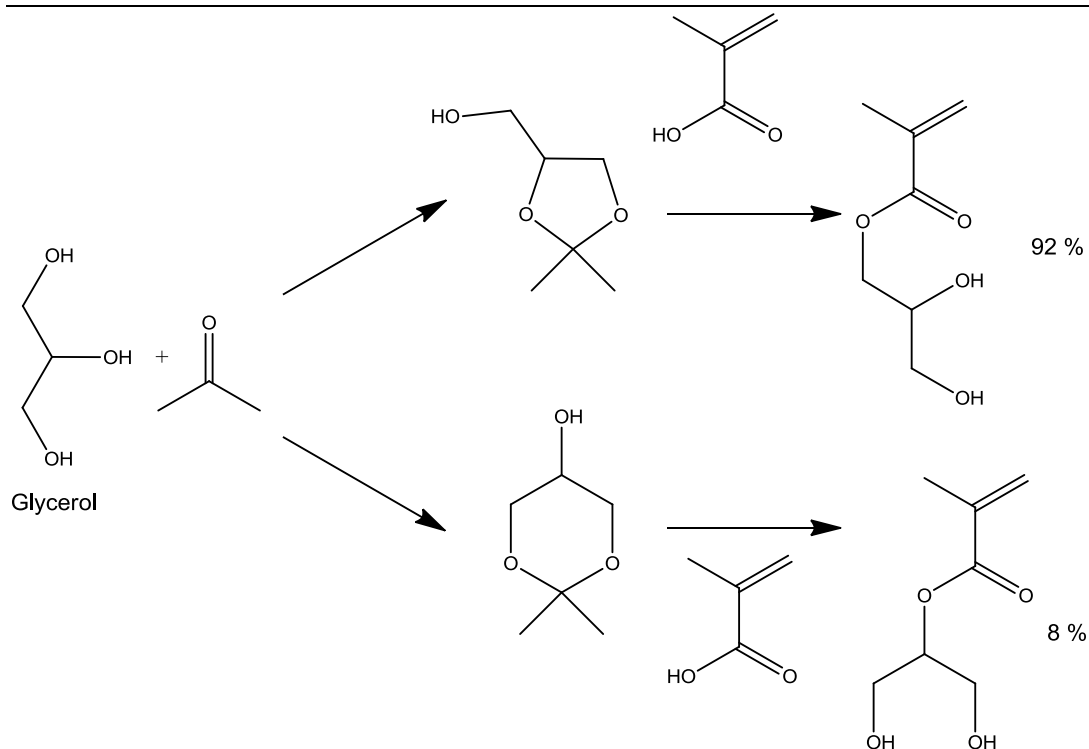
Figure 1.13. Synthetic route to glycerol monomethacrylate starting from glycerol used by Cognis.[51] Due to poor regioselectivity, 1,3-dihydroxyisopropyl methacrylate (DHIMA) is also obtained as a minor isomeric impurity (8 %).

In previous work within the Armes group, GMA has been successfully synthesised by ATRP at room temperature either in methanol or methanol/water mixtures, with M_w/M_n below 1.30.[51] In the same work, poly(propylene oxide) and poly(ethylene oxide) macroinitiators were also used to prepare the corresponding diblock copolymers, with similarly good control. The PGMA macromonomer prepared in this work was designed to be used as a reactive steric stabiliser for the synthesis of latex particles and ultimately for the preparation of colloidosome microcapsules. The synthetic route to such PGMA macromonomers used in this thesis has been reported previously by the Armes group for the preparation of Poly(2-(methacryloyloxy)ethyl phosphorylcholine) (PMPC) macromonomers.[62] In this previous work, good control over the molecular weight distribution was only achievable for relatively low target DPs (PMPC$_{30}$ and below). Attempted synthesis of higher molecular weight PMPC macromonomers invariably lead to broad molecular weight distributions (see Figure 1.14).
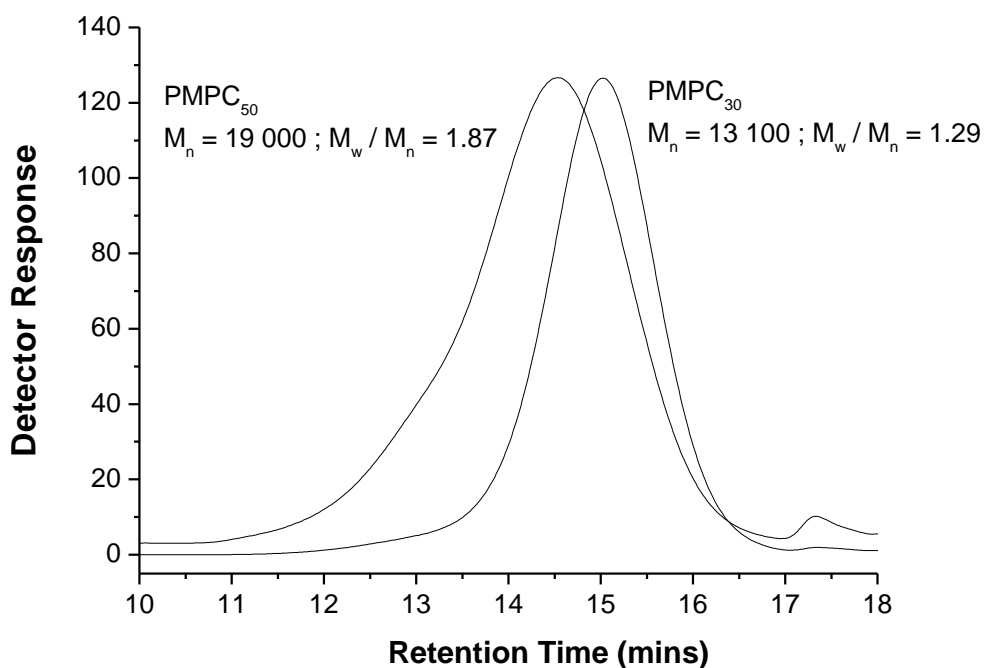
Figure 1.14. Aqueous GPC curves obtained for $PMPC_{50}$ and $PMPC_{30}$ homopolymer precursors prepared by ATRP at 20 $^{\circ}$C (vs. PEO calibration standards).[62] Reprinted with permission from [Thompson, K. L.; Bannister, I.; Armes, S. P.; Lewis, A. L., *Langmuir,* **2010,** *26*, 4693-4702.]. Copyright [2010] American Chemical Society.

The reasons for this poor control was not completely understood, however no such synthetic limits are observed for the PGMA macromonomers presented in this thesis.

As mentioned previously, routes to colloidosomes typically start with the adsorption of colloidal particles at the interface of two immiscible liquids, usually oil and water. These self-assembled structures are known as Pickering emulsions and will be discussed in more detail in the following section.

PICKERING EMULSIONS

Pickering[7] or Ramsden[8] emulsions were discovered at the turn of the last century, when it was found that solid particles could efficiently stabilise oil or water droplets. For amphiphilic surfactants at oil/water interfaces, their hydrophile-lipophile balance (HLB) determines whether a particular surfactant stabilises oil-in-water (o/w) or water-in-oil emulsions (w/o). The packing parameter of the surfactant at the oil/water interface is determined by how hydrated the polar head groups are by water and how solvated the hydrophobic tails are by the oil phase.[63] For hydrophilic surfactants, the polar head group tends to take up more room than the chain and the monolayers curve around the oil to give an o/w emulsion. The opposite is true for hydrophobic surfactants, with the area of their lipophilic chain taking up more space than the head group, hence giving w/o emulsions.[63]

In contrast to conventional surfactants colloidal particles that adsorb to the oil or air/water interface are not amphiphilic but are nevertheless surface-active. For solid particles sitting at an oil-water interface, it is the particle wettability that dictates the emulsion type. The wettability of the particle is measured by the three-phase contact angle (θ) that the particle makes at the oil/water interface (see Figure 1.15). For hydrophilic particles, ($\theta < 90°$) the majority of the particle resides in the aqueous phase,[64] thus stabilising o/w emulsions. For hydrophobic particles the converse is true and w/o emulsions are favoured. This relationship between θ and emulsion type (o/w vs. w/o) holds for cases where the oil/water volume fraction is 0.50. However, in some cases changing the volume fraction of the oil and water can lead to phase inversion.[63]
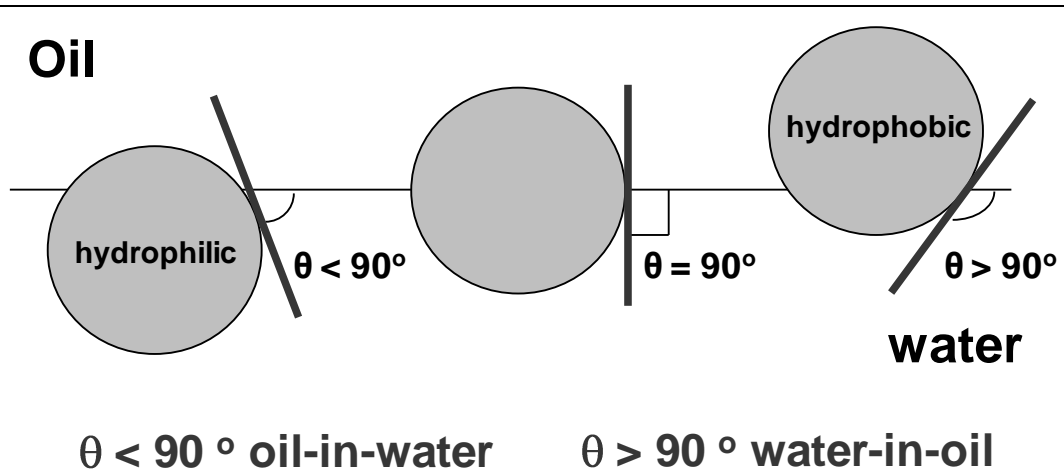
Figure 1.15. Particles sitting at the oil/water interface with varying contact angles. If the Pickering emulsifier has a contact angle at this interface below 90 °, then an oil-in-water emulsion results. However, if the contact angle is above 90 °, then a water-in-oil emulsion will be formed.[64]

Once attached to the oil/water interface, the energy required to detach the particles is given by:[64]

$$(18) \qquad E = \pi r^2 \gamma_{ow} (1 \pm \cos\theta)^2$$

Where r is the particle radius, γ_{ow} is the surface tension at the oil/water interface and θ is the particle contact angle. The sign in the brackets is negative for removal of the particle into the aqueous phase and positive for removal into the oil phase. Therefore it is easier (requires less energy) for particles to detach into the water phase if $\theta < 90°$ or detach into the oil phase if $\theta > 90°$.[64]
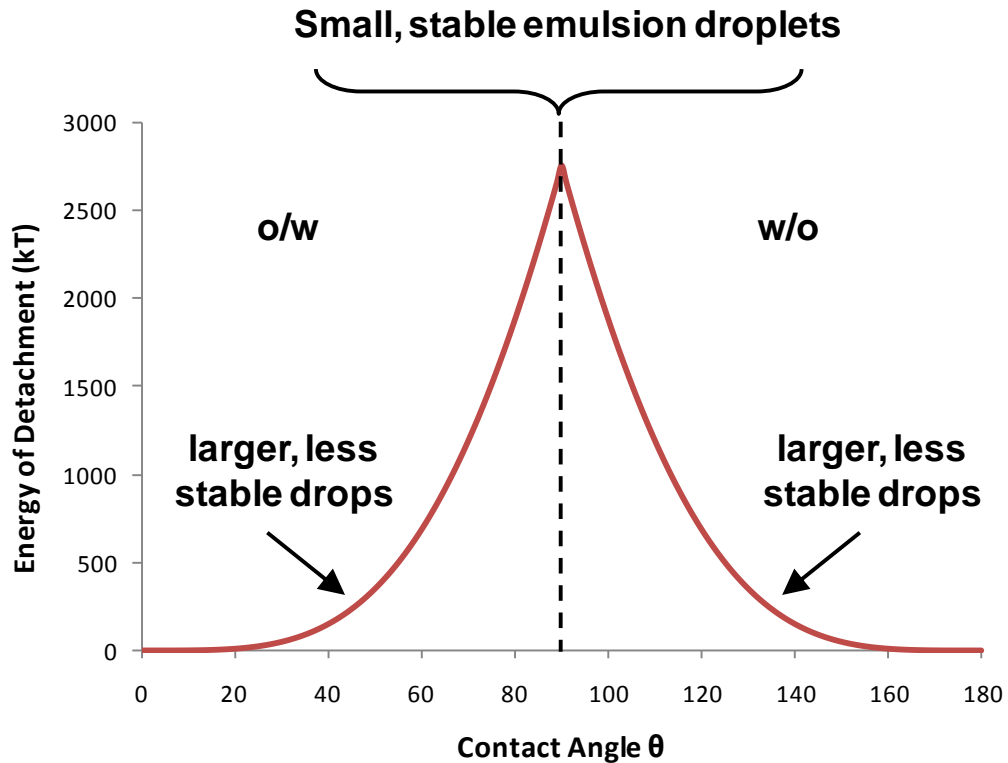
Figure 1.16. The energy of detachment versus contact angle for a particle radius of 10 nm sitting at the toluene-water interface ($\gamma_{ow} = 0.036$ Nm^{-1}).[64-65]

Equation (18) shows that the energy of detachment of a particle at the oil/water interface is heavily dependent on the three-phase contact angle θ. Figure 1.16 demonstrates this relationship for a 20 nm particle adsorbed at the toluene/water interface.[65] The calculated energy of detachment is greatest for $\theta = 90°$ and falls rapidly either side of this value. Therefore the most stable emulsions are formed when θ is close to 90° as the particles are held more strongly at the interface with a detachment energy of around 2750 kT.[65] However, larger/less stable emulsions are formed at higher and lower values of θ. In fact, when the contact angle is less than 20° or greater than 160° the detachment energy is significantly smaller (< 10 kT).[64] Hence highly hydrophilic or hydrophobic particles that exclusively reside in either the aqueous or oil phases do not act as effective Pickering emulsifiers.
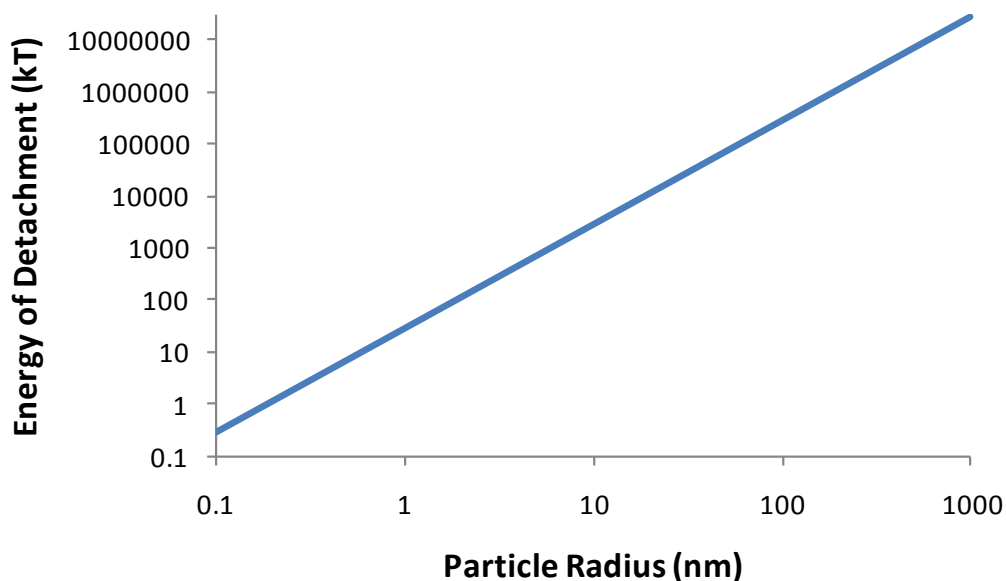
Figure 1.17. Variation of the calculated theoretical detachment energy with particle radius for a spherical particle adsorbed at the toluene/water interface (γ_{ow} = 0.036 Nm^{-1}) with a contact angle of 90° at 298K.[64]

In addition to the contact angle, equation (18) also shows the detachment energy is proportional to the square of the particle radius. Figure 1.17 shows how the calculated detachment energy varies with particle radius for a particle adsorbed at the toluene/water interface with a contact angle of 90°. Clearly, very large detachment energies would be required to remove particles larger than 10 nm radius from the droplet interface, hence they can be considered to be irreversibly adsorbed. However, particles with radii less than of < 1 nm have detachment energies similar to that of surfactant molecules (< 10 kT). In this case only weak, reversible adsorption is anticipated at the oil-water interface.[63-64]

This high energy of particle attachment makes Pickering emulsions far more stable than surfactants, with the adsorbed particles providing a strong steric barrier to droplet coalescence. Colloidal particles such as silica sols[66-67] and polystyrene latexes[68] have been shown to be effective Pickering emulsifiers. Stimulus-responsive particulate emulsifiers have also been developed, with either inversion or demulsification being achieved in response to changes in solution pH[69-70] or temperature.[71]
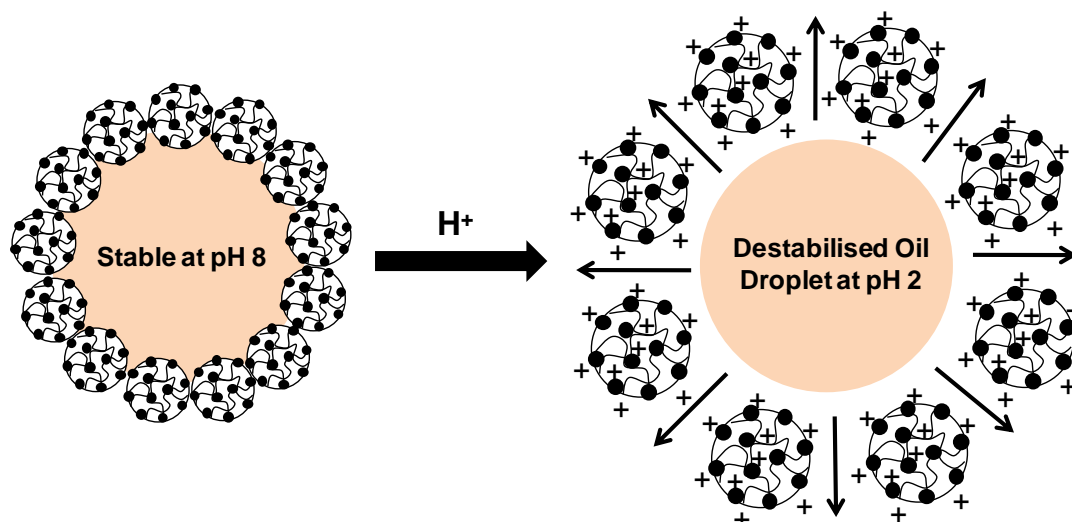
Figure 1.18. Schematic representation of the pH-induced demulsification of a Pickering emulsion stabilised using poly(4-vinylpyridine)-silica nanocomposite particles.[72-73]

Fujii *et al.*[72-73] prepared pH-responsive lightly cross-linked poly(4-vinylpyridine)-silica nanocomposite particles. These particles acted as effective Pickering emulsifiers at pH 8-9, but spontaneous demulsification occurred upon the addition of acid. The 4-vinylpyridine units become protonated at low pHs imparting cationic microgel character to the nanocomposite particles. The highly swollen cationic microgel particles have less affinity for the oil phase and hence desorb from the oil/water interface, leading to droplet coalescence and ultimately demulsification (see Figure 1.18). Similar pH-responsive behaviour was found for Pickering emulsions prepared with sterically-stabilised poly(2-vinylpyridine) latexes.[74]

Binks et al.[71] prepared stimulus-responsive polystyrene particles using a poly[2-(dimethylamino)ethyl methacrylate-*block*-methyl methacrylate] (PDMA-b-PMMA) steric stabiliser. Such particles stabilised o/w Pickering emulsions at pH 8.1 and 25 °C, using *n*-hexadecane as the oil phase. Under these conditions the particles are weakly hydrophilic and are preferentially wetted by the aqueous phase. Once formed, these o/w emulsions were heated to 70 °C (i.e. above the LCST of the PDMA stabilising block) and although the emulsions remained stable significant coalescence occurred. In contrast, phase inversion from o/w to w/o was observed if the latex and oil phases were pre-heated to 70 °C prior to homogenisation. This phase inversion occurs due to a disruption of the hydrogen bonds around the PDMA

stabiliser causing an increase in its hydrophobicity. Thus at elevated temperatures the particles are preferentially wetted by the oil phase and form w/o emulsions. The temperature at which the emulsions are prepared dictates whether they will be o/w or w/o. As a result, this system can be described as temperature-dependent rather than temperature-responsive; once formed, phase inversion or demulsification does not occur upon varying the temperature.

The preparation of colloidosomes requires an additional means of particle stabilisation at the interface of a Pickering emulsion in order to form a more robust microcapsule shell. The following section will explore the various colloidal particles and techniques that have been used to prepare stable colloidosomes.

COLLOIDOSOME MICROCAPSULES

Velev and co-workers reported the first colloidosome-type structures in 1996 in a series of three papers, where latex particles were assembled around emulsion droplets.[75-77] They reported the formation of both hollow spherical supraparticles[75] where the latex particles were adsorbed at the water/oil interface (see Figure 1.19), along with ball-like aggregates[76] where the latex particles penetrated the bulk of the oil droplets. It was found that the negatively-charged sulphate-stabilised polystyrene particles did not effectively stabilise emulsion droplets in their original form. Therefore, the surface of the particles had to be 'sensitised' using the amino acid lysine; these surface-modified particles were found to adsorb at the oil/water droplet interface. The particles were then 'bound' within the assembled microspheres using a strong coagulant (casein, HCl and $CaCl_2$), that was known to aggregate the latex particles in aqueous solution. This stabilisation was sufficient for the capsules to survive extraction of the n-octanol droplets with excess ethanol. The third paper in the series introduces the inverted water-in-oil system of microspheres, where the latex particles are ordered around water droplets[77] suspended in n-octanol.
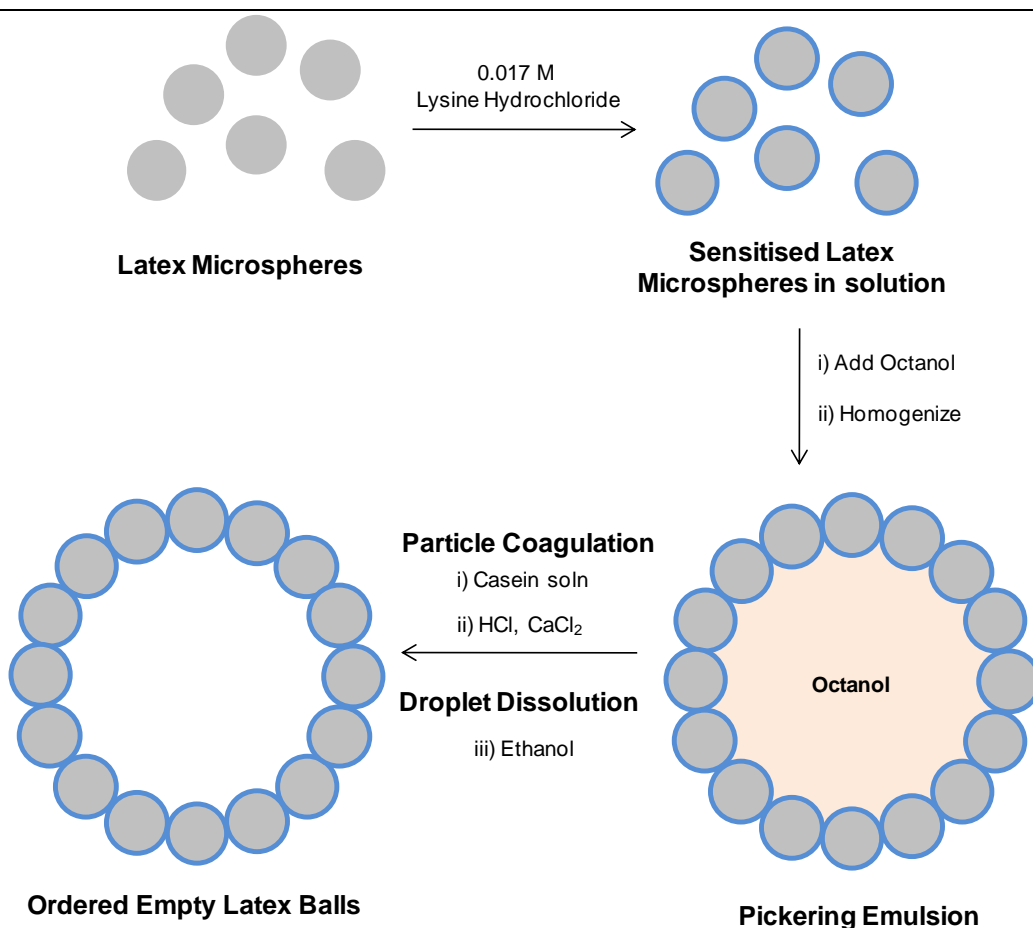
Figure 1.19. Route to shell-like supraparticles formed from a Pickering emulsion of sensitised latex microspheres and n-octanol. The neighbouring latex particles are locked in place using a strong coagulating agent, which then allows the dissolution of the n-octanol droplet template in excess ethanol.[75]

Preparation by thermal annealing

The term 'colloidosome' was first introduced by Dinsmore *et al*,[78] who prepared microcapsules by the self-assembly of micrometer-sized carboxylated polystyrene latex particles at the surface of oil-in-water emulsion droplets. Once the droplet surface was covered by particles, the colloidosome shell was formed by fusing these particles together. This was achieved by sintering, where the emulsion was heated to just above the T_g of the latex particles (~ 105 ^{o}C) in order to fuse them together (see Figure 1.20). In order to heat the emulsion to this temperature 50 % glycerol was added to increase the boiling point of the aqueous phase. In principle, the interstitial gaps between adjacent fused particles can be tuned by varying the sintering duration.
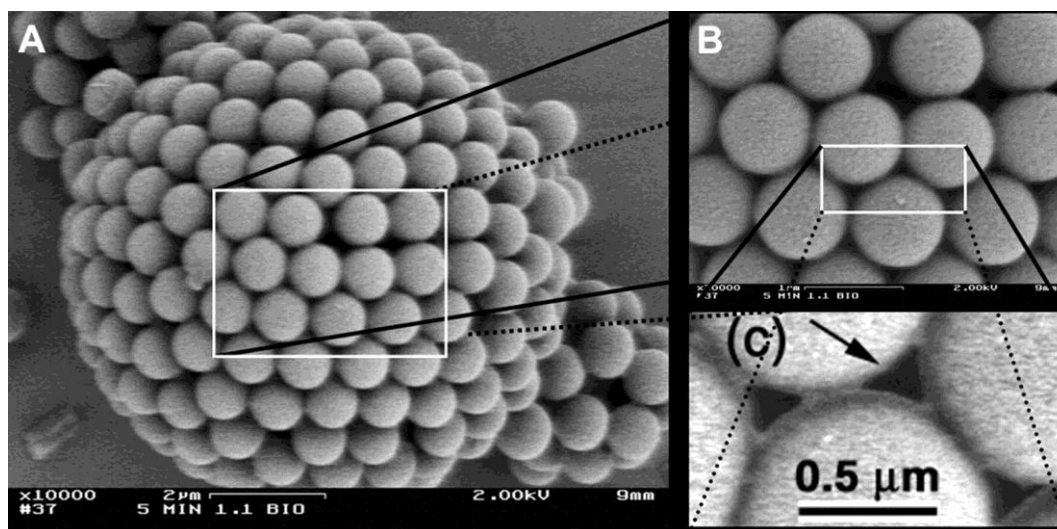
Figure 1.20. A 10 μm colloidosome prepared by thermal annealing of a oil-in-water emulsion stabilised by 0.90 μm polystyrene latex particles and sintered at 105 °C for 5 min.[78] From [Dinsmore, A. D.; Hsu, M. F.; Nikolaides, M. G.; Marquez, M.; Bausch, A. R.; Weitz, D. A., *Science,* 2002, *298*, 1006-1009]. Reprinted with permission from AAAS.

Extending the work of Dinsmore *et al*.,[78] Hsu *et al*.[79] also reported sintering as a means achieving structural integrity for the colloidosomes. After 2 h of sintering, individual particles were no longer visible, suggesting that the annealing process was complete. The shells were indented and broken with microcantilevers and the strain response due to the shell deformation was measured. The typical force required to break sintered colloidosomes increased for longer annealing times, thus longer sintering times resulted in stronger capsules, as expected.

The use of copolymer latex particles with lower T_g values than that of polystyrene allows a significant reduction in the sintering temperature. This could be potentially beneficial for the encapsulation of thermally-sensitive compounds. Routh *et al*.[80-81] used a poly(styrene-co-n-butyl acrylate) latex to prepare water-core colloidosomes of a few micrometers in size. The lower T_g of these colloidal particles meant that sintering could occur under milder conditions, typically between 35 and 65 °C. In this particular example, the particles alone were not efficient Pickering emulsifiers, hence a co-surfactant (Span 80) was added to promote colloidosome formation.

Recently, Nomura and Routh[82] prepared colloidosomes at room temperature using a poly(methyl methacrylate-co-n-butyl acrylate) latex without the need for added surfactant. A small amount of ethanol was added to the continuous oil phase so as to coagulate the latex particles and so fix the colloidosome structure.

One potential problem with colloidosome preparation by thermal annealing is that it is often difficult to avoid inter-colloidosome fusion. As well as particles within one shell being sintered together, particles in neighbouring shells can become fused, causing agglomeration of the microcapsules. This can be reduced to some extent by conducting the sintering process at lower solids and maintaining efficient stirring. Recently, Salari *et al.*[83] overcame this problem by adding poly(styrene-block-ethylene-co-propylene) (PS-b-EP) to a Pickering emulsion prior to annealing to act as a steric stabiliser for the colloidosome microcapsules. The original polystyrene particles used to prepare the Pickering emulsion were synthesised using soap-free emulsion polymerisation. These were then emulsified in the presence of salt with either n-heptane or n-decane to give a water-in-oil emulsion. The PS-b-EP copolymer was then added to this Pickering emulsion and heated to 50 ^{o}C. The n-decane has a plasticising effect on the polystyrene allowing sintering to occur below the latex T_g of the latex. It was found that significant agglomeration occurred in the absence of any PS-b-EP copolymer, whereas colloidosome aggregation is reduced significantly if the copolymer is added prior to heat treatment (see Figure 1.21).
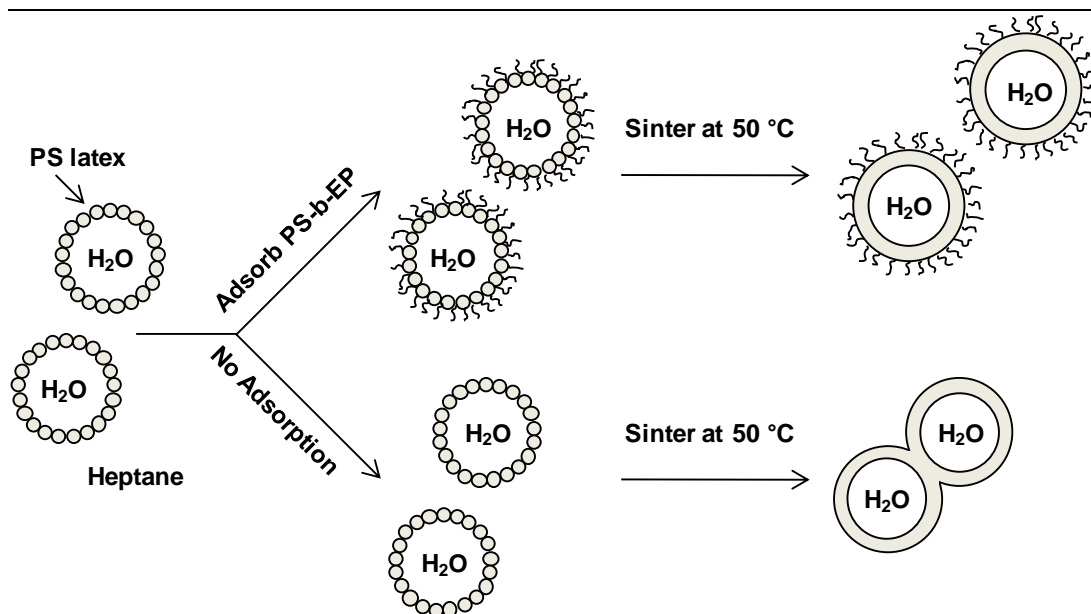
Figure 1.21. Adsorption of a PS-b-EP copolymer onto water-in-oil colloidosomes prepared with an aqueous solution of polystyrene latex and n-heptane.[83] PS-b-EP adsorption prevents inter-colloidosome fusion when the Pickering emulsions are sintered at 50 °C.

Polyelectrolyte complexation and layer-by-layer deposition

In addition to preparing colloidosomes by thermal annealing Dinsmore *et al.*[78] also explored an alternative method of colloidosome stabilisation based on the electrostatic adsorption of an oppositely-charged polyelectrolyte onto the particle surface. Thus high molecular weight, cationic poly-L-lysine was adsorbed onto the surface of anionic colloidosomes. This method proved to be effective as the latex particles became trapped at the oil/water interface. This protocol also enhanced the elastic properties of the colloidosomes: they were more flexible and deformable when compared to colloidosomes prepared by sintering.
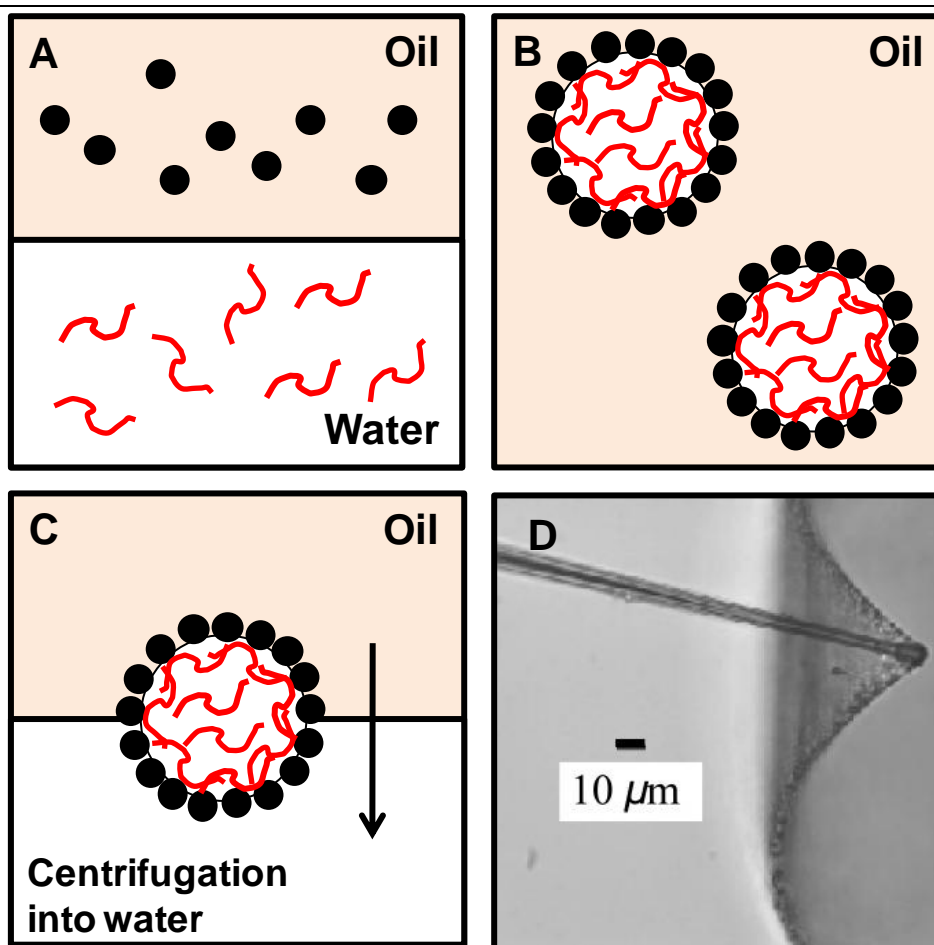
Figure 1.22. A schematic representation of the preparation of colloidosomes by polyelectrolyte complexation according to Gordon *et al*.[84] (A) An aqueous solution of poly(-L-lysine) is homogenised with the oil phase containing 1.3 µm cross-linked polystyrene particles. (B) The poly-L-lysine absorbs onto the anionic latex particles locking in the colloidosome super-structure (150-400 µm). (C) The colloidosomes can be transferred into an aqueous continuous phase via centrifugation. The strength of the resulting capsules can be assessed by deformation using microcantilevers (D).[84] Image D reprinted with permission from [Gordon, V. D.; Xi, C.; Hutchinson, J. W.; Bausch, A. R.; Marquez, M.; Weitz, D. A., *J. Am. Chem. Soc.,* 2004, *126*, 14117-14122]. Copyright [2004] American Chemical Society.

This polymer adsorption approach to colloidosomes was later developed by Gordon *et al*.[84] 1.3 µm cross-linked polystyrene latex particles were dispersed in toluene as an oil phase and emulsified with an aqueous solution of poly-L-lysine. The latex self-assembled at the droplet interface and the cationic poly-L-lysine adsorbed onto the anionic PS latex, locking together neighbouring particles.[78] It was demonstrated

that these capsule membranes are inflated by osmotic pressure from the internal polyelectrolyte. Since added salt reduces the osmotic pressure of polyelectrolytes in aqueous solution, a non-mechanical release trigger for such capsules was devised. In 1 M NaCl solution the capsules became entirely deflated, but no encapsulation/release studies were carried out.

Lawrence et al.[85] assembled anionic poly(*N*-isopropylacrylamide-co-acrylic acid) microgel particles around n-octanol droplets to form w/o colloidosomes. In this case, the colloidosomes were stabilised by addition of a cationic diblock copolymer, poly(butadiene-b-N-methyl-4-vinylpyridinium iodide). This produced robust capsules that could survive the removal of the droplet interface with excess ethanol and also be transferred into water. Once dispersed in water, the colloidosomes exhibited a significant reduction in size when heated above the LCST of PNIPAM. This potentially gives a temperature-triggered release response, although no triggered release of actives was demonstrated in this work.

Caruso *et al.*[86-87] reported the formation of silica/polymer microcapsules using a sacrificial colloidal template. Cationic poly(diallyldimethylammonium chloride) (PDADMAC) was adsorbed onto polystyrene particles of around 600 nm diameter. SiO_2 nanoparticles (~25 nm) were then adsorbed onto the PDADMAC coated polystyrene. The resulting wall thickness was dependent on the number of layer-by-layer deposition cycles. The colloidal template can then be removed either by calcination or dissolution in organic solvents. Fe_3O_4,[88] TiO_2,[89] and Laponite nanoparticles[90] have also been used to prepare hollow inorganic capsules onto a sacrificial template using this approach. One disadvantage of this technique is that the hollow core can only be achieved by template calcination or dissolution. Therefore loading of the capsule with actives would have to occur after the calcination/dissolution step, which could prove problematic. Moreover, layer-by-layer deposition is restricted to low particle concentrations, typically < 5%.

Gel trapping technique

A novel form of colloidosome stabilisation has also been achieved by using an aqueous gel as the internal phase. In these cases, the aqueous interior of the colloidosome is gelled to form a solid-like core. This means improved support for the colloidosome shell and also better structural integrity, which aids transfer into the

aqueous phase. Cayre and co-workers[91] used amine-functionalised polystyrene latex particles for the preparation of colloidosomes. These latex particles were then assembled around water-in-sunflower oil emulsion droplets where the aqueous phase contained 1.5 % agarose at 75 ^{o}C (see Figure 1.23). These emulsions were then cooled to 20 °C to allow gelation of the agarose in the aqueous cores. The gelled cores confer sufficient structural integrity to enable colloidosome transfer from the oil continuous phase into water. The colloidosome super-structure was further strengthened by cross-linking of the amine groups on the particle surface using glutaraldehyde, which binds the particles within the microcapsule shell. Although glutaraldehyde cross-linking strengthened the resulting colloidosomes, it is important to emphasise that the gelled core was essential for successful particle transfer into water. Colloidosomes prepared purely by glutaraldehyde cross-linking simply collapsed when transfer into the aqueous phase was attempted. The preparation of colloidosomes by cross-linking alone will be discussed later. Cayre and co-workers also demonstrated that swelling of the polystyrene particles occurred at 75 ^{o}C when tricaprylin was used as the oil phase. By varying the temperature and exposure time of the colloidosomes to the hot tricaprylin, the size of the interstices between adjacent latex particles could be tuned, which could be important for encapsulation applications. Nobel *et al.*[92] prepared 'hairy' colloidosomes by the same method using the self-assembly of polymeric microrods and Duan *et al.*[93] prepared magnetic colloidosomes using magnetite nanoparticles trapped in an agarose gel.
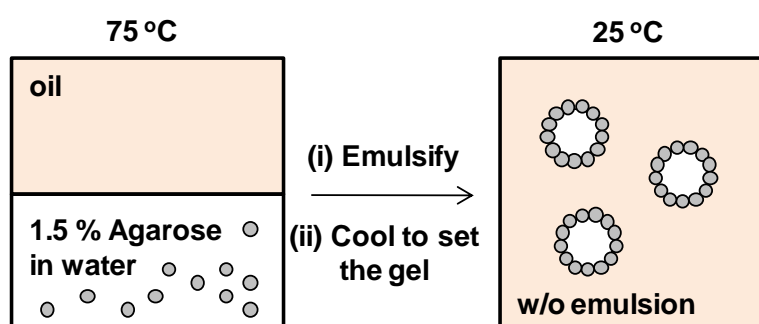
Figure 1.23. Preparation of colloidosomes by the gel-trapping technique. Colloidosomes prepared with an aqueous phase containing particles and 1.5 % agarose. This is then homogenised with sunflower oil at 75 ^{o}C. The w/o emulsion is then cooled to allow gelation of the aqueous cores and the colloidosomes can then be transferred from the continuous oil phase into water.[91]

More recently, this agarose gel technique has been used for the formation of matrix assisted colloidosomes, where almost 100 % encapsulation efficiency of water-soluble biomolecules has been demonstrated. This was achieved by using a reverse phase layer-by-layer encapsulation method.[94] An aqueous mixture of agarose, biomolecules and amino PS latex were emulsified with mineral oil at 45 °C and allowed to cool to form w/o colloidosomes. The reverse phase layer-by-layer deposition process was carried out by placing the colloidosomes in 1-butanol solutions first containing a negatively-charged polymer and then containing a positively-charged polymer. The resulting beads were washed twice with ethanol and finally transferred into water by gentle centrifugation. A colloidosome sample dispersed in water comprising seven polyelectrolyte layers was shown to retain 100% of its encapsulated biomolecules (BSA-FITC) after one week. However, this colloidosome fabrication route is rather time-consuming.

An alternative gelled-core colloidosome system was prepared by Wang and co-workers.[95-96] Instead of using agarose to gel the aqueous cores, in situ gelation of an alginate core was utilised. A shell of porous $CaCO_3$ microparticles was templated around a water-in-oil emulsion. Aqueous D-glucono-δ-lactone was added to the aqueous phase, which caused a gradual lowering of the solution pH due to its slow hydrolysis. Ca^{2+} ions were released from the $CaCO_3$ and ionically cross-linked the alginate chains in solution to form gelled cores.

Colloidosome-like structures using silica particles have also been prepared by using an oil phase that sets upon cooling,[97-98] in an approach analogous to aqueous gel trapping. This was achieved by emulsifying silica particles dispersed in a molten wax within an aqueous phase (at 75 °C). When the emulsion was cooled, the oil phase crystallises to form a wax and the particles become immobilised at the interface (a colloidosome-like structure). This technique was actually exploited to prepare so-called Janus particles by modification of the particle surface exposed to the aqueous phase. Once the surface modification was complete, the wax was dissolved in chloroform and the Janus particles were released for further studies.

Polymer trapping/Pickering Emulsion Polymerisation

In some cases colloidosome stabilisation can be achieved by a further polymerisation step that takes place either inside or on the surface of the Pickering emulsion. This

traps the particles at the interface, allowing the template to be removed. A functionalised silica sol modified to contain ATRP initiator groups has been shown to act as a Pickering stabiliser for paraffin oil-in-water emulsions.[99] Once a stable Pickering emulsion was formed, atom transfer radical polymerisation of 2-hydroxyethyl methacrylate was conducted from the surface of the silica particles. PHEMA becomes lightly cross-linked when polymerised in water due to dimethacrylate impurities in HEMA monomer, hence novel capsules are produced. The disadvantage of this route is that the silica particles have to be specially modified to incorporate the ATRP initiator groups.

The alternative to polymerising from the surface of the Pickering emulsion is to conduct the polymerisation in the droplet interior, where the oil phase contains or is itself, a monomer. So-called "Pickering emulsion polymerisation" has been frequently used to create a wide range of microcapsules. Poly(methyl methacrylate) particles have been adsorbed around monomer droplets and used as mini-reaction vessels for the copolymerisation of styrene and divinylbenzene.[100] This copolymerisation took place within the oil phase, creating colloidosomes (typically 5-30 μm in diameter) reinforced by a cross-linked polystyrene network. The same technique has been used to prepare both TiO_2[101] and ZnO[102] stabilised colloidosomes. Thermo-responsive silica/PNIPAM microcapsules have also been prepared by the polymerisation of NIPAM monomer inside water droplets stabilised by hydrophobic silica particles.[103] These capsules can be dispersed in water and the volumetric shrinkage ratio above the LCST of PNIPAM was measured as a function of cross-linker density. As more cross-linker was incorporated into the formulation, a smaller volumetric shrinkage ratio was observed, as expected.
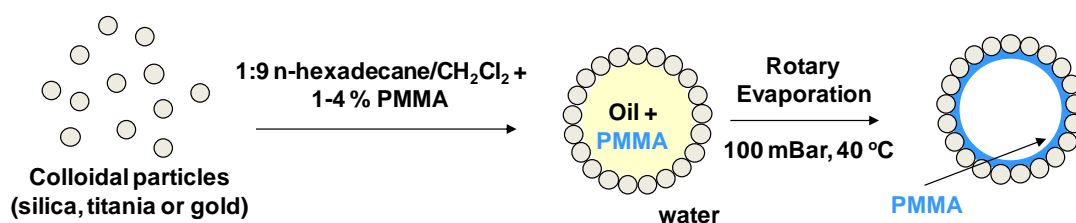
Figure 1.24. Formation of colloidosomes by precipitation of PMMA onto the inner wall of a Pickering emulsion droplet.[104-105]

Instead of an interfacial polymerisation, a preformed polymer can be precipitated onto the inside of the Pickering emulsion to lock the particles together. This was achieved by Cayre *et al*.,[104-105] who prepared a Pickering emulsion with an aqueous phase containing nanoparticles (silica or gold) and an oil phase consisting of poly(methyl methacrylate) dissolved in a 1:9 n- hexadecane/dichloromethane mixture by weight. Once formed, the emulsion was then subjected to rotary evaporation at 40 $^\circ$C. This removes dichloromethane and the core becomes n-hexadecane-rich, which is a poor solvent for poly(methyl methacrylate). As a result, the polymer precipitates onto the internal capsule walls, trapping the colloidal particles at the interface (see Figure 1.24).

Colloidosome Formation via Covalent Cross-linking

Techniques such as thermal annealing, gel trapping and Pickering emulsion polymerisation almost always involve heating the system to some extent, whether it is to sinter neighbouring particles, to initiate polymerisation or to prevent the gelling agent from setting prior to emulsification. Although such heat treatment is often essential for colloidosome formation, it is not ideal for the encapsulation of more thermally sensitive compounds or biological entities such as enzymes. Covalent-cross-linking therefore provides a potential route for locking in the colloidosome structure at room temperature, by careful design of the colloidal particle and/or the chemical cross-linker.

In 2003 Croll *et al*.[106-107] prepared poly(divinylbenzene-alt-maleic anhydride) microspheres and assembled them at the oil/water interface (see Figure 1.25A). These microspheres were then cross-linked from the aqueous continuous phase (at 20 vol % solids) by addition of various polyamines forming amide linkages and ammonium carboxylate ionic links. The capsule stability was enhanced when the molecular weight of the polyamine cross-linker was increased. Low molecular weight tetraethylene pentamine (TEPA, ~189 g/mol) did not lead to capsule formation. It not stated whether addition inter-colloidosome cross-linking occurred between adjacent capsules.
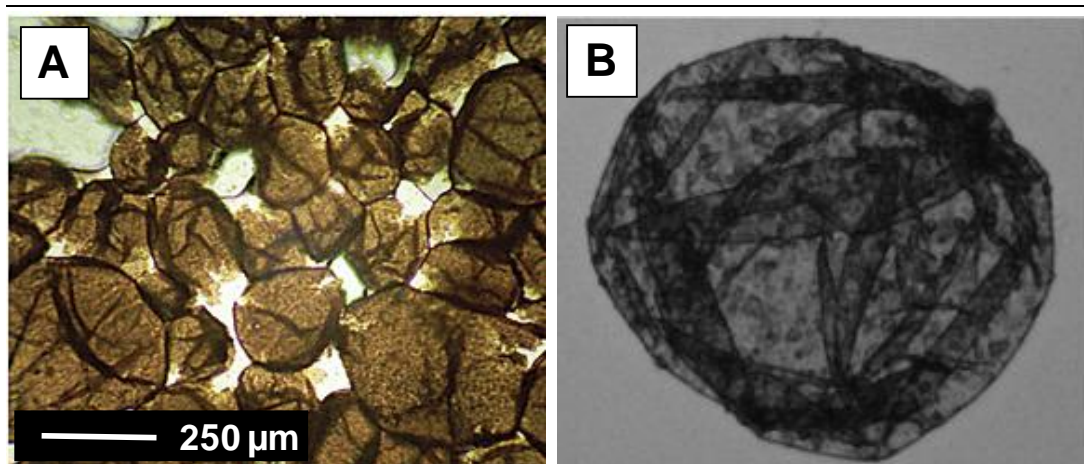
Figure 1.25. Colloidosomes prepared by covalent cross-linking of latex particles. Optical microscopy images of (A) colloidosomes prepared with poly-(divinylbenzene-alt-maleic anhydride) microspheres cross-linked from the aqueous continuous phase by addition of polyamines[106] and (B) poly(2-dimethylaminoethyl methacrylate)-block-poly(methyl methacrylate) stabilised PS latex cross-linked with 1,2-Bis(2-iodoethyloxy)ethane.[108] Reprinted with permission from [Croll, L. M.; Stöver, H. D. H., *Langmuir,* 2003, *19*, 5918-5922] and [Yuan, Q.; Cayre, O. J.; Fujii, S.; Armes, S. P.; Williams, R. A.; Biggs, S., *Langmuir,* 2010, *26*, 18408-18414]. Copyright [2003, 2010] American Chemical Society.

Lin *et al*.[109] reported the covalent cross-linking of CdSe nanoparticles at planar water/toluene interfaces. The CdSe nanoparticles are covered with reactive vinylbenzene groups that are polymerised at the interface at 60 $^{\circ}$C using a radical initiator. When this protocol was attempted at the curved interface of water droplets, some cracking of the shell was observed. This problem could possibly be due to the elevated temperature required for the free-radical cross-linking. Following this work, Skaff and coworkers[110] assembled norbornene-functionalised CdSe/ZnS core/shell quantum dots at the interface of water droplets in toluene. They then conducted ring-opening metathesis polymerisation (ROMP) using a water-soluble Ru-based Grubbs catalyst to lock in the quantum dot super-structure at room temperature. This water-soluble catalyst led to efficient cross-linking at the interface. A more hydrophobic catalyst led to inter-colloidosome cross-linking and also cross-linked particles throughout the toluene phase, as the reaction was not confined to the interface. This highlights the potential problems with the covalent cross-linking route. When cross-linking is conducted from the continuous phase, inter-colloidosome fusion is always

a potential problem. Moreover, any excess non-adsorbed particles in the same phase as the cross-linker could become cross-linked in solution, potentially causing cross-linker wastage and particle flocculation.

Walsh *et al*[111] prepared a series of polyethyleneimine-stabilised polystyrene latex particles (PEI-PS) that acted as effective Pickering emulsifiers for o/w emulsions using sunflower oil, dodecane, isononyl isononanoate and methyl myristate. Such Pickering emulsions were cross-linkable from either the internal oil or external aqueous phases by poly(propylene glycol) and poly(ethylene glycol) diglycidyl ethers respectively. It was found that surprisingly minimal inter-colloidosome cross-linking occurred in the case of the water soluble cross-linker, even at 50 vol % solids.

Arumugam *et al.*[112] prepared 35-60 μm magnetic colloidosomes by assembling terpyridine thiol-functionalised FePt nanoparticles around water droplets suspended in toluene and then cross-linked them via complexation of the terpyridine with Fe(II) ions. More recently, Weitz and co-workers[113] prepared water-in-oil emulsions using primary amine-functionalised PNIPAM microgels. These microgels were cross-linked from the aqueous phase using glutaraldehyde to produce novel thermo-responsive microcapsules. Presumably, since cross-linking is confined to the internal phase, no inter-colloidosome fusion can take place, leading to discrete microcapsules. Confocal microscopy studies with fluorescently-tagged microgels suggested the presence of excess microgels in the bulk of the droplets. It is not known whether this has any detrimental effect on the colloidosome cross-linking protocol, such as microgel aggregation within the water droplet. As with the work of Lawrence *et al.,*[85] the resulting colloidosomes display a significant reduction in size at higher temperature, leading to a potential temperature-triggered release mechanism. Yuan *et al.*[108] recently reported the preparation of cross-linked colloidosomes using a poly(2-dimethylaminoethyl methacrylate)-poly(methyl methacrylate) block copolymer as a steric stabiliser for polystyrene particles, which were then cross-linked at the oil-water interface using 1,2-bis(2-iodoethyloxy)ethane (BIEE) (see Figure 1.25B). Inter-colloidosome fusion is supposedly avoided in this case since the cross-linker is believed to be confined to the oil phase. However, BIEE is likely to partition into the aqueous phase as well seeing as it has been used previously to prepare shell cross-linked micelles in aqueous solution.[114] One

disadvantage of this cross-linking chemistry is that the reaction is relatively slow, often taking several days at 20 °C for successful colloidosome formation.

Encapsulation and Release

Clearly, there are many routes for the preparation of colloidosomes. One obvious application is the controlled encapsulation and release of actives. However, there are surprisingly few reports on the actual encapsulation performance of such microcapsules. Yow and Routh[81] reported the release profiles for fluorescein sodium salt encapsulated inside water-core colloidosomes prepared from poly(styrene-co-n-butyl acrylate) latexes sintered at 49 °C for 5, 30 or 60 minutes. Scanning electron microscopy images of the annealed colloidosomes showed that longer sintering times led to smoother microcapsule shells. Release profiles (see Figure 1.26) for encapsulated fluorescein were almost identical from within colloidosomes annealed for 5 and 30 minutes, with 100 % dye being released within a few hours in both cases. Colloidosomes sintered for 60 minutes released the dye more slowly, as expected. However all of the dye was still released within 24 h. Such encapsulation times are obviously far too short for most commercial applications. For example, the desired retention time for fragrances within microcapsules for laundry formulations is months/years.
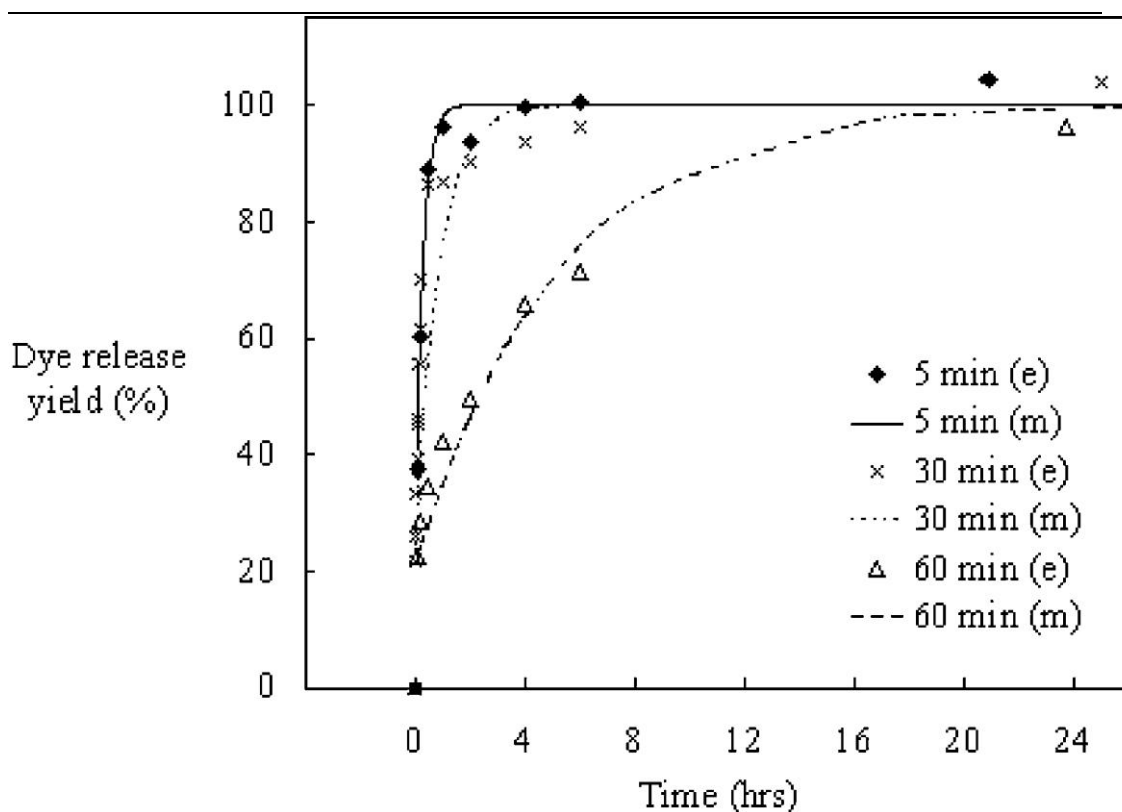
Figure 1.26. Dye release profile for colloidosomes prepared from poly(styrene-co-n-butyl acrylate) latexes sintered at 49 °C for 5, 30 and 60 minutes. Dotted line = release model, data points = experimental data.[81] Reprinted with permission from [Yow, H. N.; Routh, A. F., *Langmuir,* 2009, *25,* 159-166.]. Copyright [2009] American Chemical Society.

Colloidosomes are typically prepared from spherical particles, which even when closely packed together on a planar surface will exhibit interstices between neighbours. In principle, the dimensions of these interstices should dictate the permeability of the resulting microcapsule. However, the curvature of the colloidosome surface necessarily introduces packing defects of much larger dimensions. The nature of these packing defects has been discussed at length in the literature: for monodisperse spheres, a minimum of 12 packing defects must be present in order for these particles to pack fully around a larger sphere.[115-116] These defects are often referred to as line defects or grain-boundary scars[117] and have been experimentally observed by bright field and fluorescence microscopy studies of silica-[116] and polystyrene-[118] stabilised water droplets, respectively. Taking into account geometrical constraints, perfect hexagonal packing of monodisperse spheres of diameter d on a planar surface leads to interstices with an estimated size of

approximately 0.15 × d (see Figure 1.27).[93] However, as mentioned above, pentagonal defects must occur within this packing as a result of the surface curvature. A pentagonal arrangement of spheres leads to an estimated interstitial size of 0.70 × d. This suggests that only actives larger than 0.7 times the sphere diameter are certain to remain inside the colloidosome. This suggests that encapsulation of molecular species is likely to be problematic. Clearly, in some cases these interstices can be reduced in size (e.g. thermal annealing of latex particles) or perhaps blocked, but closing all of these individual holes is a significant challenge which may explain the poor encapsulation efficiency of the colloidosome systems discussed earlier.[81]
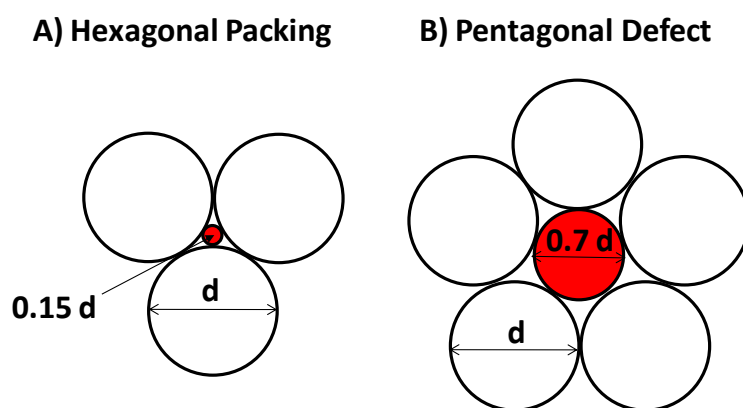
Figure 1.27. A) Hexagonal and B) pentagonal packing of monodisperse spheres. It can be seen that the diameter of the interstices formed between particles are 15 % and 70 % the sphere diameter respectively.[93]

Duan *et al.*[93] used CdTe nanoparticles as probes for their magnetic colloidosomes. Three Fe_3O_4 sols of 4, 5 and 8 nm were used to form the colloidosome shells in this study. According to geometrical considerations, colloidosomes prepared with the 5 nm Fe_3O_4 nanoparticles should have a size cut-off of 3.5 nm (i.e. 0.7 d). To test this hypothesis, two different sized CdTe nanoparticles were placed inside the colloidosomes, 2.8 nm (fluorescence emission at 540 nm) and 4 nm (fluorescence emission at 650 nm). The colloidosomes were then repeatedly washed with water. It was found that the smaller 2.8 nm CdTe nanoparticles were washed away, while the larger 4 nm particles remained inside the capsules (see Figure 1.28). This confirms that colloidosomes can successfully retain colloidal material, as long as the active is larger than the pentagonal defects within the colloidosome shell. A similar study was also performed by Dinsmore *et al.,*[78] whereby they used fluorescently-labelled

polystyrene particles to probe the permeability of their colloidosomes. They found that colloidosomes prepared from 1.3 µm particles cross-linked with poly-L-lysine (theoretical cut off 0.7d = 0.91 µm) were completely impermeable to 1 µm PS beads but allowed 0.1 µm to pass through the shell and enter the colloidosome. Similarly Lee and Weitz[119] found that low molecular weight fluorescent molecules such as calcein (622.55 gmol^{-1}) freely diffuse into colloidosomes prepared from double emulsions, whereas high molecular weight FITC-dextran, (2,000,000 gmol^{-1}) could not. The diffusion of calcein could be prevented by including poly(lactic acid) in the middle oil phase, which essentially fills the interstitial voids between the silica nanoparticles.
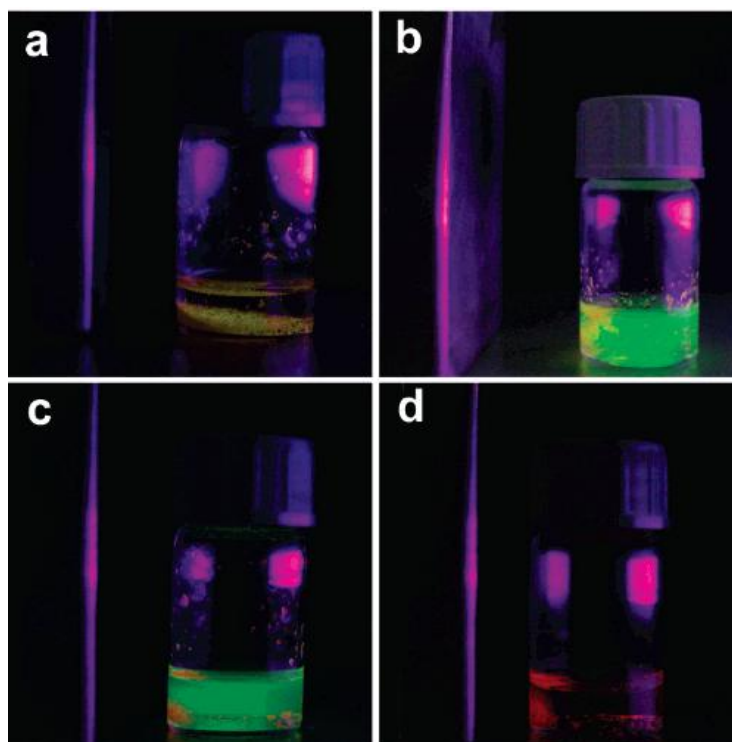
Figure 1.28. (a) Fluorescence photographs of 5.0 nm Fe$_3$O$_4$ NP colloidosomes loaded with both 2.8 and 4 nm CdTe NPs, (b) freshly transferred into water, (c) immersed in water for 10 min and (d) dispersed in water after removal the released CdTe NPs by washing with water. Reprinted with permission from [Duan, H. W.; Wang, D. Y.; Sobal, N. S.; Giersig, M.; Kurth, D. G.; Mohwald, H., *Nano Lett.,* **2005,** *5*, 949-952]. Copyright [2005] American Chemical Society. [93]

Rossenberg *et al.*[120-121] recently conducted a series of release experiments from hydrogels covered with a monolayer of spherical particles. They varied the diameters

of these particles in order to achieve different pore sizes and monitored the release of small molecules aspirin and caffeine and higher molecular weight dextran (3000-5000 gmol^{-1}). They concluded that, although transport of the molecules through the colloidal layer is retarded when compared to the uncoated hydrogel, diffusion is largely independent of the particle diameter (and therefore pore size). The exception is if the particle radius is the same size as the diffusing molecule, or if the shell consists of multi-layers,[121] such as in the work of Kim *et al*.[122]
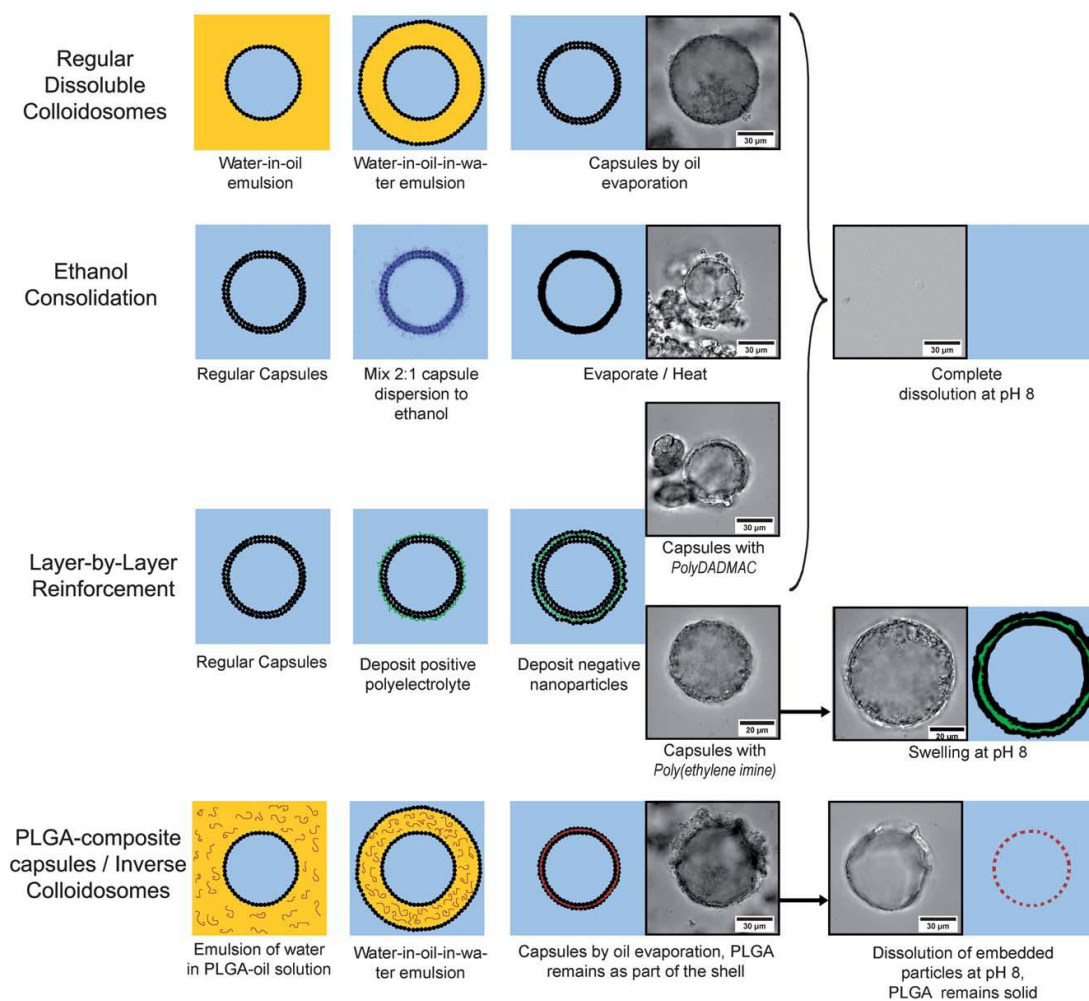
Figure 1.29. Preparation of regular dissoluble colloidosomes (top row) and the different strategies to reduce their permeability.[123] [San Miguel, A.; Behrens, S. H., *Soft Matter,* **2011,** *7*, 1948-1956] – *Reproduced by permission of The Royal Society of Chemistry.*

The permeability of colloidosomes prepared from particle multi-layers has also been investigated. Behrens and co-workers recently reported the preparation of stimulus-responsive colloidosomes that completely dissolved in response to a pH trigger.[124]

These colloidosomes were prepared from double emulsions of pH-responsive poly(methyl methacrylate-co-methacrylic acid) particles. Since the template for these colloidosomes is a double emulsion, they consist of multi-layers of the responsive particles. Firstly, a water-in-oil emulsion was prepared by homogenisation of an aqueous solution of latex particles (pH 3.25, 0.25 M NaCl) and dichloromethane. This emulsion was then re-homogenised with another aqueous solution of the same particles (pH 3.39, 0.025M NaCl) to give a water-in-oil-in-water emulsion. The hydrophobicity of the particles is tuned by changing the NaCl concentration in the aqueous phase. This therefore allows the same type of particles to stabilise both the inner and outer emulsion droplets. The dichloromethane oil phase is then removed by slow evaporation at room temperature; the particles at the original interface remain in contact due to Van der Waals forces. The resultant capsules are stable below pH 7, but upon increasing the pH to 8 the capsules completely dissolved within 1 minute, leading to a potential pH-triggered release. However, it is recognised by the authors that these capsules were of little practical use since their intrinsic permeability prior to the release trigger was simply too high; most of the encapsulated small molecules would already have been released before the colloidosomes were triggered. Therefore subsequent work[123] focused on ways to control the permeability of these capsules prior to the triggered release (see Figure 1.29). The methods investigated included solvent annealing ('ethanol consolidation'), layer-by-layer reinforcement by addition of charged polyelectrolytes and inclusion of poly(lactic-co-glycolic acid) in the oil phase prior to dichloromethane evaporation. All three methods gave a significant reduction in permeability at pH 6 prior to capsule dissolution, relative to the unmodified capsules.

PROJECT MOTIVATION

The motivation behind this Procter and Gamble project was to investigate colloidosomes as a potential route to the encapsulation of perfume oils in laundry products. The perfume oil is the most expensive component of the laundry formulation and the vast majority of this is lost during the washing machine rinse cycle. Encapsulation allows the perfume to be more efficiently trapped within the ~10 μm mesh size of fabrics. The current industry standard is microcapsules based on melamine-formaldehyde (MF).[125] The release trigger for such capsules is mechanical fracture by the application of an external force, i.e. the capsules

deposited on the fabric are crushed by the movement of the consumer and releases the perfume oil.[126] One problem with the current system is that there is always some residual formaldehyde present in the final product.[126] Formaldehyde is toxic and the current EU maximum concentration in any finished product is 0.2 %.[127] Any new system would need to offer at least as good, if not better, encapsulation performance than the current MF capsules. Ideally, next-generation microcapsules should have the following properties:[126]

1. Encapsulate the fragrance in its original form with minimum change and maximum retention.

2. Protect the fragrance from interaction with the environment and premature release on storage.

3. Completely release the fragrance when and where desired.

Laundry products often require shelf-lives of up to 18 months, meaning encapsulation would need to be long term.

The Present Work

The present work focuses on the preparation of colloidosome microcapsules by covalent cross-linking of latex particles via their steric stabiliser chains. A controlled radical polymerisation technique (atom transfer radical polymerisation) has been used to prepare a series of well-defined macromonomers. These macromonomers have been used in the synthesis of sterically-stabilised latex particles by either emulsion or dispersion polymerisation. The macromonomers and corresponding latex particles are analysed by a wide range of techniques, including gel permeation chromatography, nuclear magnetic resonance spectroscopy, dynamic light scattering, disc centrifuge photosedimentometry and x-ray photoelectron spectroscopy.

The sterically-stabilised latexes are then assessed as Pickering emulsifiers using high shear homogenisation using a various oils. In all cases stable o/w emulsions were obtained. The latex super-structure is then 'locked in' by the covalent cross-linking of the stabiliser chains between adjacent latex particles. The Pickering emulsions and covalently cross-linked colloidosomes are analysed by optical and scanning electron microscopy, conductivity and laser diffraction measurements. The covalently cross-

linked colloidosomes are challenged by the addition of either non-ionic surfactant or excess alcohol to examine the efficacy of the cross-linking chemistry.

The permeability of these microcapsules is assessed using oil-soluble small molecule dyes and also bespoke oil-dispersible nanoparticles. The dyes and nanoparticles are encapsulated in the oil phase and released into the aqueous phase by a suitable pH trigger, with the rate of release being conveniently monitored by UV/Vis spectrophotometry and fluorescence microscopy.

Finally, stirred cell membrane emulsification is assessed as a method of producing both Pickering emulsions and colloidosomes with narrower droplet size distributions. The dispersion cell parameters were systematically varied in order to achieve the optimum operating conditions. The overhead stirring speed (shear), oil injection rate and membrane type all influence the size and uniformity of the oil droplets that are produced. Droplet size distributions were assessed using optical microscopy and laser diffraction and compared to that of an emulsion prepared by conventional homogenisation. As expected, emulsification led to significantly narrower droplet size distributions.

REFERENCES

1. Yow, H. N.; Routh, A. F., *Soft Matter,* **2006,** *2*, 940-949.

2. Read, T.-A.; Sorensen, D. R.; Mahesparan, R.; Enger, P. O.; Timpl, R.; Olsen, B. R.; Hjelstuen, M. H. B.; Haraldseth, O.; Bjerkvig, R., *Nat Biotech,* **2001,** *19*, 29-34.

3. Yoshii, H.; Soottitantawat, A.; Liu, X.-D.; Atarashi, T.; Furuta, T.; Aishima, S.; Ohgawara, M.; Linko, P., *Innovative Food Science & Emerging Technologies,* **2001,** *2*, 55-61.

4. Choudary, B. M.; Prasad, B. P.; Kantam, M. L., *J. Agric. Food Chem.,* **1989,** *37*, 1422-1425.

5. Mathiowitz, E.; Jacob, J. S.; Jong, Y. S.; Carino, G. P.; Chickering, D. E.; Chaturvedi, P.; Santos, C. A.; Vijayaraghavan, K.; Montgomery, S.; Bassett, M.; Morrell, C., *Nature,* **1997,** *386*, 410-414.

6. Peppas, N. A.; Brannon-Peppas, L., *J. Control. Release,* **1996,** *40*, 245-250.

7. Pickering, S. U., *Journal of the Chemical Society,* **1907,** *91*, 2001-2021.

8. Ramsden, W., *Proceedings of the Royal Society of London,* **1903,** *72*, 156-164.

9. Lovell, P. A.; El-Aasser, M. S., *Emulsion Polymerisation and Emulsion Polymers*. John Wiley and Sons, Chichester UK: 1997.

10. Odian, G., *Principles of Polymerization*. 4th ed.; John Wiley & Sons, Inc., Hoboken, New Jersey: 2004.

11. Osmond, D. W. J.; Thompson, H. H. Dispersion Polymerisation. GB893429, 1962.

12. Rohm&Haas Polymer dispersions in organic liquid media and methods of preparation. GB934038, 1963.

13. Arshady, R., *Colloid Polym. Sci.,* **1992,** *270*, 717-732.

14. Paine, A. J.; Luymes, W.; McNulty, J., *Macromolecules,* **1990,** *23*, 3104-3109.

15. Shen, S.; Sudol, E. D.; El-Aasser, M. S., *Journal of Polymer Science Part A: Polymer Chemistry,* **1993,** *31*, 1393-1402.

16. Dawkins, J. V.; Taylor, G., *Journal of the Chemical Society, Faraday Transactions 1: Physical Chemistry in Condensed Phases,* **1980,** *76*, 1263-1274.

17. Lascelles, S. F.; Malet, F.; Mayada, R.; Billingham, N. C.; Armes, S. P., *Macromolecules,* **1999,** *32*, 2462-2471.

18. Kawaguchi, S.; Ito, K., *Adv Polym Sci,* **2005,** *175*, 299-328.

19. Ali, A. M. I.; Pareek, P.; Sewell, L.; Schmid, A.; Fujii, S.; Armes, S. P.; Shirley, I. M., *Soft Matter,* **2007,** *3*, 1003-1013.

20. Stevens, M. P., *Polymer Chemistry: an Introduction*. 3rd ed.; Oxford University Press: Oxford, 1999; p 175.

21. Hunter, R. J., *Introduction to Modern Colloid Science*. Oxford University Press: Oxford, 1993; p 20.

22. Gilbert, R. G., *Emulsion Polymerisation - A Mechanistic approach*. Academic Press: London, 1995.

23. Napper, D. H., *Polymeric Stabilization of Colloidal Dispersions*. Academic Press, Inc (London) 1983.

24. Fitch, R. M., *Polymer Colloids - A Comprehensive Introduction*. Academic Press, Inc (London): 1997.

25. Shay, J. S.; English, R. J.; Spontak, R. J.; Balik, C. M.; Khan, S. A., *Macromolecules,* **2000,** *33*, 6664-6671.

26. Matyjaszewski, K.; Spanswick, J., *Materials Today,* **2005,** *8*, 26-33.

27. Webster, O. W., *Science,* **1991,** *251*, 887-893.

28. Szwarc, M., *Nature,* **1956,** *178*, 1168-1169.

29. Sawamoto, M., *Prog. Polym. Sci.,* **1991,** *16*, 111-172.

30. Hawker, C. J.; Hedrick, J. L.; Malmstrom, E. E.; Trollsas, M.; Mecerreyes, D.; Moineau, G.; Dubois, P.; Jerome, R., *Macromolecules,* **1998,** *31*, 213-219.

31. Wang, J. S.; Matyjaszewski, K., *J. Am. Chem. Soc,* **1995,** *117*, 5614-5615.

32. Kato, M.; Kamigaito, M.; Sawamoto, M.; Higashimura, T., *Macromolecules,* **1995,** *28*, 1721-1723.

33. Hawker, C. J.; Bosman, A. W.; Harth, E., *Chem. Rev.,* **2001,** *101*, 3661-3688.

34. Chiefari, J.; Chong, Y. K.; Ercole, F.; Krstina, J.; Jeffery, J.; Le, T. P. T.; Mayadunne, R. T. A.; Meijs, G. F.; Moad, C. L.; Moad, G.; Rizzardo, E.; Thang, S. H., *Macromolecules,* **1998,** *31*, 5559-5562.

35. Matyjaszewski, K.; Xia, J. H., *Chem. Rev,* **2001,** *101*, 2921-2990.

36. Rizzardo, E.; Hill, W.; Cacioli, P. Polymerisation Process and Polymers Produced Thereby. 4,581,429, 1986.

37. Georges, M. K.; Veregin, R. P. N.; Kazmaier, P. M.; Hamer, G. K., *Macromolecules,* **1993,** *26*, 2987-2988.

38. Matyjaszewski, K.; Gnanou, Y.; Leibler, L., *Macromolecular Engineering.* Wiley-VCH, Weinheim: 2007; Vol. 1.

39. Moad, G.; Chiefari, J.; Chong, Y. K.; Krstina, J.; Mayadunne, R. T. A.; Postma, A.; Rizzardo, E.; Thang, S. H., *Polym. Int.,* **2000,** *49*, 993-1001.

40. Donovan, M. S.; Sanford, T. A.; Lowe, A. B.; Sumerlin, B. S.; Mitsukami, Y.; McCormick, C. L., *Macromolecules,* **2002,** *35*, 4570-4572.

41. Sumerlin, B. S.; Donovan, M. S.; Mitsukami, Y.; Lowe, A. B.; McCormick, C. L., *Macromolecules,* **2001,** *34*, 6561-6564.

42. Convertine, A. J.; Sumerlin, B. S.; Thomas, D. B.; Lowe, A. B.; McCormick, C. L., *Macromolecules,* **2003,** *36*, 4679-4681.

43. Kamigaito, M.; Ando, T.; Sawamoto, M., *Chem. Rev,* **2001,** *101*, 3689-3745.

44. Ando, T.; Kato, M.; Kamigaito, M.; Sawamoto, M., *Macromolecules,* **1996,** *29*, 1070-1072.

45. Brandts, J. A. M.; van de Geijn, P.; van Faassen, E. E.; Boersma, J.; van Koten, G., *J. Organomet. Chem.,* **1999,** *584*, 246-253.

46. Percec, V.; Barboiu, B.; Neumann, A.; Ronda, J. C.; Zhao, M. Y., *Macromolecules,* **1996,** *29*, 3665-3668.

47. Ando, T.; Kamigaito, M.; Sawamoto, M., *Tetrahedron,* **1997,** *53*, 15445-15457.

48. Xia, J. H.; Gaynor, S. G.; Matyjaszewski, K., *Macromolecules,* **1998,** *31*, 5958-5959.

49. Haddleton, D. M.; Kukulj, D.; Duncalf, D. J.; Heming, A. M.; Shooter, A. J., *Macromolecules,* **1998,** *31*, 5201-5205.

50. Kajiwara, A.; Matyjaszewski, K.; Kamachi, M., *Macromolecules,* **1998,** *31*, 5695-5701.

51. Save, M.; Weaver, J. V. M.; Armes, S. P.; McKenna, P., *Macromolecules,* **2002,** *35*, 1152-1159.

52. He, L.; Read, E. S.; Armes, S. P.; Adams, D. J., *Macromolecules,* **2007,** *40*, 4429-4438.

53. Krishnan, R.; Srinivasan, K. S. V., *Macromolecules,* **2003,** *36*, 1769-1771.

54. Ma, I. Y.; Lobb, E. J.; Billingham, N. C.; Armes, S. P.; Lewis, A. L.; Lloyd, A. W.; Salvage, J., *Macromolecules,* **2002,** *35*, 9306-9314.

55.　Inoue, Y.; Matyjaszewski, K., *Macromolecules,* **2004,** *37*, 4014-4021.

56.　Xia, J. H.; Johnson, T.; Gaynor, S. G.; Matyjaszewski, K.; DeSimone, J., *Macromolecules,* **1999,** *32*, 4802-4805.

57.　Li, Y. T.; Armes, S. P.; Jin, X. P.; Zhu, S. P., *Macromolecules,* **2003,** *36*, 8268-8275.

58.　Kajiwara, A.; Matyjaszewski, K., *Macromolecules,* **1998,** *31*, 5695-5701.

59.　Beers, K. L.; Boo, S.; Gaynor, S. G.; Matyjaszewski, K., *Macromolecules,* **1999,** *32*, 5772-5776.

60.　Robinson, K. L.; Khan, M. A.; de Paz Banez, M. V.; Wang, X. S.; Armes, S. P., *Macromolecules,* **2001,** *34*, 3155-3158.

61.　Haigh, R.; Rimmer, S.; Fullwood, N. J., *Biomaterials,* **2000,** *21*, 735-739.

62.　Thompson, K. L.; Bannister, I.; Armes, S. P.; Lewis, A. L., *Langmuir,* **2010,** *26*, 4693-4702.

63.　Aveyard, R.; Binks, B. P.; Clint, J. H., *Adv. Colloid Interface Sci.,* **2003,** *100-102*, 503-546.

64.　Binks, B. P., *Curr. Opin. Colloid Interface Sci.,* **2002,** *7*, 21-41.

65.　Binks, B. P.; Lumsdon, S. O., *Langmuir,* **2000,** *16*, 8622-8631.

66.　Levine, S.; Bowen, B. D.; Partridge, S. J., *Colloids Surf.,* **1989,** *38*, 325-343.

67.　Binks, B. P.; Lumsdon, S. O., *Phys. Chem. Chem. Phys.,* **1999,** *1*, 3007-3016.

68.　Binks, B. P.; Lumsdon, S. O., *Langmuir,* **2001,** *17*, 4540-4547.

69.　Amalvy, J. I.; Armes, S. P.; Binks, B. P.; Rodrigues, J. A.; Unali, G. F., *Chem. Commun.,* **2003,** *15*, 1826-1827.

70.　Read, E. S.; Fujii, S.; Amalvy, J. I.; Randall, D. P.; Armes, S. P., *Langmuir,* **2004,** *20*, 7422-7429.

71.　Binks, B. P.; Murakami, R.; Armes, S. P.; Fujii, S., *Angew. Chem., Int. Ed.,* **2005,** *44*, 4795-4798.

72.　Fujii, S.; Armes, S. P.; Binks, B. P.; Murakami, R., *Langmuir,* **2006,** *22*, 6818-6825.

73.　Fujii, S.; Read, E. S.; Binks, B. P.; Armes, S. P., *Adv. Mater.,* **2005,** *17*, 1014-1018.

74.　Dupin, D.; Armes, S. P.; Connan, C.; Reeve, P.; Baxter, S. M., *Langmuir,* **2007,** *23*, 6903-6910.

75.　Velev, O. D.; Furusawa, K.; Nagayama, K., *Langmuir,* **1996,** *12*, 2374-2384.

76.　Velev, O. D.; Furusawa, K.; Nagayama, K., *Langmuir,* **1996,** *12*, 2385-2391.

77.   Velev, O. D.; Nagayama, K., *Langmuir,* **1997,** *13*, 1856-1859.

78.   Dinsmore, A. D.; Hsu, M. F.; Nikolaides, M. G.; Marquez, M.; Bausch, A. R.; Weitz, D. A., *Science,* **2002,** *298*, 1006-1009.

79.   Hsu, M. F.; Nikolaides, M. G.; Dinsmore, A. D.; Bausch, A. R.; Gordon, V. D.; Chen, X.; Hutchinson, J. W.; Weitz, D. A., *Langmuir,* **2005,** *21*, 2963-2970.

80.   Laib, S.; Routh, A. F., *J. Colloid Interface Sci.,* **2008,** *317*, 121-129.

81.   Yow, H. N.; Routh, A. F., *Langmuir,* **2009,** *25*, 159-166.

82.   Nomura, T.; Routh, A. F., *Langmuir,* **2010,** *26*, 18676-18680.

83.   Salari, J. W. O.; van Heck, J.; Klumperman, B., *Langmuir,* **2010,** *26*, 14929-14936.

84.   Gordon, V. D.; Xi, C.; Hutchinson, J. W.; Bausch, A. R.; Marquez, M.; Weitz, D. A., *J. Am. Chem. Soc.,* **2004,** *126*, 14117-14122.

85.   Lawrence, D. B.; Cai, T.; Hu, Z.; Marquez, M.; Dinsmore, A. D., *Langmuir,* **2007,** *23*, 395-398.

86.   Caruso, F.; Caruso, R. A.; Möhwald, H., *Science,* **1998,** *282*, 1111-1114.

87.   Caruso, F.; Caruso, R. A.; Möhwald, H., *Chem. Mater.,* **1999,** *11*, 3309-3314.

88.   Caruso, F.; Spasova, M.; Susha, A.; Giersig, M.; Caruso, R. A., *Chem. Mater.,* **2000,** *13*, 109-116.

89.   Caruso, F.; Shi, X. Y.; Caruso, R. A.; Susha, A., *Adv. Mater.,* **2001,** *13*, 740-744.

90.   Caruso, R. A.; Susha, A.; Caruso, F., *Chem. Mater.,* **2001,** *13*, 400-409.

91.   Cayre, O. J.; Noble, P. F.; Paunov, V. N., *J. Mater. Chem.,* **2004,** *14*, 3351-3355.

92.   Noble, P. F.; Cayre, O. J.; Alargova, R. G.; Velev, O. D.; Paunov, V. N., *J. Am. Chem. Soc.,* **2004,** *126*, 8092-8093.

93.   Duan, H. W.; Wang, D. Y.; Sobal, N. S.; Giersig, M.; Kurth, D. G.; Mohwald, H., *Nano Lett.,* **2005,** *5*, 949-952.

94.   Mak, W. C.; Bai, J.; Chang, X. Y.; Trau, D., *Langmuir,* **2009,** *25*, 769-775.

95.   Wang, C. Y.; Liu, H. X.; Gao, Q. X.; Liu, X. X.; Tong, Z., *ChemPhysChem,* **2007,** *8*, 1157-1160.

96.   Liu, H. X.; Wang, C. Y.; Gao, Q. X.; Liu, X. X.; Tong, Z., *Int. J. Pharm.,* **2008,** *351*, 104-112.

97.   Hong, L.; Jiang, S.; Granick, S., *Langmuir,* **2006,** *22*, 9495-9499.

98. Jiang, S.; Granick, S., *Langmuir,* **2008,** *24*, 2438-2445.

99. Chen, Y. H.; Wang, C. Y.; Chen, J. X.; Liu, X. X.; Tong, Z., *Journal of Polymer Science Part a-Polymer Chemistry,* **2009,** *47*, 1354-1367.

100. Bon, S. A. F.; Cauvin, S.; Colver, P. J., *Soft Matter,* **2007,** *3*, 194-199.

101. Chen, T.; Colver, P. J.; Bon, S. A. F., *Adv. Mater.,* **2007,** *19*, 2286-2289.

102. Chen, W.; Liu, X.; Liu, Y.; Kim, H.-I., *Colloid Polym. Sci.,* **2010,** *288*, 1393-1399.

103. Cejková, J.; Hanus, J.; Stepánek, F., *J. Colloid Interface Sci.,* **2010,** *346*, 352-360.

104. Cayre, O. J.; Biggs, S., *J. Mater. Chem.,* **2009,** *19*, 2724-2728.

105. Cayre, O. J.; Biggs, S., *Advanced Powder Technology,* **2010,** *21*, 19-22.

106. Croll, L. M.; Stöver, H. D. H., *Langmuir,* **2003,** *19*, 5918-5922.

107. Croll, L. M.; Stover, H. D. H., *Langmuir,* **2003,** *19*, 10077-10080.

108. Yuan, Q.; Cayre, O. J.; Fujii, S.; Armes, S. P.; Williams, R. A.; Biggs, S., *Langmuir,* **2010,** *26*, 18408-18414.

109. Lin, Y.; Skaff, H.; Böker, A.; Dinsmore, A. D.; Emrick, T.; Russell, T. P., *J. Am. Chem. Soc.,* **2003,** *125*, 12690-12691.

110. Skaff, H.; Lin, Y.; Tangirala, R.; Breitenkamp, K.; Böker, A.; Russell, T. P.; Emrick, T., *Adv. Mater.,* **2005,** *17*, 2082-2086.

111. Walsh, A.; Thompson, K. L.; Armes, S. P.; York, D. W., *Langmuir,* **2010,** *26*, 18039-18048.

112. Arumugam, P.; Patra, D.; Samanta, B.; Agasti, S. S.; Subramani, C.; Rotello, V. M., *J. Am. Chem. Soc.,* **2008,** *130*, 10046-10047.

113. Shah, R. K.; Kim, J. W.; Weitz, D. A., *Langmuir,* **2010,** *26*, 1561-1565.

114. Sugihara, S.; Armes, S. P.; Lewis, A. L., *Angewandte Chemie International Edition,* **2010,** *49*, 3500-3503.

115. Fortuna, S.; Colard, C. A. L.; Troisi, A.; Bon, S. A. F., *Langmuir,* **2009,** *25*, 12399-12403.

116. Einert, T.; Lipowsky, P.; Schilling, J.; Bowick, M. J.; Bausch, A. R., *Langmuir,* **2005,** *21*, 12076-12079.

117. Bausch, A. R.; Bowick, M. J.; Cacciuto, A.; Dinsmore, A. D.; Hsu, M. F.; Nelson, D. R.; Nikolaides, M. G.; Travesset, A.; Weitz, D. A., *Science,* **2003,** *299*, 1716-1718.

118. Lipowsky, P.; Bowick, M. J.; Meinke, J. H.; Nelson, D. R.; Bausch, A. R., *Nat. Mater.,* **2005,** *4*, 407-411.

119. Lee, D.; Weitz, D. A., *Adv. Mater.,* **2008,** *20*, 3498-3503.

120. Rosenberg, R. T.; Dan, N. R., *J. Colloid Interface Sci.,* **2010,** *349*, 498-504.

121. Rosenberg, R. T.; Dan, N. R., *J. Colloid Interface Sci.,* **2011,** *354*, 478-482.

122. Kim, J. W.; Fernandez-Nieves, A.; Dan, N.; Utada, A. S.; Marquez, M.; Weitz, D. A., *Nano Lett.,* **2007,** *7*, 2876-2880.

123. San Miguel, A.; Behrens, S. H., *Soft Matter,* **2011,** *7*, 1948-1956.

124. San, M. A.; Scrimgeour, J.; Curtis, J. E.; Behrens, S. H., *Soft Matter,* **2010,** *6*, 3163-3166.

125. P&G; Coated perfume particles. US Patent number US 5066419, 1991.

126. Bône, S.; Vautrin, C.; Barbesant, V.; Truchon, S.; Harrison, I.; Geffroy, C., *CHIMIA International Journal for Chemistry,* **2011,** *65*, 177-181.

127. De Groot, A. C.; Flyvholm, M.-A.; Lensen, G.; Menné, T.; Coenraads, P.-J., *Contact Dermatitis,* **2009,** *61*, 63-85.

Chapter Two

Synthesis of Sterically-Stabilised Latexes Using Well-defined Poly(glycerol monomethacrylate) Macromonomers

INTRODUCTION

Polymer latexes have a wide range of commercial applications, ranging from coating and adhesives to binders and foams.[1] Conventional surfactants such as sodium dodecyl sulfate are commonly used as stabilisers to prepare such latexes.[2] However, such physically-adsorbed small molecules are relatively mobile and tend to migrate towards interfaces within latex films.[3,4] This phenomenon can be detrimental to the physical properties of such films.[5] The problem of surfactant migration can be solved by the use of polymerisable surfactants or macromonomers, which become chemically grafted onto latex particles during polymerisation.[6] The benefits of reactive stabilisers in heterophase polymerisation have been known for some time.[7,8] Such sterically-stabilised latexes are particularly resistant towards destabilisation induced by high shear or electrolyte addition and typically exhibit good freeze-thaw stability.[9,10]

Routes to Macromonomers

There are two general routes to vinyl-capped macromonomers. The first route involves using a suitable vinyl-functionalised initiator and the second route is based on the post-polymerisation modification of the polymer chain-ends. The former route was exploited by Lascelles *et al.*[11], who conducted the oxyanionic polymerisation of tertiary amine methacrylates in THF using a potassium 4-vinylbenzyl alkoxide initiator (see Figure 2.1).
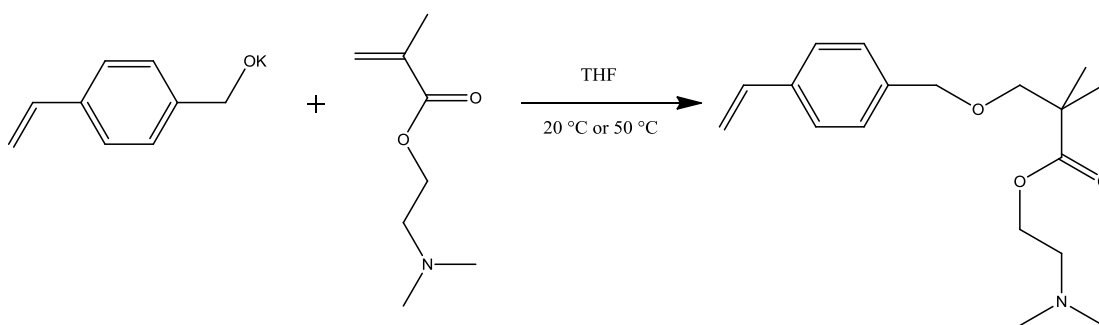
Figure 2.1. Reaction scheme for the synthesis of 2-(dimethylamino)ethyl methacrylate-based macromonomers via oxyanion-mediated polymerisation with a styrene-functionalised initiator, as reported by Lascelles et al.[11]

Similarly, Atom Transfer Radical Polymerisation (ATRP) has been used to prepare both hydrophilic and hydrophobic macromonomers using allyl-, vinyl acetate, and vinyl ether-based initiators.[12,13,14] Although the use of vinyl-functionalised initiators offers an attractive one-pot route to macromonomers, the choice of vinyl group is often rather limited since it must not participate in the polymerisation. A potentially more versatile route is post-polymerisation modification of the polymer chain ends, allowing for a larger range of different macromonomers. For example, ATRP has been used to prepare macromonomers by post-polymerisation reaction of the terminal bromine group with either acrylic or methacrylic groups.[15] An alternative strategy is to modify the initiator group in a second step after the *in situ* polymerisation, so as to afford a polymerisable end-group.[16-21] This approach clearly requires facile chemistry, but can lead to higher efficiencies than those achieved by substitution of terminal halogen atoms, since the fidelity of the halogen functionality is often compromised under monomer-starved conditions. Recently, Topham *et al.*[22] reported the preparation of macromonomers by a combination of ATRP and click chemistry. An azido α-functionalised ATRP initiator was used to produce well-defined homopolymers with terminal azide functionality. These homopolymer precursors were then efficiently clicked using either propargyl methacrylate or propargyl acrylate to yield near-monodisperse (meth)acrylate-capped macromonomers. Other research groups have reported similar syntheses.[23,24]

Very recently within the Armes group, the preparation of polystyrene latexes using near-monodisperse macromonomers (M_w/M_n ~ 1.2 to 1.3) based on a biomimetic monomer, 2-(methacryloyloxy)ethyl phosphorylcholine (MPC) was reported.[25] The synthesis of these well-defined MPC-based macromonomers involved two steps: (i) ATRP of MPC using a tertiary amine-functionalised initiator and (ii) quaternisation of the tertiary amine chain-ends using excess 4-vinylbenzyl chloride in methanol at room temperature. However, this strategy only proved to be effective for relatively low molecular weight (target degree of polymerisation < 35) macromonomers: if higher molecular weight macromonomers (target degree of polymerisation > 40) were targeted, substantial loss of control during the ATRP of MPC was observed and only rather polydisperse precursors were obtained (M_w/M_n ~ 1.6 to 2.0).

Controlled-structure PGMA-based Polymers and Nano-structures

PGMA chains are known to be good anchoring blocks for the synthesis of sterically-stabilised magnetite nanoparticles.[26] GMA has also been used for the synthesis of various types of shell cross-linked (SCL) micelles.[27] In the latter context, PGMA blocks can be readily cross-linked with divinyl sulfone in aqueous alkaline solution or converted into polyacid blocks via esterification using succinic anhydride.[28] PGMA can also act as the coronal steric stabiliser of SCL micelles.[29] In addition, Rimmer and co-workers have utilised the highly hydrophilic character of GMA for the preparation of biocompatible amphiphilic hydrogel networks[30]. PGMA has also been used as a RAFT macro-CTA for the aqueous dispersion polymerisation of HPMA. This formulation has produced various block copolymer nanoparticles with spherical, worm-like and vesicular morphologies.[31,32]

The Present Work

In this Chapter, well-defined styrene-functionalised macromonomers have been prepared based on the hydrophilic methacrylic monomer, glycerol monomethacrylate (GMA). This monomer has previously been polymerised to high conversions with reasonable control ($M_w/M_n < 1.30$) using an ATRP formulation in methanol at 20 $^{\circ}$C.[32] Unlike the unexpected synthetic limitations observed for the MPC-based macromonomers reported earlier,[25] excellent control over the ATRP of GMA for target degrees of polymerisation ranging from 20 to 70 is demonstrated in the present work. The resulting series of six near-monodisperse PGMA macromonomers was evaluated for the synthesis of sterically-stabilised polystyrene latexes using either aqueous emulsion or alcoholic dispersion polymerisation and also for the synthesis of sterically-stabilised poly(2-hydroxypropyl methacrylate) latexes using aqueous dispersion polymerisation.

The work presented herein has already formed the basis of a publication in *Macromolecules*.[34] This Chapter consists of the synthesis of PGMA macromonomers and latex particles reported in this publication along with some additional unpublished results. The hydroxy-functional nature of these sterically-stabilised latexes will be utilised in later Chapters for the covalent cross-linking of latex-based Pickering emulsions to form colloidosome microcapsules.

EXPERIMENTAL DETAILS

Materials

Glycerol monomethacrylate (GMA) and 2-hydroxypropyl methacrylate were kindly donated by Cognis Performance Chemicals (Hythe, UK) and used without further purification. 4-Vinylbenzyl chloride (90 %), Cu(I)Cl (99.995 %) and 2,2′-bipyridine (bpy, 99%) were purchased from Aldrich and were used as received. Styrene (Aldrich) was passed through a column of basic alumina to remove inhibitor and then stored at -20 °C prior to use. 2,2'-Azobisisobutyronitrile (AIBN; BDH) and 2,2'-azobis(isobutyramidine) dihydrochloride (AIBA; 97%; Aldrich, UK) were used as received. Methanol was purchased from Fisher and was used as received. De-ionised water was used in all experiments. Silica gel 60 (0.0632-0.2 mm) was obtained from Merck (Darmstadt, Germany). NMR solvents (D_2O, CD_3OD, $CDCl_3$ and d_5-pyridine) were purchased from Aldrich.

Synthesis of 2-(Dimethylamino)ethyl-2-bromoisobutyrylamide ATRP Initiator

N,N-Dimethylethylenediamine (6.00 g, 0.068 mol), triethylamine (27.27 g, 0.27 mol) and dichloromethane (120 ml) were placed in a 500 ml three-necked round-bottomed flask and purged with nitrogen for 30 minutes. A white precipitate of triethylammonium bromide was formed on addition of 2-bromoisobutyryl bromide (15.49 g, 0.067 mol) to this reaction mixture, which was stirred for a further 5 h at 20^oC. The precipitate was removed by filtration, the reaction solution was washed three times with $NaHCO_3$ solution and dried over $MgSO_4$. The dichloromethane was removed under reduced pressure to afford a pale brown liquid (11.5 g; 72% yield). ^{1}H NMR (400 MHz, CD_3OD): δ 1.88 (6H, s, 2 x CH_3), 2.26 (6H, s, N(CH_3)$_2$), 2.45 (2H, t, $J = 7.0$ Hz, (CH$_3$)$_2$NCH_2), 3.31 (2H, t, $J = 7.0$ Hz, CH_2NHCOO(CH$_3$)$_2$Br).

Homopolymerisation of GMA via ATRP

2-(Dimethylamino)ethyl-2-bromoisobutyrylamide (0.300 g, 1.25 mmol), bpy (0.390 g, 2.5 mmol) and GMA (10.0 g, 62.4 mmol) were weighed into a 25 ml round-bottomed flask and degassed. Methanol (12 ml) was degassed and transferred into the reaction solution under nitrogen. The Cu(I)Cl catalyst (0.120 g, 1.25 mmol) was added to the stirred solution which turned dark brown, indicating the onset of

polymerisation. After 24 h, the reaction solution was diluted with methanol and passed through a silica column to remove the spent Cu(II) catalyst. The product was then dried on a vacuum line overnight to afford a white powder (8.0 g; 77 % yield).

Quaternisation of PGMA Homopolymer Precursor

The PGMA$_{50}$ homopolymer (7.00 g, 0.85 mmol) was dissolved in methanol (20 ml). 4-Vinylbenzyl chloride (0.430 g, 2.55 mmol; 4-VBC/polymer molar ratio = 3:1) was added and the reaction solution stirred at room temperature for 48 h. The excess solvent was removed under reduced pressure and the resulting solid was dissolved in water. The excess 4-vinylbenzyl chloride was extracted three times with cyclohexane. The aqueous solution was then freeze-dried from water overnight to afford a white powder (6.0 g; 84 % yield).

Aqueous Emulsion Polymerisation of Styrene

PGMA$_{50}$ macromonomer (0.50 g) was weighed into a 100 ml round-bottomed flask and dissolved in water (44.5 g). This solution was purged with nitrogen for 30 minutes before being heated to 70 ^{o}C under a nitrogen blanket. The AIBN initiator (0.050 g) was dissolved in styrene (5.0 g) and purged with nitrogen before being injected into the reaction vessel. The solution turned milky-white within 1 h and was stirred for 24 h at 70 ^{o}C. The latexes were purified by three centrifugation/redispersion cycles, replacing each successive supernatant with pure water.

Alcoholic Dispersion Polymerisation of Styrene

PGMA$_{50}$ macromonomer (0.50 g) was weighed into a 100 ml three-necked round-bottomed flask fitted with a condenser and nitrogen inlet and dissolved in 44.5 g of a 90:10 mixture of methanol/water. This solution was purged with nitrogen for 30 minutes before being heated to 70 ^{o}C under a nitrogen blanket. The AIBN initiator (0.050 g) was dissolved in styrene (5.00 g) and purged with nitrogen before being injected into the reaction vessel. The solution turned milky-white within 1 h and was stirred for 24 h at 70 ^{o}C. The latexes were purified by three centrifugation/redispersion cycles replacing each successive supernatant with the

methanol/water mixture followed by a further three redispersion cycles using pure water.

Aqueous Dispersion Polymerisation of 2-Hydroxypropyl Methacrylate

$PGMA_{50}$ macromonomer (0.50 g) was placed into a 100 ml round-bottomed flask, along with HPMA monomer (5.00 g) and water (44.5 g). The reaction vessel was degassed by five evacuation / nitrogen purge cycles and subsequently heated to $70^{o}C$. AIBA initiator (0.050 g) was dissolved in water (5.0 g) and purged with nitrogen before being inject to reaction vessel at $70 ^{o}C$. The reaction turned milky-white within 1 h and was stirred for 24 h before being allowed to cool to room temperature. The resulting PHPMA latexes were purified by three centrifugation/redispersion cycles, replacing each successive supernatant with de-ionised water.

Freeze-Thaw and Salt Stability Experiments

Selected PMPC-PS latexes (10.0 w/v % solids content) were frozen at $-20 ^{o}C$ and then allowed to thaw at room temperature. Flocculation was judged by visual inspection and confirmed by DLS measurements. Various PGMA-PS latexes (1.0 ml; 2.0 w/v % solids content) were transferred via pipette into sample vials to which 1.0 ml aliquots of various aqueous $MgSO_4$ solutions were added (0.02 M – 1.00 M). This dilution produced 1.0 % aqueous latex dispersions in 0.01 M – 0.50 M $MgSO_4$. Colloidal (in)stability was again judged by visual inspection and confirmed by DLS measurements.

Polymer Characterisation

^{1}H NMR Spectroscopy

All ^{1}H NMR spectra were recorded in either $CDCl_3$, D_2O, CD_3OD or d_5-pyridine using a 400 MHz Bruker Avance-400 spectrometer.

FT-IR Spectroscopy

Each sample (1.0 mg) was ground up with 150 mg of KBr to afford a fine powder
and compressed into a pellet by applying a pelletisation pressure of 8 tonnes for ten
minutes. The FTIR spectra were recorded using a Nicolet Magna (series II)
spectrometer at 4.0 cm^{-1} resolution and 64 scans were recorded per spectrum.

Gel Permeation Chromatography (GPC)

The molecular weight and polydispersity of the PGMA$_n$ homopolymer precursor
were determined by DMF GPC at 70°C. The GPC set-up comprised three Polymer
Laboratories PL gel 10 μm MIXED-B columns in series with a Viscotek TriSEC
model 302 refractive detector. The flow rate was 1.0 ml min^{-1} and the mobile phase
contained 10 mmol LiBr. Ten near-monodisperse poly(methyl methacrylate)
standards (M_p = 2,000 – 300,000 g mol^{-1}) were used for calibration. Data were
analysed using Viscotek TriSEC 3.0 software.

Dynamic Light Scattering (DLS)

The intensity-average hydrodynamic diameter of each latex was obtained by DLS
using a Malvern Zetasizer NanoZS instrument. Aqueous solutions of 0.01 w/v %
latex were analysed using disposable plastic cuvettes and results were averaged over
three consecutive runs. Deionised water used to dilute each latex was ultra-filtered
through a 0.20 μm membrane to remove dust.

Disc Centrifuge Photosedimentometry (DCP)

The weight-average diameters (D_w) of the polystyrene latexes were measured using a
CPS disc centrifuge photosedimentometer model number DC24000. Samples of
around 0.1% (0.10 ml) were injected in an aqueous spin fluid consisting of a sucrose
gradient (15 ml). The gradient for polystyrene samples was from 2% - 8% sucrose,
whereas the gradient used for the PHPMA sample was 4% to 12% sucrose. The
density of the polystyrene latex particles was taken to be 1.05 g cm^{-3}, while that of
the PHPMA latex was taken to be 1.17 g cm^{-3}. This is a reasonable assumption for
latex diameters of around 1 μm, where the thickness of the steric stabiliser layer is
negligible compared to the particle size. For smaller latexes (particularly for

diameters of less than 200 nm), the stabiliser layer thickness becomes significant, resulting in a significant reduction in the effective particle density. Since an accurate particle density is required when calculating the weight-average particle diameter, D_w, any uncertainty in density produces an associated error in D_w.[35]

Scanning Electron Microscopy (SEM)

SEM studies were performed using a FEI Sirion field emission scanning electron microscope at a beam current of 244 μA and an operating voltage of 5 kV. Samples were dried onto aluminum stubs and sputter-coated with a thin layer of gold prior to examination to prevent sample charging.

X-ray Photoelectron Spectroscopy (XPS)

XPS spectra were acquired using a Kratos Axis ULTRA 'DLD' x-ray photoelectron spectrometer equipped with a monochromatic Al-Kα x-ray source (hν = 1486.6 eV) and operating at a base pressure of 10^{-8} to 10^{-10} mbar. Latex particles were dried on indium foil prior to XPS measurements.

RESULTS AND DISCUSSION

The two-step synthesis route used in this study to obtain well-defined PGMA-based macromonomers is outlined in Figure 2.2.

A)

B)
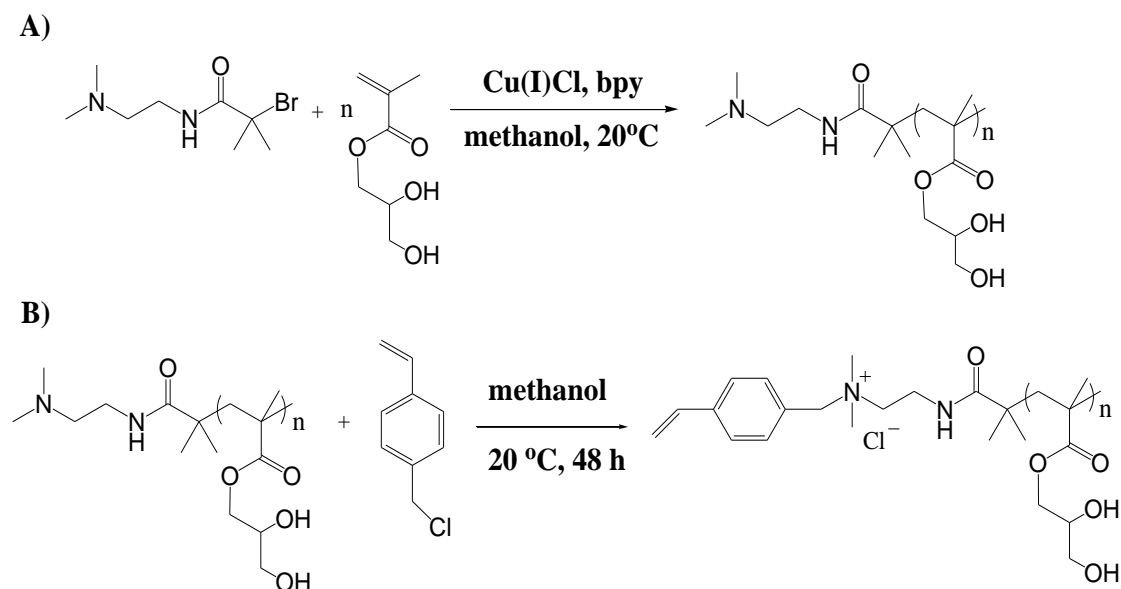
Figure 2.2. Two-step synthesis of PGMAn macromonomers: (a) ATRP of GMA monomer at 20 $^{\circ}$C in methanol for 16-24 h; (b) post-polymerisation quaternisation of tertiary amine end-groups with 4-vinylbenzyl chloride at 20 $^{\circ}$C.

Homopolymerisation of GMA via ATRP

Various $PGMA_n$ homopolymer precursors were prepared with target degrees of polymerisation, n, ranging from 20 to 70 (see Table 2.1). Good molecular weight control was achieved for the targeted homopolymers, with the actual degree of polymerisation calculated from ^{1}H NMR lying close to that targeted.

Table 2.1. Conversion and molecular weight data for PGMA homopolymer precursors synthesised at 20 ^{o}C in methanol and the degrees of quaternisation for the corresponding PGMA$_n$ macromonomers achieved using 4-VBC in methanol in 20 ^{o}C (4-VBC/amine molar ratio = 3.0 in each case). GPC data were obtained using poly(methyl methacrylate) standards.

Target DP	Conversion (%)	DP (NMR)	Mn (GPC)	Mw/Mn (GPC)	Degree of Quaternisation (%)
20	100	22	20 000	1.19	99
30	100	32	32 000	1.27	100
40	100	38	41 700	1.25	99
50	99	53	49 000	1.21	100
60	100	62	57 700	1.24	100
70	100	72	64 700	1.33	100

The polymerisation kinetics was first order with respect to monomer and the linear evolution of molecular weight with conversion indicates that these homopolymerisations possess good living character, as expected (see Figure 2.3). This is in marked contrast to the results recently reported for the synthesis of PMPC macromonomers, where good control over the ATRP of MPC using the 2-(dimethylamino)ethyl-2-bromoisobutyrylamide initiator was only demonstrated for relatively low degrees of polymerisation.[25]

The molecular weight distribution of each PGMA$_n$ homopolymer was unimodal, see Figure 2.4. Polydispersities of < 1.30 are consistent with those achieved in earlier work where GMA was prepared in methanol by ATRP.[32] It is particularly noteworthy that low polydispersities were obtained for higher target degrees of polymerisation (40 to 70), since this was found empirically to be a significant limitation of the synthesis of the analogous MPC-based macromonomers using the same two-step route.[25]
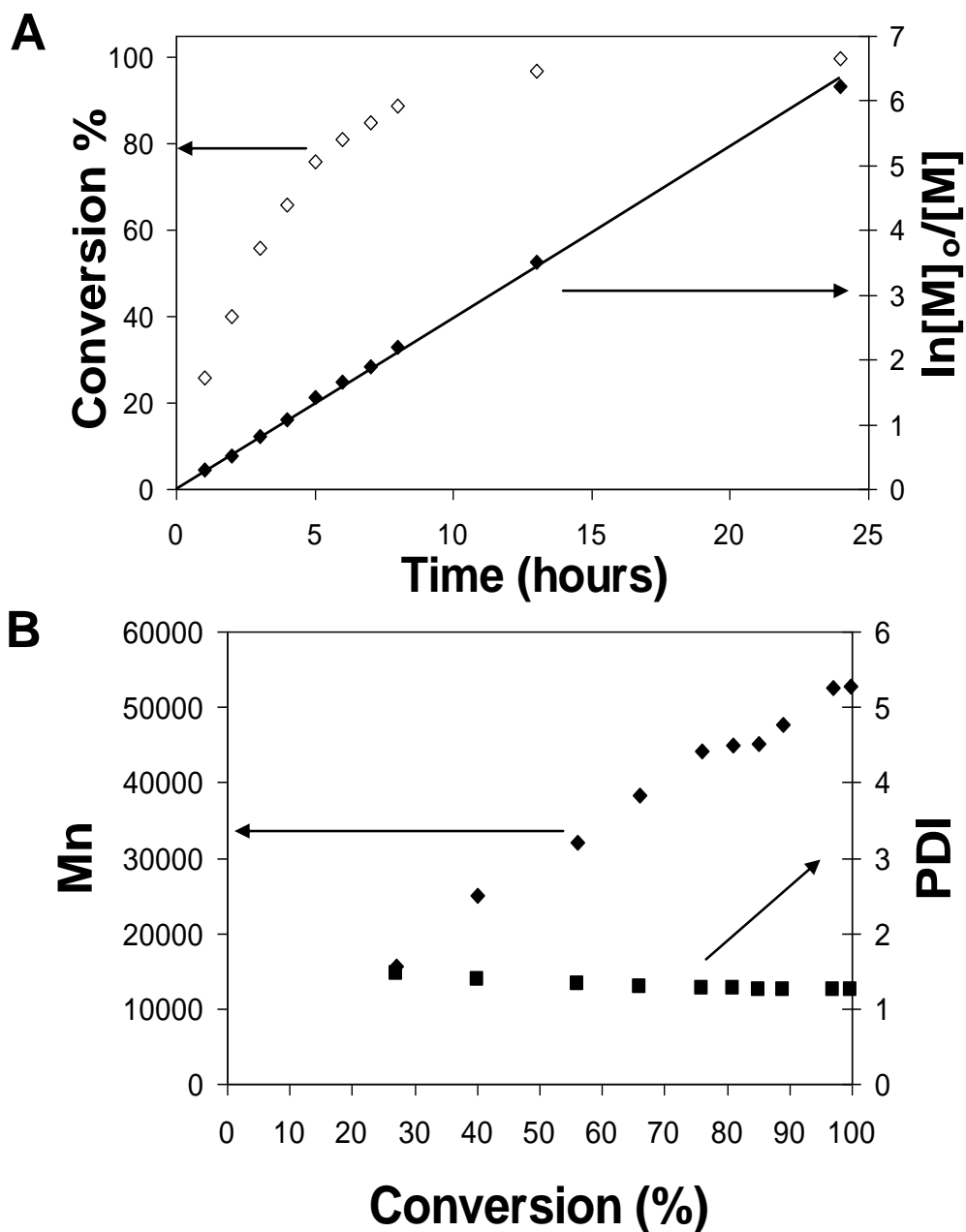
Figure 2.3. (a) Conversion vs. time and semi-logarithmic plot and (b) evolution of
M_n and polydispersity vs. conversion for the homopolymerisation of GMA at 20 ^{o}C
in methanol for 24 h. Reaction conditions: [GMA]: [Initiator]: [CuCl]: [bpy] = 50: 1:
1: 2.
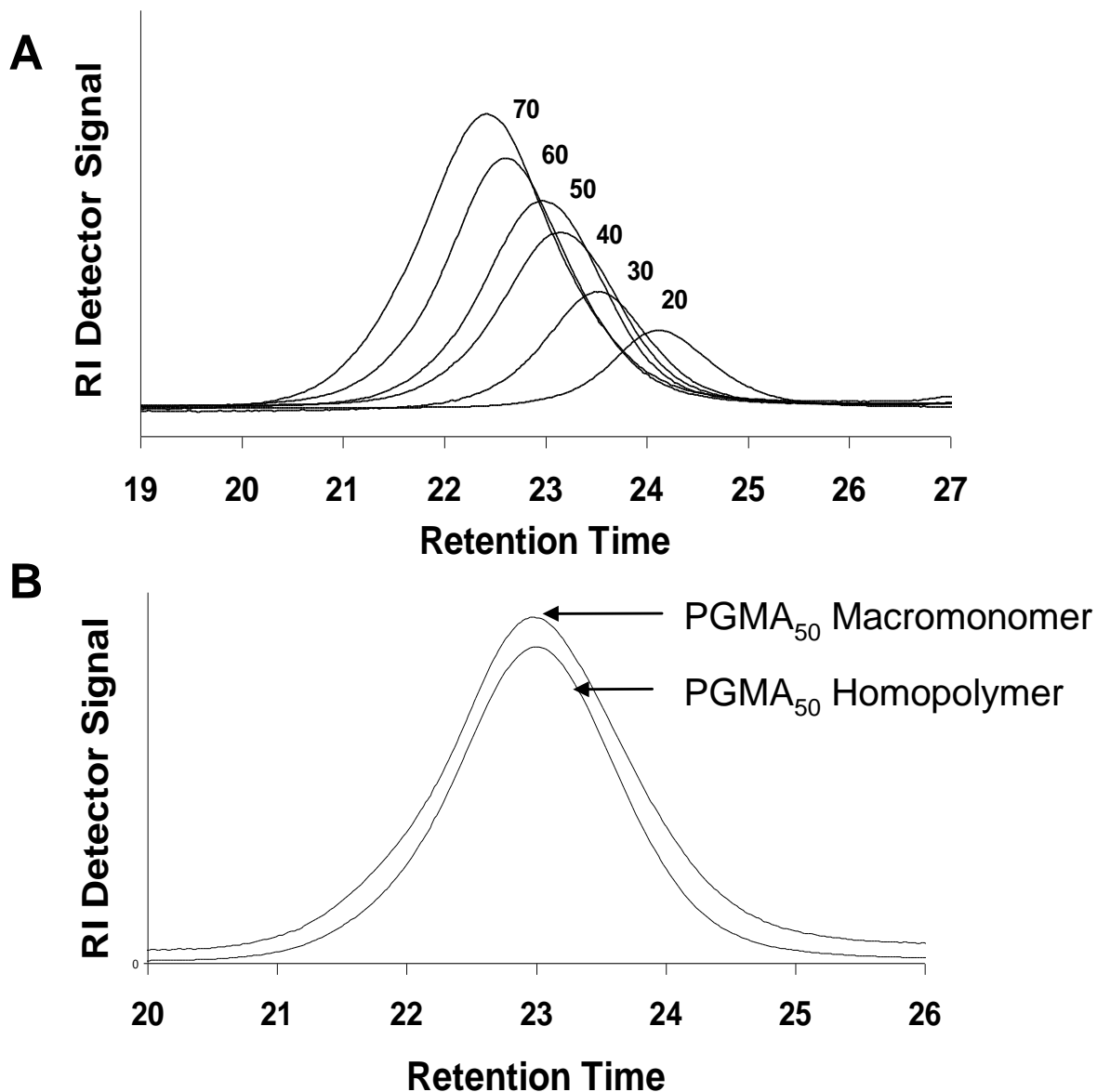
Figure 2.4. (a) Representative GPC curves for $PGMA_n$ homopolymer precursors prepared by ATRP at 20 ^{o}C (vs. PMMA standards). (b) Comparison of the GPC traces obtained for $PGMA_{50}$ homopolymer and $PGMA_{50}$ macromonomer. Quaternisation using 4-vinylbenzyl chloride under mild conditions clearly has no deleterious effect on the molecular weight distribution.

Quaternisation of PGMA Homopolymer Precursors

Well-defined macromonomers based on all six of the PGMA$_n$ homopolymers were synthesised as shown in Figure 2.2. Assigned ^{1}H NMR spectra for the 2-(dimethylamino)ethyl-2-bromoisobutyrylamide initiator, the PGMA$_{20}$ homopolymer precursor and the corresponding PGMA$_{30}$ macromonomer are shown in Figure 2.5.
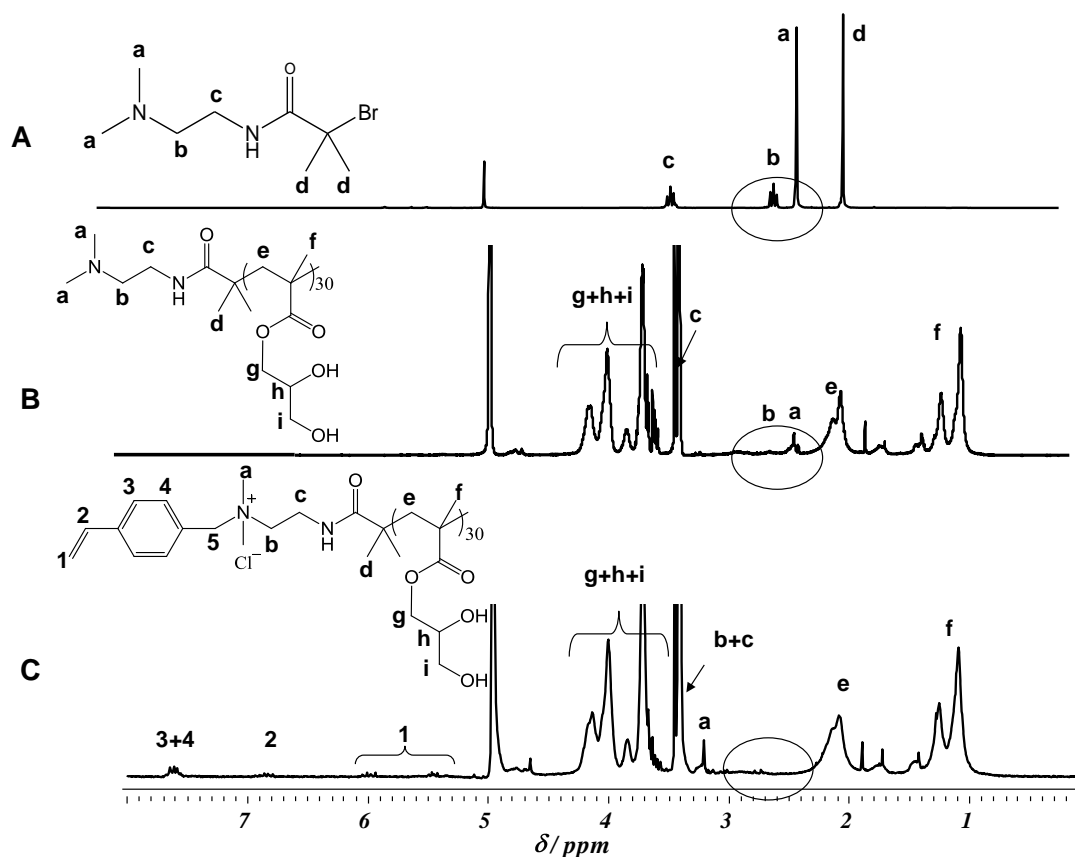
Figure 2.5. ^{1}H NMR spectra recorded in CD$_3$OD for: (a) 2-(dimethylamino)ethyl-2-bromoisobutyrylamide initiator; (b) PGMA$_{30}$ homopolymer precursor prior to quaternisation; (c) fully quaternised PGMA$_{30}$ macromonomer.

Quaternisation of the precursor with 4-VBC leads to distinct shifts in the NMR signals due to the six dimethylamino and two adjacent azamethylene protons in the initiator from δ 2.5 and δ 2.7 to δ 3.2 and δ 3.4, see Figure 2.5. When 100 % quaternisation is achieved, the original initiator end-group signals are no longer visible at δ 2.5 - 2.7. After purification to remove excess 4-VBC, new aromatic, benzylic and vinyl signals due to the 4-vinylbenzyl group can be observed at δ 5.2 - 7.7, thus confirming successful quaternisation. Comparison of the integrals of these new aromatic signals compared to those due to the PGMA backbone at δ 0.6-1.6,

allows the mean degree of quaternisation to be calculated. For all target DPs, more than 99 % end-group functionalisation was achieved as judged by ^{1}H NMR spectroscopy. Clearly, the accuracy of these NMR measurements is progressively reduced for higher PGMA DPs due to the weaker intensity of the end-group signals. Nevertheless, these signals were always visible for all target DPs. However, if even higher molecular weight macromonomers were required (e.g. DPs > 100), then end-group analysis via UV spectroscopy may be a more accurate method of determining end-group functionality, as this is a much more sensitive technique compared to ^{1}H NMR spectroscopy.

Preparation of PGMA$_n$-Latex Particles

These PGMA-based macromonomers were evaluated as potential reactive steric stabilisers for latex syntheses, as illustrated in Figure 2.6. Three routes were employed to prepare PGMA-stabilised polystyrene (PS) and poly(2-hydroxypropyl methacrylate) (PHPMA) particles. PGMA-PS latexes were prepared by both aqueous emulsion and alcoholic dispersion polymerisation, producing mean diameters of approximately 100-200 nm and 1100 nm, respectively. PGMA-PHPMA latexes of 700-1000 nm were also successfully prepared by aqueous dispersion polymerisation.
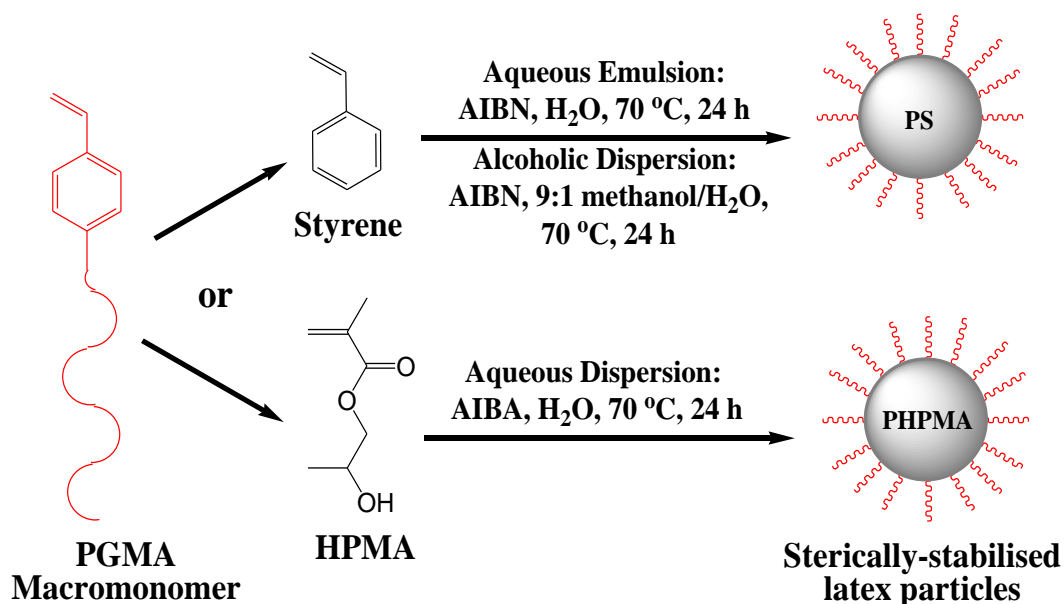
Figure 2.6. Reaction scheme for the synthesis of PGMA-stabilised polystyrene latex via both aqueous emulsion and alcoholic dispersion polymerisation and poly(2-hydroxypropyl methacrylate) latex via aqueous dispersion polymerisation.

Aqueous Emulsion Polymerisation of Styrene

Table 2.2 shows the particle size data for the aqueous emulsion polymerisation of styrene at 70 $^{\circ}$C using the AIBN initiator in the presence of the PGMA$_{50}$ macromonomer. Oil soluble initiators in aqueous emulsion polymerisation are rare; however we found empirically it to be the best choice. Attempted reactions with water soluble initiators such as ammonium persulfate or 2,2'-azobis(isobutyramidine) dihydrochloride (AIBA) led to highly flocculated particles. Figure 2.7 shows a scanning electron micrograph of PGMA$_{50}$-PS latex particles prepared with the cationic AIBA initiator. Dynamic light scattering gives an intensity-average diameter of 381 nm with a polydispersity index of 0.20. However, the SEM image indicates a primary particle diameter of 100-200 nm, which is similar to those latexes successfully prepared with the AIBN initiator, albeit somewhat more polydisperse. Such a large discrepancy between the SEM and DLS sizes indicates significant particle flocculation. Indeed, this flocculation is observed by the more sensitive technique of disc centrifuge photosedimentometry (DCP). DCP detects a primary particle size of approximately 250 nm along with larger flocs, which lead to a weight-average diameter to 374 ± 131 nm. FT-IR and ^{1}H NMR studies indicate that the PGMA$_{50}$ macromonomer has been incorporated into the latex. However, the degree of flocculation suggests that it does not act as an efficient stabiliser in this case. One possible explanation is that the majority of the PGMA stabiliser chains have actually been incorporated *inside* the particles, rather than being expressed at the surface. However, it remains unclear why this should be the case for such water-soluble initiators. As yet, the reason for this unusual behaviour is not fully understood, but the poor results obtained with these aqueous initiators in emulsion polymerisation appear to be reproducible. This colloid stability problem was not observed for latexes prepared using PMPC$_{30}$ macromonomers synthesised by the same two-step protocol.[25] Due to these preliminary findings it was decided that all further emulsion polymerisation syntheses should be conducted using the neutral AIBN initiator, since no particle flocculation was observed in this case. Although uncommon, there are reports of successful particle synthesis in the presence of hydrophobic initiators.[36, 37] One suggestion is that the polymerisation proceeds by a conventional emulsion polymerisation mechanism, with initiating radicals originating from the aqueous phase due to a water-soluble initiator fraction.[37, 38]

Table 2.2. Latex yield, particle size data and stabiliser contents for PGMA$_n$-PS latexes prepared by aqueous emulsion polymerisation using 10.0 w/v % stabiliser based on styrene at 70 ^{o}C in water with AIBN for 24 h. Size distributions were determined by disc centrifuge photosedimentometry (DCP) and dynamic light scattering (DLS), while latex yields were determined by gravimetry and stabiliser contents were determined by analysing latexes dissolved in d$_5$-pyridine using ^{1}H NMR spectroscopy.

Entry No	Stabiliser Type	Initial stabiliser concentration w/v %	Latex yield %	SEM diameter nm	DCP diameter nm	DLS diameter nm (PDI)	Stabiliser content w/w %	Γ mg m^{-2}
1	none	0	0	-	-	-	-	-
2	PGMA$_{50}$ homopolymer	10	12	546	580 ± 100	641 (0.17)	1.25	1.3
3	PGMA$_{50}$ macromonomer	10	69	90	163 ± 40	120 (0.03)	9.4	1.8
4	PGMA$_{50}$ macromonomer	20	95	88	133 ± 39	130 (0.09)	19.8	3.8
5	PGMA$_{20}$ macromonomer	10	40	180	185 ± 30	185 (0.00)	5.8	1.9
6	PGMA$_{30}$ macromonomer	10	85	94	144 ± 37	123 (0.05)	5.7	1.3
7	PGMA$_{40}$ macromonomer	10	66	89	118 ± 20	116 (0.04)	8.3	1.8
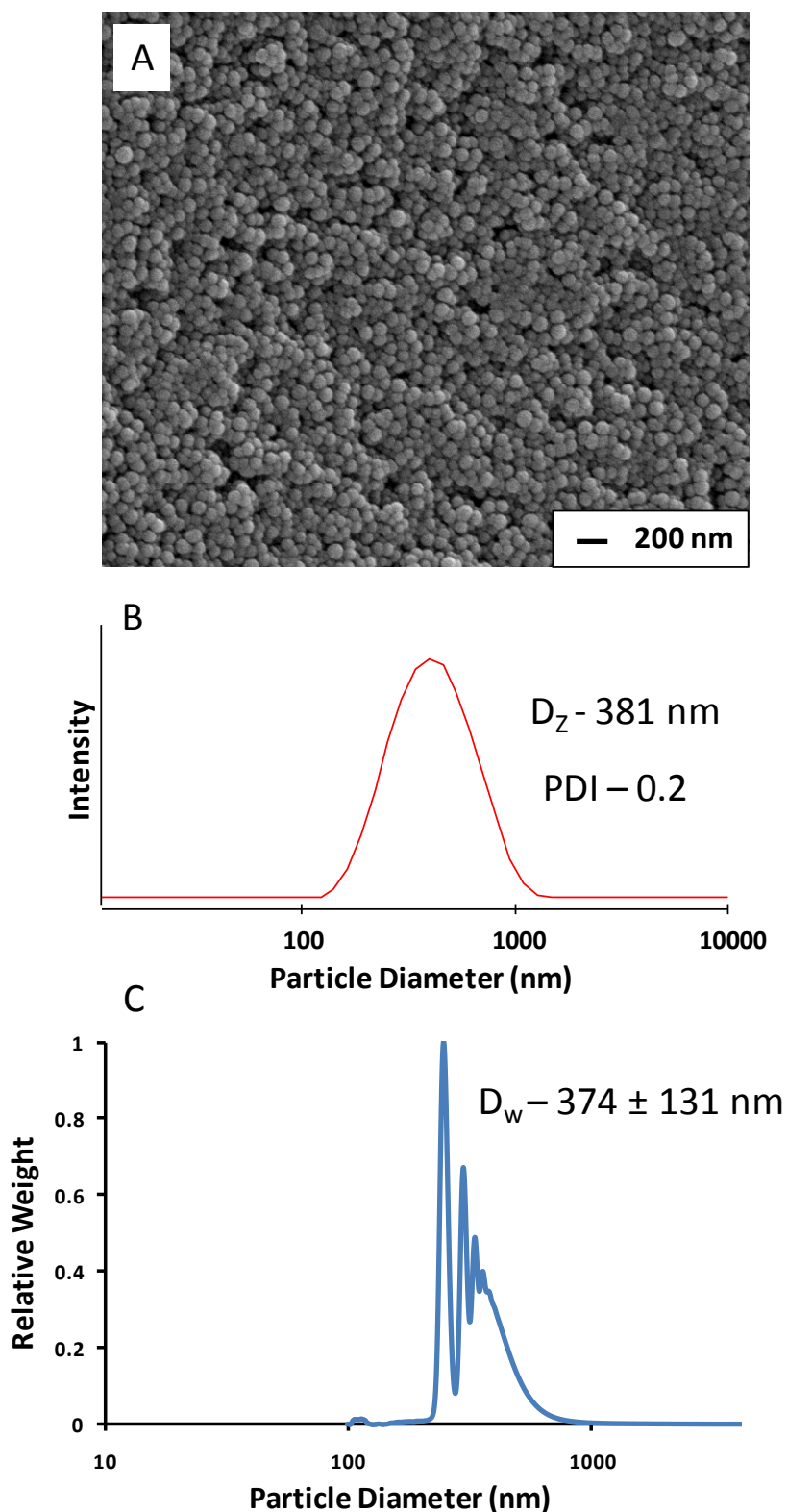
Figure 2.7. (A) Scanning electron microscopy image and corresponding particle size distributions determined by (B) dynamic light scattering and (C) disc centrifuge photosedimentometry for a PGMA$_{50}$-PS latex prepared by aqueous emulsion polymerisation using the cationic AIBA initiator at 60 °C.

PGMA$_{50}$-PS latexes of around 100 nm in diameter are produced with polydispersities ranging from 0.03 to 0.09 using AIBN, as judged by dynamic light scattering (DLS) and disc centrifuge photosedimentometry (DCP). The lower molecular weight macromonomers (DPs 20, 30 and 40) also gave stable latex dispersions. The PGMA$_{20}$ and PGMA$_{30}$ macromonomer gave slightly larger latex diameters than those prepared with the PGMA$_{40}$ and PGMA$_{50}$ macromonomers. This is attributed to the shorter stabiliser chains offering less efficient steric stabilisation. For the smaller latexes, there is some discrepancy observed between the intensity-average diameters (D$_z$) produced by DLS and the weight-average diameters from DCP (D$_w$), since the former values should always be higher than the latter for any latex size distribution with a finite width. However, for latex diameters of less than 200 nm, the thickness of the hydrated PGMA stabiliser layer becomes significant relative to the mean particle diameter, resulting in a substantial reduction in the effective particle density. Since an accurate particle density is required for DCP analysis, any uncertainty in the particle density produces an associated error in D$_w$, as previously discussed by Cairns et al.[35] In summary, the DLS data shown in Table 2.2 are all correct, but the DCP data are subject to significant systematic errors, particularly for the smaller latexes. This error becomes negligible for all the larger latexes shown in Table 2.3 and Table 2.4.

As expected, a control experiment conducted in the absence of any stabiliser led to gross precipitation with no latex formation; charge-stabilised PS latex particles cannot be formed under such conditions due to the non-ionic nature of the AIBN initiator. A second control experiment conducted in the presence of the PGMA$_{50}$ homopolymer precursor produced mainly coagulum with a small fraction of a significantly larger, more polydisperse latex compared to that formed in the presence of macromonomer (compare entry 2 with entries 3-7 in Table 2.2). This obvious difference in size is highlighted by SEM when comparing Figure 6a and 6b. These control experiments demonstrate that the use of the macromonomers (rather than the homopolymer precursors) is essential for producing small, uniform latexes, since such stabilisers confer efficient steric stabilisation.

Unfortunately, the latex yields obtained for these PGMA$_{50}$-PS latexes are disappointingly low, ranging from 40 – 85 %. Since relatively little coagulum is observed for this formulation, this low yield is attributed to poor monomer conversion rather than precipitated polystyrene. This low conversion could be related to the relatively low aqueous solubility of the AIBN initiator used in these latex syntheses.[39]
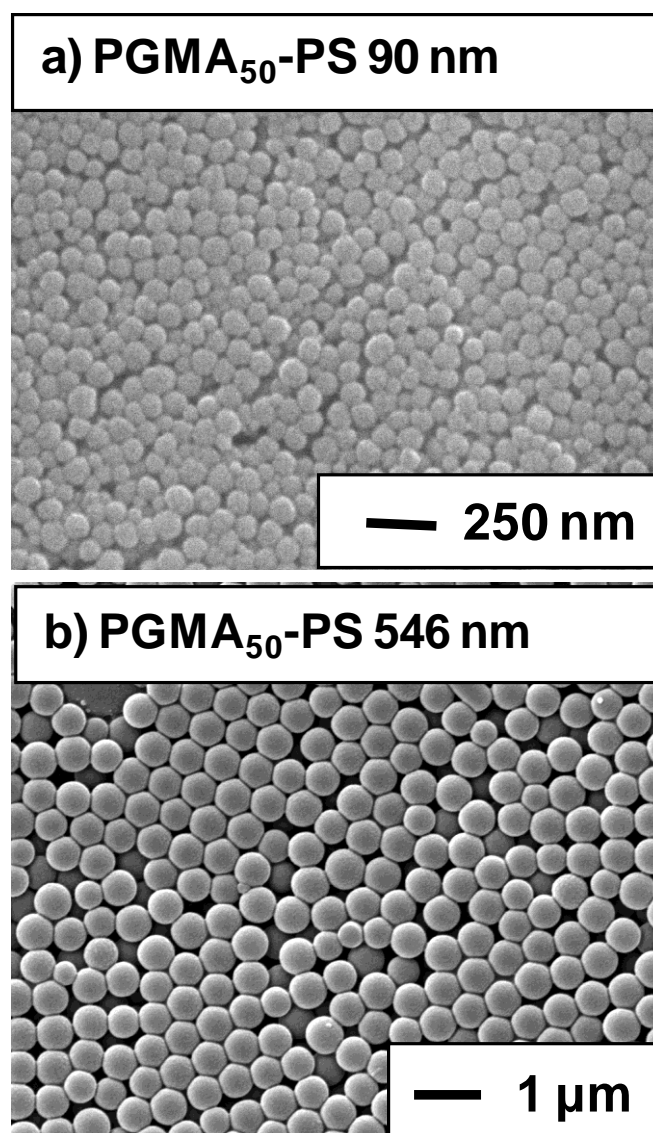
Figure 2.8. Scanning electron micrographs of latexes prepared using the (a) PGMA$_{50}$ *macromonomer* and (b) PGMA$_{50}$ *homopolymer precursor* by aqueous emulsion polymerisation

^{1}H NMR analysis of the dried latexes allows calculation of the amount of PGMA macromonomer or homopolymer incorporated into the latex particles (see Figure 2.9). In the case of aqueous emulsion polymerisation, the PGMA content comprises 1.25 to 19.8 % of the latex by mass (Table 2.2) depending on the type and amount of stabiliser used. Assuming that all of the PGMA chains are located on the outside of the latex, this corresponds to an adsorbed amount, Γ, of approximately $1.3 - 3.8$ mg m^{-2}. The lowest stabiliser content (1.25 w/w %) was obtained when using the homopolymer precursor. This is consistent with the poor grafting expected from the precursor since it lacks a polymerisable group. In contrast when the PGMA macromonomers is used higher stabiliser contents and absorbed amounts are observed as expected. This is attributed to the polymerisable nature of the macromonomer chains allowing for better grafting of the chains onto the latexes.
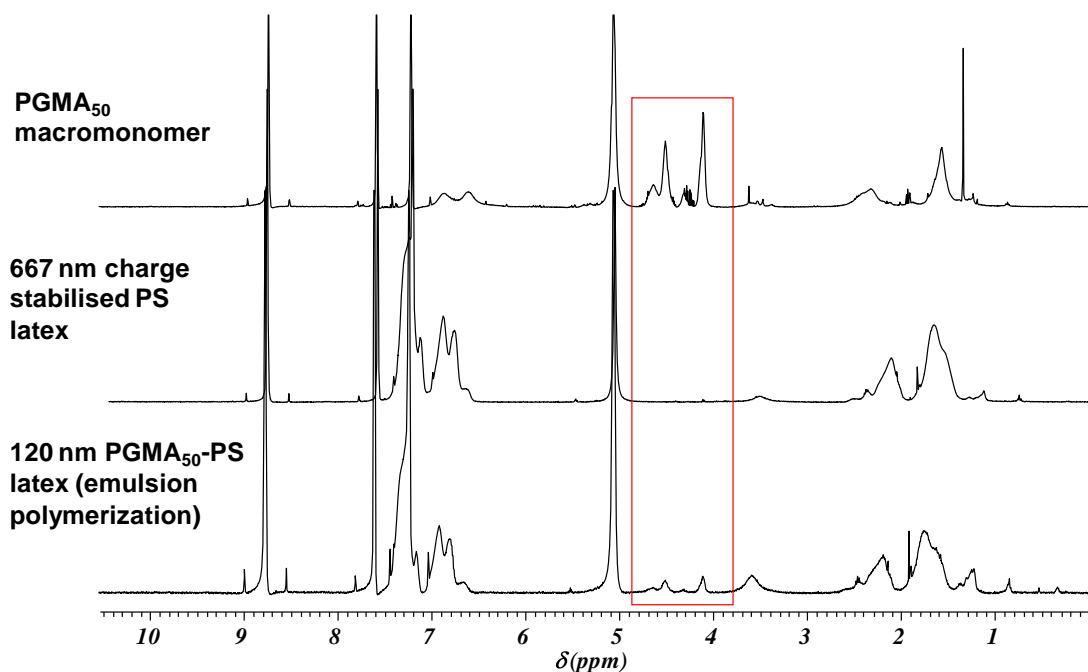
Figure 2.9. ^{1}H NMR spectra recorded in d$_5$-pyridine of the PGMA$_{50}$ macromonomer, a charge stabilised polystyrene latex and the 120 nm PGMA$_{50}$-PS latex prepared by aqueous emulsion polymerisation. Note the absence of any macromonomer peaks in the control experiment.

Alcoholic Dispersion Polymerisation of Styrene

Alcoholic dispersion polymerisation in a 9:1 methanol/water mixture was successfully used to prepared larger, micrometer-sized polystyrene latexes (see Table 2.3). Although no definite trend was observed between mean particle diameter and macromonomer chain length by DLS, a small reduction in particle diameter was observed by DCP when the mean degree of polymerisation of the macromonomer was increased from 20 to 50. There is also a concomitant reduction in latex polydispersity and the $PGMA_{50}$ macromonomer again produced the most uniform particles (see entry 6 in Table 2.3). A control experiment conducted in the absence of any macromonomer led to gross precipitation with essentially no latex formation. In addition, much larger (~2800 nm) latex particles were produced in the presence of the $PGMA_{50}$ homopolymer precursor albeit with a latex yield of only 50 % (the rest being coagulum, see entries 1 and 2 in Table 2.3 and the SEM image in Figure 2.10).

Table 2.3. Latex yield and particle size data for selected $PGMA_n$-PS latexes prepared by alcoholic dispersion polymerisation using 10 wt. % stabiliser based on styrene at 70 ^{o}C for 24 h in 9:1 methanol/water using AIBN initiator (SEM - scanning electron microscopy; DCP - disc centrifuge photosedimentometry; DLS - dynamic light scattering; latex yields determined by gravimetry).

Entry No	Stabiliser Type	Latex yield (%)	SEM diameter / nm	DCP diameter / nm	DLS diameter / nm (PDI)
1	None	0	-	-	-
2	$PGMA_{50}$ homopolymer	50	2700	2760 ± 521	2800 (0.32)
3	$PGMA_{20}$ macromonomer	90	1300	1599 ± 640	1840 (0.40)
4	$PGMA_{30}$ macromonomer	85	910	1085 ± 76	1100 (0.15)
5	$PGMA_{40}$ macromonomer	100	900	990 ± 105	1100 (0.10)
6	$PGMA_{50}$ macromonomer	100	980	980 ± 106	1100 (0.03)
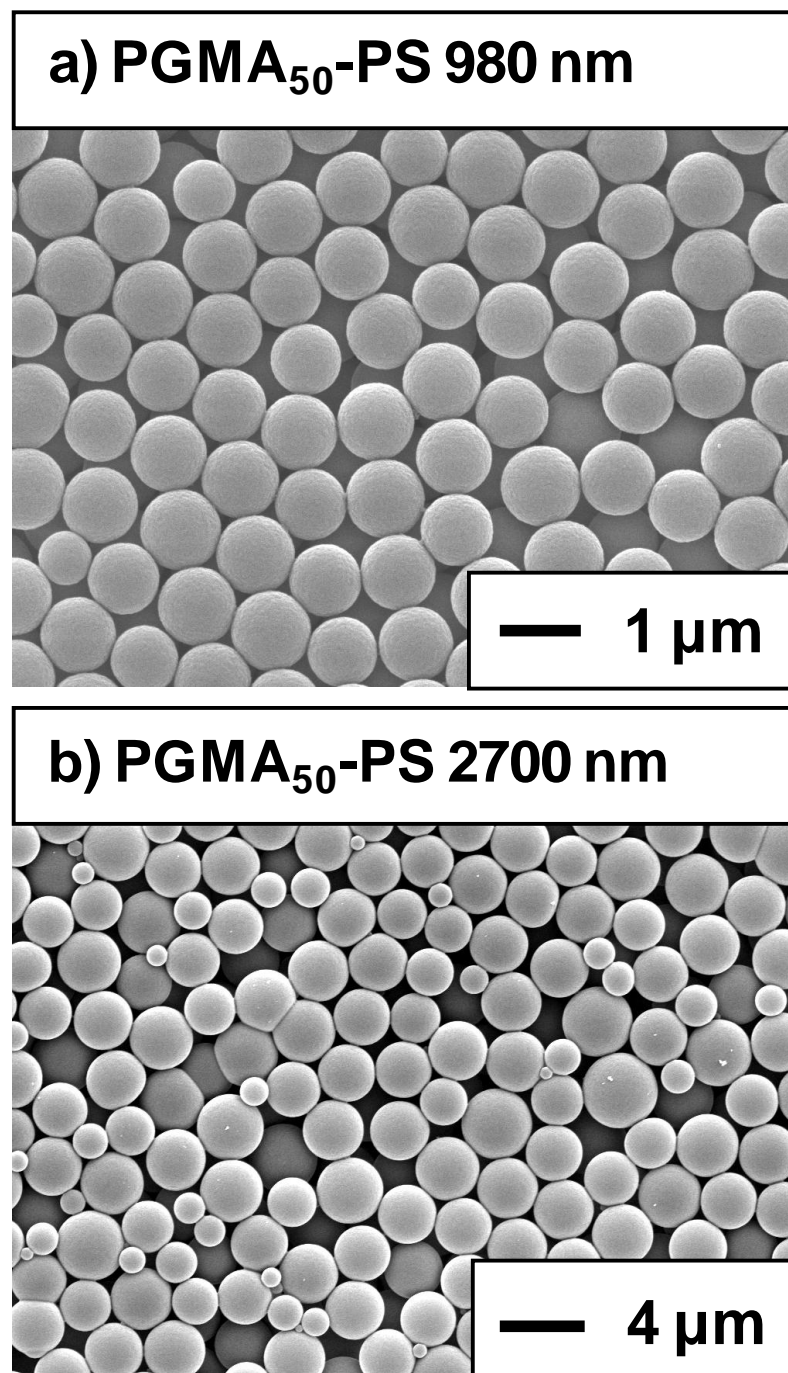
Figure 2.10. Scanning electron micrographs of latexes prepared using the (a) PGMA$_{50}$ *macromonomer* and (b) PGMA$_{50}$ *homopolymer precursor* by alcoholic dispersion polymerisation at 70 °C in a 9:1 methanol/water mixture.

Aqueous Dispersion Polymerisation of 2-Hydroxypropyl Methacrylate

This latex is rather unusual, since both the core and the steric stabiliser chains contain hydroxyl functionality. Initially, the latex synthesis was carried out at 60 °C, which suggests a half-life for the AIBA initiator of approximately 10 h. However, in this initial experiment, only around 50 % monomer conversion was achieved. SEM imaging of the resulting latex particles also show an unusual non-spherical surface morphology, which is attributed to the relatively low monomer conversion (see Figure 2.11). In order to increase the latex yield, all subsequent syntheses were conducted at 70 °C. This resulted in much higher conversions and a well-defined spherical particle morphology in all cases.

1 µm
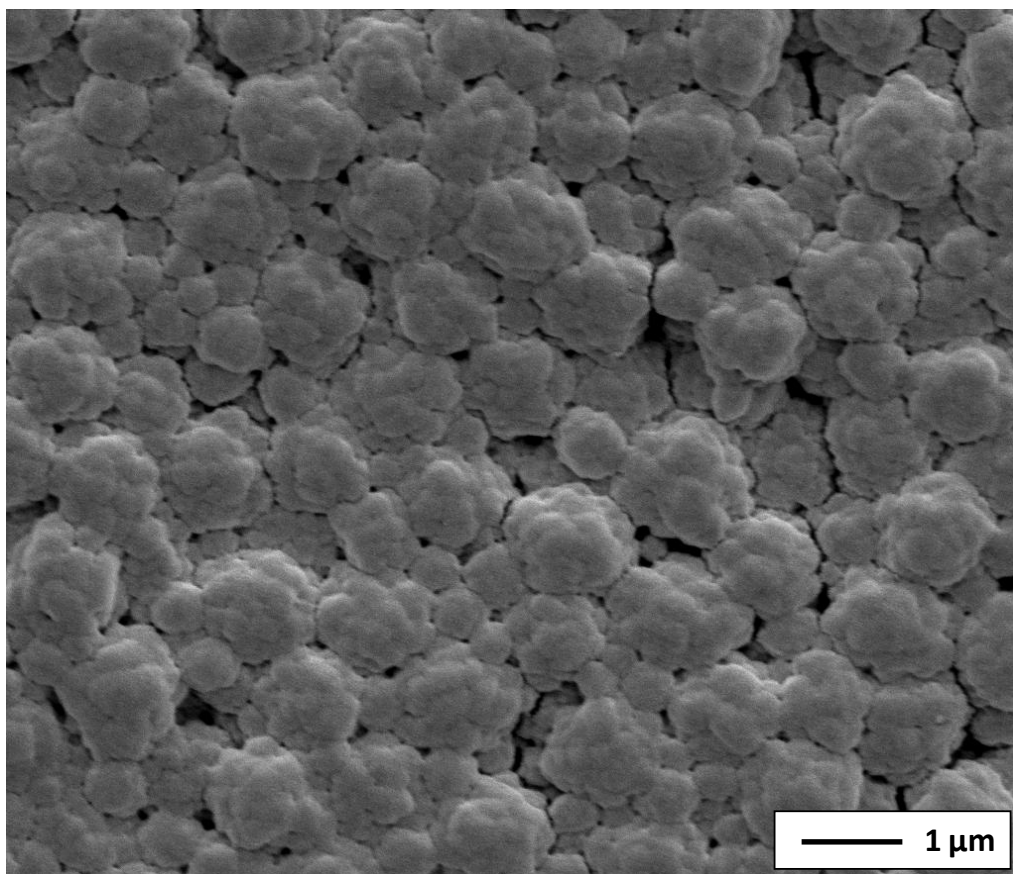
Figure 2.11. Scanning electron microscopy image obtained for a $PGMA_{50}$-PHPMA latex prepared by aqueous dispersion polymerisation at 60 °C using AIBA initiator. Note the non-spherical morphology obtained in this case.

Table 2.4 summarises the results obtained for the synthesis of PGMA-PHPMA latexes by aqueous dispersion polymerisation at 70 °C. In this case, no particular trend was observed between latex particle diameter and macromonomer chain length but the $PGMA_{50}$ macromonomer again produced more monodisperse particles. Control experiments conducted either in the absence of any macromonomer or in the presence of the $PGMA_{50}$ homopolymer precursor both led to gross precipitation of PHPMA, as expected (see entries 1 and 2 in Table 2.4 and the SEM image in Figure 2.12). This further confirms the importance of the polymerisable styrenic group on the macromonomer chain to confer effective steric stabilisation. It is perhaps worth emphasising here that, in contrast to aqueous emulsion polymerisation, using a water-soluble initiator (AIBA) in conjunction with a PGMA stabiliser did not lead to any detrimental particle flocculation with such aqueous dispersion polymerisation formulations.

Table 2.4. Latex yield and particle size data for $PGMA_n$-PHPMA latexes prepared by aqueous dispersion polymerisation using 10 wt. % stabiliser based on HPMA at 70 °C for 24 h in water using AIBA initiator.

Entry No	Stabiliser Type	Latex yield (%)	SEM diameter / nm	DCP diameter / nm	DLS diameter / nm (PDI)
1	None	0	-	-	-
2	$PGMA_{50}$ homopolymer	0	-	-	-
3	$PGMA_{20}$ macromonomer	86	1020	1036 ± 164	1490 (0.37)
4	$PGMA_{30}$ macromonomer	99	765	790 ± 145	950 (0.09)
5	$PGMA_{40}$ macromonomer	100	720	744 ± 100	1110 (0.14)
6	$PGMA_{50}$ macromonomer	100	855	880 ± 143	1070 (0.06)
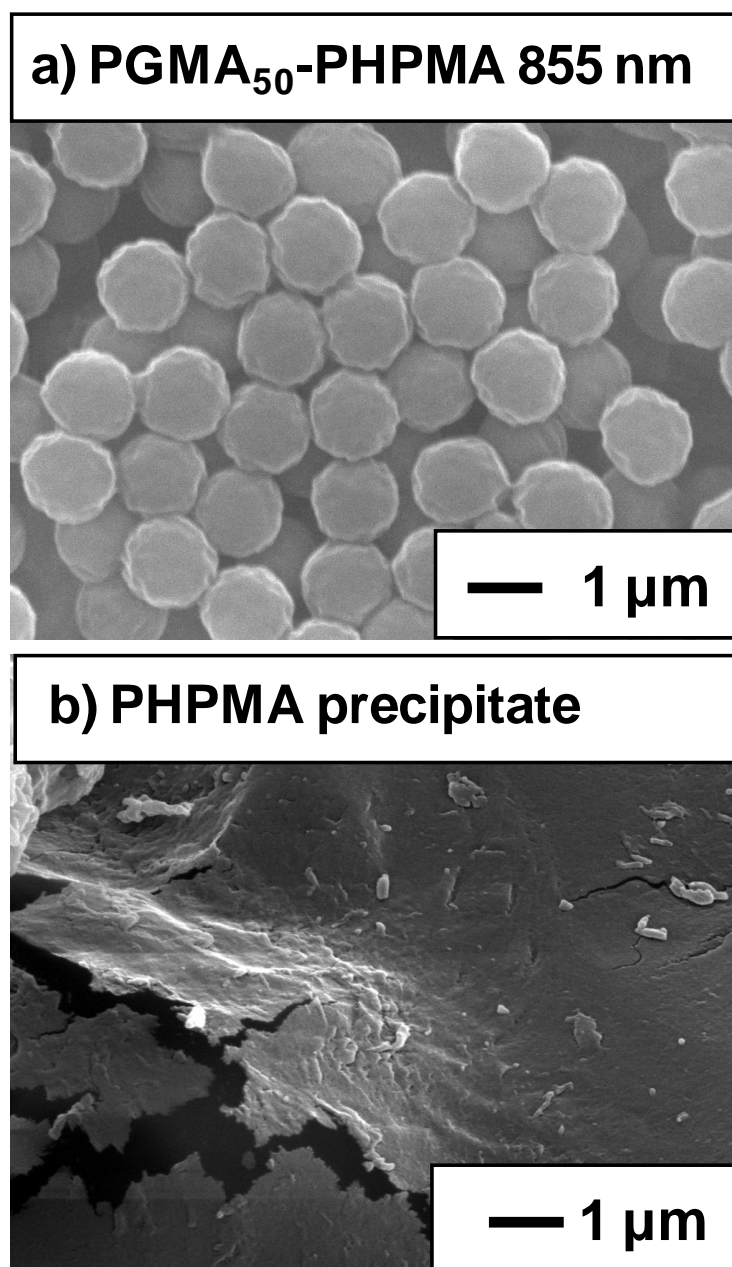
Figure 2.12. Scanning electron micrographs of (a) a latex prepared using the PGMA$_{50}$ *macromonomer* and (b) the amorphous PHPMA precipitate obtained in the attempted aqueous dispersion polymerisation of 2-hydroxypropyl methacrylate in the presence of the PGMA$_{50}$ *homopolymer precursor* at 70 °C.

Latex Surface Characterisation

FT-IR spectra were recorded for the $PGMA_{50}$ macromonomer, selected $PGMA_{50}$-
stabilised polystyrene latexes and a polystyrene precipitate. The distinctive ester
carbonyl stretch due to the GMA repeat units of the macromonomer chains is
observed at around 1730 cm^{-1} (see Figure 2.13). The same band appears in the
$PGMA_{50}$-stabilised polystyrene latex prepared by aqueous emulsion polymerisation.
This confirms the presence of the PGMA stabiliser in this latex, but does not provide
any information regarding its spatial location. It is perhaps noteworthy that this
carbonyl band is not observed in the much larger $PGMA_{50}$-PS latex prepared by
alcoholic dispersion polymerisation. However, this negative result was not
unexpected due to the much lower stabiliser content of this latex (< 1 wt. %).
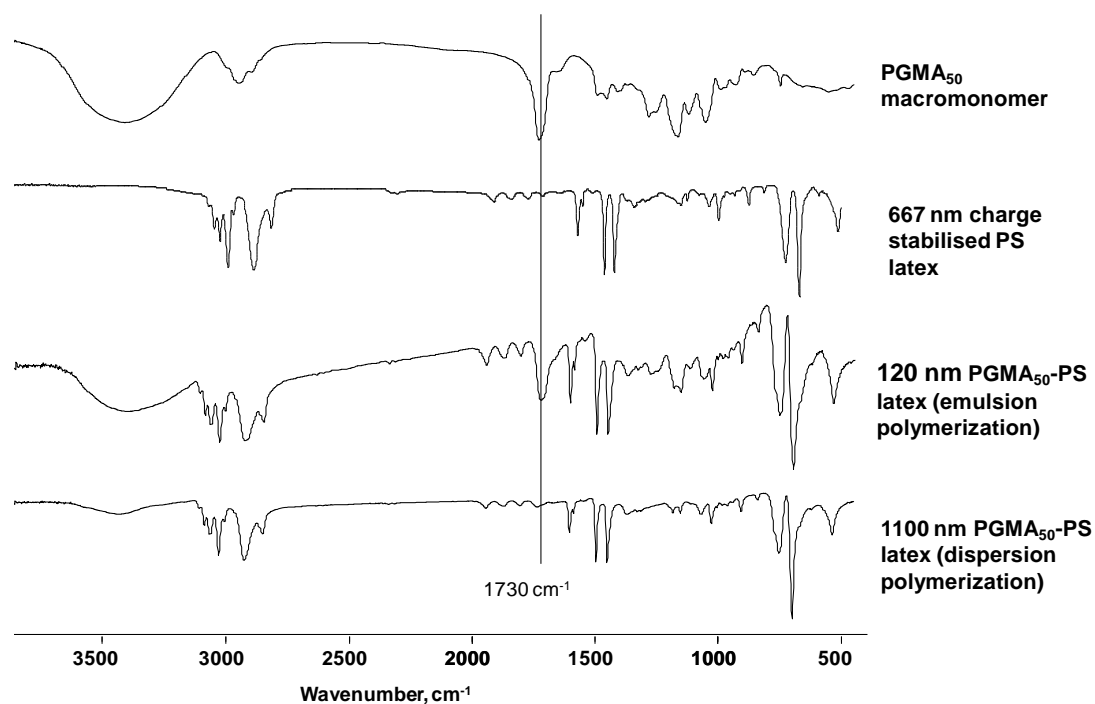
Figure 2.13. FT-IR spectra recorded for $PGMA_{50}$ macromonomer, charge-stabilised
polystyrene latex prepared in the absence of any macromonomer and two $PGMA_{50}$-
stabilised polystyrene latexes prepared by aqueous emulsion and alcoholic dispersion
polymerisation, respectively. Note the prominent carbonyl ester band at around 1730
cm^{-1} observed for the spectrum of the 120 nm $PGMA_{50}$-stabilised polystyrene latex.
This band is absent in the 1100 nm $PGMA_{50}$-stabilised polystyrene latex since its
stabiliser content is too low.
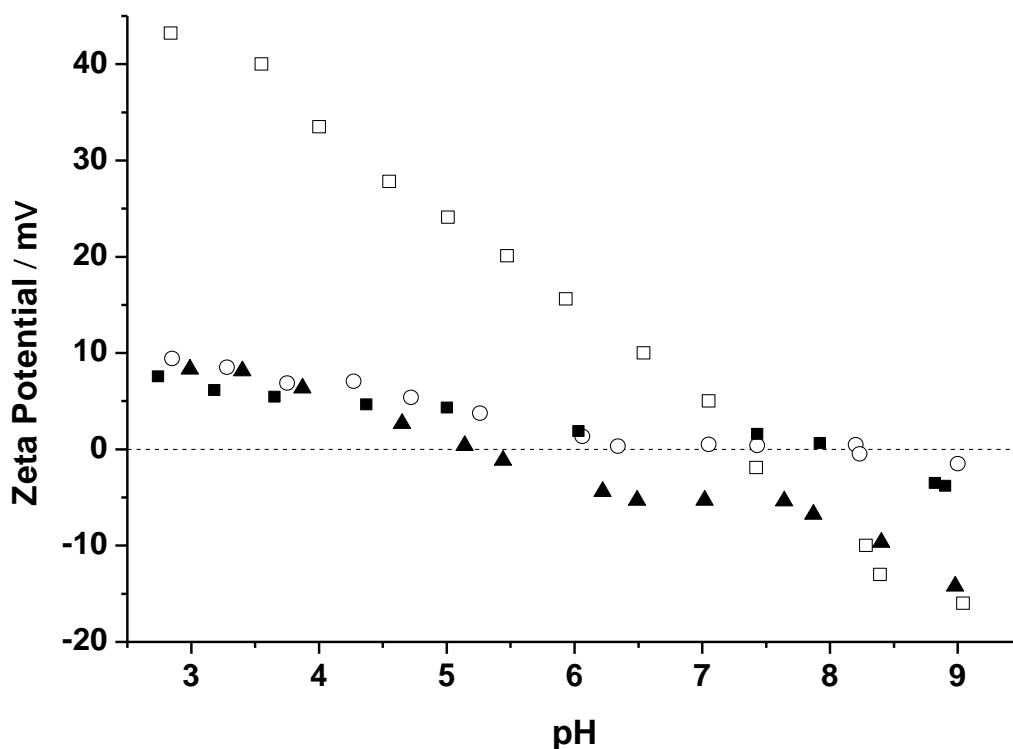
Figure 2.14. Aqueous electrophoresis curves observed for a 1100 nm $PGMA_{50}$-PS latex (▲), 120 nm $PGMA_{50}$ (■), a $PGMA_{50}$-PHPMA latex (○) and also a 667 nm charge-stabilised PS latex prepared in the absence of macromonomer using a cationic azo initiator AIBA (□). The presence of the non-ionic PGMA chains effectively shields the underlying surface charge.

Further evidence for the presence of the PGMA chains being incorporated into these latexes is provided by aqueous electrophoresis and XPS analysis (see Figure 2.14 and Figure 2.15); both are surface-specific techniques. Aqueous electrophoresis shows that the $PGMA_{50}$-PS latexes display only a relatively modest change in zeta potential ($\pm$ 10 mV) as a function of pH; much larger changes are observed for a cationic charge-stabilised PS latex examined under the same conditions. This indicates that the non-ionic $PGMA_n$ chains are located at the latex surface and shield the underlying cationic charge arising from the quaternised reacted styrene group.
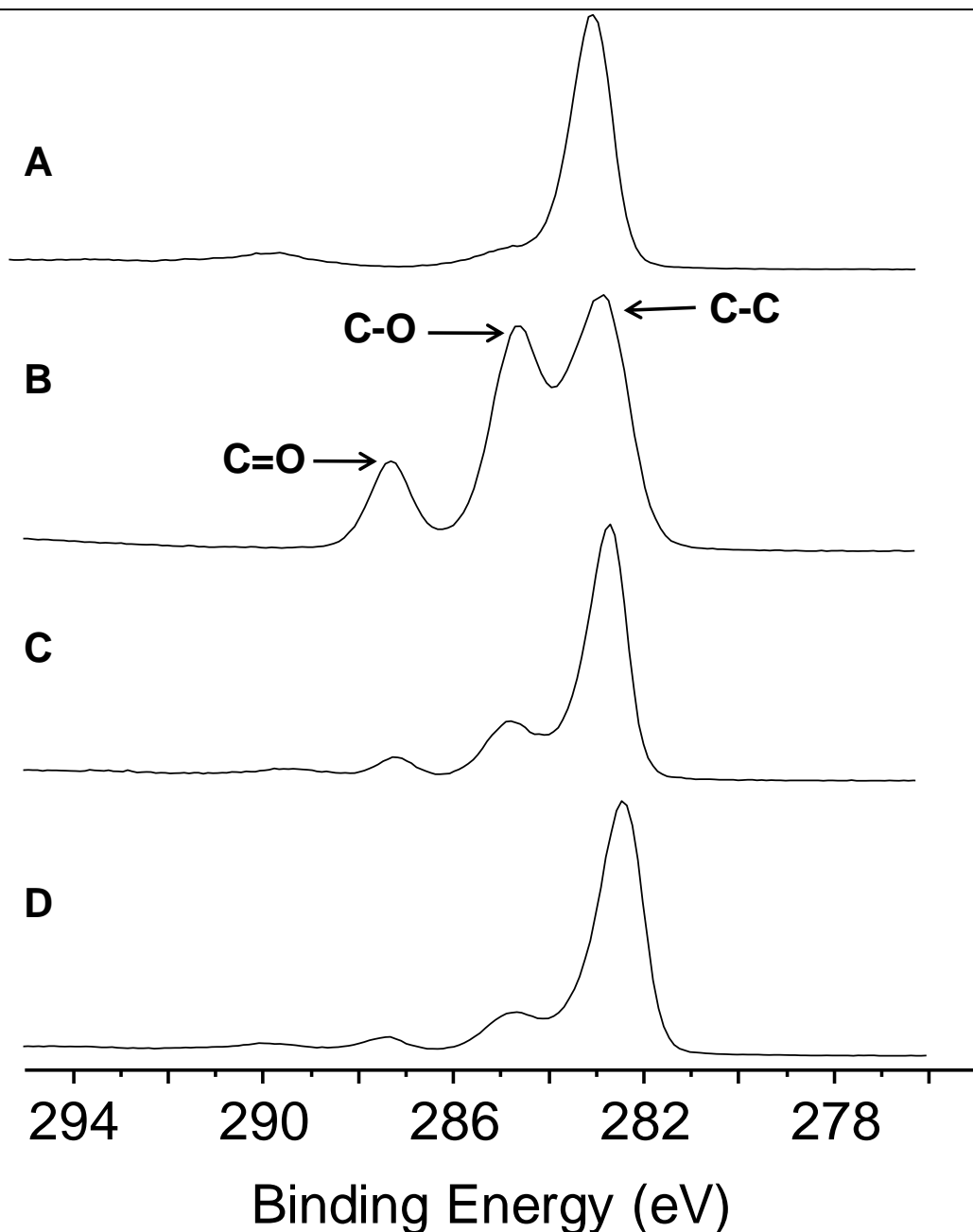
Figure 2.15. XPS core-line C1s spectra for (a) a polystyrene precipitate prepared in the absence of macromonomer, (b) the PGMA$_{50}$ macromonomer and (c, d) the 120 nm and 1100 nm PGMA$_{50}$-PS latexes, respectively. There is clear evidence for C-O and C=O species in the latter two spectra, which confirms the presence of the PGMA chains at the surface of each latex.

Comparing the X-ray photoelectron spectra recorded in the C1s region for the PGMA$_{50}$ macromonomer, the precipitated polystyrene homopolymer and both PGMA$_{50}$-PS latexes, it is clear that the PGMA$_{50}$ macromonomer is present in both latexes (see Figure 2.15A). The C-O and C=O signals arising from the PGMA$_{50}$ macromonomer are present both sterically stabilised latexes, but absent from the PS precipitated control. Moreover, since XPS has a typical analysis depth of around 2-8 nm, the PGMA stabiliser chains must be located at (or very near) the latex surface. It is also possible to estimate the surface coverage of the PGMA$_{50}$ chains on the latex particles using the carbonyl signals due to the ester groups in the PGMA macromonomer, since no such signals are observed for the precipitated polystyrene homopolymer. Using this approach, surface coverages of 42 % and 25 % are estimated for PGMA$_{50}$-PS latexes prepared by aqueous emulsion and alcoholic dispersion polymerisation, respectively. Unfortunately, due to the similar chemical structures of PGMA and PHPMA, it was not possible to directly confirm the presence of the PGMA macromonomer chains in the PHPMA latexes by either FT-IR, ^{1}H NMR or XPS. However, the aqueous electrophoretic data again indicate very low zeta potentials over a wide pH range. This suggests that the surface charge from the underlying cationic AIBA initiator and quaternised styrene end group of the macromonomer is effectively screened by the non-ionic PGMA chains.

Having demonstrated that the PGMA-based macromonomers are indeed located at the latex surface and thus act as steric stabilisers, the colloid stability of selected latexes was evaluated by two methods: (i) a single freeze-thaw cycle at -20 ^{o}C and (ii) addition of varying concentrations of MgSO$_4$ (see Table 2.5). A charge-stabilised polystyrene latex flocculated substantially on addition of just 0.01 M MgSO$_4$ and also failed to redisperse after a freeze-thaw cycle. However, each latex stabilised using the PGMA$_n$-based macromonomers (where n = 20, 30, 40 or 50) remained stable at up to 0.50 M MgSO$_4$ and also readily redispersed after a freeze-thaw cycle, as judged by DLS. Clearly, the chemically-grafted PGMA stabiliser chains confer substantially enhanced colloidal stability, as expected for sterically-stabilised latexes.

Table 2.5. Colloid stability of selected latexes in the presence of added salt and after one freeze-thaw cycle at -20 ^{o}C.

Latex	DLS diameter **before** freeze-thaw (nm)	DLS diameter **after** freeze-thaw (nm)	MgSO$_4$ concentration / M					
			0.01	0.05	0.10	0.20	0.30	0.50
AIBA-PS	667	aggregation	✖	✖	✖	✖	✖	✖
PGMA$_{20}$-PS	1840	1971	✓	✓	✓	✓	✓	✓
PGMA$_{30}$-PS	1100	1990	✓	✓	✓	✓	✓	✓
PGMA$_{40}$-PS	1110	1200	✓	✓	✓	✓	✓	✓
PGMA$_{50}$-PS	120	120	✓	✓	✓	✓	✓	✓
PGMA$_{50}$-PS	1100	1200	✓	✓	✓	✓	✓	✓
PGMA$_{50}$-PHPMA	1070	1108	✓	✓	✓	✓	✓	✓

✖ indicates substantial particle aggregation (coagulation)   ✓ indicates no change in DLS diameter within experimental error

CONCLUSIONS

A series of well-defined styrene-functionalised poly(glycerol monomethacrylate)-based macromonomers have been synthesised by combining use of a tertiary amine-functional ATRP initiator with post-polymerisation quaternisation using 4-vinylbenzyl chloride. Target degrees of polymerisation can be systematically varied from 20 to 70 with good molecular weight control and relatively low polydispersities ($M_w/M_n < 1.30$). Selected hydrophilic macromonomers were evaluated as reactive polymeric stabilisers for the polymerisation of styrene and HPMA under either emulsion or dispersion conditions. Near-monodisperse, sterically-stabilised polystyrene latexes of micrometer dimensions were obtained via dispersion polymerisation in the presence of the $PGMA_{50}$ macromonomers, whereas only flocculated, poorly-defined particles were observed if the non-quaternised $PGMA_{50}$ homopolymer precursor was utilised. Also complete precipitation occurred in the absence of any stabiliser. This serves to illustrate the essential role played by the terminal polymerisable styrene group in determining the final particle morphology. Near-monodisperse polystyrene latexes of around 120 nm diameter were also obtained via emulsion polymerisation using the same macromonomer. Varying the molecular weight of the macromonomer affected the latex particle size distribution; more uniform particles were achieved in the presence of higher molecular weight macromonomers. FT-IR confirmed the presence of the stabiliser in the smaller latexes and XPS studies indicated that the chemically-grafted macromonomer was present at (or very near) the latex surface, as expected. Compared to a charge-stabilised polystyrene latex, these sterically-stabilised latexes proved to be highly resistant to the addition of electrolyte, as expected. Finally, the tolerance of these new sterically-stabilised latexes towards freeze-thaw cycling was enhanced for higher molecular weight macromonomers.

REFERENCES

1. Urban, D.; Takamura, K. *Polymer Dispersions and their Industrial Applications*. Wiley-VCH Verlag GmbH, Weinheim, **2002**.

2. Gilbert, R. G. *Emulsion Polymerisation: A Mechanistic Approach*, Academic Press, London, **1995.**

3. Chern, C. S. *Prog. Polym. Sci.,* **2006**, *31*, 443.

4. Zhao, C. L.; Holl, Y.; Pith, T.; Lambla, M. *Colloid Polym. Sci.,* **1987**, *265*, 823.

5. Steward, P. A.; Hearn, J.; Wilkinson, M. C. *Adv. Colloid Interface Sci,* **2006,** *86*, 195.

6. Aramendia, E.; Mallégol, J.; Jeynes,C.; Barandiaran, M. J.; Keddie, J. L.; Asua J. M. *Langmuir*, **2003**, *19*, 3212.

7. Bromley, C. W. A., *Colloids and Surfaces*, **1986**, *17*, 1.

8. Ito, K.; Yokoyama, S.; Arakawa, F., *Polymer Bulletin*, **1986**, *16*, 345.

9. Ottewill, R. H.; Satgurunathan, R. *Colloid Polym. Sci.,* **1995,** *273*, 378.

10. Capek, I. *Adv. Colloid Interface Sci,* **2009,** *99*, 77

11. Lascelles, S. F.; Malet, F.; Mayada, N. C.; Billingham, N. C.; Armes, S. P. *Macromolecules*, **1999**, *32*, 2462.

12. Wang, X. S.; Lascelles, S. F.; Jackson, R. A.; Armes, S. P. *Chem. Commun.* **1999**, 1817.

13. Matyjaszewski, K.; Gaynor, S. G.; Kulfan, A.; Podwika, M. *Macromolecules,* **1997**, *30*, 5192.

14. Matyjaszewski, K.; Beers, K. L.; Kern, A.; Gaynor, S. G. *J. Polym. Sci., Part A: Polym. Chem.* **1998**, *36*, 823.

15. Muehlebach, A.; Rime, F. *J. Polym. Sci., Part A: Polym. Chem.* **2003**, *41*, 3425.

16. Schoen, F.; Hartenstein, M.; Mueller, A. H. E. *Macromolecules* **2001**, *34*, 5394.

17. Ishizu, K.; Tahara, N. *Polymer* **1996**, *37*, 2853.

18. Ishizu, K.; Yamashita, M.; Ichimura, A. *Polymer* **1997**, *38*, 5471.

19. Ishizu, K.; Yamashita, M.; Ichimura, A. *Macromol. Rapid Commun.* **1997**, *18*, 639.

20. Uchida, T.; Furuzono, T.; Ishihara, K.; Nakabayashi, N.; Akashi, M. *J. Polym. Sci., Part A: Polym. Chem.* **2000**, *38*, 3052.

21. Bon, S. A. F.; Morsley, S. R.; Waterson, C.; Haddleton, D. M. *Macromolecules* **2000**, *33*, 5819.

22. Topham, P. D.; Sandon, N.; Read, E. S.; Madsen, J.; Ryan, A. J.; Armes, S. P. *Macromolecules* **2008**, *41*, 9542.

23. Mantovani, G.; Ladmiral, V.; Tao, L.; Haddleton, D. M., *ChemComm*, **2005**, 2089.

24. Vogt, A. P.; Sumerlin, B. S., *Macromolecules*, **2006**, *39*, 5286

25. Thompson, K. L.; Bannister, I.; Armes, S. P.; Lewis, A. L. *Langmuir,***2010**, *26*, 4693.

26. Yuan, J. J.; Armes, S. P.; Takabayashi, Y.; Prassides, K.; Leite, C. A. P.; Galembeck, F.; Lewis, A. L. *Langmuir*, **2006**, *22*, 10989.

27. Liu, S. Y.; Save, M.; Weaver, J. V. M. ; Armes, S. P.; *Langmuir*, **2002**, *18*, 8350.

28. Fujii, S. ; Cai, Y. ; Weaver, J. M. V. ; Armes, S. P., *J. Am. Chem. Soc.,* **2005**, *127*, 7304.

29. Pilon, L. N. ; Armes, S. P. ; Findlay, P. ; Rannard, S. P., *Langmuir*, **2005**, *21*, 3808.

30. Haigh, R.; Rimmer, S.; Fullwood, N. J. *Biomaterials*, **2000**, *21*, 735.

31. Li, Y.; Armes, S. P., *Angew. Chem., Int. Ed.,* **2010,** *49*, 4042.

32. Blanazs, A.; Madsen, J.; Battaglia, G.; Ryan, A. J.; Armes, S. P., *J. Am. Chem. Soc.,* **2011**, ASAP, DOI: 10.1021/ja206301a

33. Save, M.; Weaver, J. V. M.; Armes, S. P., McKenna, P. *Macromolecules*, **2002**, *35*, 1152.

34. Thompson, K. L.; Armes, S. P.; York, D. W.; Burdis, J. A., *Macromolecules,* **2010,** *43*, 2169.

35. Cairns, D. B.; Armes, S. P.; Bremer, L. G. B. *Langmuir*, **1999**, *15*, 8052.

36. Chen, S.; Jiang, L.; Dan, Y., *J. Appl. Polym. Sci.,* **2011,** *121*, 3322.

37. Luo, Y.; Schork, F. J., *Journal of Polymer Science Part A: Polymer Chemistry,* **2002,** *40*, 3200.

38. Nomura, M.; Suzuki, K., *Ind. Eng. Chem. Res.,* **2004,** *44*, 2561.

39. Capek, I., *Adv. Colloid Interface Sci.,* **2001,** *91*, 295.

Chapter Three

Covalently Cross-linked Colloidosomes

INTRODUCTION

Colloidosomes are microcapsules whose shells are composed of colloidal particles that have been fused together to provide the shell with additional stability.[1] In recent years colloidosomes have received considerable attention due to their potential importance in the area of microencapsulation. As was described in Chapter One, routes to colloidosomes are commonly based on the self-assembly of colloidal particles at the interface between two immiscible liquids, typically water and oil; such so-called Pickering emulsions have been recognised for over a century.[2] The preparation of colloidosomes involves reinforcement of the particle adsorption at the interface of these Pickering emulsions in order to form more robust, and ideally less permeable, microcapsule shells.

Velev and co-workers reported the first colloidosome-type structures in 1996 where latex particles were adsorbed onto emulsion droplet templates.[3-5] This group described the formation of both hollow spherical "supraparticles"[3] where surfactant-sensitised latex particles were adsorbed at the water/n-octanol interface and also "ball-like aggregates"[4] where the latex particles penetrated the bulk of the oil droplets. The term 'colloidosome' was first introduced by Dinsmore *et al,*[6] who prepared microcapsules by the self-assembly of micron-sized polystyrene or poly(methyl methacrylate) latex particles at the surface of either oil-in-water or water-in-oil emulsion droplets. Once the droplet surface was covered by particles the colloidosome shell was formed by thermal annealing, whereby the emulsion was heated to just above the T_g of the polystyrene latex particles (~ 105 ^{o}C) using a glycerol co-solvent. Laïb and Routh used a low T_g poly(styrene-co-n-butyl acrylate) latex to prepare colloidosomes[7] that could be annealed under relatively mild conditions, typically between 35 and 65 ^{o}C. Another form of colloidosome stabilisation utilised an aqueous gelator within the internal phase.[8] Here in situ gelation ensures structural integrity and both 'hairy'[9] and 'magnetic'[10] colloidosomes have been prepared this way. This Chapter will examine the preparation of colloidosomes via the covalent cross-linking of neighbouring latex particles.

Previous reports of covalent cross-linking

Poly(divinylbenzene-alt-maleic anhydride) microspheres assembled at the oil/water interface have been cross-linked from the aqueous continuous phase by addition of polyamines.[11] Skaff and coworkers[12] assembled norbornene-functionalised CdSe/ZnS quantum dots at the water/toluene interface and then conducted ring-opening metathesis polymerisation (ROMP) using a water-soluble Ru-based Grubbs catalyst to lock in the quantum dot super-structure. More recently, Shah *et al.*[13] prepared water-in-oil emulsions using primary amine-functionalised poly(*N*-isopropylacrylamide) microgels, followed by cross-linking within the aqueous droplets using glutaraldehyde to produce novel thermo-responsive microcapsules.

The Present Work

In this Chapter the $PGMA_{50}$-PS particles described in Chapter Two are used for the preparation of covalently cross-linked colloidosomes at the oil-water interface. The aim was to assemble these latex particles around oil droplets and cross-link them in place via their surface hydroxy groups. An oil-soluble polymeric diisocyanate was chosen as an appropriate cross-linker since it would readily react with the PGMA stabiliser chains at room temperature. The effects of oil type and latex size on the resulting colloidosomes are investigated and the microcapsules are challenged with either excess alcohol or non-ionic surfactant. Methods to anneal the surface of these microcapsules using co-solvent mixtures are also explored. The route to covalently cross-linked colloidosomes described in this Chapter has already resulted in publications in Chemical Communications[14] and Macromolecules.[15]

EXPERIMENTAL DETAILS

Materials.

Glycerol monomethacrylate (GMA) was kindly donated by Cognis UK Ltd (Hythe, UK) and used without further purification. 4-Vinylbenzyl chloride (4-VBC; 90 %), Cu(I)Cl (99.995 %) 2,2′-bipyridine (bpy, 99 %), n-dodecane, sunflower oil, fluorescein and tolylene 2,4-diisocyanate-terminated poly(propylene glycol) [PPG-TDI] were all purchased from Aldrich and were used as received. Styrene and pyrrole (Aldrich) were passed through a column of basic alumina to remove inhibitor and then stored at -20 °C prior to use. 2,2'-Azobisisobutyronitrile (AIBN; BDH) and ammonium persulfate (APS, Aldrich) were used as received. Methanol and ethanol were purchased from Fisher and were used as received. De-ionised water was used in all experiments. Silica gel 60 (0.0632-0.2 mm) was obtained from Merck (Darmstadt, Germany). NMR solvents (D_2O, CD_3OD, $CDCl_3$ and d_5-pyridine) were purchased from Fisher.

Preparation of PGMA$_{50}$ Macromonomer

The PGMA$_{50}$ macromonomer was prepared as reported in Chapter Two.[16]

Preparation of PGMA$_{50}$-PS Latex via Aqueous Emulsion Polymerisation

The sub-micrometer sized PGMA$_{50}$-PS particles were prepared by the aqueous emulsion polymerisation protocol described in Chapter Two.[16] The mean diameter of the resulting latex particles was assessed by scanning electron microscopy, disk centrifuge photosedimentometry and dynamic light scattering (see Table 3.1).

Preparation of PGMA$_{50}$-PS Latex via Alcoholic Dispersion Polymerisation

The micrometer sized PGMA$_{50}$-PS particles were prepared by the alcoholic dispersion polymerisation protocol described in Chapter Two.[16] The mean diameter of the resulting latex particles was assessed by scanning electron microscopy, disk centrifuge photosedimentometry and dynamic light scattering (see Table 3.1). The protocol was repeated utilising 0.050 g fluorescein-o-methacrylate (1 wt % based on styrene) to prepare a fluorescently-labelled latex for fluorescence microscopy experiments, see Table 3.1 for particle size details. For clarity, each of the latexes used in this study will be denoted by their intensity average diameter.

Colloidosome Preparation

PPG-TDI (0.025 g) was weighed into a sample vial and then dissolved in 5.0 ml oil (e.g. *n*-dodecane, sunflower oil or isononyl isononoate). This solution was then homogenised with 5.0 ml of 0.4 - 10.0 wt % aqueous latex for 2 minutes using a IKA Ultra-Turrax T-18 homogeniser with a 10 mm dispersing tool operating at 12,000 rpm. The resulting stable milky-white emulsion was allowed to stand at 20 $^{\text{o}}$C for 0-60 minutes to allow the cross-linking reaction to proceed.

Cyclohexane Annealing of Colloidosomes

Colloidosomes were prepared as described above, but using 5.0 ml of a 4:1 *n*-dodecane/cyclohexane mixture as the oil phase instead of pure *n*-dodecane. The resulting stable milky-white emulsion (average droplet diameter = 99 ± 80 μm) was split between five vials, with four of these emulsions being heated to 50$^{\text{o}}$C in an oven for 15, 30, 45 and 60 minutes, respectively.

Polymer Characterisation

^{1}H NMR Spectroscopy

All ^{1}H NMR spectra were recorded in either CDCl$_3$, D$_2$O, CD$_3$OD or d$_5$-pyridine using a 400 MHz Bruker Avance-400 spectrometer.

DMF GPC

The molecular weight and polydispersity of the PGMA homopolymer precursor were determined by DMF GPC at 70°C. The GPC set-up comprised three Polymer Laboratories PL gel 10 μm 'Mixed B' columns in series with a Viscotek TriSEC model 302 refractive detector. The flow rate was 1.0 ml min^{-1} and the mobile phase contained 10 mmol LiBr. Ten near-monodisperse PMMA standards (M$_p$ = 2,000 – 300,000 g mol^{-1}) were used for calibration purposes and data were analysed using Viscotek TriSEC 3.0 software.

Dynamic Light Scattering (DLS)

Intensity-average hydrodynamic diameters of the three latexes were obtained by DLS using a Malvern Zetasizer NanoZS instrument. Aqueous solutions of 0.01 wt % latex were analysed using disposable curvettes, and the results were averaged over three consecutive runs. The deionised water used to dilute each latex was ultra-filtered through a 0.20 μm membrane so as to remove dust.

Colloidosome Characterisation

Conductivity Measurements

The conductivities of the emulsions immediately after preparation were measured using a digital conductivity meter (Hanna model Primo 5). A high conductivity (typically > 10 μS cm^{-1}) indicated that all emulsions in this work were water-continuous. These results were confirmed using the so-called 'drop test': one drop of the emulsion was added to both pure water and oil, and its ease of dispersion was assessed by visual inspection. Relatively rapid dispersion into water was observed in all cases, which confirmed that the continuous phase of the emulsion was water.

Laser Diffraction

A Malvern Mastersizer 2000 instrument equipped with a small volume Hydro 2000SM sample dispersion unit (ca. 50 ml), a HeNe laser operating at 633 nm, and a solid-state blue laser operating at 466 nm was used to size the emulsions. The stirring rate was adjusted to 1,000 rpm in order to avoid creaming of the emulsion during analysis. The mean droplet diameter was taken to be the volume mean diameter ($D_{4/3}$), which is mathematically expressed as $D_{4/3} = \Sigma D_i^4 N_i / \Sigma D_i^3 N_i$. The standard deviation for each diameter provides an indication of the size distribution. After each measurement, the cell was rinsed once with ethanol, followed by three times with doubly-distilled water, the glass walls of the cell were carefully wiped with lens cleaning tissue to avoid cross-contamination, and the laser was aligned centrally on the detector.

Optical Microscopy

Optical microscopy images were recorded using a Motic DMBA300 digital biological microscope with a built in camera and Motic Images Plus 2.0 ML software.

Fluorescent Microscopy

Parallel fluorescence and brightfield microscopy was carried out using a Nikon Eclipse LV100 microscope. The fluorescence excitation and emission wavelengths were controlled by a B-2A filter block (Nikon). Fluorescent images were captured using a high sensitivity EMCCD Andor iXon+ 897 camera (512x512 pixels). Brightfield (diascopic) images were captures using a Luminera 2.1 CCD camera.

Scanning Electron Microscopy (SEM)

SEM studies were performed using a FEI Sirion field emission scanning electron microscope using a beam current of 244 μA and a typical operating voltage of 20 kV. Colloidosome samples were washed repeatedly with ethanol to remove any traces of oil. Samples were dried onto aluminium stubs and sputter-coated with a thin layer of gold prior to examination so as to prevent sample charging.

Differential Scanning Calorimetry (DSC)

DSC (Perkin Elmer Pyris1) was used to measure the T_g of the PGMA$_{50}$-PS latexes and covalently cross-linked colloidosomes. The samples were heated from 25 °C to 150 °C at a heating rate of 10 °C/min.

Packing Efficiency Calculation

According to the recent work of Balmer *et al.*[17], the following equation was used to estimate a packing efficiency (P) for 107 nm and 1188 nm PGMA$_{50}$-PS particles adsorbed onto dodecane droplets:

$$P = \frac{N r_l^2}{4(r_d + r_l)^2} \qquad (1)$$

$$N = \frac{4P(r_d + r_l)^2}{r_l^2} \qquad (2)$$

Where N = number of latex particles per oil droplet, P = latex packing efficiency, r_d = mean radius of the oil droplet (as determined by laser diffraction) and r_l = mean radius of the latex particles (as determined by DLS). P was calculated for lower latex concentrations (0.35 – 1.2 wt %) where it was determined by visual inspection of the creamed emulsion that essentially all latex particles in solution had adsorbed onto the oil droplets (this was confirmed by gravimetric analysis of the aqueous phase below the creamed emulsion).

RESULTS AND DISCUSSION

The synthetic route for the preparation of covalently cross-linked colloidosomes from well-defined poly(glycerol monomethacrylate) macromonomers is outlined in Figure 3.1.
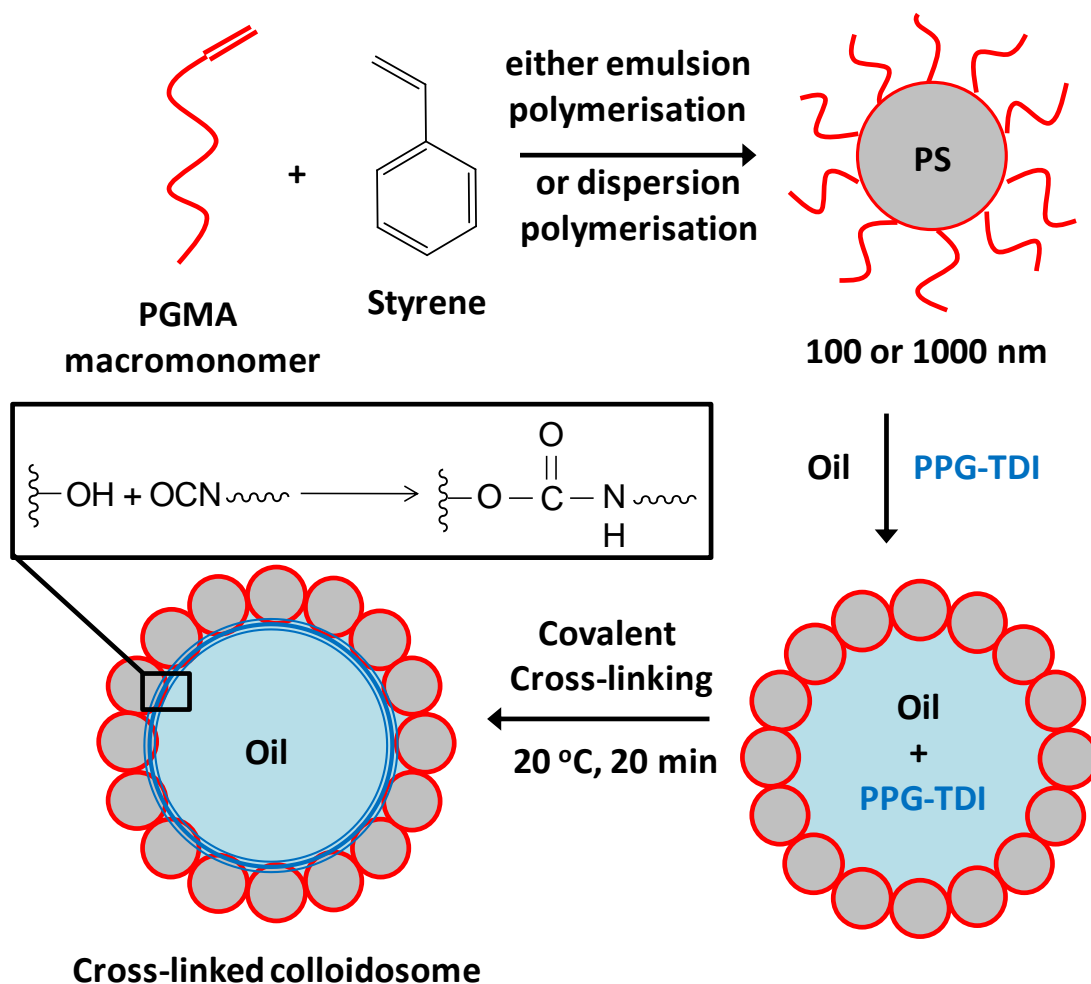
Figure 3.1. Covalently cross-linked colloidosomes prepared by self-assembly of PGMA$_{50}$-PS latex particles around oil droplets in the presence of the oil-soluble PPG-TDI cross-linker.

The first step is to prepare PGMA$_{50}$-PS latexes via either aqueous emulsion or alcoholic dispersion polymerisation (as described in Chapter 2).[16] Transmission and scanning electron micrographs of two such latexes are shown in Figure 3.2 and particle characterisation data for the three latexes used in this Chapter appears in Table 3.1. These latexes were then homogenised with various oils to obtain oil-in-water Pickering emulsions.
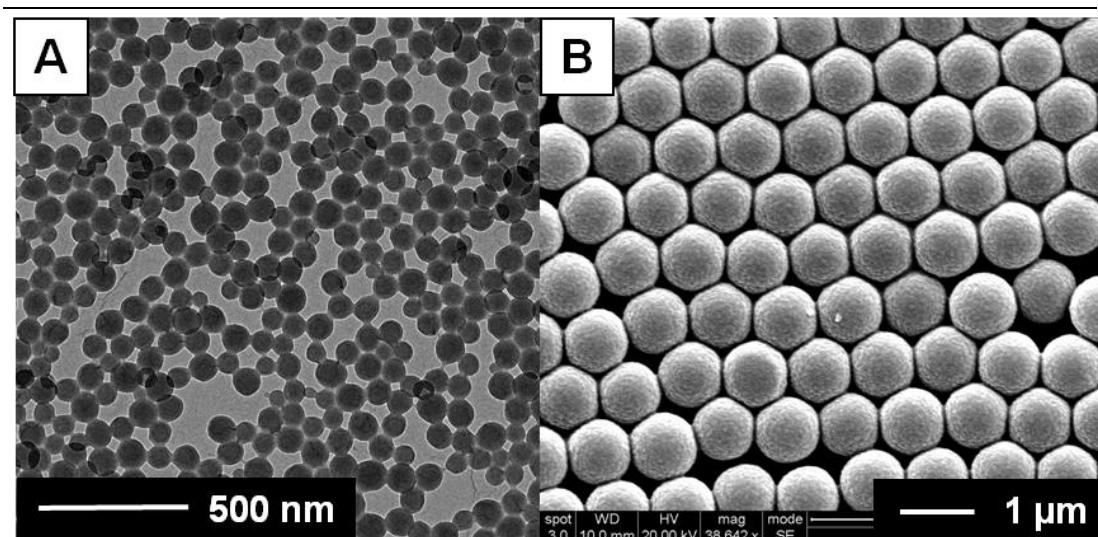
Figure 3.2. Transmission electron microscopy image of A) 107 nm PGMA$_{50}$-PS latex particles prepared by aqueous emulsion polymerisation (entry 1, Table 1) and scanning electron microscopy image of B) 1188 nm PGMA$_{50}$-PS latex particles prepared by alcoholic dispersion polymerisation (entry 2, Table 1).

Table 3.1. Summary of the three sterically-stabilised latexes prepared using the PGMA$_{50}$ macromonomer.

Entry No	SEM diameter /nm	DCP diameter /nm	DLS diameter (PDI) /nm	Stabiliser Content /%	Γ /mg m^{-2}
1	80	112 ± 14	107 (0.04)	9.8	1.5
2	837	851 ± 71	1188 (0.06)	0.9	1.3
3^{a}	813	893 ± 59	1015 (0.08)	1.1	1.6

a- contains 1 wt % fluorescein-*o*-methacrylate comonomer (based on styrene).

Having determined that these emulsions were always of the oil-in-water type (via conductivity measurements and the drop-test) a suitable cross-linker was selected. An oil-soluble cross-linker was considered desirable since this avoids the need to remove any excess cross-linker and should also confine the cross-linking reaction to within the oil droplets. Thus cross-linking only occurs within individual colloidosomes and not between them, allowing their production at high solids (50 vol %). The cross-linker chosen was tolylene 2,4-diisocyanate-terminated poly(propylene glycol) [PPG-TDI], which readily reacts with the hydroxy groups from the PGMA stabiliser to form robust urethane bonds with no small molecule by-

products (see Figure 3.3). This commercially available polymeric cross-linker is significantly less toxic than small molecule diisocyanates because it is non-volatile. Moreover, its insolubility in water prevents partitioning between the oil droplets and the aqueous continuous phase.
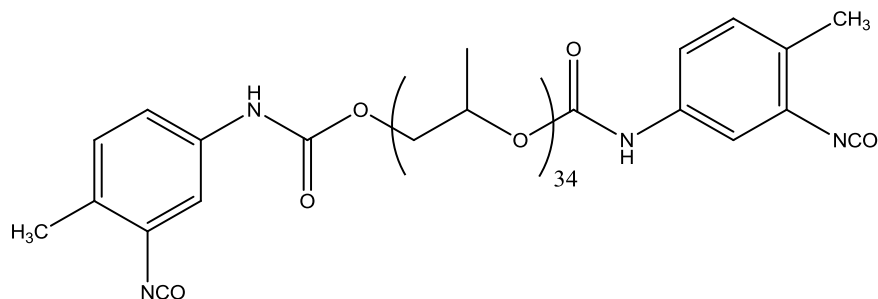
Figure 3.3. Chemical structure of the tolylene 2,4-diisocyanate-terminated poly(propylene glycol) (PPG-TDI) cross-linker.

PPG-TDI was dissolved in the oil phase prior to emulsification; after homogenisation the Pickering emulsion was allowed to stand without stirring at 20 °C for 20-30 minutes to allow cross-linking to occur. In principle, cross-linking can occur between OH groups *on the same latex particle* as well as between neighbouring latex particles. However, calculation of the effective isocyanate / OH molar ratio used is somewhat problematic, since this depends on the latex contact angle (θ) at the oil/water interface (and this parameter is not known). If we assume that θ is 90°, which is almost certainly an over-estimate, we calculate an isocyanate / OH molar ratio of approximately 1:1 for the 107 nm $PGMA_{50}$-PS latex when employed at a concentration of 1.0 wt % (assuming that all the $PGMA_{50}$ macromonomer chains are located at the latex surface and all the latex is adsorbed onto the oil droplets). Thus there is sufficient polymeric cross-linker to react with every single hydroxy group located at the oil droplet surface. This suggests that significant wastage of the PPG-TDI cross-linker can occur via *intra-particle* cross-linking while still allowing efficient *inter-particle* cross-linking to be achieved.

Table 3.2. Summary of the mean droplet diameter and latex incorporation efficiency for various oil-in-water colloidosomes prepared using three PGMA$_{50}$-PS latexes and PPG-TDI cross-linker with n-dodecane, sunflower oil and isononyl isononanoate as the oil phase. 5.0 ml of aqueous latex was homogenised at 12,000 rpm for 2 mins with 5.0 ml of oil containing 0.025 g of PPG-TDI cross-linker.

Latex	Latex Diameter (DLS)/ nm	Oil	Latex Concentration /wt %	Droplet Diameter /μm	Latex Adsorption Efficiency [a] /%
1	107	n-dodecane	0.35	112 ± 47	> 99
			0.66	59 ± 28	> 99
			0.8	49 ± 23	> 99
			1.2	33 ± 17	> 99
			2.00	26 ± 13	89
			3.46	25 ± 12	51
			5.00	25 ± 14	36
2	1188	n-dodecane	1.90	225 ± 115	> 99
			2.70	160 ± 94	> 99
			4.80	91 ± 35	> 99
			9.40	60 ± 28	80
		sunflower oil	5.00	65 ± 25	95
		isononyl isononanoate	5.00	83 ± 32	90
3	1015	n-dodecane	5.00	92 ± 48	80

a- As judged by gravimetric analysis of the creamed aqueous phase.

Table 3.2 shows the volume-average droplet diameter, D$_{4/3}$, obtained for cross-linked colloidosomes prepared using the three latexes with either n-dodecane, sunflower oil or isononyl isononate as the oil phase. n-Dodecane was chosen as a model oil for further studies.

Determination of the Latex Packing Efficiency on *n*-Dodecane Droplets

It was found that increasing the latex concentration in the aqueous phase reduces the mean droplet diameter, as expected.[18] Also, a significantly higher concentration of the larger latexes (entries 2 and 3, Table 3.1) is required compared to the smaller latex (entry 1, Table 3.1) to compensate for the much lower specific surface areas of the former emulsifiers. In most cases high latex adsorption efficiency is obtained during colloidosome construction, often with more than 99 % of the latex becoming adsorbed at the oil-water interface and negligible excess latex remaining in aqueous solution.

Figure 3.4 shows the relationship between the latex concentration and mean droplet diameter of colloidosomes prepared with the 107 nm $PGMA_{50}$-PS latex and *n*-dodecane as the oil phase. Increasing the latex concentration decreases the mean droplet diameter, until a plateau at 25 μm is reached at around 2.0 wt %. Higher latex concentrations do not lead to any further reduction in droplet size but merely to excess latex particles in solution. This observation is consistent with those reported previously.[18-20] In those cases where no excess latex could be detected in solution, a packing efficiency (P) for the particles adsorbed onto the *n*-dodecane droplets was calculated using an equation previously reported by Balmer *et al.*[17] for large latex particles coated with small silica particles (see equation 1). In the case of *n*-dodecane droplets stabilised by the 107 nm $PGMA_{50}$-PS latex particles, a packing density of 0.85 ± 0.01 is calculated. Hexagonally close packing of spheres on a *planar* surface leads to a maximum P value of 0.91,[17] but the curvature of the oil droplet surface will inevitably lead to packing defects that lower the theoretical packing efficiency. Balmer *et al.*[17] examined the packing efficiency of a relatively polydisperse 20 nm silica sol onto a monodisperse poly(2-vinylpyridine) (P2VP) latex core. They found an experimental packing efficiency of 0.69 ± 0.04, which was somewhat lower than the calculated theoretical maximum packing efficiency of 0.86 ± 0.04. This maximum P value was calculated by taking into account the curvature of the small silica sol packing onto the core particle. In the current work, adsorbing a 107 nm latex onto 25 μm oil cores leads to significantly less curvature of the droplet surface due to the larger difference between the latex and droplet diameters. Therefore the approximation made in equation (1) is less likely to incur any significant error. A

packing efficiency of 0.85 is a reasonable value for this colloidosome system, since it lies between that observed experimentally for the silica/P2VP nanocomposite system and perfect hexagonal packing on a planar surface (0.69 and 0.91, respectively). Using P = 0.85, it was calculated that the minimum concentration (derived from N, see equation 2) of 107 nm latex required for monolayer coverage of a 25 μm droplet should be 1.54 wt %, which is consistent with the experimental data shown in Figure 3.4A. Therefore, under these particular emulsification conditions there is no significant advantage in using latex concentrations above this upper limit of 1.54 wt %, since the droplet diameter will remain constant at 25 μm and any excess latex simply resides in the aqueous phase. A value of P for the larger 1188 nm latex packing around n-dodecane droplets was also calculated (again for the cases where no excess latex could be detected in solution). The same packing efficiency of 0.85 was obtained in this case, with a limiting droplet diameter of 60 μm being achievable at a latex concentration of 7.3 wt % or above (see Figure 3.4B). This suggests that efficient packing of these near-monodisperse PGMA$_{50}$-PS latex spheres is achievable irrespective of the latex size. The same calculated value of P is consistent with both sets of particles having the same surface chemistry and thus adsorbing and packing in a similar way on the n-dodecane droplet surface. Consequently, there appears to be an optimum latex concentration for a given latex diameter and oil type that enables the minimum droplet diameter to be obtained, with essentially all the latex particles being adsorbed onto the oil droplets with comparable packing efficiencies. It is noteworthy that this situation differs from that reported by Walsh et $al.,$[21] who found that polyamine-stabilised latexes were never fully adsorbed on n-dodecane droplets (i.e. were always present in excess in the aqueous continuous phase). The inset in Figure 3.4B shows a high magnification optical microscopy image of a typical individual colloidosome microcapsule prepared with 1015 nm fluorescently-labelled latex particles in which hexagonal close-packing of the latex spheres is clearly observed, along with the boundary scar defects reported by Bausch and co-workers that are characteristic of the packing of small spheres around a larger sphere.[22]
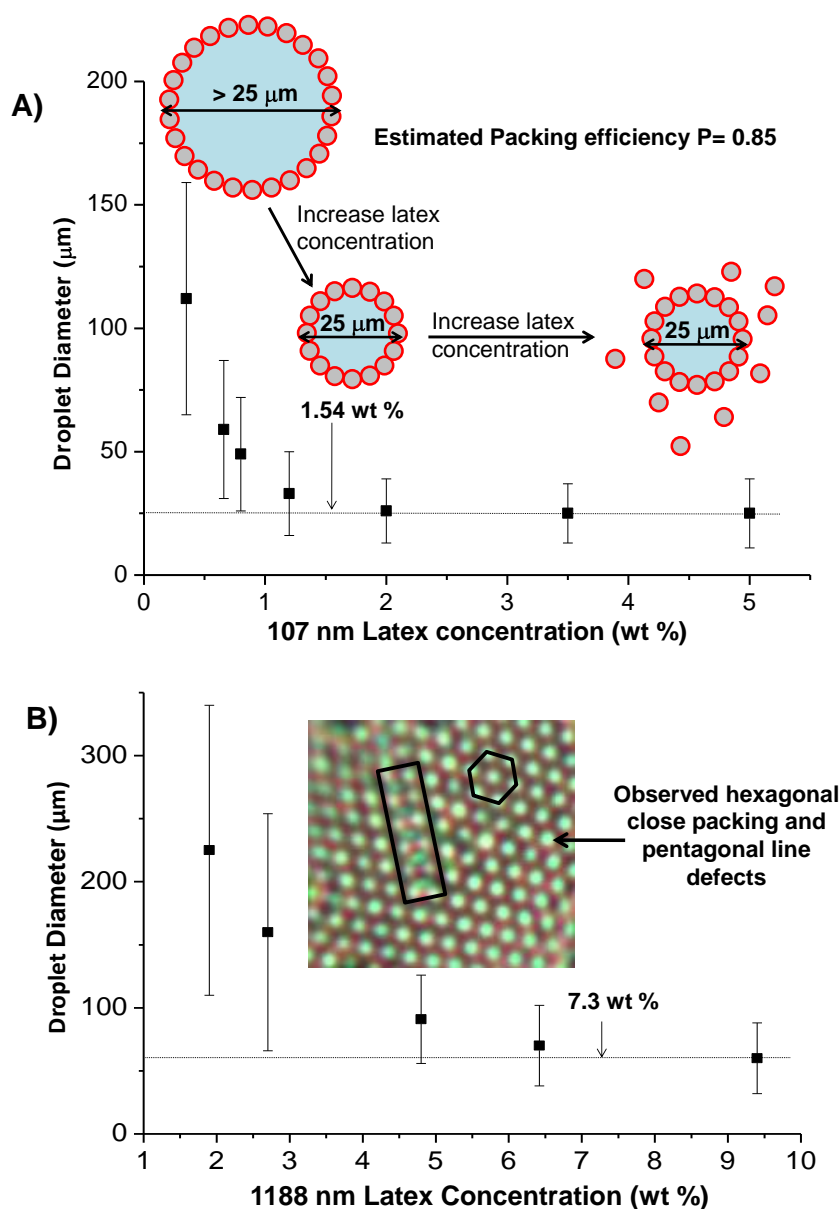
Figure 3.4. Relationship between latex concentration and mean droplet diameter for colloidosomes prepared with (A) 107 nm PGMA$_{50}$-PS particles using *n*-dodecane as the oil phase. The minimum droplet diameter is 25 μm, with further increase in latex concentration leading to excess particles in solution and (B) 1188 nm PGMA$_{50}$-PS particles and *n*-dodecane as the oil phase particles using *n*-dodecane as the oil phase. The minimum possible droplet diameter is 60 μm. An estimated packing efficiency of 0.85 ± 0.01 was calculated in both cases. The inset image shown in (B) is a fluorescence microscopy image of the top of a single emulsion droplet prepared using a fluorescently-labelled 1015 nm PGMA$_{50}$-PS latex. The error bars represent the standard deviation of the measured volume average droplet size distribution.

Alcohol and Surfactant Challenges

Successful cross-linking was assessed by an alcohol challenge, whereby a small aliquot of colloidosome was diluted with excess ethanol (which is a common solvent for both the water and oil phases)[23] and observed by optical and fluorescence microscopy (see Figure 3.5).
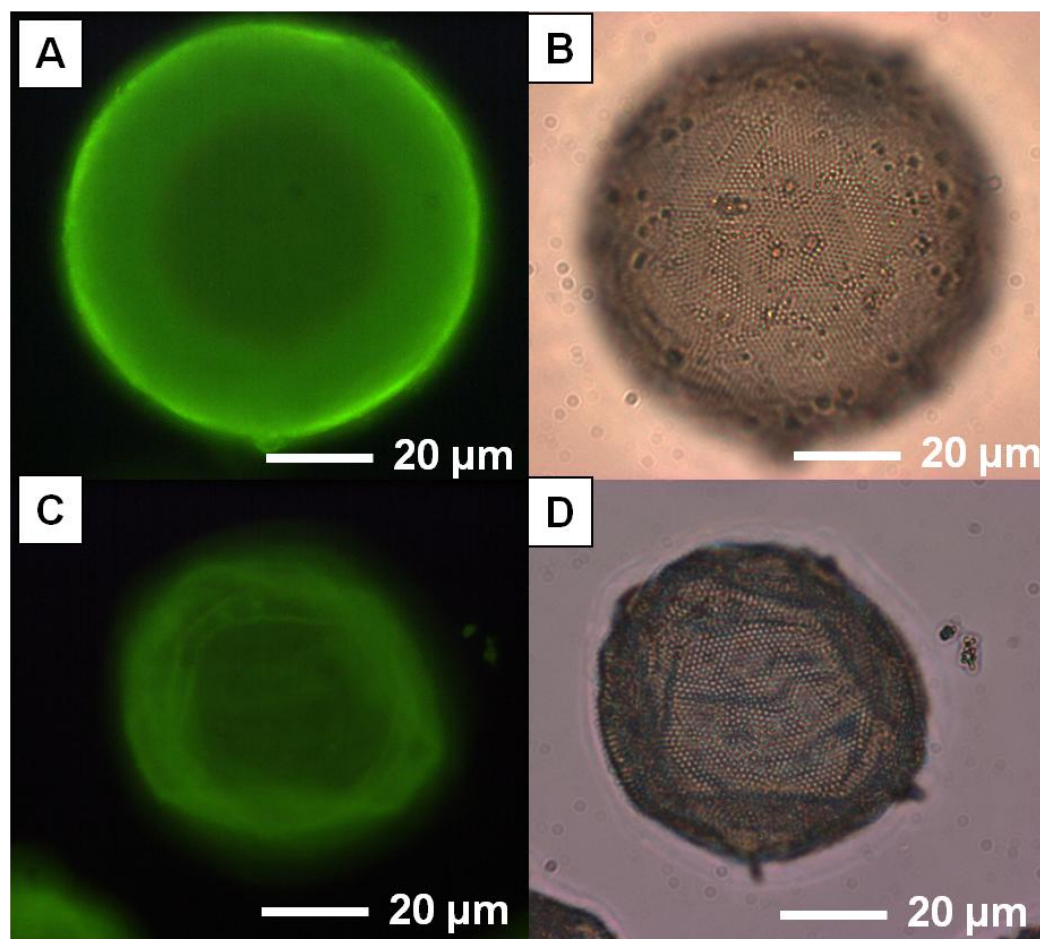
Figure 3.5. (A) Fluorescence microscopy image of a PPG-TDI cross-linked colloidosome prepared with 1015 nm fluorescently-labelled $PGMA_{50}$-PS latex and *n*-dodecane (B) bright field image of the same colloidosome (note that the individual latex particles on the colloidosome surface can be resolved). (C) Fluorescent microscopy image of the collapsed colloidosome obtained after washing with excess ethanol (D) bright field image of the same ethanol washed colloidosome (again the individual latex particles can be seen).

When the non-cross-linked Pickering emulsion is subjected to such a challenge, no microcapsules are observed by optical microscopy and only latex debris is visible by SEM (Figure 3.6A). In contrast, when covalently cross-linked colloidosomes are

challenged with ethanol, intact microcapsules are observed by both optical and scanning electron microscopy. Figure 3.6B and 5C shows SEM images of colloidosomes prepared with either 107 nm or 1188 nm PGMA$_{50}$-PS latex (see entries 1 and 2 in Table 3.1). Such capsules also collapse during ethanol evaporation (i.e. prior to UHV conditions). A lower magnification image shows a large population of cross-linked colloidosomes observed for a typical sample, showing that this is an efficient route to produce colloidosomes.

Further evidence of successful cross-linking is provided by challenging the non-cross-linked Pickering emulsions and covalently cross-linked colloidosomes with a surfactant. It is well known that surfactants can displace adsorbed particles from the oil-water interface.[24-25] However, the PPG-TDI cross-linked colloidosomes exhibited excellent stability when subjected to a surfactant challenge: addition of a non-ionic surfactant (Triton X-100) produced minimal change in volume-average droplet diameter (see Figure 3.7). In contrast, non-cross-linked Pickering emulsions exposed to Triton X-100 exhibited a significant reduction in volume-average droplet diameter from 129 ± 68 μm to 38 ± 18 μm, with the latter value being very close to the mean diameter obtained for a Triton X-100-stabilised emulsion. This observation suggests that this surfactant had displaced the latex particles as the primary emulsion stabiliser, as depicted in Figure 3.8A.
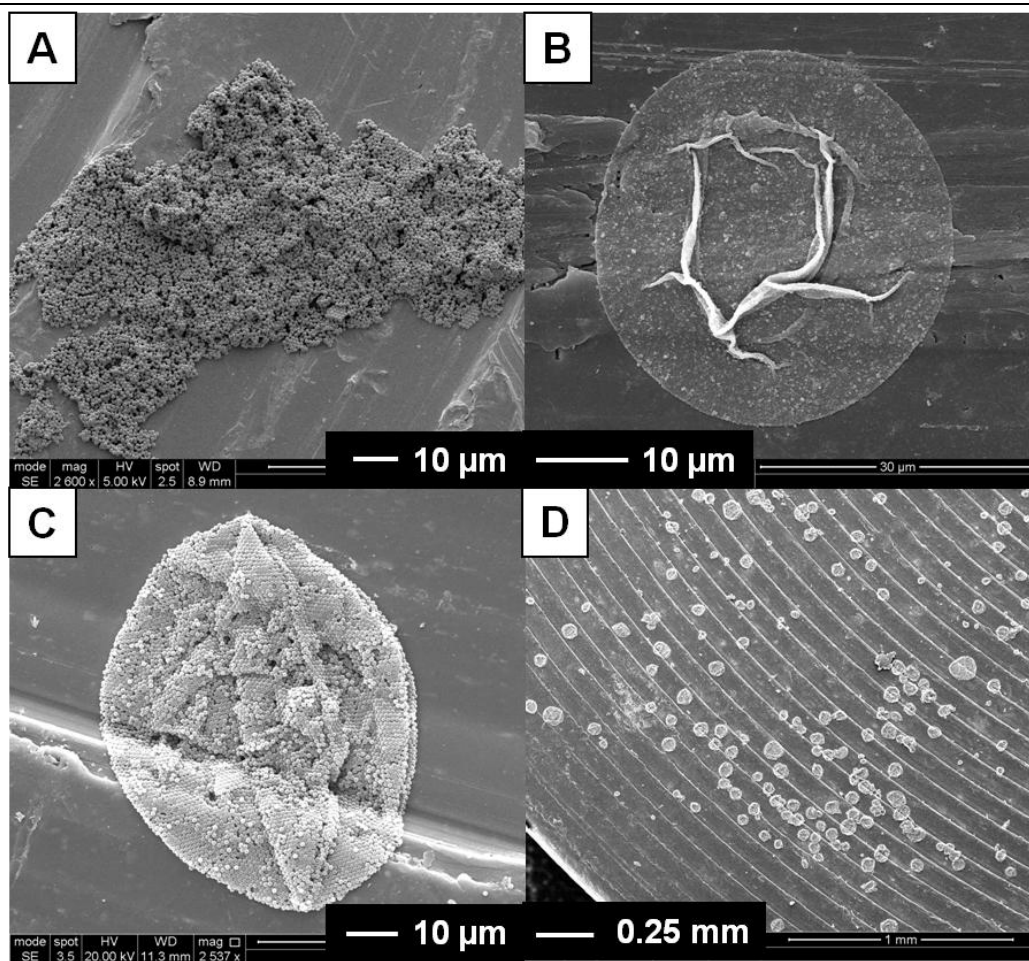
Figure 3.6. Scanning electron microscopy images obtained after ethanol challenges of (A) latex debris obtained with a non-cross-linked Pickering emulsion prepared with 5.0 % 1188 nm PGMA$_{50}$-PS particles, (B) cross-linked colloidosomes prepared with 1.0 % 107 nm PGMA$_{50}$-PS particles, (C) cross-linked colloidosomes prepared with 5.0 % 1188 nm PGMA$_{50}$-PS particles and (D) a lower magnification image of sample C showing multiple colloidosomes. The oil phase was *n*-dodecane in each case.

Non cross-linked *n*-dodecane/water emulsions

Before Triton X-100
(129 ± 68 μm)

After Triton X-100
(38 ± 18 μm)

Triton X-100
stabilised emulsion
(34 ± 13 μm)

Droplet Diameter (μm)

Cross-linked colloidosomes

Before Triton X-100
(112 ± 47 μm)

After Triton X-100
(116 ± 58 μm)

Droplet Diameter (μm)
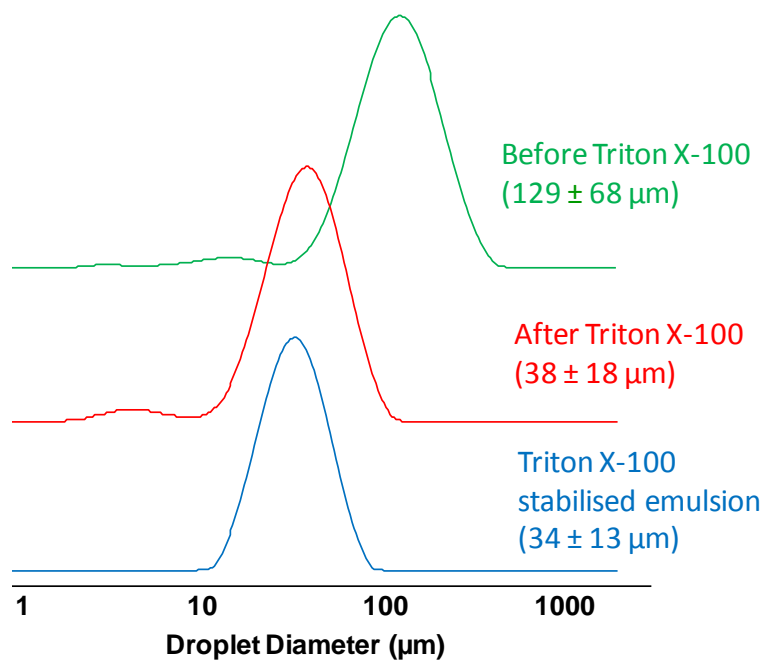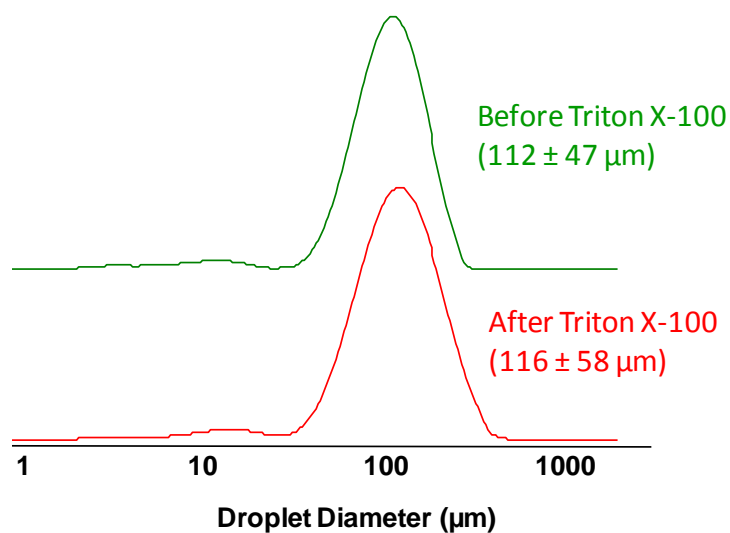
Figure 3.7. Laser diffraction (Malvern Mastersizer) particle size distribution curves obtained for both non-crosslinked (top) and crosslinked (bottom) 107 nm PGMA$_{50}$-PS latex-stabilised *n*-dodecane-in-water emulsions, before and after addition of Triton X-100 surfactant. A Triton X-100-stabilised *n*-dodecane-in-water emulsion is provided as a reference.

This conclusion was supported by visual inspection of the (lower) aqueous phase that formed once the oil droplets within the colloidosome microcapsules had been allowed to cream on standing at 20 ^{o}C. For cross-linked colloidosomes prepared with the 107 nm PGMA$_{50}$-PS latex, this aqueous phase always remained transparent (for latex concentrations < 1.54 %) even after the addition of Triton X-100 surfactant (see Figure 3.8C). In contrast, the aqueous phase always became milky for the Pickering emulsions, indicating that non-cross-linked latex particles are easily displaced from the oil-water interface by the surfactant (see Figure 3.8B). DLS studies of the isolated aqueous phase confirmed the presence of the displaced latex in the latter case.
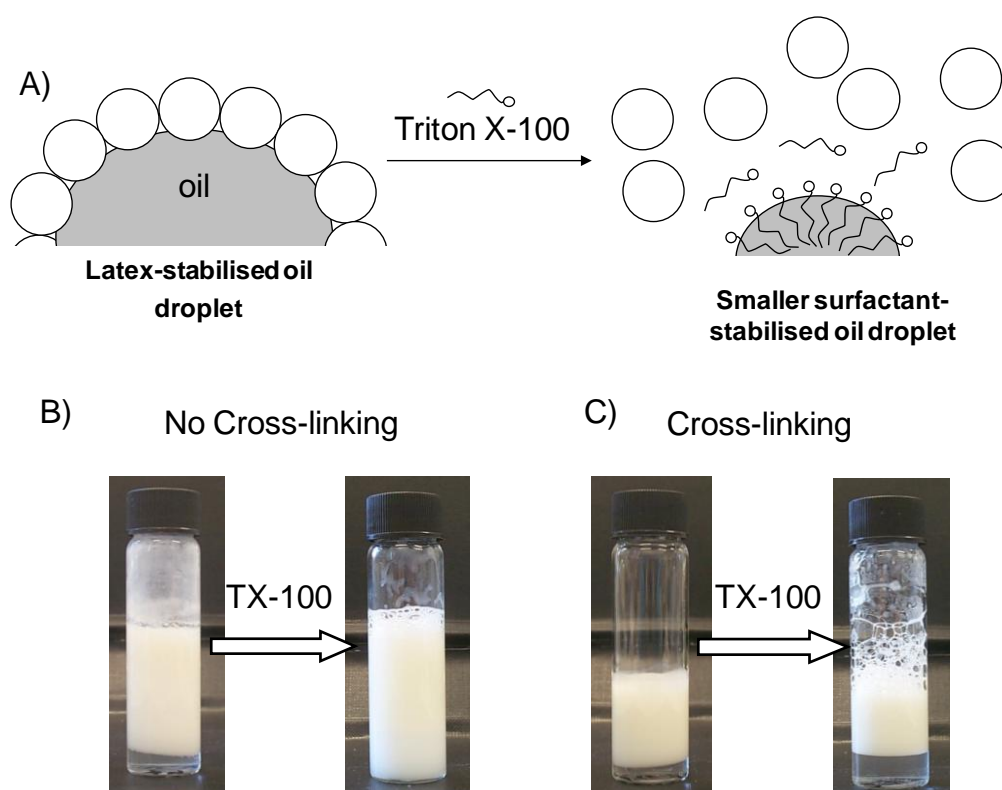
Figure 3.8. A) Schematic representation of a surfactant challenge to a non-cross-linked Pickering emulsion, where the Triton X-100 surfactant replaces the PGMA$_{50}$-PS particles at the droplet interface and results in a reduction in the average droplet diameter. Digital photographs obtained for (B)a non-cross-linked Pickering emulsion and (C) PPG-TDI cross-linked colloidosomes before and after a surfactant challenge. Note the clear lower aqueous phase in the latter case, suggesting that no particle replacement has occurred.

Confirming the Absence of Inter-colloidosome Fusion

When cross-linking at such high solids (50 vol %) the question of whether any inter-colloidosome fusion occurs arises. It was hypothesised that due to the hydrophobic oil soluble nature of the PPG-TDI, the cross-linker should be confined to the internal oil phase. This suggests that the chances of any cross-linking between adjacent colloidosomes capsules would be highly unlikely. To investigate this further laser diffraction studies as a function of cross-linking time were carried out. These confirmed that the cross-linking reaction is indeed confined to the droplet phase, as expected.

Figure 3.9 shows representative droplet size distributions recorded for freshly-prepared covalently cross-linked colloidosomes and on standing for 3 h and 330 h after homogenisation. Immediately after homogenisation cross-linking was not yet complete, as judged by the alcohol challenge and optical microscopy studies. Thus the initial droplet size distribution is essentially that of the original Pickering emulsion. Three hours after homogenisation, intact colloidosomes are observed by optical microscopy, but minimal change is observed in the volume-average droplet diameter. A similar size distribution was obtained 330 h after the initial homogenisation. This indicates that the PPG-TDI cross-linker is indeed confined to the oil phase and minimal inter-colloidosome cross-linking occurs even at 50 vol % solids. Given the known high reactivity of diisocyanate groups towards water, a water-soluble equivalent of the oil-soluble PPG-TDI cross-linker is simply not feasible: such cross-linking chemistry must necessarily be restricted to the oil droplet phase. Very recently, similar results have been obtained for covalently cross-linked colloidosomes prepared with a polyamine-functionalised latex using three different polymeric cross-linkers in turn.[21] In this case, cross-linking was also achievable from the external aqueous phase. Surprisingly, no inter-colloidosome fusion occurred using this external cross-linker, despite the relatively high solids content utilised (50 vol %). This is a potentially important advance compared to previous cross-linking protocols[11] and demonstrates that the spatial location of the cross-linker may not be as important as originally anticipated.

A)

Immediately after homogenisation

65 ± 25 µm

B)

3 hours after homogenisation

66 ± 25 µm

C)

330 h after homogenisation

71 ± 30 µm

| 0.1 | 1 | 10 | 100 | 1000 |

Droplet Diameter (µm)
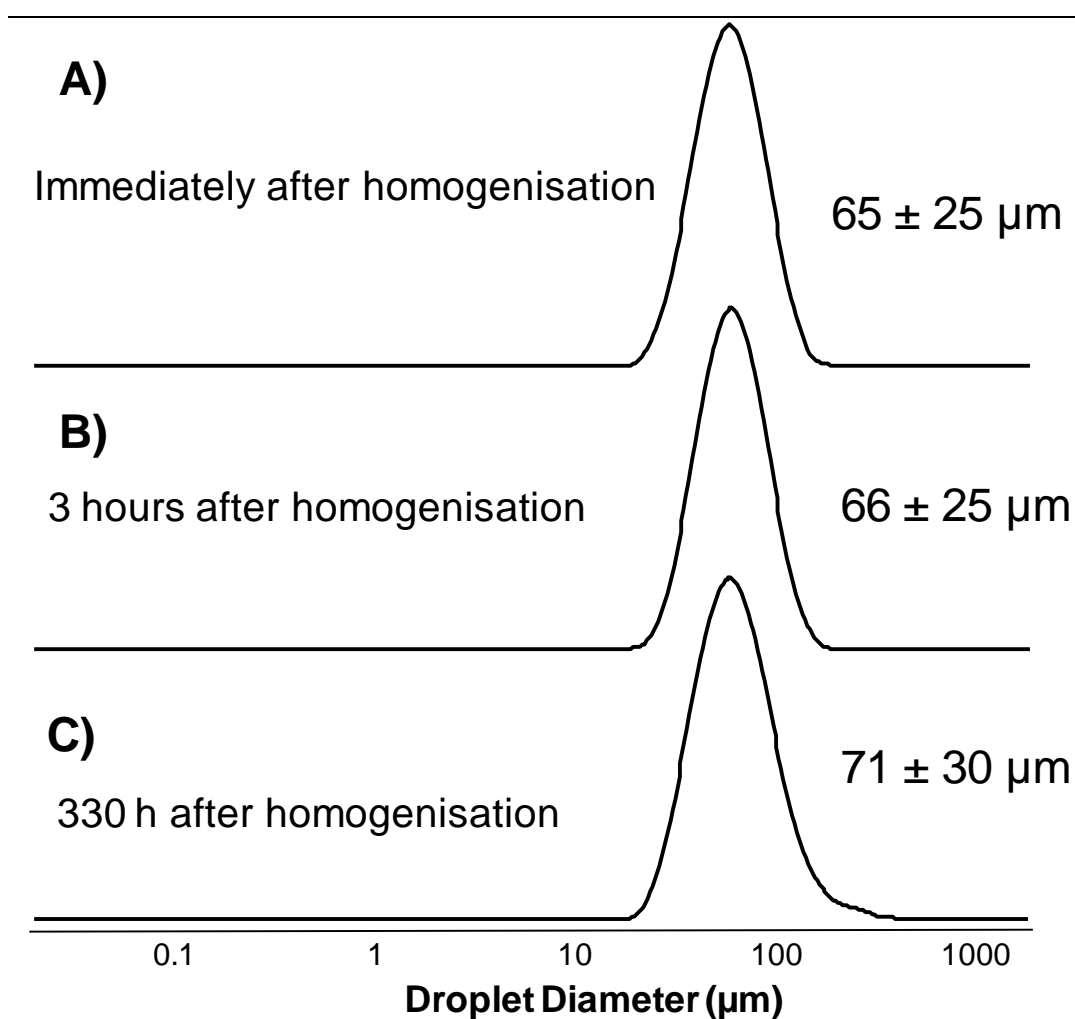
Figure 3.9. Laser diffraction particle size distribution curves obtained using a Malvern Mastersizer for cross-linked colloidosomes prepared with 1188 nm PGMA$_{50}$-PS latex particles (5.0 wt %) and sunflower oil (A) immediately after homogenisation (when cross-linking is incomplete as judged by an ethanol challenge combined with optical microscopy), (B) 3 h after homogenisation when cross-linking is now complete and (C) 330 h (two weeks) after homogenisation. Little difference in these droplet size distributions is observed confirming that minimal inter-colloidosome fusion occurs during cross-linking since the cross-linker is confined to the oil phase. PPG-TDI concentration 5 mg/ml of oil.

The majority of colloidosomes in this work were prepared using approximately 5 mg/ml of PPG-TDI dissolved in 5.0 ml of the appropriate oil phase. As mentioned earlier this concentration ensures there is more than enough cross-linker to react with all the PGMA units present at the colloidosome inner surface. It is perhaps worth mentioning that varying the PPG-TDI concentration has minimal effect on the droplet size distribution for this system. Figure 3.10 shows an example of colloidosomes prepared with varying concentrations of cross-linker. At 5 mg/ml or below the mean droplet diameter is essentially constant, with little or no dependence on the PPG-TDI concentrations.

PPG-TDI	Droplet Diameter
1 mg/ml	56 ± 25 μm
2 mg/ml	54 ± 20 μm
5 mg/ml	53 ± 21 μm
10 mg/ml	78 ± 87 μm
20 mg/ml	65 ± 67 μm
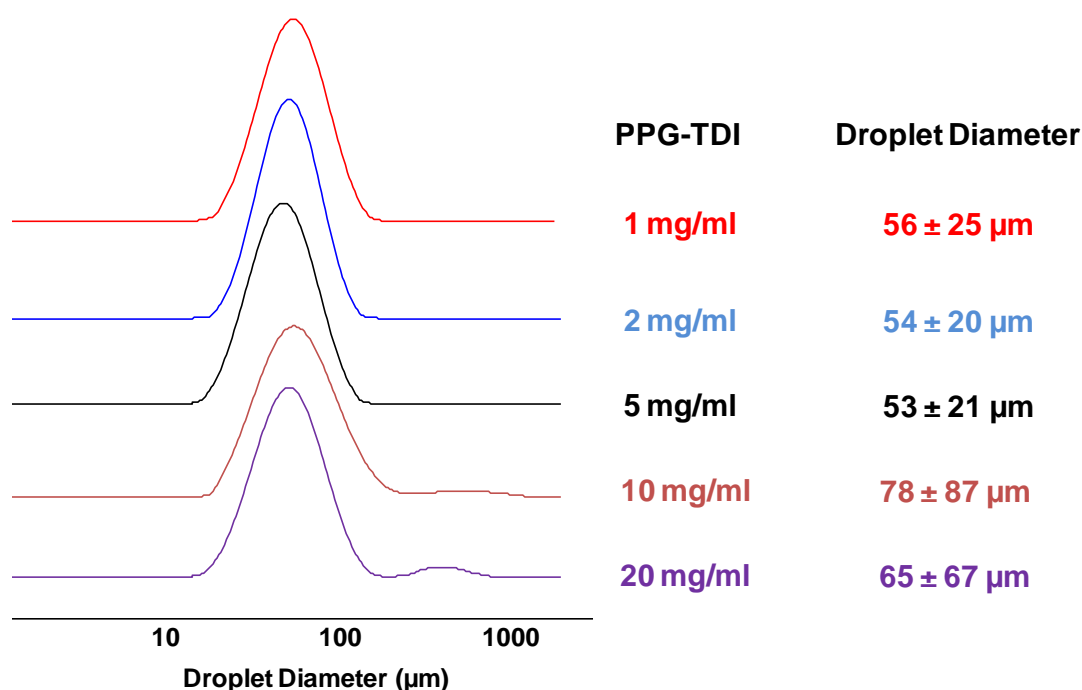
Figure 3.10. Laser diffraction particle size distributions obtained for colloidosomes prepared with varying concentrations of PPG-TDI cross-linker in the oil phase. An aqueous solution of 1.0 wt % 107 nm $PGMA_{50}$-PS latex was used in each case and the oil phase was sunflower oil. Emulsification was conducted at 12,000 rpm for 2.0 minutes at 20 °C.

When the cross-linker concentration was increased to 10 or 20 mg/ml, laser diffraction studies detected some larger droplets, which increase the volume-average diameter of the emulsion. This could be an indication of some emulsion instability such as droplet coalescence, although it is important to emphasise that no

demulsification was observed. However, given that the cross-linker is present in excess, it is not necessary to increase the concentration further for colloidosome formation. Thus this potential reduction in stability is not a significant problem. Also, successful colloidosomes were prepared for all cross-linker concentrations examined. It was thought that, at extremely high cross-linker concentrations, there might be a significant amount of mono-reacted diisocyanate (due to the large excess of cross-linker) which may well hinder colloidosome formation. However, this is not the case for the concentration range investigated. Furthermore, increasing the PPG-TDI concentration did not strengthen the microcapsules towards collapse after the ethanol challenge. Presumably, the resulting cross-links are either too flexible or additional reaction is mainly mono-functional which does not aid capsule strength.

Spectroscopic Detection of the PPG-TDI Cross-linker

Since the cross-linker chosen is polymeric in nature, it was hoped that this would aid it spectroscopic detection, in order to prove that it is indeed reacting with the GMA groups on the latex. Colloidosomes prepared using PPG-TDI were extensively washed with ethanol prior to dissolution in d_5-pyridine. Subsequent ^{1}H NMR studies confirmed the presence of the polymeric cross-linker, suggesting that successful cross-linking had indeed occurred (see Figure 3.11).

Control experiments using dihydroxy-capped PPG of comparable molecular weight confirmed that this non-reactive species was completely removed during the ethanol wash. Thus the PPG-TDI must be chemically grafted via the PGMA chains, rather than merely physically occluded within the colloidosomes. It is perhaps worth emphasising that the polymeric nature of the PPG-TDI cross-linker is actually essential for its detection, since NMR is a relatively insensitive technique. NMR analysis of dried cross-linked colloidosomes prepared with the 1188 nm latex was also attempted. In this case, the PPG-TDI peaks were barely detectable due to the larger latex diameter (and correspondingly much lower PGMA content).

.
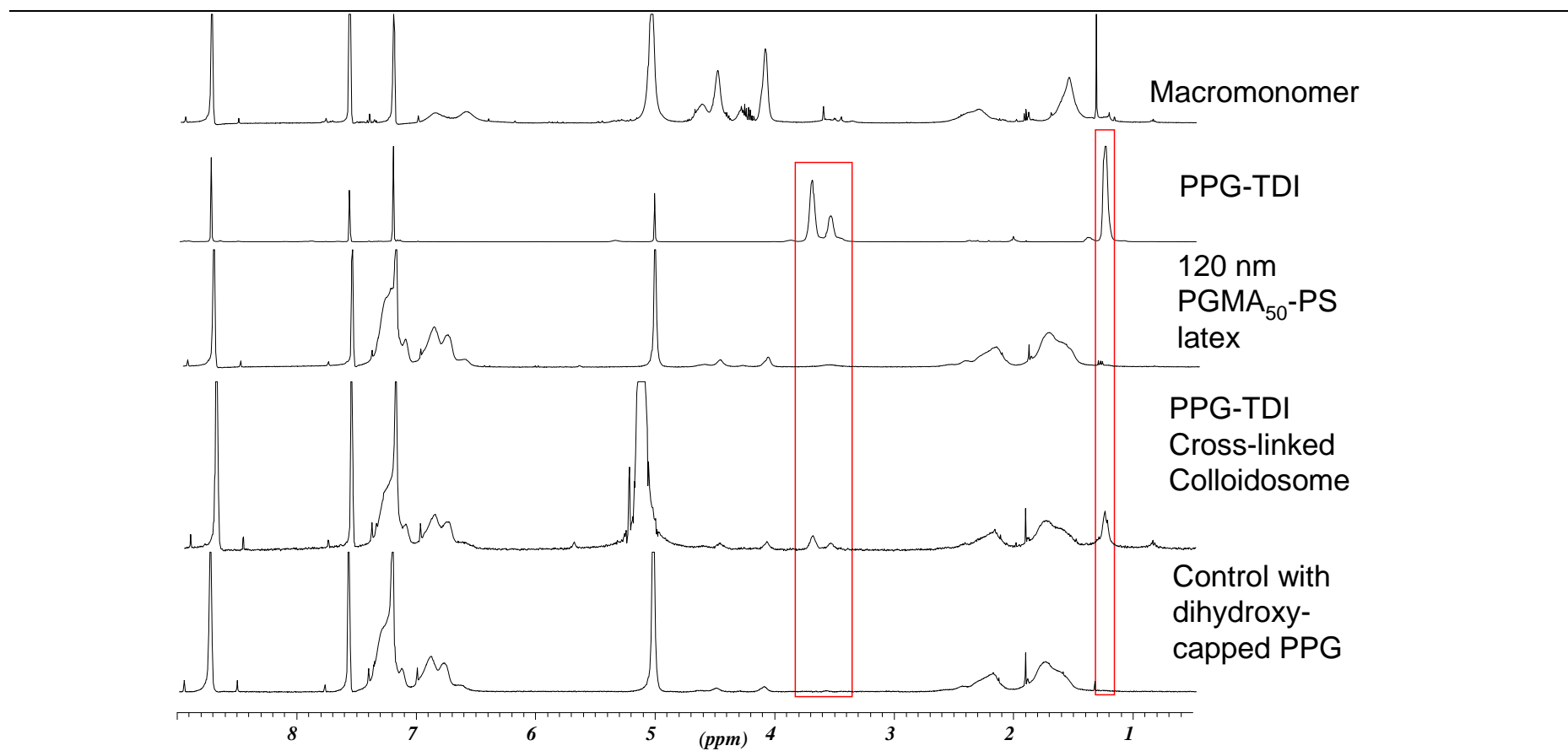
Figure 3.11. ^{1}H NMR spectra recorded in d_5-pyridine for PGMA$_{50}$ macromonomer, PPG-TDI cross-linker, 107 nm PGMA$_{50}$-PS latex particles and cross-linked colloidosomes after repeatedly washing with ethanol to remove excess cross-linker.
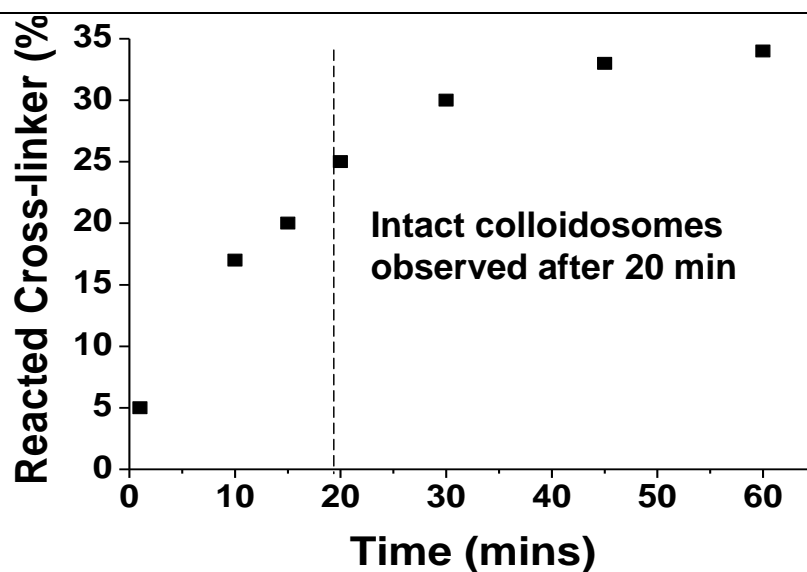
Figure 3.12. Increase in the proportion of reacted PPG-TDI cross-linker within the colloidosome with reaction time. Aliquots taken from the colloidosome reaction solution were quenched at various time intervals by washing with excess ethanol. Quenched colloidosomes were then dried and dissolved in d^5-pyridine for ^{1}H NMR analysis.

^{1}H NMR also proved to be very useful for monitoring the kinetics of colloidosome cross-linking (see Figure 3.12). The colloidosome reaction solution was sampled at various time intervals after homogenisation of the oil and aqueous phases and each aliquot was immediately quenched and washed repeatedly with excess ethanol. This sampling protocol ensures that any unreacted cross-linker is quenched with ethanol and hence removed along with the oil phase. ^{1}H NMR spectra (Figure 3.13) show the aliphatic backbone protons at δ 1.4-2.7 due to the polystyrene latex chains, along with the methylene and methine backbone protons and pendent methyl protons due to the PPG repeat units of the cross-linker at δ 3.5-3.8 and δ 1.27, respectively. Comparing the backbone signals for the polystyrene and PPG-TDI components confirms that the proportion of reacted cross-linker found within the colloidosomes increases with reaction time. Inspection of ethanol-washed reaction solutions using optical microscopy confirmed that intact colloidosomes were formed within 20 minutes at 20 °C. Thus, only ~ 20-25 % of the original PPG-TDI cross-linker is actually required to 'lock-in' the colloidosome structure and this cross-linking chemistry occurs quite rapidly under mild conditions.
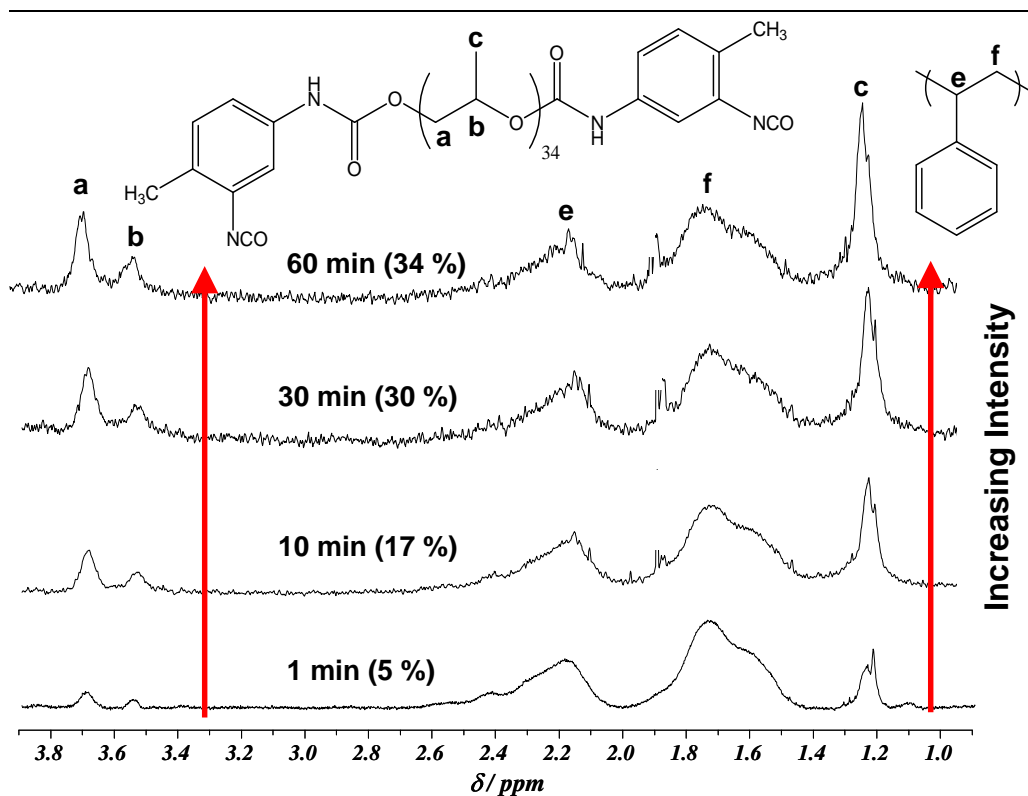
Figure 3.13. ^{1}H NMR spectra recorded for cross-linked colloidosomes sampled 1, 10, 30 and 60 minutes after homogenisation. Notice the increase in signal intensities at both 1.27 and 3.5-3.8 ppm due to the PPG-TDI cross-linker relative to the polystyrene backbone. For quantification purposes, the signals at 3.5-3.7 ppm were preferred since these were better resolved relative to the baseline.

FT-IR spectra were also recorded for these dried cross-linked colloidosomes (see Figure 3.14). Unfortunately it was not possible to confirm the presence of the new urethane bonds, since this band overlaps with the carbonyl band from the GMA units. However, a prominent band at 1097 cm^{-1} was observed in the spectra obtained for both the cross-linker and the washed/dried colloidosomes. This feature is assigned to the C-O stretch due to the PPG repeat units of the cross-linker. This again supports our findings that the PPG-TDI reacts with the GMA units on the latex surface and becomes covalently bound.
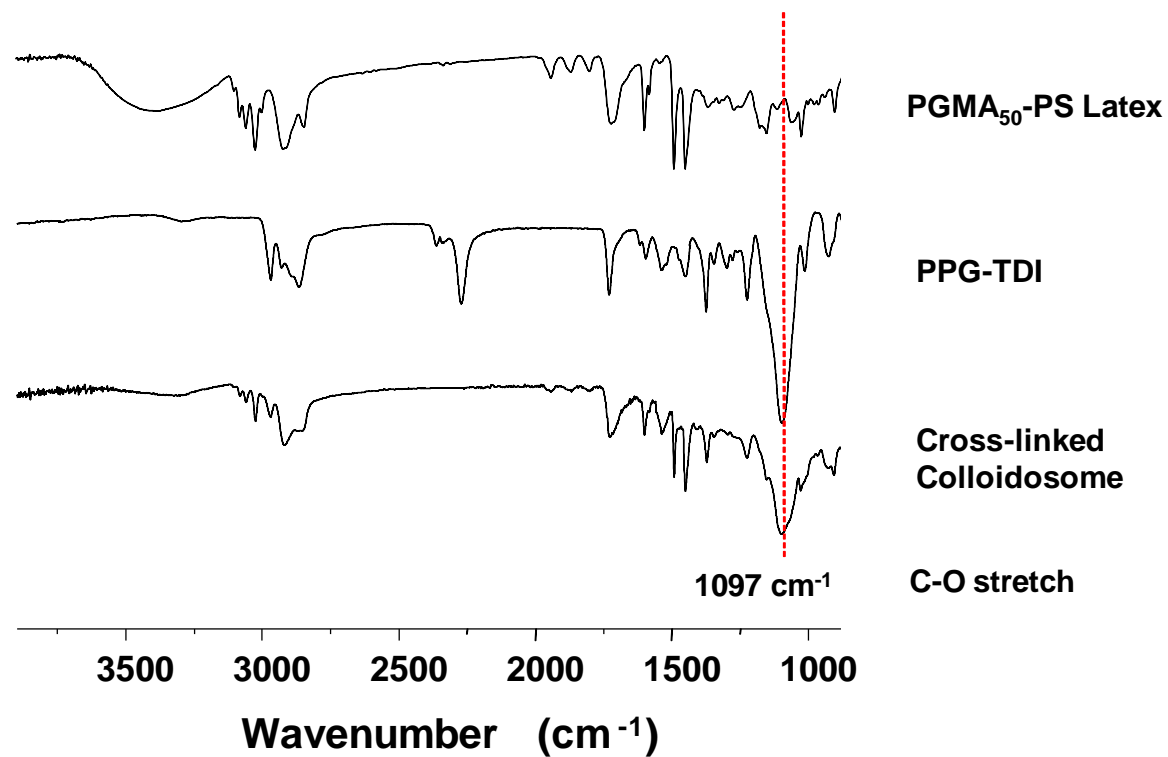
Figure 3.14. FT-IR spectra recorded for the 107 nm PGMA$_{50}$-PS latex (top), the PPG-TDI cross-linker (middle) and ethanol-washed, dried covalently cross-linked colloidosomes prepared with the 107 nm latex. Note the presence of the strong C-O stretch at 1097 cm^{-1} due to the PPG-TDI cross-linker in the colloidosome spectrum.

Solvent and Thermal Annealing of Cross-linked Colloidosomes

Although robust colloidosomes can be obtained by PPG-TDI cross-linking alone, the resulting microcapsules are expected to be highly permeable due to their many interstitial pores. Previous workers have shown that thermal annealing can reduce and potentially close these interstices.[6-7, 26] In principle, this simply involves heating the latex particles to above their glass transition temperature, which for polystyrene is approximately 105 ^{o}C. However, annealing at such a high temperature could have implications for the encapsulation of temperature-sensitive actives, and cannot be achieved for oil-in-water Pickering emulsions without the addition of high b.p. water-miscible co-solvents such as glycerol.[6]

Therefore an alternative lower temperature annealing protocol was investigated. Cyclohexane (20 vol % based on *n*-dodecane) was incorporated into the oil phase prior to emulsification at room temperature. The UCST for polystyrene in cyclohexane is 35 ^{o}C[27] and so by heating the cross-linked colloidosomes to 50 ^{o}C substantial annealing was observed well below the T_g of the latex core. The effect of cyclohexane annealing in both the presence and absence of the PPG-TDI cross-linker at 50 vol % solids is investigated and also the extent of inter-colloidosome fusion that occurs under these conditions is explored. In these experiments the 1188 nm latex is focused on, this is because colloidosome interstices formed by these larger particles are far easier to observe by SEM. Figure 3.15 shows SEM images of both cross-linked and non-cross-linked samples prepared with the 1188 nm latex, before (A and B) and after (C and D) cyclohexane annealing at 50 ^{o}C for 60 minutes.

Before heating, Figure 3.15A shows the latex debris that is always observed in the absence of cross-linking while Figure 3.15B shows an example of the collapsed colloidosome structure that is typically observed in the presence of cross-linker. After heating to 50 ^{o}C for 1 h both samples exhibit significant evidence for interstitial annealing, with microcapsules also being formed in the absence of any PPG-TDI cross-linker. However, it is emphasised that the yield of intact microcapsules prepared without any cross-linker is relatively low and many fractured and broken particles are also observed by SEM under these conditions (see Figure 3.16).
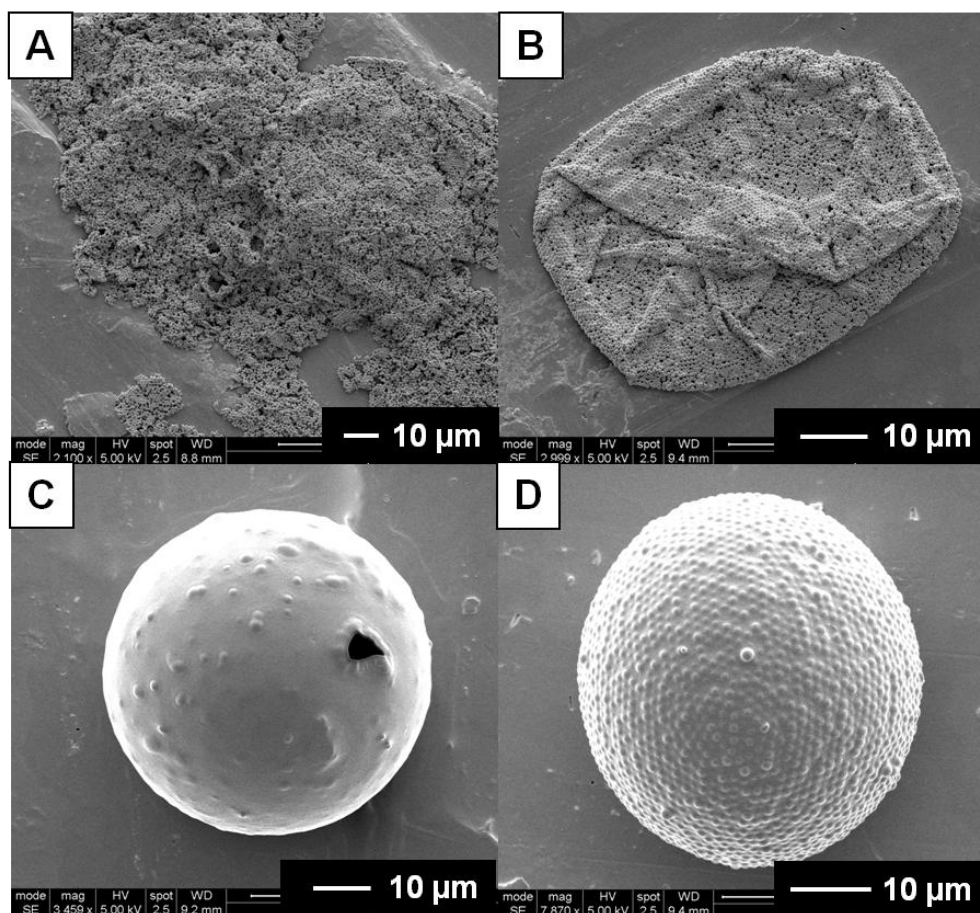
Figure 3.15. Scanning electron microscopy images of samples prepared using 5.0 % 1188 nm PGMA$_{50}$-PS latex particles and a 4:1 *n*-dodecane/cyclohexane oil mixture. (A) Only latex debris is observed in the absence of cross-linker at 20 ^{o}C. (B) A collapsed colloidosome is obtained in the presence of the PPG-TDI cross-linker at 20 ^{o}C. (C) A solvent-annealed colloidosome prepared in the absence of cross-linker after heating to 50 ^{o}C for 1 h. (D) A solvent-annealed and cross-linked colloidosome prepared in the presence of PPG-TDI cross-linker after heating to 50 ^{o}C for 1 h. Note that covalent cross-linking of the latex particles appears to hinder the extent of annealing (compare the surface texture of C with D).
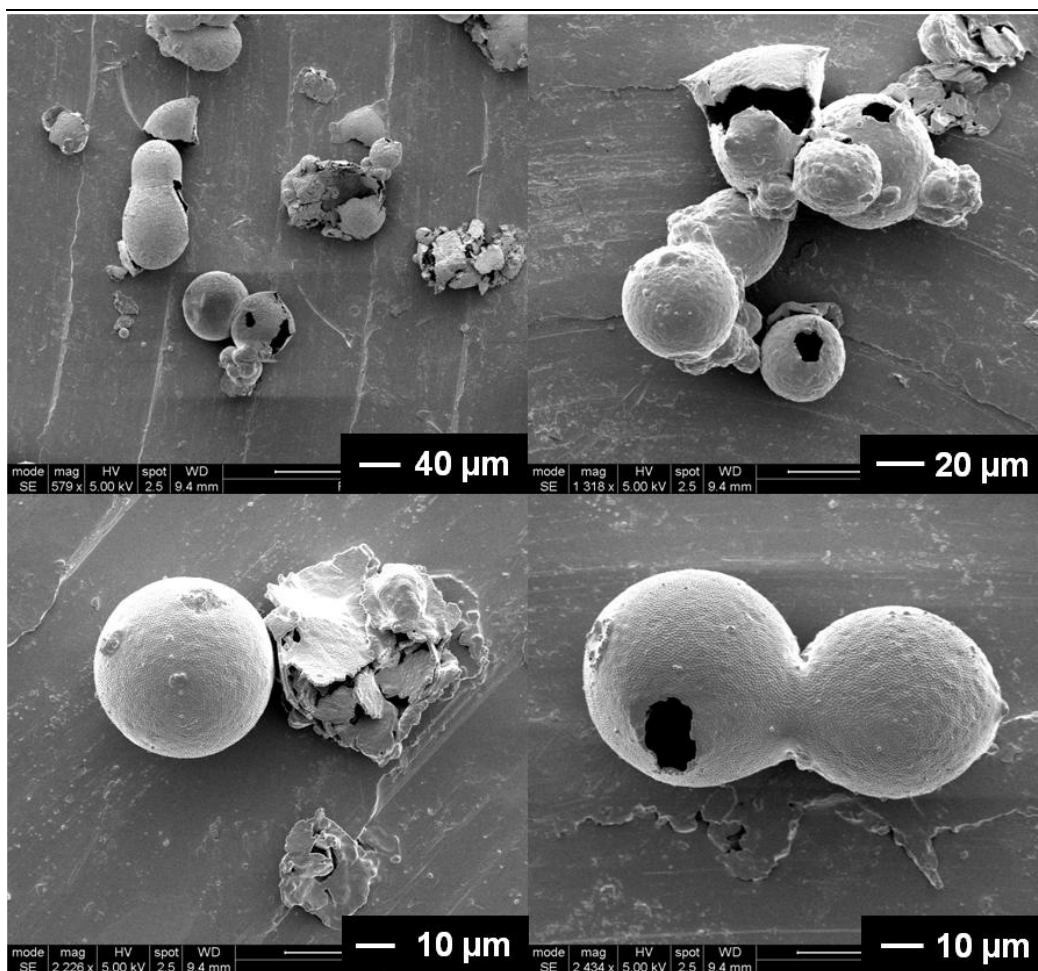
Figure 3.16. Scanning electron microscopy images of microcapsules after an ethanol challenge prepared in the absence of any PPG-TDI cross-linker, with 5.0 wt % 1188 nm $PGMA_{50}$-PS latex and 4:1 n-dodecane/cyclohexane oil phase (50 vol %), after being heating to 50 ^{o}C for 60 minutes. Note the presence of many crushed/broken capsules and the evidence for partial capsule fusion.

In contrast, all the cross-linked and annealed colloidosomes that were visible on the SEM stub remained intact. Although partial collapse is still observed under the UHV conditions required for these SEM studies, no rupture or breakage occurs compared to the non-cross-linked capsules (see Figure 3.17). Comparing the capsules in the presence and absence of cross-linker, it also appears that the extent of annealing achieved after 1 h is somewhat reduced in the presence of cross-linker (since the microcapsule surface is not as smooth as that observed in the absence of cross-linker). This difference is attributed to the PPG cross-links between latex particles potentially hindering latex coalescence.
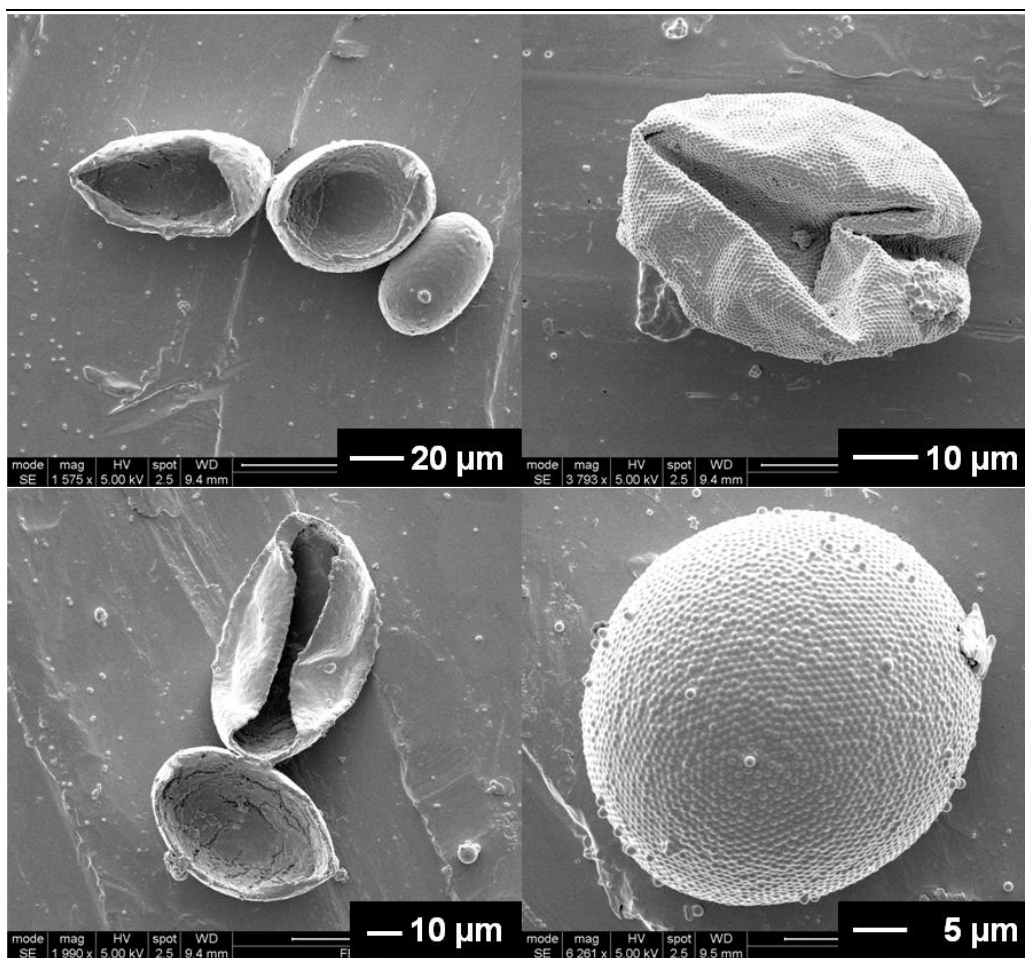
Figure 3.17. Scanning electron microscopy images of microcapsules after an ethanol challenge prepared in the presence of PPG-TDI cross-linker, with 5.0 wt % 1188 nm PGMA$_{50}$-PS latex and 4:1 n-dodecane/cyclohexane oil phase (50 vol %), after heating to 50 $^{\circ}$C for 60 minutes. Note that collapse is still observed under the UHV conditions of the SEM. However, there was no evidence for any crushed/broken capsules.

It is also noteworthy that, unlike cross-linking alone, cyclohexane annealing at 50 vol % results in a substantial amount of inter-colloidosome fusion, as illustrated in Figure 3.18. The droplet size distribution shifts to higher diameters for longer annealing times, which indicates partial agglomeration of the colloidosomes under these conditions. Similar observations have been made by others who have tried annealing at high solid contents.[7, 28] Significant dilution would be required to minimise this inter-colloidosome fusion and hence ensure discrete microcapsules, which is not likely to be commercially attractive.
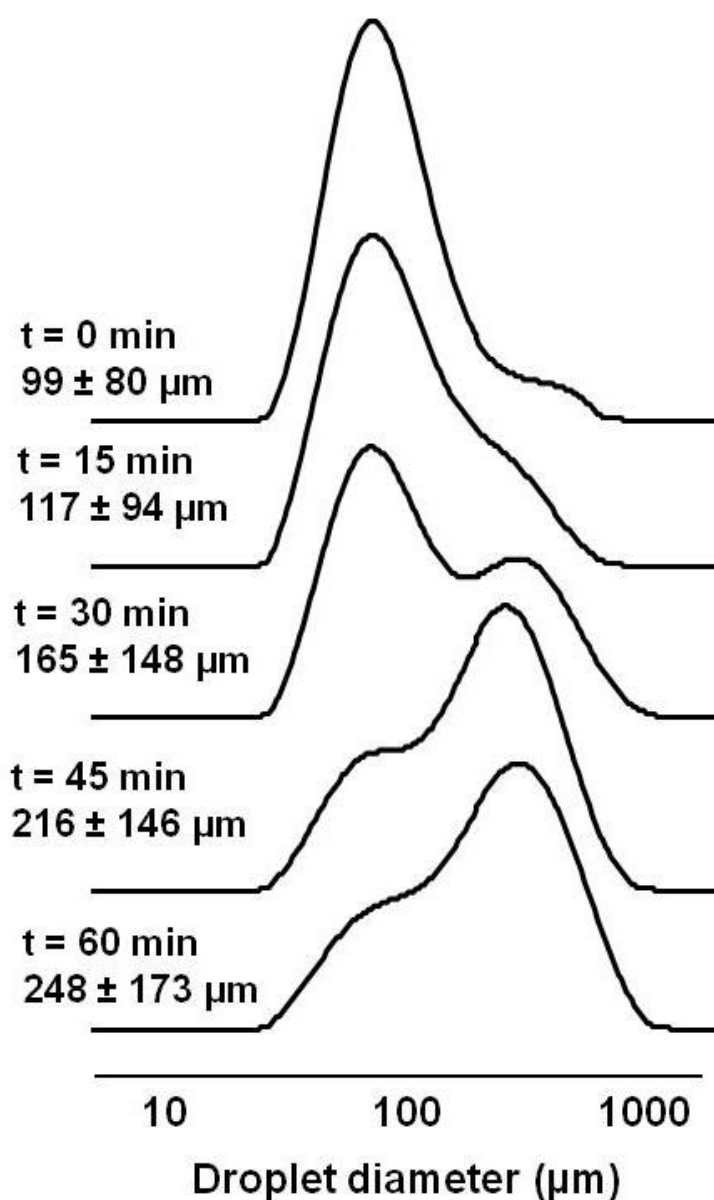
Figure 3.18. Laser diffraction particle size distribution curves obtained using a Malvern Mastersizer for cross-linked colloidosomes prepared with 1188 nm PGMA$_{50}$-PS latex and 4:1 n-dodecane/cyclohexane oil phase after annealing at 50 ^{o}C for up to 1 h. The droplet size distribution shifts to higher diameters upon increasing the annealing time, demonstrating that neighbouring capsules become fused together when annealing occurs at 50 vol %.

Interestingly, it was also found that significant thermal annealing can occur well below the latex T_g, without the addition of a cyclohexane co-solvent. The T_g of the 1188 nm $PGMA_{50}$-PS latex was 103 °C, as determined by differential scanning calorimetry. This value is in good agreement with the literature value for polystyrene of 100 °C.[27] Covalently cross-linked colloidosomes were prepared and then heat-treated at either 50, 70 or 90 °C in an oven for up to 4 h to assess the extent of annealing that could be achieved in the absence of cyclohexane co-solvent.

Figure 3.19 shows SEM images of covalently cross-linked colloidosomes after being heated to either 70 °C or 90 °C for 1 h. Substantial annealing occurs in both cases, despite this sintering temperature being 10-30 °C below the T_g of the polystyrene latex. As expected, the SEM images indicated that more annealing occurred at 90 °C, which is consistent with the higher sintering temperature. Perhaps more surprisingly, some thermal annealing occurred in the absence of any cyclohexane at 50 °C. However, the annealing times required at this relatively low temperature were far longer than those required in the presence of cyclohexane, with interstices still visible after 4 h of annealing in the former case. Biggs and co-workers[28] have also achieved annealing of similar colloidosomes at lower temperatures (86 °C). In their case the steric stabiliser for the polystyrene latex was a poly(2-dimethylaminoethyl methacrylate-block-methyl methacrylate) diblock copolymer (PDMA-b-PMMA). DSC measurements indicated a thermal transition at 107 °C attributed to the T_g of the polystyrene latex core. Two further transitions were observed at 90 and 75 °C, which were assigned to thermal transitions within the adsorbed block copolymer chains on the latex surface. Biggs and co-workers therefore conclude that "The glass transition of the adsorbed polymer shell rather than that of the PS cores allows the annealing to be successfully carried out at temperatures significantly lower than that of the core". Unlike Biggs and co-workers,[28] no separate temperature transition was observed by DSC for the $PGMA_{50}$ steric stabiliser chains. This is perhaps not surprising seeing as in contrast to PDMA, PGMA is not a thermo-responsive polymer. Therefore in this case, the observed annealing must be due to film formation of the polystyrene core and not due to any secondary transition of the steric stabiliser shell.
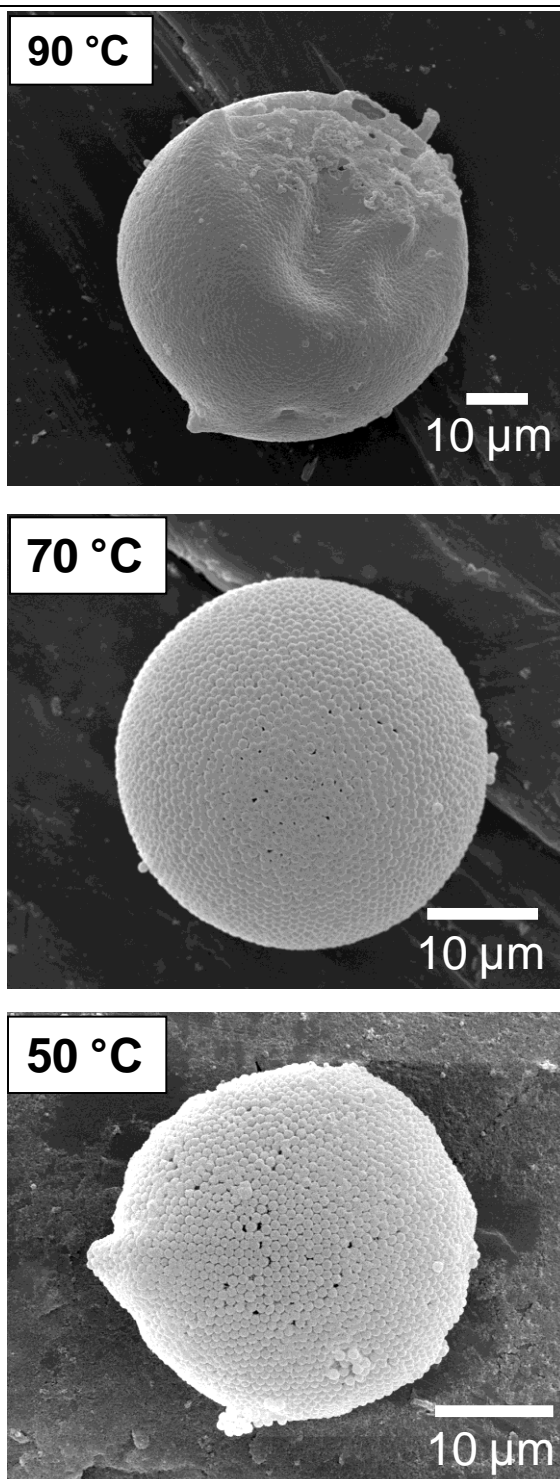
Figure 3.19. Scanning electron microscopy images of cross-linked colloidosomes prepared with 5.0 wt % 1188 nm PGMA$_{50}$-PS and *n*-dodecane. The sample was split between three vials and these aliquots were annealed at 90 °C or 70 °C (for 1 hour) or 50 °C (for 4 hours).

In fact Tsavalas and co-workers[29-30] have shown that the apparent T_g of 'wet' latexes can be significantly lower than that of the dry powders due to a plasticisation effect of the aqueous solvent. Therefore this is likely to be the reason for the observed annealing below the T_g of polystyrene core. In addition the extent of sintering is governed by two main factors, the sintering temperature (T_{si}) and the sintering time (t_{si}) (see equation 3).[31-32]

$$Sin\theta_{si} = \frac{x_{si}}{a} = \left(\frac{\gamma_{w/p}}{a_o \eta_p} t_{si} \right)^{1/2} \qquad (3)$$

Where θ_{si} is the sintering angle, x_{si} is the sintering neck radius, a is the sintered particle radius, $\gamma_{w/p}$ is the water-polymer interfacial tension, a_0 is the initial particle radius, η_p is the viscosity of polymer and t_{si} is the sintering time, as portrayed in Figure 3.20. The sintering temperature T_{si} influences both the η_p and $\gamma_{w/p}$ of the polymer latex.
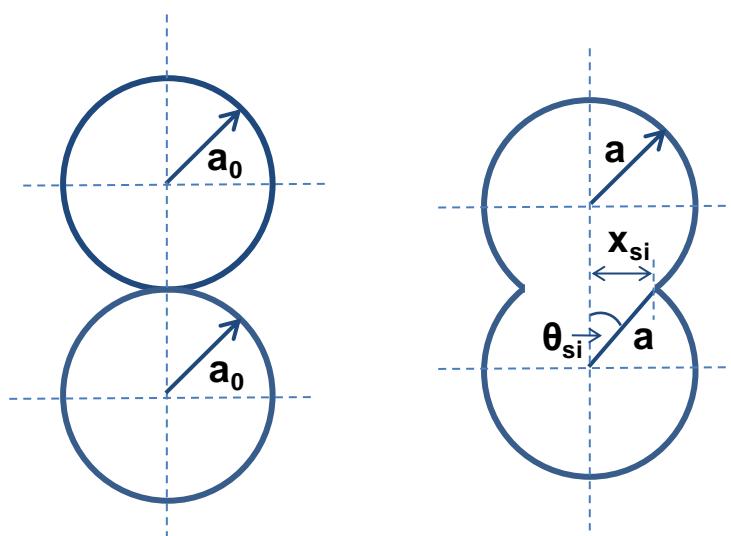
Figure 3.20. Schematic representation of a sintering sequence for two latex spheres.[31]

In the case of these PGMA-PS latex-based colloidosomes, the thermal annealing observed below the latex T_g is attributed to plasticisation by the aqueous phase and the relatively long t_{si}. This is also consistent with the significantly longer sintering time required at 50 °C compared to 90 °C, and demonstrates the how sintering time and temperature can be optimised to achieve well-annealed colloidosome shells.

CONCLUSIONS

A convenient route to covalently cross-linkable colloidosomes has been established using hydroxy-functionalised sterically-stabilised polystyrene latexes and a cheap, commercially available oil-soluble polymeric diisocyanate. Varying the latex concentration allows the mean oil droplet diameter to be tuned to some extent. Above a certain critical latex concentration, which corresponds to the limiting droplet diameter (and depends on the latex diameter), any additional latex simply remains in the aqueous phase. Below this critical concentration, larger oil droplets are obtained, but in each case we estimate an experimental latex packing efficiency of approximately 0.85 ± 0.01. This relatively efficient packing is supported by high magnification fluorescent images of the surface of individual colloidosomes, since hexagonal close-packing within the self-assembled latex monolayer is observed. The cross-linking reaction is confined to the oil phase, with no evidence for any inter-colloidosome fusion even at 50 vol %. In contrast, significant agglomeration can occur when cyclohexane-mediated annealing of the colloidosomes is attempted. In addition, thermal annealing can also occur at temperatures as low as 50 °C in the absence of cyclohexane. However, it should be noted that, at this reduced, temperature the extent of annealing is not as complete as in the presence of cyclohexane, despite far longer annealing times.

The relative merits of utilising two different sized latexes have also become readily apparent during the course of this Chapter. The micrometer-sized latexes prepared by dispersion polymerisation facilitate imaging of the resulting colloidosomes by SEM and fluorescence/optical microscopy. On the other hand, the smaller 107 nm latex prepared by emulsion polymerisation allows detection of the PPG-TDI cross-linker and monitoring of the cross-linking reaction by ^{1}H NMR spectroscopy. However, the same quantitative analysis of the latex packing fraction can be applied in both cases.

REFERENCES

1. Yow, H. N.; Routh, A. F., *Soft Matter,* **2006,** *2*, 940-949.

2. Pickering, S. U., *Journal of the Chemical Society,* **1907,** *91*, 2001-2021.

3. Velev, O. D.; Furusawa, K.; Nagayama, K., *Langmuir,* **1996,** *12*, 2374-2384.

4. Velev, O. D.; Furusawa, K.; Nagayama, K., *Langmuir,* **1996,** *12*, 2385-2391.

5. Velev, O. D.; Nagayama, K., *Langmuir,* **1997,** *13*, 1856-1859.

6. Dinsmore, A. D.; Hsu, M. F.; Nikolaides, M. G.; Marquez, M.; Bausch, A. R.; Weitz, D. A., *Science,* **2002,** *298*, 1006-1009.

7. Laib, S.; Routh, A. F., *J. Colloid Interface Sci.,* **2008,** *317*, 121-129.

8. Cayre, O. J.; Noble, P. F.; Paunov, V. N., *J. Mater. Chem.,* **2004,** *14*, 3351-3355.

9. Noble, P. F.; Cayre, O. J.; Alargova, R. G.; Velev, O. D.; Paunov, V. N., *J. Am. Chem. Soc.,* **2004,** *126*, 8092-8093.

10. Duan, H. W.; Wang, D. Y.; Sobal, N. S.; Giersig, M.; Kurth, D. G.; Mohwald, H., *Nano Lett.,* **2005,** *5*, 949-952.

11. Croll, L. M.; Stöver, H. D. H., *Langmuir,* **2003,** *19*, 5918-5922.

12. Skaff, H.; Lin, Y.; Tangirala, R.; Breitenkamp, K.; Böker, A.; Russell, T. P.; Emrick, T., *Adv. Mater.,* **2005,** *17*, 2082-2086.

13. Shah, R. K.; Kim, J. W.; Weitz, D. A., *Langmuir,* **2010,** *26*, 1561-1565.

14. Thompson, K. L.; Armes, S. P., *Chem. Commun.,* **2010,** *46*, 5274-6.

15. Thompson, K. L.; Armes, S. P.; Howse, J. R.; Ebbens, S.; Ahmad, I.; Zaidi, J. H.; York, D. W.; Burdis, J. A., *Macromolecules,* **2010,** *43*, 10466-10474.

16. Thompson, K. L.; Armes, S. P.; York, D. W.; Burdis, J. A., *Macromolecules,* **2010,** *43*, 2169-2177.

17. Balmer, J. A.; Armes, S. P.; Fowler, P. W.; Tarnai, T.; Gaspar, Z.; Murray, K. A.; Williams, N. S. J., *Langmuir,* **2009,** *25*, 5339-5347.

18. Aveyard, R.; Binks, B. P.; Clint, J. H., *Adv. Colloid Interface Sci.,* **2003,** *100-102*, 503-546.

19. Tambe, D. E.; Sharma, M. M., *Adv. Colloid Interface Sci.,* **1994,** *52*, 1-63.

20. Frelichowska, J.; Bolzinger, M.-A.; Chevalier, Y., *J. Colloid Interface Sci.,* **2010,** *351*, 348-356.

21. Walsh, A.; Thompson, K. L.; Armes, S. P.; York, D. W., *Langmuir,* **2010,** *26*, 18039-18048.

22. Bausch, A. R.; Bowick, M. J.; Cacciuto, A.; Dinsmore, A. D.; Hsu, M. F.; Nelson, D. R.; Nikolaides, M. G.; Travesset, A.; Weitz, D. A., *Science,* **2003,** *299*, 1716-1718.

23. It is worth emphasising that neither methanol nor 2-propanol are suitable in this regard. The former is not miscible with n-alkanes, while the latter is a poor solvent for the PGMA stabiliser chains (and hence the latex).

24. Binks, B. P.; Desforges, A.; Duff, D. G., *Langmuir,* **2006,** *23*, 1098-1106.

25. Vashisth, C.; Whitby, C. P.; Fornasiero, D.; Ralston, J., *J. Colloid Interface Sci.,* **2010,** *349*, 537-543.

26. Yow, H. N.; Routh, A. F., *Langmuir,* **2009,** *25*, 159-166.

27. *Polymer Handbook*. 2nd ed.; Wiley Interscience: New York, p IV-248.

28. Yuan, Q.; Cayre, O. J.; Fujii, S.; Armes, S. P.; Williams, R. A.; Biggs, S., *Langmuir,* **2010,** *26*, 18408-18414.

29. Jiang, B.; Tsavalas, J.; Sundberg, D., *Langmuir,* **2010,** *26*, 9408-9415.

30. Tsavalas, J. G.; Sundberg, D. C., *Langmuir,* **2010,** *26*, 6960-6966.

31. Bellehumeur, C. T.; Kontopoulou, M.; Vlachopoulos, J., *Rheol. Acta,* **1998,** *37*, 270-278.

32. Bellehumeur, C. T.; Bisaria, M. K.; Vlachopoulos, J., *Polym. Eng. Sci.,* **1996,** *36*, 2198-2207.

Chapter Four

Release of Encapsulated Species from Covalently Cross-linked Colloidosomes

INTRODUCTION

Colloidosome-based microcapsules have received attention in recent years for their potential application in the encapsulation and release of actives. It has been suggested by Dinsmore and co-workers[1] that the capsule permeability can be tuned by dictating the size of the interstices between adjacent particles.[2] In principle, smaller interstices can be achieved either by using smaller particles to construct the colloidosome shell or by thermal annealing of the shell once formed.

Yow and Routh[3] looked at the effect that sintering time had on the release profiles from the aqueous cores of latex-based colloidosomes using fluorescein in its sodium salt form as a model active. Their colloidosome shells consisted of poly(styrene-co-butyl acrylate) latexes of around 180 nm as determined by DLS. This low T_g copolymer shell was sintered at 50 °C for either 5, 30 and 60 minutes. Although there was little difference between the release from colloidosomes annealed for 5 and 30 minutes, the longest sintering time did lead to slower dye release. Nevertheless, these encapsulation times are too short to be commercially attractive.

The Present Work

This Chapter describes encapsulation and release experiments performed using the cross-linked colloidosome microcapsules described in Chapter 3. The small molecule dye fluorescein was chosen for the initial release experiments. It was selected because it is oil-soluble in its protonated form, but becomes water-soluble at high pH when its carboxylic acid group becomes ionised. This allowed its encapsulation inside the colloidosome oil cores, with release being triggered as desired by increasing the external aqueous pH. The effect of varying the PGMA$_{50}$-PS latex diameter, cyclohexane annealing time and conducting polymer overlayer deposition on the release profile of fluorescein is investigated. Selected results were presented in an earlier publication in Macromolecules[4]; this Chapter discusses these data along with some further as-yet unpublished results. The ability of these cross-linked colloidosomes to encapsulate relatively large oil-dispersible latex particles, as opposed to small molecule dyes, is also investigated.

EXPERIMENTAL DETAILS

Materials

Glycerol monomethacrylate (GMA) was kindly donated by Cognis UK Ltd (Hythe, UK) and used without further purification. 4-Vinylbenzyl chloride (4-VBC; 90 %), Cu(I)Cl (99.995 %) 2,2′-bipyridine (bpy, 99 %), *n*-dodecane, sunflower oil, fluorescein and tolylene 2,4-diisocyanate-terminated poly(propylene glycol) [PPG-TDI] were all purchased from Aldrich and were used as received. Styrene and pyrrole (Aldrich) were each passed through basic alumina columns to remove inhibitor and then stored at -20 °C prior to use. 2,2'-Azobisisobutyronitrile (AIBN; BDH) and ammonium persulfate (APS, Aldrich) were used as received. Methanol and ethanol were purchased from Fisher and were used as received. De-ionised water was used in all experiments. Silica gel 60 (0.0632-0.2 mm) was obtained from Merck (Darmstadt, Germany). NMR solvents (D_2O, CD_3OD, $CDCl_3$ and d_5-pyridine) were purchased from Fisher.

Encapsulation and Release of Fluorescein from Colloidosomes

Fluorescein (1.0 mg) was weighed into a glass sample vial, along with PPG-TDI (0.025 g). This was then dissolved in the sunflower oil (5.0 ml) before homogenisation for 2.0 mins with a 1.0 or 5.0 wt % aqueous solution of 107 nm or 1188 nm $PGMA_{50}$-PS latex, respectively. The resulting emulsion was allowed to stand at 20^oC for 30 min to allow the urethane cross-linking reaction to proceed. Release studies were conducted using a PC-controlled Perkin-Elmer Lambda 25 UV/visible absorption spectrophotometer operating in time drive mode. A known mass (0.020-0.024 g) of filtered colloidosomes (or polypyrrole-coated colloidosomes, see later) was placed on top of an aqueous solution (3.0 ml, pH 9) in a disposable UV-grade cuvette equipped with a miniature magnetic stirrer bar. The absorbance at 490 nm due to the released dye was monitored as a function of time. Since the colloidosomes are less dense than water they remained buoyant and hence out of range of the transmitted beam. As a control experiment, pure oil containing the same concentration of dissolved dye was used instead of the colloidosomes.

Polypyrrole Deposition onto Colloidosomes

Fluorescein-encapsulated cross-linked colloidosomes (2.0 ml of a 50 vol %
dispersion of 89 ± 24 μm colloidosome microcapsules prepared using the 1188 nm
$PGMA_{50}$-PS latex) were transferred into a sample vial. Ammonium persulfate (0.019
g; 0.083 mmol) and pyrrole monomer (0.005 ml; 0.075 mmol) were added to these
colloidosome microcapsules, followed by mixing for 16 h at 20°C using a roller
mixer. This protocol produced polypyrrole-coated colloidosomes with a conducting
polymer mass loading of 0.66 wt. % (approximate target polypyrrole thickness = 60
nm). A second 2.0 ml aliquot was coated with 1.32 wt. % polypyrrole (using 0.038 g
APS and 0.010 ml pyrrole). The average thickness, x, of the deposited polypyrrole
overlayer on the colloidosomes can be estimated using equation 1;[5]

$$x = R \left[\left(\frac{M_{ppy}\rho_{oil}}{M_{oil}\rho_{ppy}} + 1 \right)^{1/3} - 1 \right] \tag{1}$$

where R = the mean radius of the original uncoated colloidosomes (as judged by
Malvern Mastersizer), M_{ppy} and ρ_{ppy} are the mass fractions and density of the
polypyrrole component and M_{oil} and ρ_{oil} are the mass fraction and density of the oil
droplet component. It was assumed that the adsorbed PS latex has minimal effect on
the droplet radius, density or mass fraction and so this component was not included
in the calculation. It was also assumed in the calculation that the polypyrrole
conversion was 100 % and that all of the polymer deposited onto the outside of the
colloidosomes and not as bulk polypyrrole in solution.

Synthesis of the Disulfide-Based Bifunctional ATRP Initiator, Bis[2-(2-bromoisobutyryloxy)ethyl] Disulfide (BiBOE)$_2$S$_2$

This synthesis was carried out as reported previously.[6] Bis(2-hydroxyethyl) disulfide
(15.4 g, 12.2 ml, 0.1 mol) was added to a 500 ml three-neck round bottom flask and
dissolved in dry THF (200 ml). Triethylamine (42.0 ml, 0.30 mol) was added to this
solution under a nitrogen atmosphere and the reaction solution was cooled in an ice
bath. 2-Bromoisobutyryl bromide (59.8 g, 0.26 mol) was added slowly using a
dropping funnel. The reaction turned reddish-brown. The solution was then stirred at
room temperature for a further 24 h. The insoluble triethylammonium bromide salt
was removed by filtration and the solution was concentrated by removal of the THF

under reduced pressure by rotary evaporation. The concentrated solution was stirred with 0.10 M aqueous Na_2CO_3 to hydrolyse any residual 2-bromoisobutyryl bromide. The crude product was then extracted three times with dichloromethane (DCM) using a separating funnel. The combined dichloromethane extracts were first passed through a basic alumina column before being dried with anhydrous magnesium sulfate. The DCM was removed under vacuum to give a reddish brown oil (29.2 g; yield = 65 %). This $(BiBOE)_2S_2$ initiator was analysed by ^{1}H NMR spectroscopy in $CDCl_3$ (δ, ppm): 4.45 (triplet, 2H, $-CH_2OOC-$), 2.96 (triplet, 2H, $-CH_2S-$), and 1.95 (singlet, 6H, $(CH_3)_2C-$).

Atom Transfer Radical Polymerisation of 2-(Diethylamino)ethyl Methacrylate (DEA) using a Bifunctional Disulfide Initiator

$(BiBOE)_2S_2$ initiator (0.122 g, 0.27 mmol), bpy (0.170 g, 1.80 mmol) and DEA monomer (5 g, 27 mmol) were weighted into a 25 ml round bottom flask and degassed by three vacuum/nitrogen cycles. A degassed solution of 9:1 IPA/H_2O was added to the flask and the reaction solution was purged with nitrogen for 15 minutes. Cu(I)Br (0.077 g, 0.54 mmol) was added to the reaction flask quickly under a positive nitrogen pressure and the reaction solution turned dark brown indicating the onset of polymerisation. After 24 h, the reaction was terminated by opening the flask to air and diluting the reaction solution with IPA. The solution became blue/green in colour, indicating aerial oxidation of the Cu catalyst. The spent catalyst was removed by passing the solution through a silica column. The homopolymer was then dried by removal of the IPA by rotary evaporation and further drying in a vacuum desiccator overnight to yield a clear viscous polymer. (Yield = 4.56 g, ~ 0.90 %).

Synthesis of Rhodamine B Acrylate Fluorescent Monomer

This synthesis was performed by Dr Jeppe Madsen according to the following protocol.

Rhodamine B base (0.50 g, 1.13 mmol) was weighed into a round-bottom flask and placed under nitrogen, thionyl chloride (0.50 ml, 0.82 g 6.9 mmol) was then added and the reaction solution was stirred overnight. After evaporation of the excess thionyl chloride, the resulting rhodamine B chloride was used without further purification. 2-Hydroxyethyl piperazine (0.13 g, 1.0 mmol) and rhodamine B

chloride (0.1 g, 0.2 mmol) were weighed into a round-bottom flask and co-dissolved in dichloromethane (10 ml). The mixture was stirred overnight, then transferred to a separating funnel with dichloromethane. The organic fractions were washed with saturated sodium hydrogen carbonate (50 ml) and water (50 ml), which led to coloration of the aqueous phase. The combined aqueous phases were washed with ethyl acetate (2 x 50 ml).

Absorption spectroscopy (assuming ε_{max} = 100,000 M^{-1} cm^{-1} at a λ_{max} = 567 nm)[7] revealed that the concentration of rhodamine B in the aqueous phase was approximately 1 mM.

For acrylation, 0.20 ml acryloyl chloride (0.22 g, 2.46 mmol, ~ 12 eq) was added to the aqueous 2-hydroxyethylpiperazine rhodamine B solution (200 ml, ~ 0.20 mmol) and stirred overnight at room temperature. The mixture was then transferred to a separating funnel with dichloromethane and washed with saturated sodium hydrogen carbonate solution (2 x 50 ml) to remove excess acid chloride followed by water (2 x 50 ml) and finally brine (1 x 50 ml). The organics were collected and dried by addition of anhydrous magnesium sulfate. After filtration and evaporation, followed by precipitation with petroleum ether, the product was obtained as a dark red/purple solid. Yield: 0.101 g, ~ 80 %.

^{1}H NMR (CDCl$_3$) δ 7.62 (dd, 2 H, Ar), 7.48 (dd, 1 H, Ar), 7.29 (dd, 1 H, Ar), 7.18 (d, 2H, J-9.54 Hz, Ar), 6.91 (dd, 2 H, Ar), 6.72 (d, 2H, J=2.45 Hz, Ar), 6.31 (d, 1 H, J=17.36 Hz, **H**HC=CH-), 6.04 (dd, 1H, H**H**C=CH-), 5.77 (d, 1H, J=10.27 Hz, HHC=C**H**-), 4.18 (t, 2H, J=5.62 Hz, -C**H$_2$**-O-C=O), 3.60 (q, 8H, J=7.66 Hz, N-(C**H$_2$**-CH$_3$)$_2$), 3.35 (br, 4H, C=O-N<(C**H$_2$**-CH$_2$)$_2$>N- , piperazine ring) 2.60 (t, 2H, J=5.62 Hz, >N-C**H$_2$**-), 2.34 (br, 4H, N<(CH$_2$-C**H$_2$**)$_2$>N-CH$_2$, piperazine ring), 1.27 (t, 12 H, J=7.09 Hz, N-(CH$_2$-C**H$_3$**)$_2$) ppm

PDEA-PS Latex Preparation by Alcoholic Dispersion Polymerisation

PDEA homopolymer (0.050 g) and Rhodamine B acrylate (0.0050 g) were weighed into a 10 ml round bottom flask and dissolved in an IPA/H$_2$O mixture (4.45 g, 100:0, 90:10 or 70:30). The solution was purged with nitrogen for 20 minutes before being heated to 70 °C. A solution of AIBN (0.0050 g) dissolved in styrene (0.50 g) was

then injected into the reaction flask and the reaction was stirred at 70 °C for 24 h. The crude latexes were characterised by dynamic light scattering before being purified by repeated centrifugation cycles, replacing each successive supernatant with pure IPA. This centrifugation-redispersion protocol was repeated until the supernatant was clear, indicating removal of all free unreacted Rhodamine acrylate. This was important as this impurity may interfere with fluorescence microscopy studies. Finally, the particles were redispersed in sunflower oil and placed in a vacuum desiccator overnight to remove any residual traces of IPA, which might otherwise compromise the diisocyanate cross-linking chemistry.

Encapsulation of PDEA-PS Particles

PPG-TDI (10.0 mg) was added to 1.80 ml of pure sunflower oil, to which a dispersion of PDEA-PS latex in sunflower oil (200 μl, ~ 5 wt. % solids) was added. This oil solution was then homogenised with an aqueous solution of PGMA$_{50}$-PS latex particles (2.0 ml, 1.0 wt % for the 107 nm latex and 5.0 wt % for the 1188 nm latex) at 12,000 rpm for 2.0 minutes using the Ultra-Turrax homogeniser. Droplet size distributions were measured by laser diffraction as described overleaf.

Release of the encapsulated PDEA-PS latex particles was attempted by adding a few drops of HCl (0.50 M) to the aqueous phase to allow protonation of the PDEA chains. The colloidosomes were viewed by fluorescence microscopy before and after addition of acid. They were also subjected to an alcohol challenge in order to (i) confirm that cross-linking had been successful in the presence of the PDEA-PS particles and (ii) to see if any encapsulated latex particles were visible by scanning electron microscopy.

Polymer/Colloidosome Characterisation

Dynamic Light Scattering (DLS)

Intensity-average hydrodynamic diameters for each of the three latexes were obtained by DLS using a Malvern Zetasizer NanoZS instrument at a fixed scattering angle of 173°. Aqueous dispersions of 0.01 wt % latex were analysed using disposable cuvettes and the results were averaged over three consecutive runs. The deionised water used to dilute each latex was ultra-filtered through a 0.20 μm membrane so as to remove dust.

Disc Centrifuge Photosedimentometry

Weight-average diameters (D_w) of the PDEA-PS latexes were measured using a CPS disc centrifuge photosedimentometer (model number DC24000). Samples of around 0.1% (0.10 ml) were injected in an aqueous spin fluid consisting of a sucrose gradient (15 ml). The spin fluid gradient (2% - 8% sucrose) was prepared at pH 3 to fully disperse the PDEA chains in the aqueous media. The density of the polystyrene latex particles was taken to be 1.05 g cm^{-3}. This is a reasonable assumption for latex diameters of around 1 μm, where the thickness of the steric stabiliser layer is negligible compared to the mean particle diameter. For smaller latexes (particularly for diameters of less than 200 nm), the stabiliser layer thickness becomes significant, resulting in a significant reduction in the effective particle density.[8] Since an accurate particle density is required when calculating the weight-average particle diameter, D_w, any uncertainty in particle density produces an associated error in D_w.

Laser Diffraction

A Malvern Mastersizer 2000 instrument equipped with a small volume Hydro 2000SM sample dispersion unit (ca. 50 ml), a HeNe laser operating at 633 nm, and a solid-state blue laser operating at 466 nm was used to size the emulsions. The stirring rate was adjusted to 1,000 rpm in order to avoid creaming of the emulsion during analysis. The mean droplet diameter was taken to be the volume mean diameter ($D_{4/3}$), which is mathematically expressed as $D_{4/3} = \Sigma D_i^4 N_i / \Sigma D_i^3 N_i$. The standard deviation for each diameter provides an indication of the size distribution. After each measurement, the cell was rinsed once with ethanol, followed by three times with doubly-distilled water. The glass walls of the cell were carefully wiped with lens cleaning tissue to avoid cross-contamination, and the laser was aligned centrally on the detector.

Optical Microscopy

Optical microscopy images were recorded using a Motic DMBA300 digital biological microscope with a built-in camera and Motic Images Plus 2.0 ML software.

Scanning Electron Microscopy (SEM)

SEM studies were performed using a FEI Sirion field emission scanning electron microscope using a beam current of 244 µA and a typical operating voltage of 20 kV. Colloidosome samples were washed repeatedly with ethanol to remove any traces of oil. Samples were dried onto aluminium stubs and sputter-coated with a thin layer of gold prior to examination so as to prevent sample charging.

Fluorescent Microscopy

Fluorescence microscopy was carried out using a Nikon Eclipse LV100 microscope. The fluorescence excitation and emission wavelengths were controlled by either a B-2A (Nikon, for fluorescein) or a 49004 ET - CY3 filter block (Chroma Technology Corp, for Rhodamine). Fluorescent images were captured using a high sensitivity EMCCD Andor iXon+ 897 camera (512x512 pixels). Bright field (diascopic) images were captured using a Luminera 2.1 CCD camera.

THF GPC

Molecular weights (M_n) and polydispersities (M_w/M_n) of the P(DEA$_{100}$) homopolymer was assessed by THF GPC. The GPC set-up comprised two Polymer Laboratories PL gel 5 µm MIXED-C columns. The GPC eluent was HPLC grade THF containing 2.0 % (v/v) TEA and 0.05 % (w/v) BHT at a flow rate of 1.0 ml min^{-1}. The column temperature was set at 30 $^{\circ}$C. Ten near-monodisperse poly(methyl methacrylate) (PMMA) standards (M_p = 2,000 - 300,000 g mol^{-1}) were used for calibration. Data were analysed using PL Cirrus GPC software (version 2.0) supplied by Polymer Laboratories.

X-ray Photoelectron Spectroscopy (XPS)

XPS spectra were acquired using a Kratos Axis ULTRA 'DLD' x-ray photoelectron spectrometer equipped with a monochromatic Al-Kα x-ray source (hν = 1486.6 eV) and operating at a base pressure of 10^{-8} to 10^{-10} mbar. Latex particles were dried on indium foil prior to XPS measurements.

^{1}H NMR Spectroscopy

All ^{1}H NMR spectra were recorded in either CDCl$_3$, D$_2$O, CD$_3$OD or d$_5$-pyridine using a 400 MHz Bruker Avance-400 spectrometer.

RESULTS AND DISCUSSION

Encapsulation of a Small Molecule Dye

The encapsulation/release performance of the cross-linked colloidosomes prepared in Chapter Three was investigated for a model dye molecule. The dye was required to be initially oil-soluble to ensure effective encapsulation but be subsequently capable of triggered release on adjusting the pH of the external aqueous solution. Fluorescein (pK_a ~ 6.3) was selected as an appropriate acid dye, since it is oil-soluble in its protonated form at low pH but becomes water-soluble at higher pH (see Figure 4.1).[9] Sunflower oil was selected as the droplet phase in these release experiments since it dissolved this dye more readily than *n*-dodecane. It is perhaps worth emphasising here that the cross-linking reaction between the PGMA and PPG-TDI appears to have little or no pH dependence, since it was equally successful at pH 3, 7 and 9. This is understandable, since only those PGMA chains on the inside of the colloidosomes (i.e. wetted by the oil phase) are available for reaction with the PPG-TDI. Therefore oil-in-water colloidosomes were prepared at pH 3 with fluorescein encapsulated within the oil cores and dye release was subsequently triggered as desired by increasing the pH of the aqueous continuous phase above the pK_a of the dye (see Figure 4.2 for typical visible absorption spectra and a calibration plot of the dye at pH 9).

Model Active - Fluorescein

Soluble in sunflower oil   Water-soluble at high pH
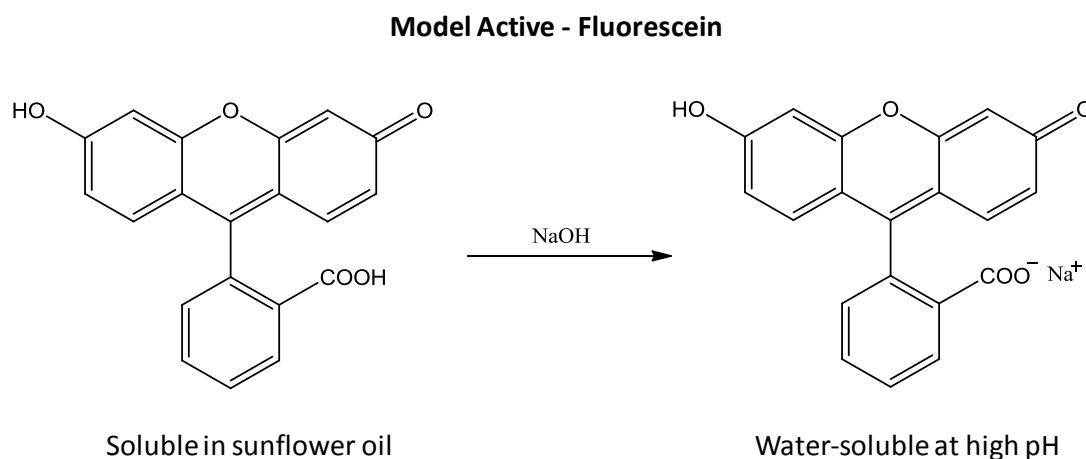
Figure 4.1. The pH dependent solubility of the fluorescein dye used for encapsulation and release studies.
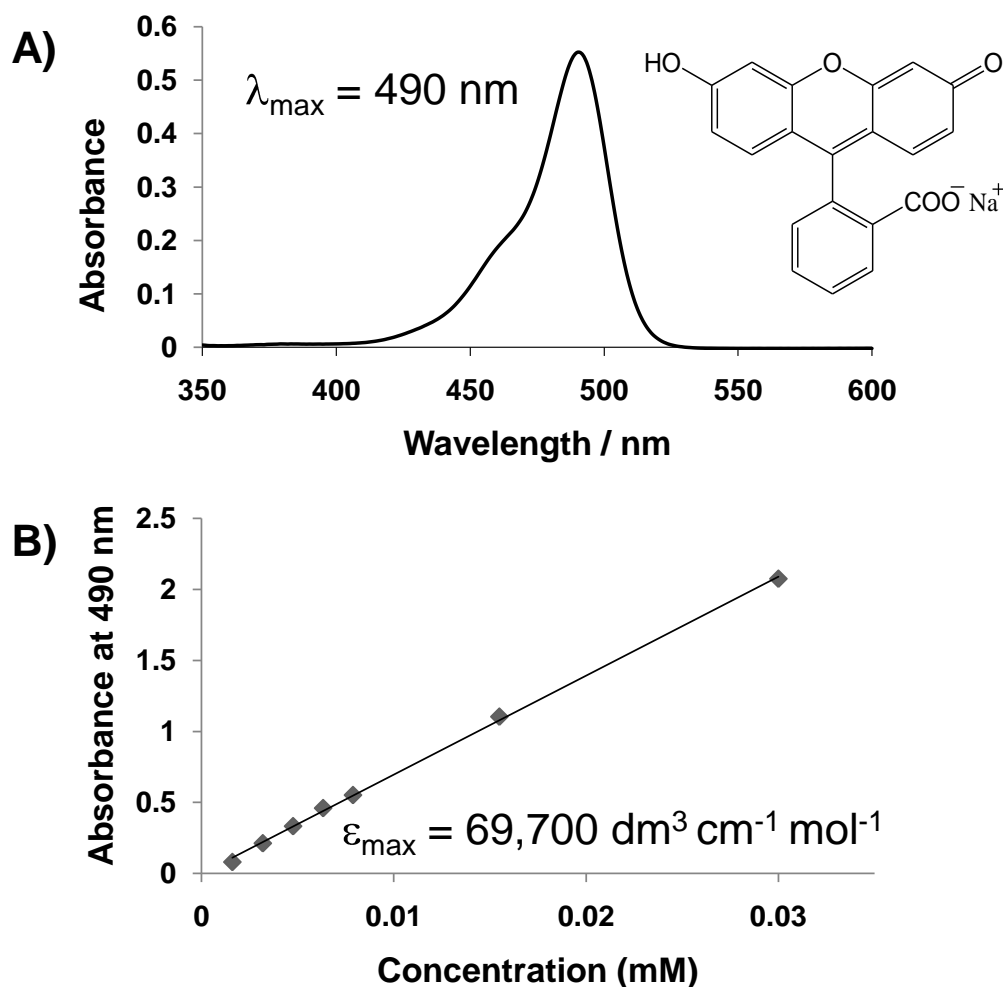
Figure 4.2. (A) Visible absorption spectrum for anionic fluorescein dye recorded at pH 9, with a λ_{max} of 490 nm and (B) absorbance vs. concentration plot for aqueous solutions of anionic fluorescein at pH 9, giving a calculated ε_{max} of 69,700 ± 3,200 $dm^3\,cm^{-1}\,mol^{-1}$.

To allow the rate of dye diffusion into the aqueous phase to be assessed when there was no microcapsule barrier, a control experiment was conducted whereby the rate of release of dye from sunflower oil alone was determined (see Figure 4.3). Unfortunately, the solely cross-linked colloidosomes proved to be highly permeable, with no significant difference in the rate of dye release being observed between the control experiment and the colloidosomes within error (see Figure 4.3). With the benefit of hindsight, given that these particles contain a large number of interstitial holes between adjacent latex particles, such high permeability towards a small molecule dye is perhaps not surprising. Varying the size of the $PGMA_{50}$-PS particles

(107 nm vs. 1188 nm) forming the colloidosome shells also had no discernable effect on the rate of release of the fluorescein dye.
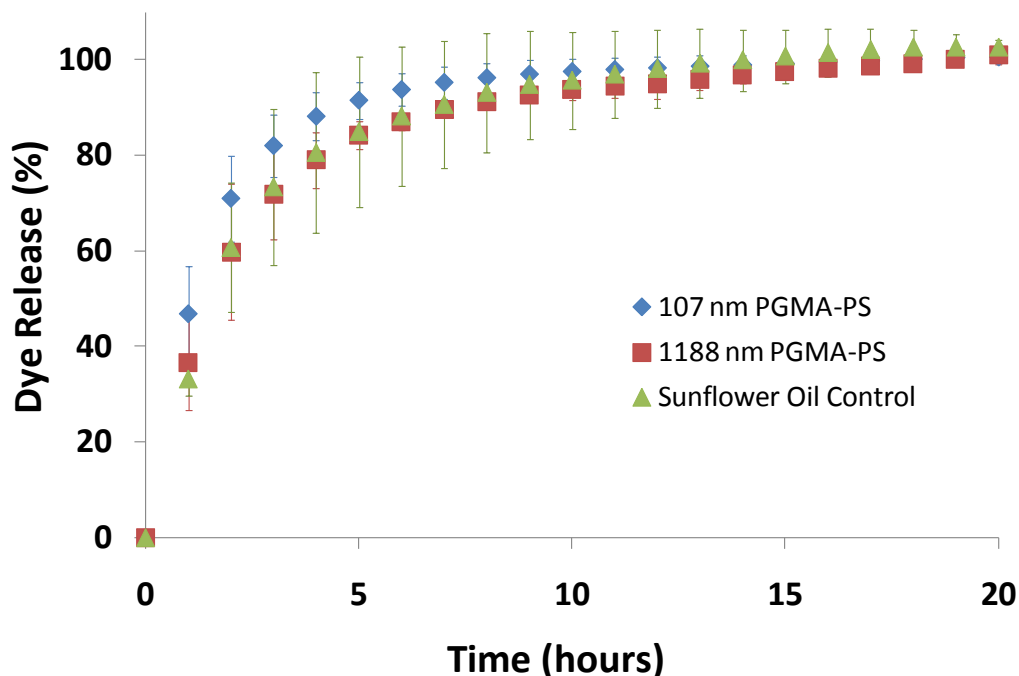
Figure 4.3. Release curves obtained at pH 9 for fluorescein dye diffusing from: sunflower oil control (green triangles), 89 ± 24 µm cross-linked colloidosomes prepared with 1188 nm $PGMA_{50}$-PS particles (red squares) and 47 ± 25 µm cross-linked colloidosomes prepared with 107 nm $PGMA_{50}$-PS particles (blue diamonds). The error bars represent the standard deviation taken from three repeat experiments.

 It has been previously suggested that the size of the particles forming the shells can control the permeability of the resulting capsules, since the particle size dictates the interstical size.[1] For the work carried out in this Chapter, this does not appear to be the case. However, it is perhaps not too unexpected since the molecule chosen for release is so small that even the 107 nm particles provide very large interstices relative to the dimensions of the fluorescein molecule. Rosenberg *et al.*[10-11] recently conducted a series of release experiments from hydrogels covered with a monolayer of spherical particles. The particle diameter was varied in order to achieve different pore sizes and the rates of release of two small molecules (aspirin and caffeine) and dextran (MW ~3000-5000) were monitored in turn. Diffusion rates were largely independent of the particle diameter (and therefore pore size), unless the diffusing

molecule was of similar dimensions to the particles forming the monolayer. This is consistent with our findings that, for a small molecule, the size of the particles making up the colloidosome shell have essentially no effect on the release profile. This can be explained if one considers the surface area available for diffusion of a small molecule. The surface area available for transport is the remaining area not occupied by the latex particles. On a planar surface, provided that all the particles have the same packing fraction, the available surface area remains constant irrespective of colloid size (see Figure 4.4). Despite the smaller latex offering significantly smaller individual interstices, the total area of all interstices remains constant. Hence it follows that if the surface area is constant regardless of latex diameter, the rate of release from within these colloidosomes should be constant.
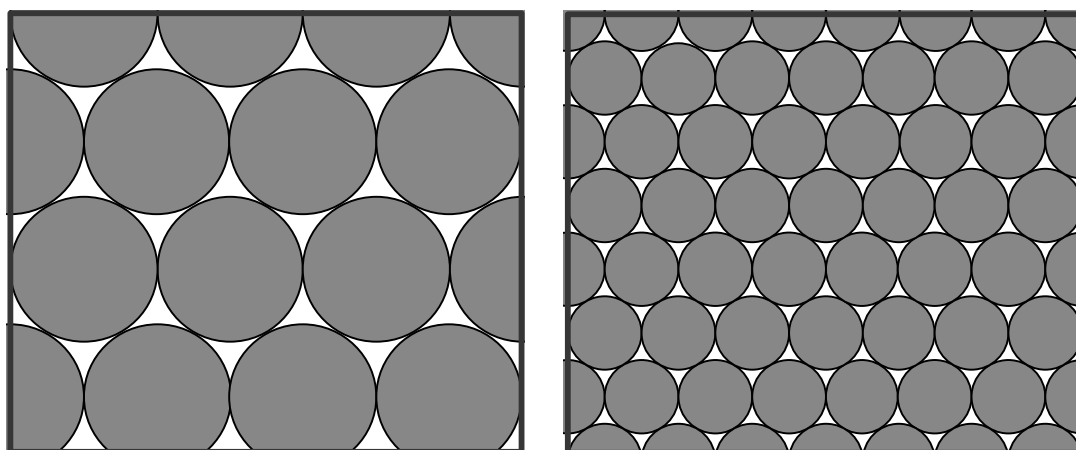
Figure 4.4. Schematic representation demonstrating that the available surface area for a planar surface covered with a monolayer of hexagonally close-packed monodisperse spheres is the same irrespective of latex diameter (provided they have the same packing density). Despite the interstices being smaller in the case of the finer particles, the overall surface area available for transport is the same in both cases.

The situation is complicated slightly by the fact that the latexes in this case are assembled around curved polydisperse oil droplets rather than on a planar surface. Taking into account the areas blocked by the PGMA$_{50}$-PS particles (P = 0.85) the available oil/water interfacial area is approximately 9 cm^2 and 5 cm^2 for the colloidosomes prepared with the 107 nm and 1188 nm PGMA$_{50}$-PS particles, respectively. This difference in surface area could account for the slightly faster rate

of fluorescein release observed from the colloidosomes prepared with the smaller 107 nm latex (blue data points in Figure 4.3). However, these data points lie within the error bars of the other release curves and so this slightly faster release is not considered significant. Surface area considerations also help to explain why no retardation occurs when compared to the control experiment performed in the absence of a microcapsule barrier. Although Rosenberg et al.[10-11] found that particle size had no effect on the release rate of model actives, they did on the other hand observe some retardation when compared to the uncoated hydrogel. They attributed this effect to the reduced surface area available for diffusion when their planar hydrogels were coated with a monolayer of particles. In the case of this work no such retardation was observed, with the dye release from the control experiment being at effectively the same rate as that for the colloidosomes. However, it is worth mentioning that the control experiment was conducted directly from sunflower oil, which is immiscible with water. Hence the interfacial surface area between the oil phase and aqueous release medium is approximately equal to the cross-sectional area of the UV-Vis cuvette (1 cm^2). This is significantly smaller than the available surface areas in the release experiments from the colloidosome capsules (9 and 5 cm^2), as the same volume of oil is divided into numerous smaller droplets. Therefore, in this particular set of experiments it is entirely reasonable that no retardation is observed when comparing the rates of release from the colloidosomes to that of the control experiment.

Figure 4.5 shows fluorescent microscopy images obtained for the release of fluorescein from cross-linked colloidosomes (initially pH 3) triggered by addition of NaOH to the microscope slide. The wavefront of base triggers rapid dye release into the surrounding aqueous phase (see the third still recorded after 18 s). In this case, release seems to occur within seconds, rather than minutes or hours as observed in the in situ UV/visible studies. However, the local concentration of the base is far greater in the case of the fluorescent microscopy studies, which probably accounts for the faster release rate.
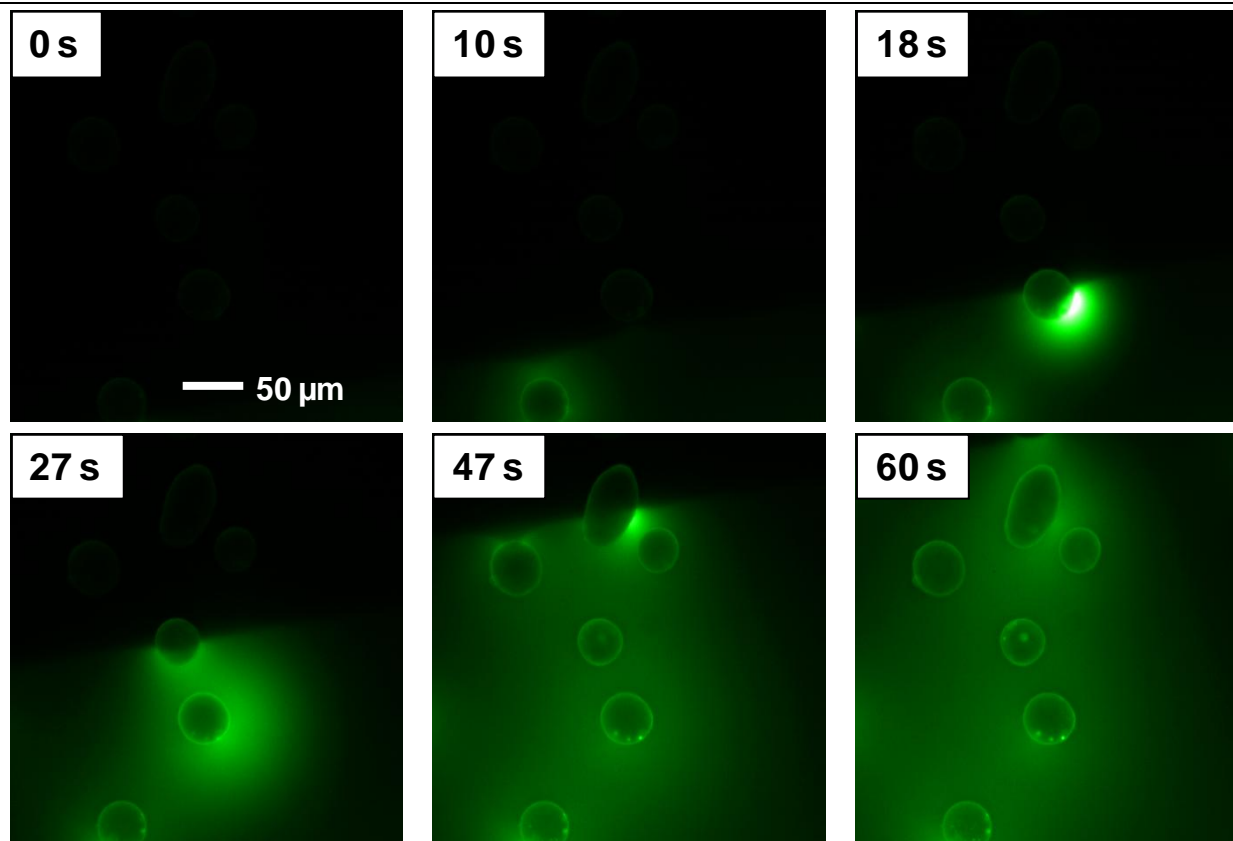
Figure 4.5. Fluorescent microscopy images of the triggered release of fluorescein from within the sunflower oil phase covalently cross-linked colloidosomes of 47 ± 23 μm prepared using the 107 nm $PGMA_{50}$-PS latex particles. Images were recorded at various time intervals after addition of 0.5 M (0.1 ml) NaOH to the microscope slide.

SEM studies described in Chapter 3 showed that cyclohexane annealing enabled
closure of the latex interstices at 50 °C. Therefore release profiles for these annealed
colloidosomes were also investigated, since the interstitial pores had been
significantly reduced. It was hoped that this would lead to a significant reduction in
the rate of dye release.
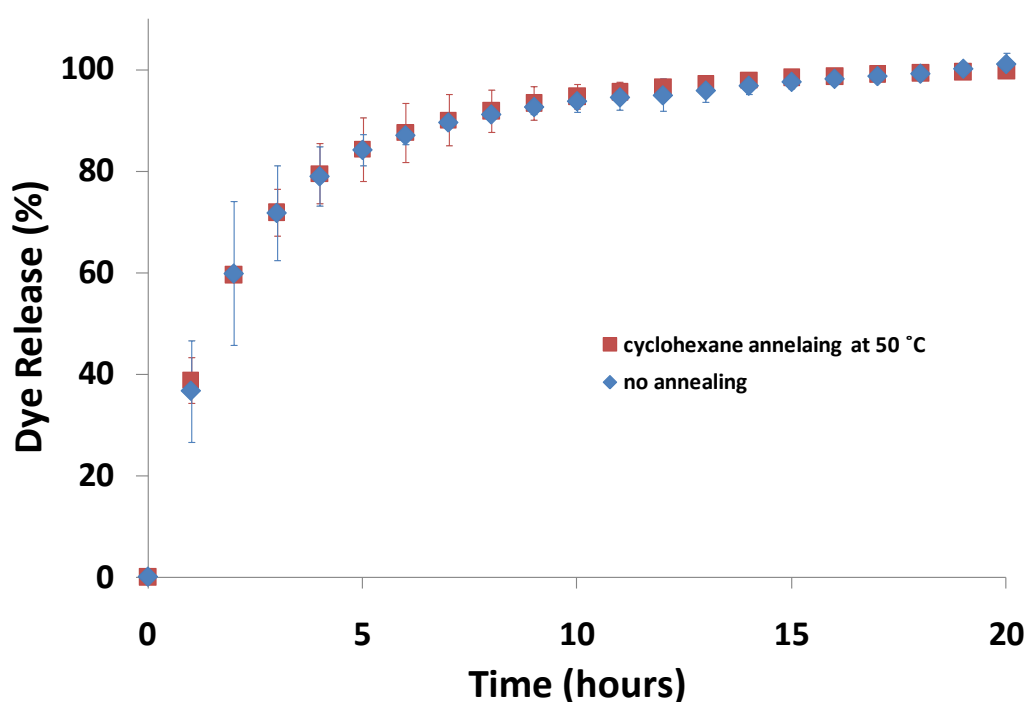
Figure 4.6. Release curves obtained at pH 9 for anionic fluorescein dye diffusing
from (a) cross-linked colloidosomes prepared with the 1188 nm PGMA$_{50}$-PS latex
(blue diamonds) and (b) cyclohexane-annealed colloidosomes prepared with the
same latex and annealed for 1 h at 50 °C using a 4:1 *n*-dodecane/cyclohexane binary
mixture as the oil phase (red squares). The error bars represent the standard deviation
taken from three repeat experiments.

Although, cyclohexane annealing appeared to close these interstitial holes as judged
by SEM, the rate of dye release was not retarded compared to either non-annealed
cross-linked colloidosomes or the control experiment involving just sunflower oil,
see Figure 4.6. One explanation for this poor retention performance is the difficulty
in ensuring that every single interstitial hole is closed in each colloidosome. Indeed,
similar results were reported by Yow and Routh[3], who investigated the release of
fluorescein in its sodium salt form from the aqueous cores of colloidosomes annealed
for up to 60 minutes at 49 °C. These workers found that, although longer latex

annealing times did lead to slower release rates, dye retention remained surprisingly poor. All encapsulated dye was released within 24 h, despite SEM images suggesting that smooth latex shells were obtained after the annealing protocol.

The problem of such interstitial pores is of course exacerbated by the inevitable packing defects that occur when small spheres pack on large spheres. In Chapter 3, a packing efficiency, P, for these latex particles assembled on cross-linked colloidosomes was calculated to be 0.85 ± 0.01. Although this packing is relatively high, there must still be some pentagonal defects that result from packing on the curved oil droplet surface. For perfectly monodisperse spheres, a minimum of 12 defects must be present in order for the particles to pack fully around a larger sphere.[12-13] These packing imperfections are often referred to as line defects or grain-boundary scars[14] and have been experimentally observed by bright field and fluorescence microscopy studies of polystyrene[15] and silica[13] stabilised water droplets respectively. It is these defects that make efficient latex annealing highly problematic. It is not only the standard interstices resulting from hexagonally close-packed spheres that have to be closed, but also the much larger pores resulting from the pentagonal defects.

An incomplete annealing step goes some way to explaining the poor retention performance of these annealed colloidosomes. However, one would expect that closing the majority of latex interstices would reduce the available surface area for diffusion sufficiently to observe at least some retardation in the rate of dye release. This appears not to be the case, with the non-annealed and annealed colloidosomes showing essentially identical release profiles (see Figure 4.6). Therefore, the permeability of the annealed PS latex shell should also be considered. The fluorescein may be able to diffuse through the annealed PS sections of the shell almost as well as through any unclosed interstitial defects. In essence, these data suggests that a ~1 μm thick polystyrene barrier is simply too permeable to efficiently encapsulate a small molecule active. The amorphous nature of the polystyrene latex appears detrimental with a relatively large free volume for the dye to permeate through.

In order to address these problems, we attempted to deposit a thin over layer of an additional polymer onto the outside of the colloidosomes, in order to both fill in the

latex interstices and also provide a thicker, less permeable barrier to dye release. Polypyrrole was chosen for this overlayer as it is easily deposited from aqueous solution using a well-known protocol previously developed by our group for micrometer-sized sterically-stabilised polystyrene latexes.[5] Polypyrrole is a black, insoluble electrically conducting polymer that can be readily synthesised in water at room temperature.[16] Since significant agglomeration of the colloidosomes occurred during cyclohexane annealing and this annealing appears to offer no tangible benefit in terms of dye release retardation, non-annealed cross-linked colloidosomes were used for the polypyrrole coating experiments. The polymerisation of pyrrole requires an acidic solution (pH < 2), but since the fluorescein dye remains water-insoluble at low pH it is not affected by the polypyrrole deposition conditions and is thus retained within the oil droplets.
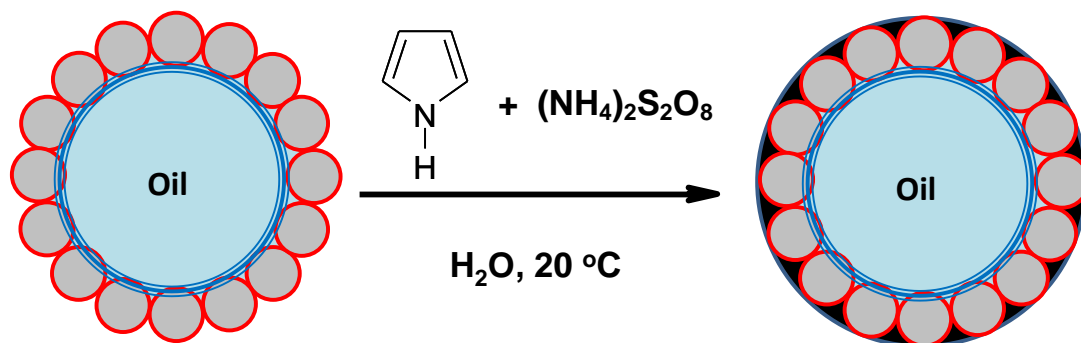
Figure 4.7. Schematic representation of the deposition of an ultrathin layer of polypyrrole (depicted as a black coating) onto covalently cross-linked colloidosomes from aqueous solution at 20 $^{\circ}$C using ammonium persulfate oxidant at pH 1.

Figure 4.7 shows a schematic representation of the polypyrrole deposition onto the outside of a cross-linked colloidosome. The polymerisation using the $(NH_4)_2S_2O_8$ oxidant occurs within minutes[17] and the efficiency of the coating formulation is such that essentially all of the polypyrrole is deposited onto the surface of the colloidosomes, with little or no polypyrrole precipitating in the bulk aqueous solution.[5] Figure 4.8 shows SEM images recorded for the colloidosomes prepared with the 1188 nm $PGMA_{50}$-PS latex both before and after conducting polymer deposition. Polypyrrole-coated colloidosomes are much less prone to collapse under UHV conditions compared to uncoated colloidosomes. This suggests that the polypyrrole overlayer reinforces the latex superstructure. Secondly, the polypyrrole

overlayer has a relatively high Hamaker constant[18] and SEM images suggest that the
polypyrrole-coated microcapsules are somewhat agglomerated. The higher
magnification images in Figure 4.8 also suggest that the polypyrrole overlayer has
filled in the latex interstices, at least to some extent.
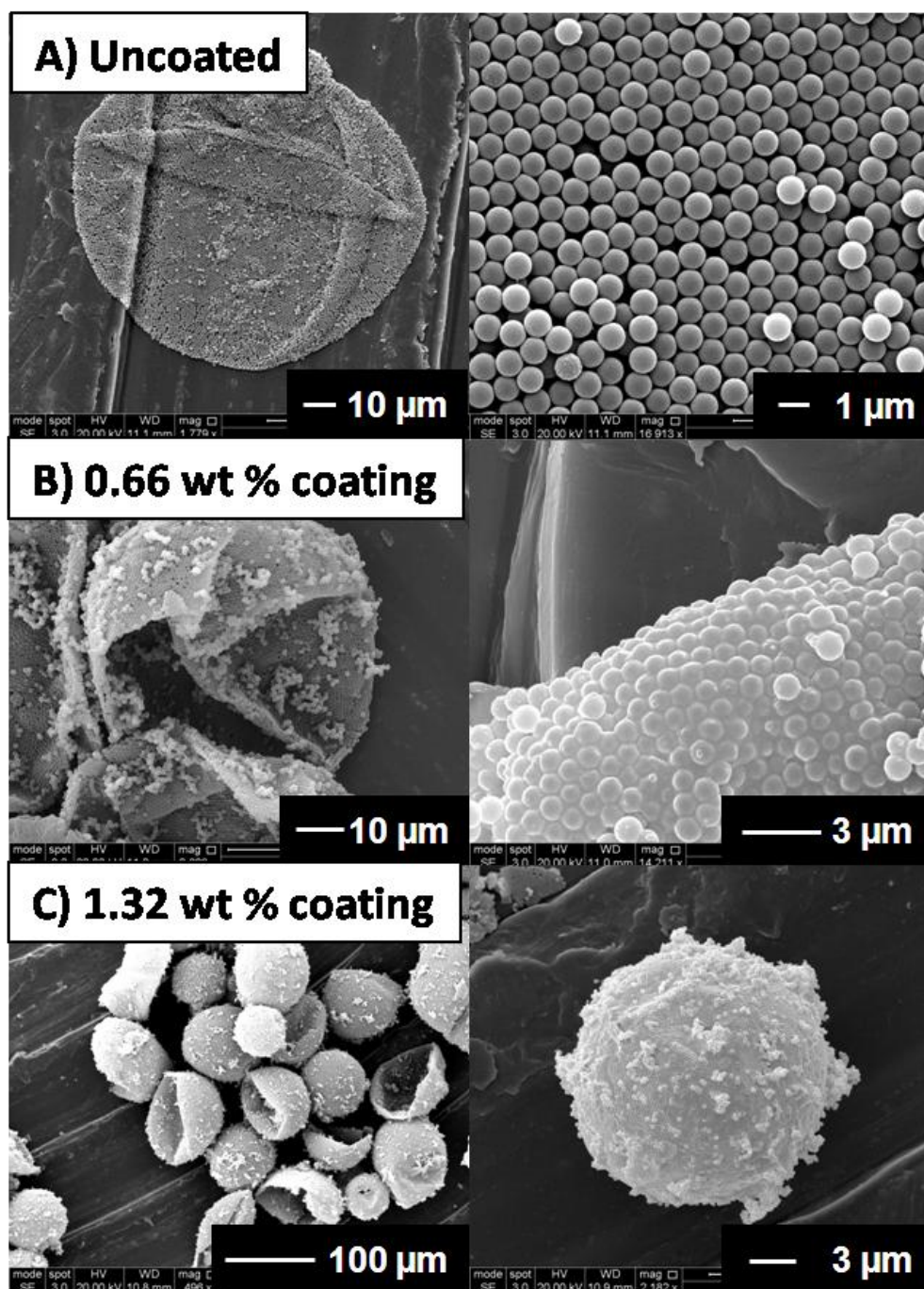
Figure 4.8. Scanning electron micrographs of cross-linked colloidosomes prepared
with 1188 nm PGMA$_{50}$-PS latex and sunflower oil encapsulated with fluorescein
dye: (A) no polypyrrole, (B) 0.06 wt % polypyrrole loading and (C) 1.32 wt %
polypyrrole loading.
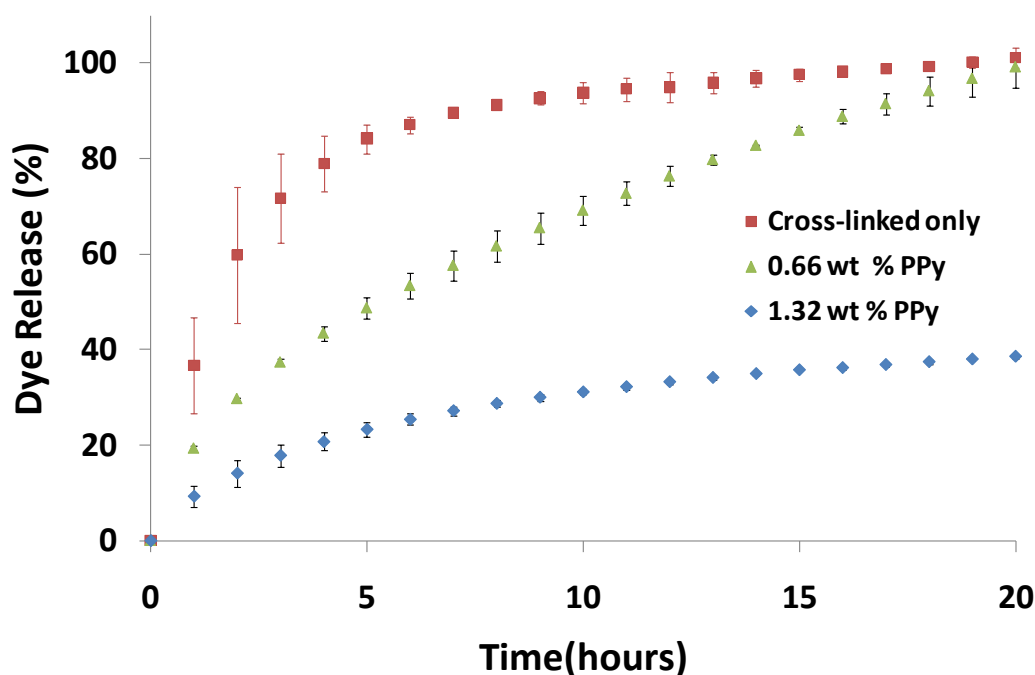
Figure 4.9. Release curves obtained at pH 9 for fluorescein dye diffusing from 89 ± 24 μm uncoated cross-linked colloidosomes prepared with (a) 1188 nm $PGMA_{50}$-PS particles (red squares), (b) cross-linked colloidosomes after coating with 0.66 wt % polypyrrole (green triangles) and (c) cross-linked colloidosomes after coating with 1.32 wt % polypyrrole (blue diamonds). The error bars represent the standard deviation taken from three repeat experiments.

This hypothesis is supported by our dye release data obtained for these microcapsules. Typical release profiles for the uncoated and coated colloidosomes are shown in Figure 4.9. From these data, the characteristic time required to release 40 % of the encapsulated dye ($t_{40\%}$) is estimated (see Table 4.1). It is clear that the polypyrrole overlayer has retarded the rate of dye release. A 0.66 wt % coating (estimated PPy thickness = 60 nm) causes $t_{40\%}$ to more than double to 3 h, but disappointingly Figure 4.9 also shows that 99 % of the dye is still released within 24 h. Doubling the PPy layer to 1.32 wt % (estimated PPy thickness = 120 nm), reduces the $t_{40\%}$ further so that only 40 % is released within the 20 h time frame of the experiment. It is also worth mentioning that the actual polypyrrole thickness could be up to half of that calculated, since the hemispheres of the PS latex protruding from the oil surface can increase the effective surface area by a factor of 2.[19] Thus

utilising an additional polypyrrole overlayer allows the release of a small molecule dye from colloidosomes to be retarded significantly.

Table 4.1. Approximate values of $t_{40\%}$ as a function of polypyrrole content. ($t_{40\%}$ is the time it takes for the release of 40 % of the encapsulated dye).

Polypyrrole Coating (%)	Polypyrrole thickness (nm)	$T_{40\%}$ (hours)
0	0	1
0.66	60	3
1.32	120	> 20

Despite some success with the polypyrrole coating protocol, many commercial applications would require encapsulated actives to have a shelf life of at least 12-18 months. This would require far more efficient encapsulation than these latex-based colloidosomes can currently offer. Any capsule based on an organic/latex particulate shell has inherent problems regarding its porosity and encapsulation performance. Our attempts to close every individual interstitial hole have proven to be problematic, especially for the larger packing defects that inevitably originate from the intrinsic 'scars' discussed earlier.[14] Even in cases where it appears that no latex interstices remain, such as in the work of Yow and Routh[3], the long-term retention of small molecules within these capsules remains a substantial technical challenge.

Bearing this in mind, it was decided that colloidosomes could potentially offer more efficient encapsulation for much larger colloidal actives. Such actives could not physically fit through the latex interstices, nor permeate through the polystyrene shell. The next part of this Chapter focuses on the encapsulation of oil-dispersible latex particles.

Encapsulation of Oil-Dispersible Latex Particles

Sterically-stabilised polystyrene latex particles were chosen, as their size can be easily tuned by changing the reaction parameters of the dispersion polymerisation protocol.[20] Latex particles were targeted that were both smaller and larger than the interstices/defects within the colloidosome shell. It was expected that efficient

encapsulation would be based purely on size exclusion: encapsulated particles smaller than the $PGMA_{50}$-PS latex interstices (and pentagonal defects) should be able to escape the colloidosome interior, while larger particles should be trapped inside and retained indefinitely.

Since the colloidosomes in this work are of the oil-in-water type, the encapsulated particles must initially be oil-dispersible. Also, in order for them to be released into the external aqueous phase (provided that they can fit through the interstices) they required a pH response that was capable of transferring them into the aqueous phase, similar to that of the fluorescein dye used in the previous section. Such particles are not commercially available and therefore they had to be designed and prepared 'in house'.

Preparation of an Oil Soluble pH Responsive Steric Stabiliser

It was decided that a suitable pH-responsive steric stabiliser should provide the route to pH-switchable latex particles. A polymeric stabiliser based on 2-(diethylamino)ethyl methacrylate (DEA) was selected. PDEA has a pK_a of around 7.3.[21] Below this value, PDEA is sufficiently hydrophilic to be water-soluble, but when its tertiary amine groups are deprotonated PDEA becomes hydrophobic. Previous work by Cheng *et al.*[22] has shown that gold particles grafted with PDEA can transfer between aqueous and organic phases by variation of the aqueous phase pH. PDEA-stabilised polystyrene particles have been previously used for the preparation of stimulus-responsive liquid marbles.[21] In this earlier work, PDEA-PS latex particles were prepared by the emulsion polymerisation of styrene in the presence of a PDEA macromonomer, which was synthesised by oxyanionic polymerisation. Due to the relatively stringent synthesis conditions that oxyanionic polymerisation requires, it was decided to prepare a reactive PDEA stabiliser by a less synthetically demanding ATRP protocol.
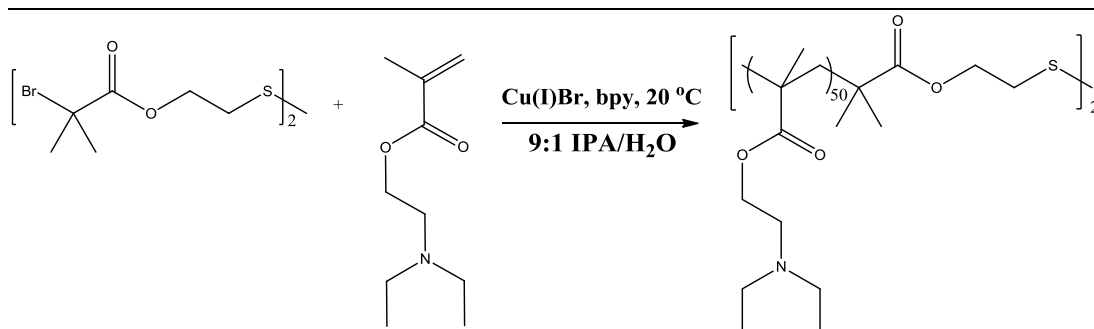
Figure 4.10. Preparation of PDEA homopolymer using a bifunctional disulfide-based ATRP initiator in a 9:1 IPA/H$_2$O mixture at 20 °C.
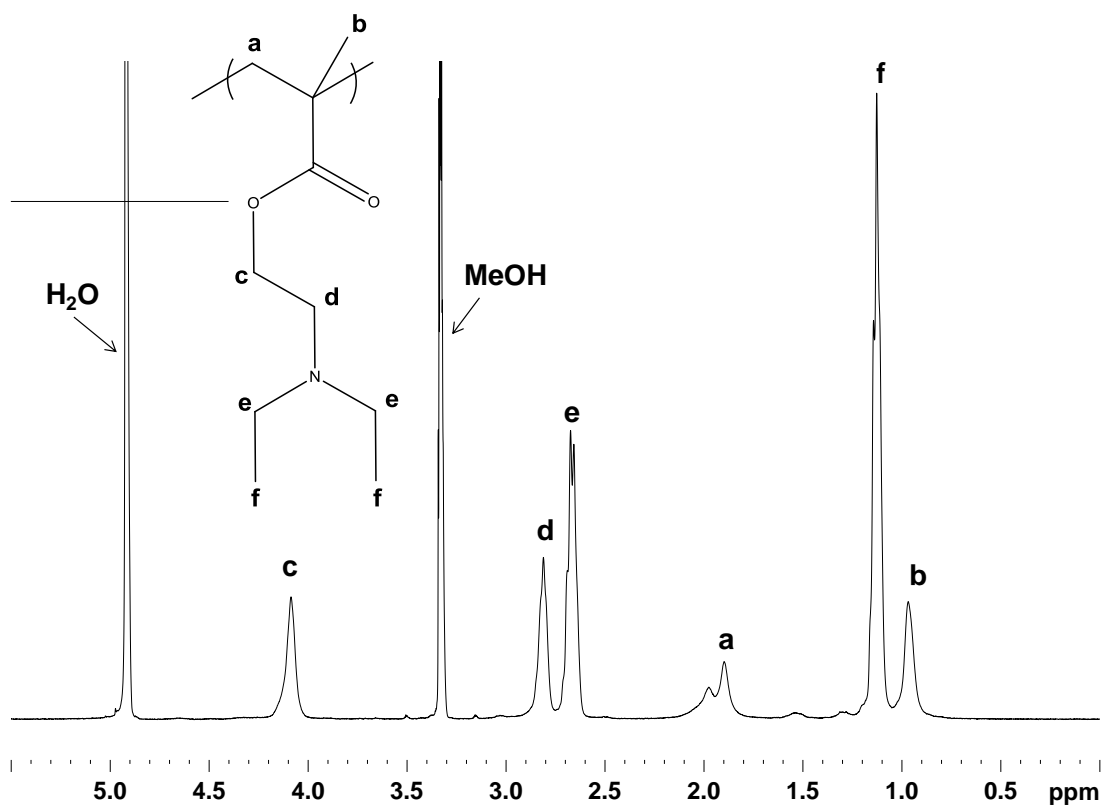
Figure 4.11. ^{1}H NMR spectrum recorded in CD$_3$OD for the PDEA$_{100}$ homopolymer prepared using the disulfide-based ATRP initiator.

The PDEA stabiliser was prepared using a bifunctional ATRP initiator containing a central disulfide bond, as illustrated in Figure 4.10. This disulfide-based initiator has been used previously in the Armes groups to prepare biocompatible thermo-responsive tri-block gellators based on the monomers 2-(methacryloyloxy)ethylphosphorylcholine and N-isopropylacrylamide.[23] The

resulting PNIPAM$_{80}$–PMPC$_{125}$-S-S-PMPC$_{125}$–PNIPAM$_{80}$ tri-block formed free standing gels at 37 °C due to inter-connecting PNIPAM core micelles. The disulfide bridges were then cleaved leading to break down of the micelle bridges and gel dissolution. The DEA polymerisation in this work went to essentially 100 % conversion within 24 h and the assigned ^{1}H NMR spectrum of the purified PDEA after copper removal is shown in Figure 4.11. The molecular weight distribution for this PDEA homopolymer is shown in Figure 4.12. This shows a monomodal trace with a relatively low polydispersity index, as expected for a controlled radical polymerisation.

M_n = 21 300
M_w/M_n = 1.31
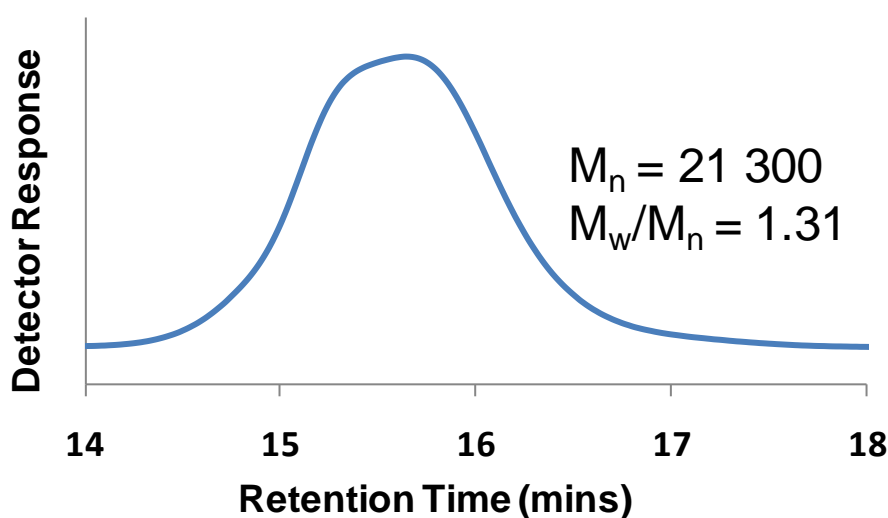
Figure 4.12. Molecular weight distribution determined by THF GPC for the PDEA$_{50}$-S-S-PDEA$_{50}$ polymer prepared by ATRP (vs. PMMA standards).

PDEA-PS Particles by Alcoholic Dispersion Polymerisation

It was found that this PDEA$_{50}$-S-S-PDEA$_{50}$ homopolymer can be used directly in alcoholic dispersion polymerisation as a reactive steric stabiliser to prepare PDEA-PS particles (Figure 4.13). It is thought that two stabilising methods of the PDEA chains are possible, either (i) the homopolymer physically adsorbs onto the growing polystyrene particles or (ii) the free radicals generated during the dispersion polymerisation of styrene cleave the central disulfide bond of the PDEA homopolymer in situ and the PDEA chains become grafted onto the particle surface via their terminal thiol groups. Evidence presented later in this Chapter confirms the

presence of the PDEA chains on the latex surface, although further work needs to be conducted to determine whether these are physically adsorbed or chemically grafted.
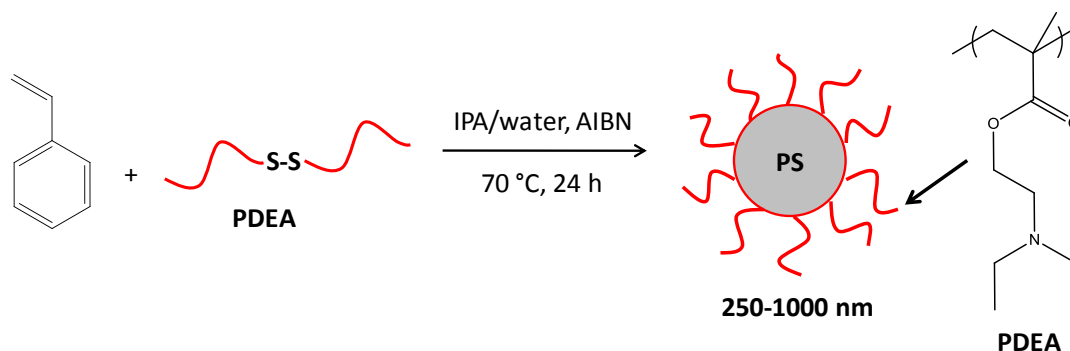
Figure 4.13. Preparation of PDEA-PS latex particles via the alcoholic dispersion polymerisation of styrene in IPA/water mixtures in the presence of the $PDEA_x$-S-S-$PDEA_x$ homopolymer at 70 °C.

Table 4.2. PDEA-PS particles prepared by alcoholic dispersion polymerisation in IPA/water mixtures at 70 °C using 10 wt % $PDEA_{50}$-S-S-$PDEA_{50}$ stabiliser and 1.0 wt % AIBN initiator based on styrene monomer.

ID	IPA/water	DLS in IPA (PDI) / nm	DLS at pH 3 (PDI) / nm	DCP / nm (at pH 3)
1	100:0	1007 (0.18)	1467 (0.30)	1032 ±155
2	90:10	474 (0.04)	580 (0.03)	516 ± 93
3	70:30	250 (0.05)	294 (0.07)	261 ± 50

This latex synthesis was carried out in the presence of 0.10 wt % (based on styrene) rhodamine B piperazine acrylate fluorescent comonomer. This was incorporated to aid visualisation of the resulting particles once they were encapsulated inside the colloidosomes. The chemical structure of this fluorescent comonomer was carefully chosen so that it would not interfere with the diisocyanate/alcohol cross-linking chemistry. The particle size data obtained for three batches of PDEA-PS latex particles are shown in Table 4.2. As expected, the particle size decreases with increasing water content in the reaction mixture. This is consistent with other reports of dispersion polymerisation syntheses conducted in alcohol/water mixtures.[20, 24] The particles also disperse readily in water at low pH, when the PDEA stabiliser chains become protonated. Therefore DLS studies could be performed in either pure IPA or in water at pH 3. For all the latexes prepared herein, dynamic light scattering gave a somewhat larger particle diameter in water at pH 3 than that measured in pure IPA. A likely reason for this is that the PDEA chains are fully protonated at pH 3 (pK_a – 7.3) and therefore occupy more volume than when solvated by IPA, leading to a larger hydrodynamic diameter. The corresponding scanning electron microscopy images for these PDEA-PS latexes are shown in Figure 4.14. Entries 1 and 3 in Table 4.2 were purified by centrifugation to remove excess monomer and stabiliser, with each successive supernatant being replaced with pure IPA. The purified particles were then centrifuged one final time and redispersed in either water at pH 3 (for aqueous electrophoresis studies) or sunflower oil (for encapsulation experiments).
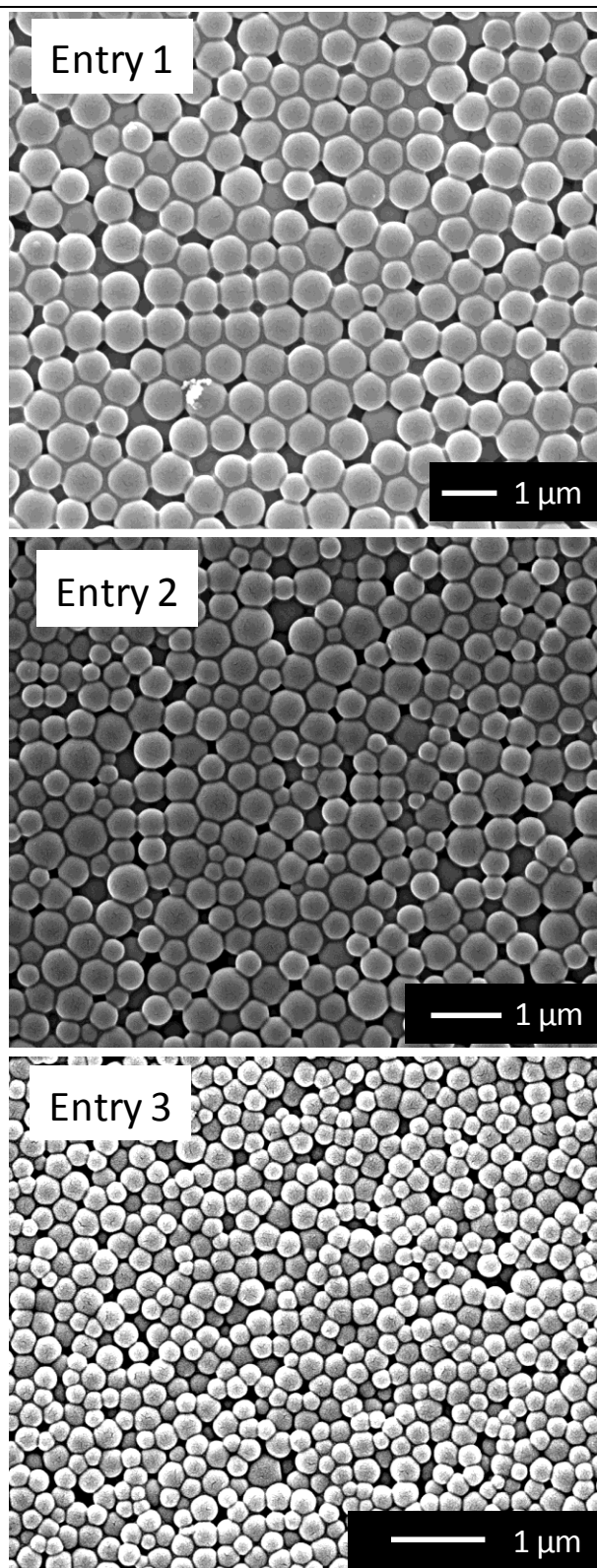
Figure 4.14. Scanning electron micrographs obtained for the PDEA-PS latexes prepared by alcoholic dispersion polymerisation at 70 °C using 100 % IPA (entry 1), 90:10 IPA/water (entry 2) or 70:30 IPA/water (entry 3).

Surface Characterisation of PDEA-PS Particles
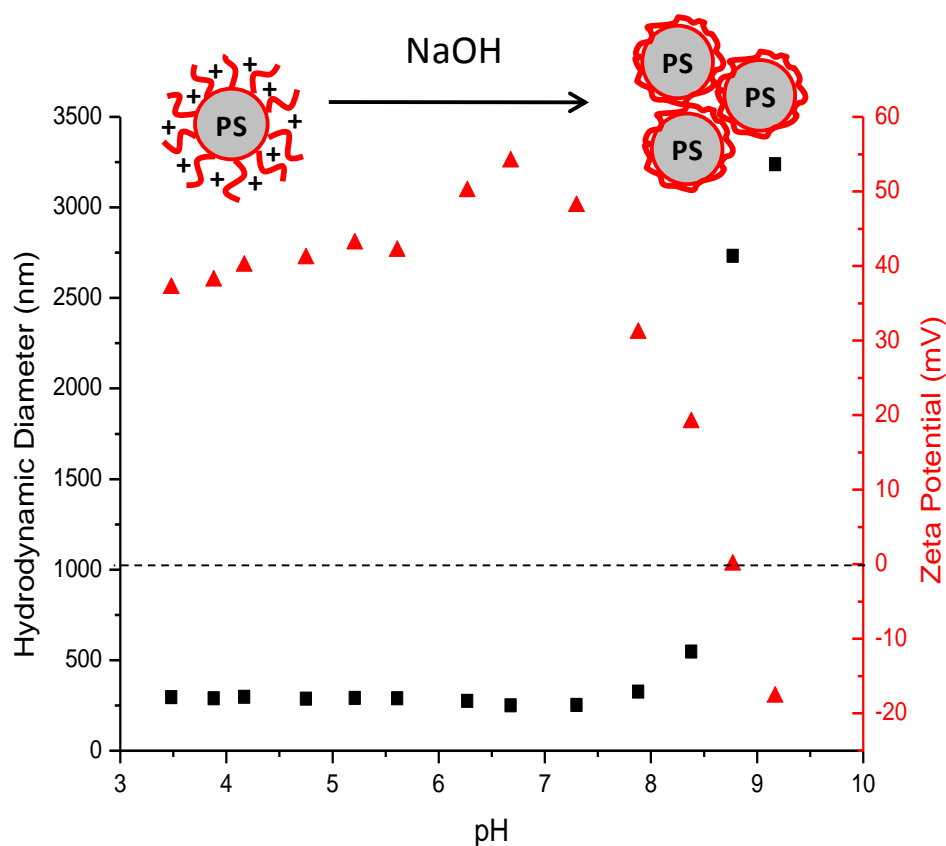
Figure 4.15. Variation of hydrodynamic diameter and zeta potential versus pH for the 250 nm PDEA-PS latex (entry 3, Table 4.2).

Combined DLS and aqueous electrophoresis studies were carried out as a function of pH as shown in Figure 4.15. The latex shows an IEP at around pH 8.7 and significant flocculation occurs above pH 8, since the PDEA chains are largely deprotonated at this pH (and thus hydrophobic). Conversely, the particles are well-dispersed and have cationic character below the pKa of the PDEA chains (due to protonation). These observations are consistent with the PDEA chains residing at the latex surface and are comparable to those reported by Dupin *et* al[21] for PDEA-PS latexes prepared by aqueous emulsion polymerisation.
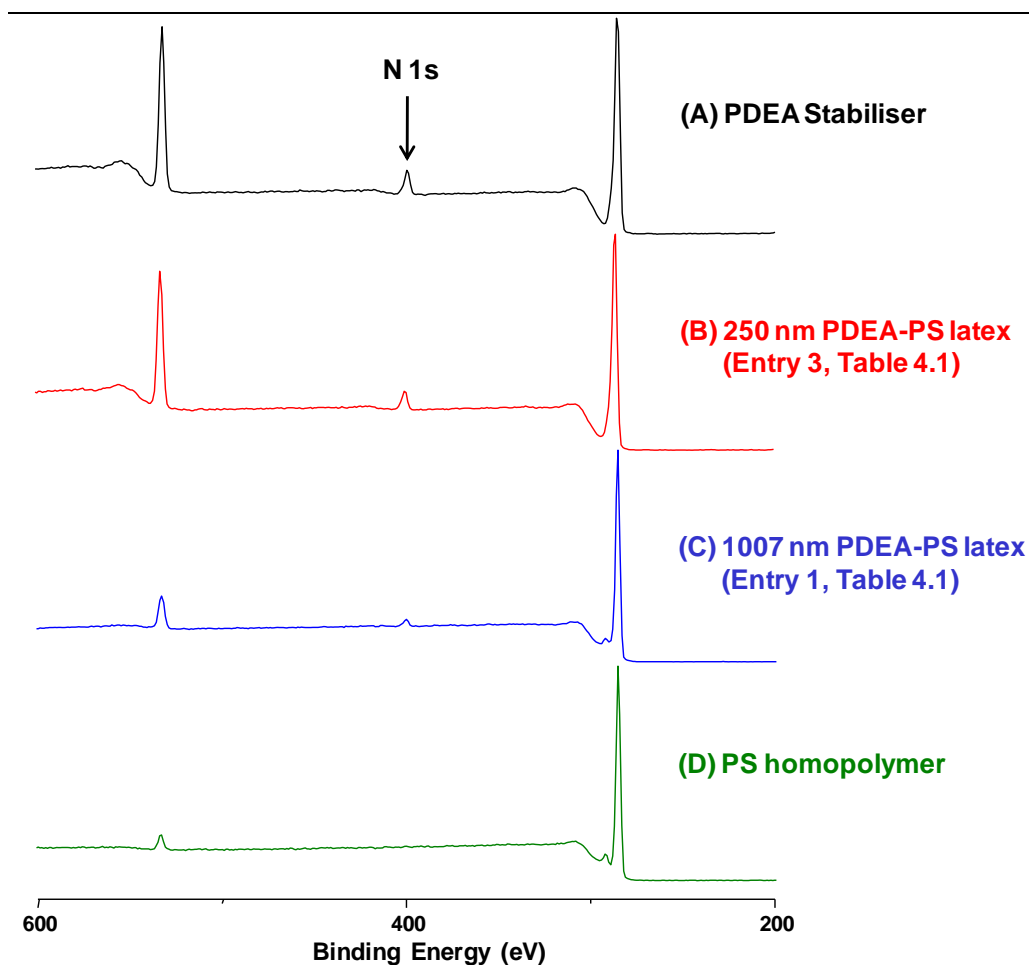
Figure 4.16. X-ray photoelectron spectra recorded for (A) the PDEA$_{50}$-S-S-PDEA$_{50}$ stabiliser, (B) the 250 nm PDEA-PS latex (entry 3, Table 4.1), (C) the 1007 nm PDEA-PS latex (entry 1, Table 4.1) and (D) a polystyrene homopolymer control prepared in the absence of the PDEA$_{50}$-S-S-PDEA$_{50}$.

Further evidence for the PDEA chains residing at the latex surface is provided by XPS analysis. Examination of the PDEA$_{50}$-S-S-PDEA$_{50}$ homopolymer stabiliser clearly shows a characteristic N1s signal originating from the tertiary amine groups (see Figure 4.16A). The same N1s signal also appears in the two spectra recorded for the PDEA-PS particles. In contrast, no N1s signal is present in the spectrum for the polystyrene homopolymer control prepared in the absence of any stabiliser. This confirms that the N1s signal on the latex surface originates from the PDEA chains, rather than from any AIBN initiator fragments.

Particle Encapsulation Studies

The PDEA-PS latex particles can be redispersed in sunflower oil in their non-protonated form. Therefore, two PDEA-PS latexes of 1007 and 250 nm (see entries 1 and 3 in Table 4.2) were encapsulated inside covalently cross-linked colloidosomes to examine their permeability towards colloidal particles.

Table 4.3. Encapsulation of 250 or 1007 nm PDEA-PS particles inside covalently cross-linked colloidosomes prepared using $PGMA_{50}$-PS latexes of either 107 or 1188 nm diameter.

Entry No	$PGMA_{50}$-PS shell thickness (DLS in water, nm)	Diameter of encapsulated PDEA-PS (DLS in IPA, nm)	Estimated interstices size from hexagonal packing (nm)	Estimated pentagonal defect size (nm)	Predicted Permeability to encapsulated particles
1	107	250	16	75	Impermeable
2	107	1007	16	75	Impermeable
3	1188	1007	180	830	Impermeable
4	1188	250	180	830	Semi-permeable

Table 4.3 shows the different encapsulation experiments that were carried out, by varying both the size of the encapsulated particles and the size of the $PGMA_{50}$-PS particles making up the colloidosome shell. Entries 1 and 2 correspond to encapsulation of PDEA-PS particles that are significantly larger than the latex particles within the colloidosome shell. In these cases it was expected that complete encapsulation should occur, since both the 250 and 1007 nm PDEA-PS particles should be unable to pass through even the pentagonal defects formed by the close-packed 107 nm $PGMA_{50}$-PS latex. Figure 4.17 shows that this is indeed the case. For comparison, Figure 4.17A shows a conventional cross-linked colloidosome prepared in the absence of encapsulated particles. As expected, these colloidosomes collapse flat upon drying. In contrast, Figure 4.17B and C shows that both the 250 nm and 1007 nm PDEA-PS latexes are clearly visible when encapsulated inside the same type of colloidosome.
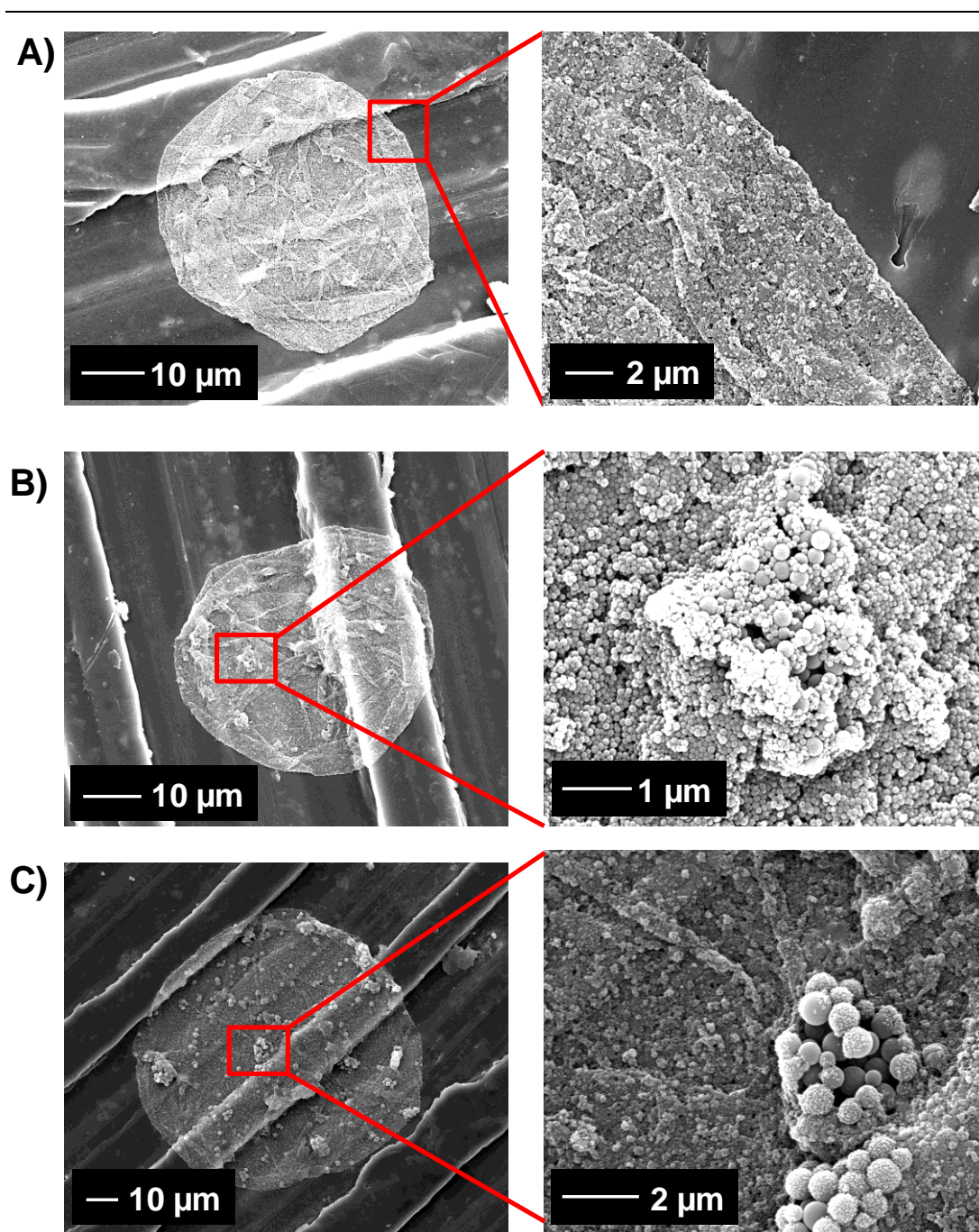
Figure 4.17. SEM images of cross-linked colloidosomes prepared with the 107 nm
PGMA$_{50}$-PS latex for (A) no encapsulation, (B) 250 nm PDEA-PS particles and (C)
1007 nm PDEA-PS particles encapsulated. Images were recorded after an alcohol
challenge.

The colloidosome no longer dries completely flat due to the particles trapped inside
the microcapsules and a more 'lumpy' surface morphology is evident. The higher
magnification image in Figure 4.17B and C shows that the PDEA-PS particles lie

beneath a layer of the 107 nm $PGMA_{50}$-PS. The encapsulated particles are too large to escape between the colloidosome interstices even during the alcohol wash protocol required for SEM. Therefore, as expected, it is relatively straightforward to encapsulate nanoparticles inside colloidosome microcapsules if the nanoparticle dimensions exceed those of the latex particles forming the shell.

Entry 3 in Table 4.3 illustrates the situation when encapsulating PDEA-PS particles of similar size to those used to form the colloidosome shell (1007 nm PDEA-PS vs. 1188 nm $PGMA_{50}$-PS). Based on the pentagonal defects within the colloidosome shell, PDEA-PS particles smaller than 0.7 x d (in this case 0.7 x 1188 = 831 nm) should in principle be able to pass through the latex interstices and hense be released into the aqueous phase when the external pH is lowered to 3. It was therefore expected that the 1007 nm PDEA-PS latex should remain encapsulated inside the colloidosomes. SEM images of the resulting colloidosomes after the alcohol challenge are shown in Figure 4.18. However, the particle sizes are too similar to be able to distinguish them and therefore it is not obvious by SEM if the particles have been successfully encapsulated. Fortunately, these encapsulated 1007 nm PDEA-PS particles were labelled with Rhodamine B, allowing their visualisation via fluorescence microscopy.
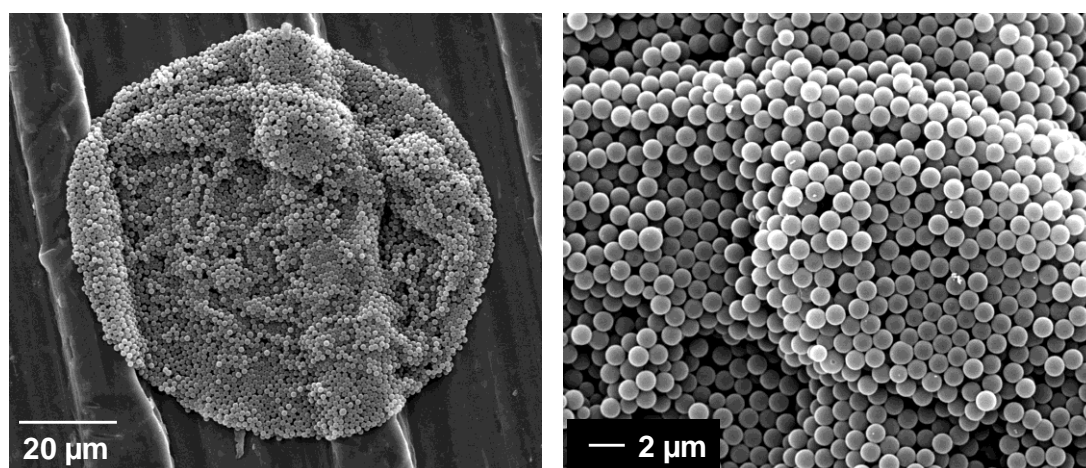
Figure 4.18. SEM images of covalently cross-linked colloidosomes after an alcohol challenge, inside which 1007 nm PDEA-PS particles have been encapsulated. The colloidosome shell was constructed using 1188 nm PGMA50-PS particles and sunflower oil. (Entry 3, Table 4.3).

Figure 4.19A shows a fluorescent microscope image of 1007 nm PDEA-PS particles encapsulated inside a colloidosome prepared with 1188 nm PGMA$_{50}$-PS particles at pH 9. In this case only the encapsulated particles are fluorescent, not those in the shell and therefore it is clear that these PDEA-PS particles are present inside the colloidosomes. Figure 4.19B and C show the same colloidosome microcapsules at pH 3, under conditions where the PDEA stabiliser chains on the encapsulated particles should become protonated. Providing that the particles can pass through the latex interstices, this change in pH should transfer them into the external aqueous phase. However, it is clear from the fluorescent microscopy images that the majority of the PDEA-PS particles remain encapsulated inside the colloidosomes. However Figure 4.19C, does show two particles highlighted by white circles that are on the outside of the microcapsules and appear to have been released from the colloidosomes. Although in principle latex particles of ~ 1 μm should not be able to fit through the PGMA$_{50}$-PS latex interstices, the latex size distribution is relatively broad as judged by SEM. Therefore these PDEA-PS particles could actually be less than 830 nm in diameter. It is also worth mentioning that these samples were equilibrated at pH 3 for one week prior to the fluorescence microscopy measurements, allowing ample time for the PDEA-PS latex to become protonated and transfer into the aqueous phase. Therefore it is apparent from the highly fluorescent cores that the majority of these particles have remained encapsulated inside the colloidosomes.

Entry 4 in Table 4.3 shows the situation for encapsulating the smaller 250 nm PDEA-PS particles inside colloidosomes prepared with the 1188 nm PGMA$_{50}$-PS latex. These PDEA-PS particles should be too large to pass through the close-packed interstices (0.15d = 178 nm). However, they should be small enough to fit through the pentagonal defects (0.7d = 831 nm). It was therefore expected that much more particle release would be observed for this smaller latex than for the encapsulation of the larger 1007 nm PDEA-PS.
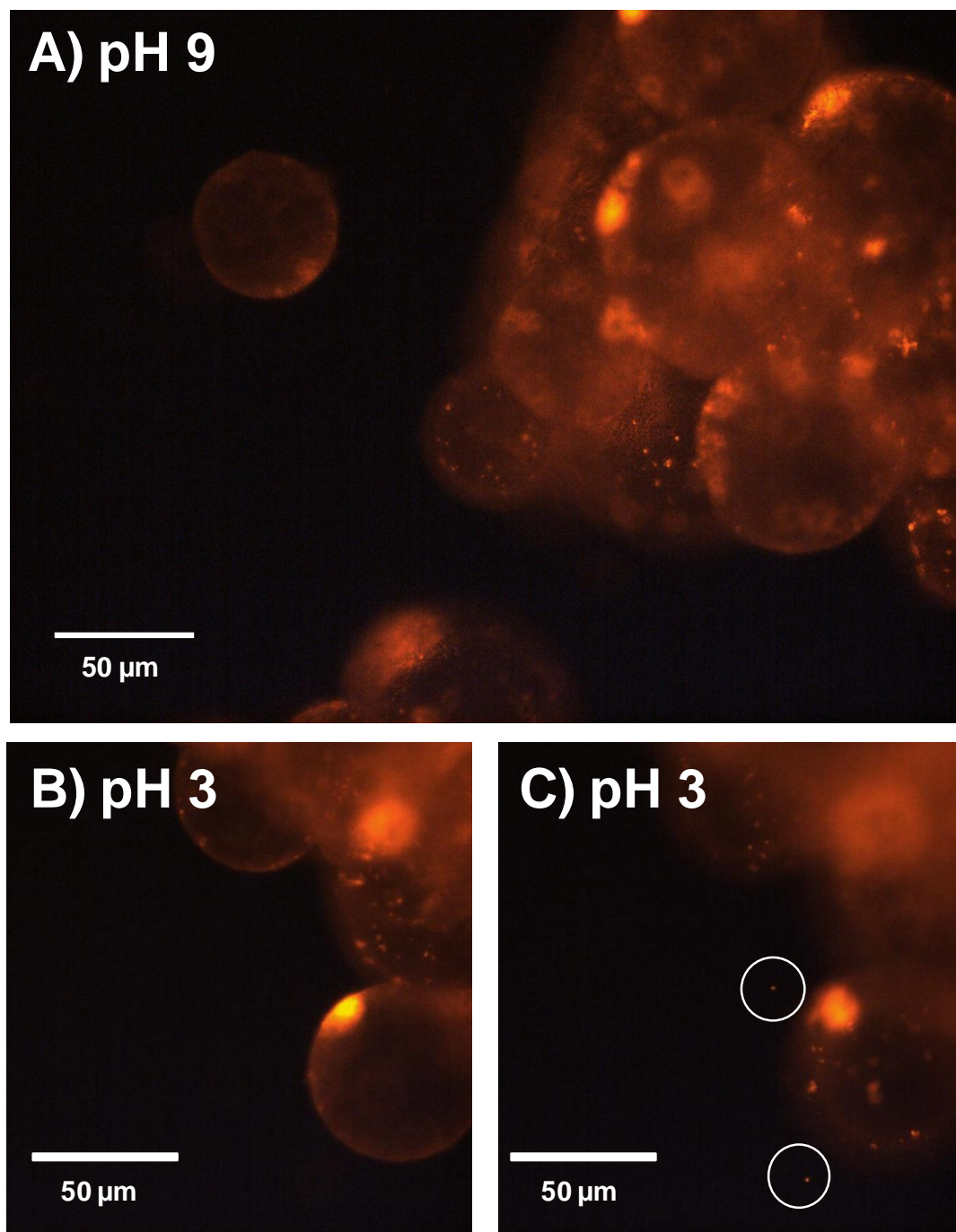
Figure 4.19. Fluorescent microscopy studies recorded for a 1007 nm Rhodamine B-labelled PDEA-PS latex encapsulated inside colloidosome microcapsules prepared using the 1188 nm PGMA$_{50}$-PS particles (Entry 3, Table 4.3). (A) pH 9, (B) pH 3 and (C) same capsules as (B) viewed at a different focal plane. Note the two latex particles circled in white that are visible outside the colloidosomes in (C).
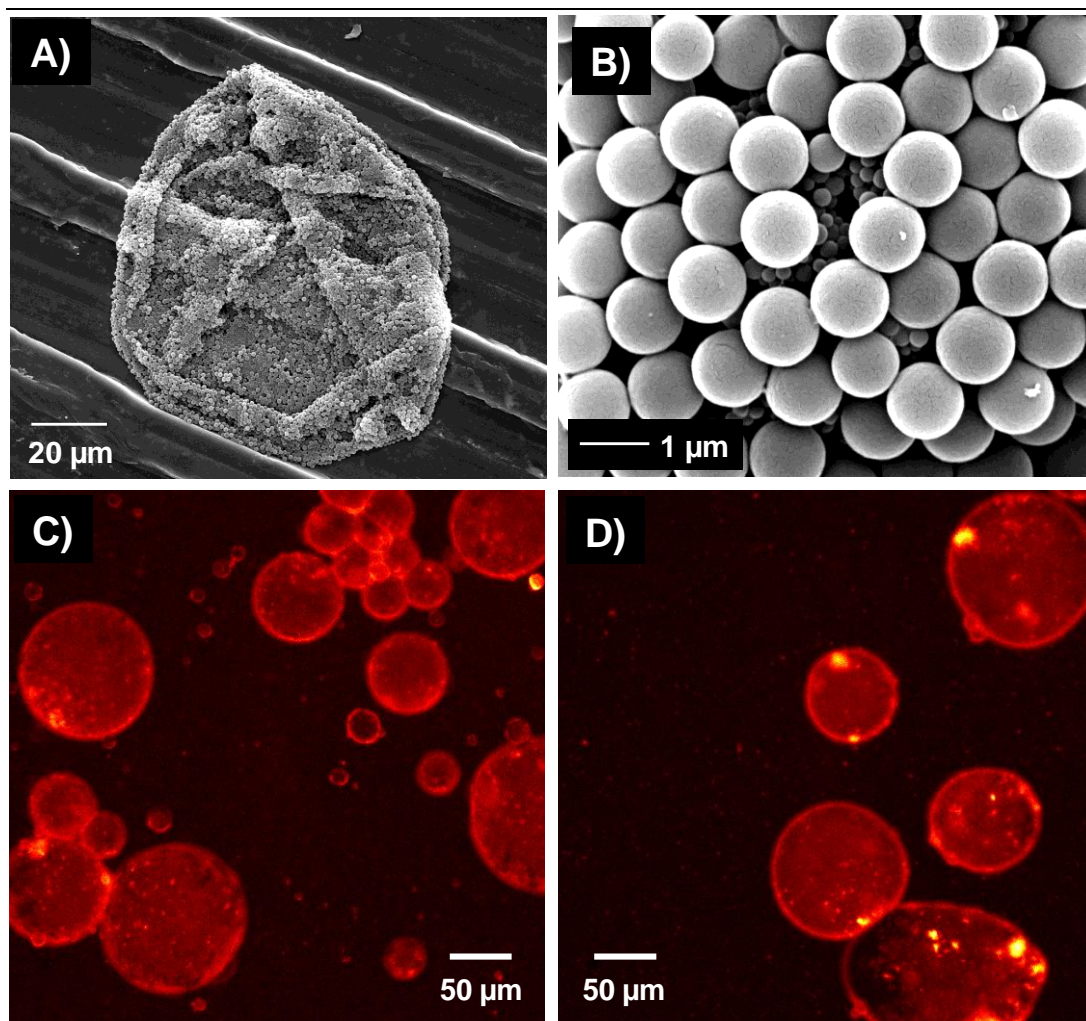
Figure 4.20. Microscopy images of 250 nm PDEA-PS latex particles encapsulated inside colloidosomes prepared with 1188 nm PGMA50-PS latex (entry 4, Table 4.3). (A) SEM image of the colloidosome obtained after an alcohol challenge, (B) higher magnification image of (A). Fluorescence microscopy images of these colloidosomes with the aqueous phase adjusted to (C) pH 9 and (D) at pH 3.

Figure 4.20 shows the SEM and fluorescence microscopy images for the resulting covalently cross-linked colloidosomes. Both imaging techniques provide good evidence for encapsulation of the 250 nm PDEA-PS particles. The high magnification SEM image in Figure 4.20 B confirms that at least some of the encapsulated particles remain inside the colloidosome even after repeated washing with alcohol. The 250 nm PDEA-PS particles were found to be somewhat less fluorescent than their larger counterparts. Therefore a more sensitive camera was required to detect their fluorescence in this case (see Figure 4.20 C and D). It is not conclusive from these fluorescence microscopy images whether there has been any

particle release upon adjusting the pH from 9 to 3. The instrument resolution does not allow visualisation of individual 250 nm particles. However, the colloidosome core remains highly fluorescent even at pH 3, suggesting significant particle retention. Again, these samples were left for one week at pH 3 prior to imaging to allow ample time for particle release. As explained earlier, there must be at least 12 pentagonal defects within the colloidosome shell. Although small molecules diffuse rapidly through the latex interstices, this should not be possible for sufficiently large particles. In principle, the 250 nm PDEA-PS latex should be able to pass through the pentagonal defects, although it may be unlikely that all of the encapsulated particles will be released. In addition, the PDEA chains must become protonated in order for transfer into the aqueous phase to occur. It is assumed that this protonation occurs close to the oil/water interface. Thus it is conceivable that particles may become partially protonated via the smaller hexagonal interstices and get effectively trapped at the interface. Such partially protonated particles may be unable to pass through the small interstices and unable to transfer back into the sunflower oil. Therefore the apparently high degree of particle retention is perhaps not too surprising for particles of this intermediate size. In addition, there is some evidence for 250 nm PDEA-PS particle flocculation when dispersed in sunflower oil. The particles settle under gravity within 24 hours in sunflower oil, whereas they remain stable in IPA and pH 3 water over the same time period. This could be the source of the 'hot spots' observed by fluorescence microscopy in Figure 4.20. The presence of larger particle flocs could also explain the high particle encapsulation performance for latexes of this size. Nonetheless the size exclusion encapsulation capability of covalently cross-linked colloidosomes has been demonstrated.

In order to investigate the size cut-off for these colloidosomes further, smaller PDEA-PS particles would need to be prepared (< 100 nm). These particles should pass through all the interstices and significantly less retention would be expected in this case. However, it is difficult to achieve the required degree of size control using the alcoholic dispersion polymerisation protocol employed here. Adding more water to the synthesis (i.e. 60:40 IPA/water) does not reduce the particle size further but instead leads to a larger, more polydisperse latex (DLS diameter = 641 nm, PDI = 0.15). This is presumably because the IPA/water mixture becomes a poor solvent for the PDEA stabiliser chains. In principle, such particles could be prepared by

alcoholic dispersion polymerisation via RAFT.[25] However, time constraints meant that such studies are beyond the scope of this thesis.

CONCLUSIONS

Small molecule dye release studies have been conducted on these colloidosomes both with and without annealing of the latex particles and also with an additional conducting polymer coating. The cross-linked colloidosomes failed to retard dye release when compared to a control experiment involving just sunflower oil. More surprisingly, no improvement was observed when cyclohexane annealing was conducted in order to close the latex interstices. This suggests that either this annealing was incomplete and/or that the annealed shells are highly permeable. Coating the non-annealed cross-linked colloidosomes with a thin overlayer of polypyrrole offers some improvement with respect to dye release, with thicker coatings leading to slower release, as expected. However, such latex-based microcapsules do not currently provide a practical means of encapsulating small molecules over relatively long time scales (e.g. months or years). Nevertheless, colloidosomes may yet offer potential biological applications where encapsulation of relatively large entities (cells, enzymes etc.) is desired in combination with high permeability of small molecules (e.g. nutrients or reaction products) across the microcapsule wall. In this case the cross-linked stabiliser chains should act as a macromolecular 'mesh' to aid retention of the encapsulated large bio-actives. This proof of principle has been demonstrated by the successful encapsulation of pH-responsive PDEA-PS latex particles. The encapsulated particles were dispersible in both sunflower oil and water below the pK_a of the PDEA stabiliser chains (pH 7.3). This pH-responsive behaviour allowed latex particles to be transferred from the oil core into the surrounding aqueous phase via a pH trigger. Fluorescence microscopy experiments confirmed the hypothesis that actives larger than the colloidosome interstices are retained inside these microcapsules. Furthermore, SEM also provided evidence for PDEA-PS latex encapsulation, even after repeated washings with alcohol. These preliminary experiments confirm that colloidosomes can encapsulate relatively large actives through a size exclusion mechanism.

REFERENCES

1.   Dinsmore, A. D.; Hsu, M. F.; Nikolaides, M. G.; Marquez, M.; Bausch, A. R.; Weitz, D. A., *Science,* **2002,** *298*, 1006-1009.

2.   Lee, D.; Weitz, D. A., *Adv. Mater.,* **2008,** *20*, 3498-3503.

3.   Yow, H. N.; Routh, A. F., *Langmuir,* **2009,** *25*, 159-166.

4.   Thompson, K. L.; Armes, S. P.; Howse, J. R.; Ebbens, S.; Ahmad, I.; Zaidi, J. H.; York, D. W.; Burdis, J. A., *Macromolecules,* **2010,** *43*, 10466-10474.

5.   Lascelles, S. F.; Armes, S. P., *Adv. Mater.,* **1995,** *7*, 864.

6.   Madsen, J.; Armes, S. P.; Bertal, K.; Lomas, H.; MacNeil, S.; Lewis, A. L., *Biomacromolecules,* **2008,** *9*, 2265-2275.

7.   Nguyen, T.; Francis, M. B., *Org. Lett.,* **2003,** *5*, 3245-3248.

8.   Cairns, D. B.; Armes, S. P.; Bremer, L. G. B., *Langmuir,* **1999,** *15*, 8052-8058.

9.   Lavis, L. D.; Rutkoski, T. J.; Raines, R. T., *Anal. Chem.,* **2007,** *79*, 6775-6782.

10.   Rosenberg, R. T.; Dan, N. R., *J. Colloid Interface Sci.,* **2010,** *349*, 498-504.

11.   Rosenberg, R. T.; Dan, N. R., *J. Colloid Interface Sci.,* **2011,** *354*, 478-482.

12.   Fortuna, S.; Colard, C. A. L.; Troisi, A.; Bon, S. A. F., *Langmuir,* **2009,** *25*, 12399-12403.

13.   Einert, T.; Lipowsky, P.; Schilling, J.; Bowick, M. J.; Bausch, A. R., *Langmuir,* **2005,** *21*, 12076-12079.

14.   Bausch, A. R.; Bowick, M. J.; Cacciuto, A.; Dinsmore, A. D.; Hsu, M. F.; Nelson, D. R.; Nikolaides, M. G.; Travesset, A.; Weitz, D. A., *Science,* **2003,** *299*, 1716-1718.

15.   Lipowsky, P.; Bowick, M. J.; Meinke, J. H.; Nelson, D. R.; Bausch, A. R., *Nat. Mater.,* **2005,** *4*, 407-411.

16.   Armes, S. P., *Synth. Met.,* **1987,** *20*, 365-371.

17.   Bjorklund, R. B., *Journal of the Chemical Society, Faraday Transactions 1: Physical Chemistry in Condensed Phases,* **1987,** *83*, 1507-1514.

18.   Markham, G.; Obey, T. M.; Vincent, B., *Colloids Surf.,* **1990,** *51*, 239-253.

19.   Maeda, S.; Armes, S. P., *Synth. Met.,* **1995,** *73*, 151-155.

20.   Lacroix-Desmazes, P.; Guyot, A., *Macromolecules,* **1996,** *29*, 4508-4515.

21.   Dupin, D.; Armes, S. P.; Fujii, S., *J. Am. Chem. Soc.,* **2009,** *131*, 5386-5387.

22.   Cheng, L.; Liu, A.; Peng, S.; Duan, H., *ACS Nano,* **2010,** *4*, 6098-6104.

23.   Li, C.; Madsen, J.; Armes, S. P.; Lewis, A. L., *Angewandte Chemie International Edition,* **2006,** *45*, 3510-3513.

24.   Terence, C., *Colloids Surf.,* **1981,** *3*, 119-129.

25.   Li, Y. T.; Armes, S. P., *Angew. Chem., Int. Ed.,* **2010,** *49*, 4042-4046.

Chapter Five

Preparation of Pickering Emulsions and Colloidosomes by Stirred Cell Membrane Emulsification

INTRODUCTION

Pickering emulsions are most frequently prepared by simple high shear homogenisation of the immiscible oil and water phases. Control over the mean droplet size can be controlled to some extent by varying parameters such as particle size and concentration.[1-2] However, only poor control over the uniformity of the resulting droplets is achieved, with rather broad droplet size distributions generally being obtained. Over recent years various techniques have emerged that can narrow emulsion droplet size distributions. Previously, Binks and co-workers reported the preparation of highly uniform Pickering emulsions using a surfactant-stabilised emulsion as a template.[3] The droplet size distribution of a polydisperse precursor emulsion was "size-fractionated" by shearing using a Couette cell[4] and the adsorbed surfactant was gradually replaced at the droplet interface by dialysis in the presence of the either polystyrene or silica particles. However, this process is rather time-consuming and relatively high shear rates are required, which may not be suitable for relatively delicate actives such as cells or enzymes. Highly monodisperse Pickering emulsions have been recently prepared using microfluidic devices.[5-8] Although this approach produces highly uniform emulsions (typically with coefficients of variation below 5 %),[7] droplets are typically generated one at a time. This disadvantage can be addressed by designing massively parallel microfluidic devices to enhance throughput,[9] but occasional blockages may well be difficult to diagnose and rectify. Thus a robust and convenient means of achieving significantly better control over the droplet size distribution for Pickering emulsions has remained somewhat elusive.

Membrane emulsification

In principle, membrane emulsification can produce near-monodisperse emulsion droplets on a scale far larger than that can be achieved conveniently via microfluidics. In addition, the former technique generally requires far less energy input compared to conventional homogenisation.[10]

In membrane emulsification, the droplet phase is typically pumped through a membrane consisting of a series of well-defined pores into the continuous phase, which contains the emulsifier. Ceramic, metal, glass and polymeric membranes have each been used successfully.[10] The droplets are detached by shear forces acting at the

membrane surface (see Figure 5.1). Shear can be created by (i) cross-flow of the
continuous phase over the membrane surface, (ii) membrane rotation/vibration or
(iii) by mechanical stirring.[10] This force should be sufficient to detach the droplets
from the membrane surface but not so large that it causes further droplet break-up.
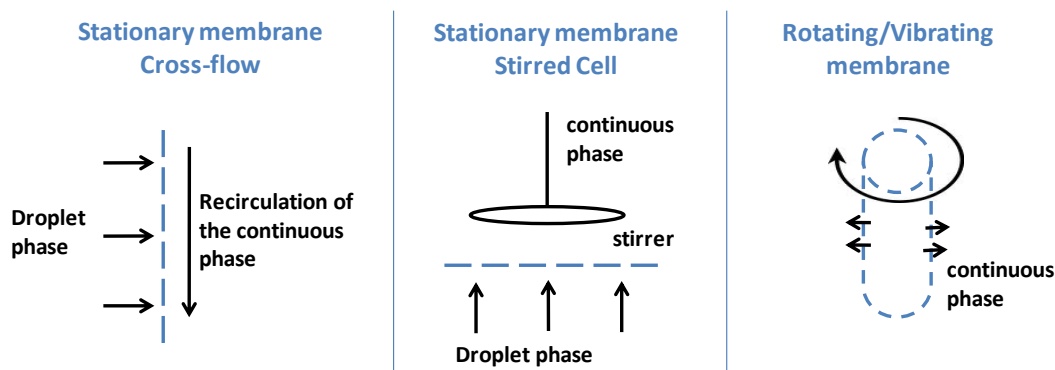
Figure 5.1. Three techniques for generating surface shear within a membrane
emulsification set-up. Oil droplets can be broken off by shear forces due to cross-
flow of the continuous phase or mechanical stirring or membrane rotation.

Previous reports of Membrane Emulsification for the preparation of Pickering emulsions

Although there have been a number of literature reports of the use of membrane
emulsification for the preparation of near-monodisperse emulsion droplets, the
majority of these studies have focused on surfactant-stabilised emulsions.[10-12] There
are very few reports concerning the formation of low polydispersity Pickering
emulsions. Yuan *et al.*[13] recently reported a pilot-scale membrane emulsification
technique to prepare silica-stabilised emulsions in an attempt to gain better control
over the droplet size distribution. Both cross-flow and rotating membrane
emulsification were investigated. In each case, stable Pickering emulsions were
obtained with somewhat narrower droplet size distributions compared to those
produced via rotor-stator homogenisation under otherwise identical conditions. The
rotating membrane technique was amenable to small volumes of continuous phase
(30 ml) and yielded droplets in the region of 150-500 μm diameter with coefficients
of variation ranging from 32 to 80 %, as judged by optical microscopy. However,

due to the limitations of the laser drilling technique used to manufacture the membrane pores, droplet diameters below approximately 50 µm cannot be achieved.[13] In contrast, the cross-flow system produced droplets with significantly smaller diameters (< 10 µm) with coefficients of variation as low as 35 %. However, optimisation of the cross-flow emulsification conditions required a significant amount of test material, with each experiment requiring approximately one litre of the continuous phase. This is potentially a disadvantage when using more specialised or expensive particulate emulsifiers (as in the present work).

The Present Work

Herein low polydispersity oil-in-water Pickering emulsions are prepared using the PGMA$_{50}$-PS latex particles discussed in Chapter 2 in conjunction with a stirred-cell membrane emulsification system. The advantage of this set-up is that emulsions can be conveniently produced using less than 100 ml of the aqueous continuous phase. This allows a large number of small scale experiments to be conducted easily and reproducibly without utilising substantial quantities of latex emulsifier. Moreover, the hydroxyl groups on the PGMA stabiliser chains allow *in situ* cross-linking to obtain the corresponding low polydispersity colloidosomes. The work described in the present Chapter has resulted in a publication in Langmuir.[14]

EXPERIMENTAL

Materials

Glycerol monomethacrylate (GMA) was kindly donated by Cognis UK Ltd (Hythe, UK) and used without further purification. 4-Vinylbenzyl chloride (4-VBC; 90 %), Cu(I)Cl (99.995 %) 2,2′-bipyridine (bpy, 99 %), sunflower oil and tolylene 2,4-diisocyanate-terminated poly(propylene glycol) [PPG-TDI] were all purchased from Aldrich and were used as received. Styrene (Aldrich) was passed through a column of basic alumina to remove inhibitor and then stored at -20 °C prior to use. 2,2'-Azobisisobutyronitrile (AIBN; BDH) was used as received. Methanol and ethanol were purchased from Fisher and were used as received. De-ionised water was used in all experiments. Silica gel 60 (0.0632-0.2 mm) was obtained from Merck (Darmstadt, Germany).

Macromonomer Synthesis

The $PGMA_{50}$ macromonomer was prepared using atom transfer radical polymerisation as described in Chapter 2.[15]

Rhodamine 6G piperazine methacrylate synthesis

The rhodamine 6G piperazine methacrylate was kindly prepared by Mr Nicholas Warren according to the following two-step protocol.[16] The structure of the final product is shown in Figure 5.2.
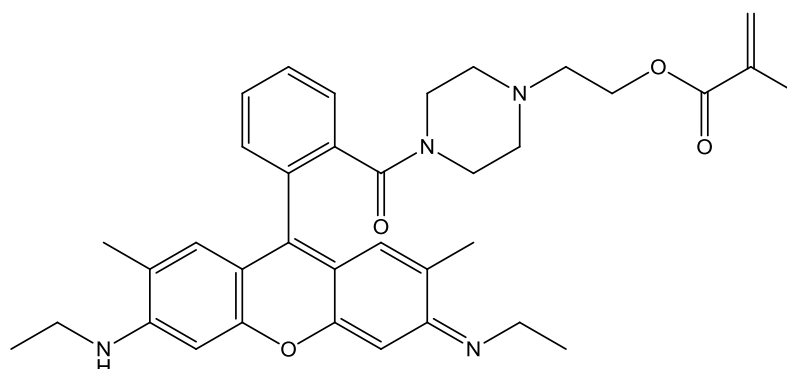
Figure 5.2. Structure of the rhodamine 6G piperazine methacrylate used to prepare fluorescently-labelled $PGMA_{50}$-PS latex particles of 150 nm diameter.

Step 1. Preparation of rhodamine 6G 4-(2-hydroxyethyl)piperazine amide

In a 100 ml round-bottomed flask, rhodamine 6G (10.0 g, 0.021 mol) was dissolved in *N*-(2-hydroxyethyl)piperazine (20.0 g, 0.154 mol). The flask was fitted with a reflux condenser, placed under nitrogen and heated to 90 °C for approximately 24 h. After cooling, the solution was dissolved in the minimum amount of methanol and poured into 500 ml water. After filtering, the aqueous solution was saturated with sodium chloride and extracted with 50 ml aliquots of a 2:1 isopropanol: dichloromethane mixture until only a faint colour remained in the aqueous phase. The combined organic phases were dried over anhydrous sodium sulfate, filtered and evaporated. The product was obtained as a dark red powder (7.2 g, 65 % yield) and used without further purification.

^{1}H NMR (400 MHz, 3:1 CDCl$_3$: CD$_3$OD) δ 7.52 (m, 2H), 7.37 (m, 1H), 7.16 (m, 1H), 6.73 (s, 2H), 6.55 (s, 2H), 3.46 (t, 1H, J = 5.50 Hz), 3.40 (t, 2H, J = 5.62 Hz), 3.29 (q, 7.27 Hz), 3.16 (br m, 2H + MeOH), 2.94 (br t, 2H, J~5.1 Hz), 2.54 (br t, 2H, J~5.0 Hz), 2.40 (t, 1H, J = 5.38 Hz), 2.24 (t, 2H, J = 5.62 Hz), 1.97 (s, 6H), 1.17 (t, 6H, J = 7.21 Hz) ppm

^{13}C NMR (400 MHz, 3:1 CDCl$_3$: CD$_3$OD) δ 170.42, 160.21, 159.08, 157.63, 138.00, 136.75, 133.94, 133.05, 132.82, 132.27, 130.42, 128.20, 116.52, 96.66, 61.20, 55.50, 52.98, 46.41, 41.25, 20.00, 16.23 ppm

MS (EI+), m/z = 527 Da

Step 2. Synthesis of rhodamine 6G 4-(2-(methacryloyloxy)ethyl)piperazine amide

In a 100 ml round-bottomed flask was placed rhodamine 6G 4-(2-hydroxyethyl)piperazine amide (neutral form, 1.0051 g, 1.9 mmol) and methacrylic acid (20.0 ml, 20.3 g, 0.236 mol). To this mixture was added 50 ml chloroform and 12.6 mg BHT. Once a homogeneous solution had formed, methacrylic anhydride was added (2 ml, 2.07 g, 13.4 mmol). After 40 h, 2 ml methanol was added to quench residual methacrylic anhydride and the reaction mixture was stirred for a further 2 h at 20 °C. Chloroform was evaporated at 30 °C under reduced pressure and the residue was poured into 200 ml diethyl ether. After filtration and washing

with diethyl ether, the solid residue was partitioned between dichloromethane (100 ml) and water (50 ml). Sodium hydrogen carbonate was added until gas evolution ceased and the aqueous phase was washed with aliquots of dichloromethane (3 x 50 ml). The combined organic solutions were washed with water (five 50 ml portions) and finally with a saturated sodium bromide solution (50 ml). The organic phase was dried over anhydrous sodium sulfate, filtered and evaporated. After precipitation into diethyl ether, the dark red solid product (0.859 g, 76 % yield) had a purity of at least 95 % as judged by ^{1}H NMR.

^{1}H NMR (400 MHz, 3:1 CDCl$_3$: CD$_3$OD) δ 7.78 (m, 2H), 7.65 (m, 1H), 7.46 (m,1H), 7.00 (s, 2H), 6.85 (s, 2H), 6.09 (s, 1H), 5.63 (s, 1H), 4.23 (t, 2H, J = 5.62 Hz), 3.55 (q, 4H, J = 7.15 Hz), 3.41 (br m, 4H), 2.65 (t, 2H, J = 5.75 Hz), 2.37 (br m, 2H), 2.32 (br m, 2H), 2.21 (s, 6H), 1.93 (br s, 3H), 1.40 (t, 6H, J = 7.21 Hz) ppm

^{13}C NMR (400 MHz, 3:1 CDCl$_3$: CD$_3$OD) δ 173.16, 167.20, 156.97, 156.08, 153.43, 136.05, 131.51, 130.28, 129.69, 128.97, 127.51, 126.05, 119.66, 113.49, 93.64, 61.84, 56.32, 53.47, 52.69, 47.53, 41.79, 38.44, 19.80, 18.52, 13.76 ppm

ES (EI+) m/z = 595 Da

Latex Synthesis by either Aqueous Emulsion Polymerisation or Alcoholic Dispersion Polymerisation

PGMA$_{50}$ macromonomer (0.500 g) was weighed into a 100 ml round-bottomed flask and dissolved in 50.0 g of either water (aqueous emulsion polymerisation) or a 9:1 methanol/water mixture (alcoholic dispersion polymerisation). This solution was purged with nitrogen for 30 minutes before being heated to 70°C under a nitrogen blanket. The AIBN initiator (0.050 g) was dissolved in styrene (5.00 g) and purged with nitrogen before being injected into the reaction vessel. The solution turned milky-white within 1 h and was stirred for 24 h. In the case of aqueous emulsion polymerisation the latexes were purified by three centrifugation/redispersion cycles, with each successive supernatant being replaced with pure water. In the case of alcoholic dispersion polymerisation the latexes were purified by six centrifugation/redispersion cycles, with each successive supernatant being replaced

three times by a 9:1 methanol/water mixture, followed by a further three cycles using pure water. A scale-up synthesis using the same protocol at 70°C was also conducted with PGMA$_{50}$ macromonomer (5.00 g), AIBN initiator (0.50 g), styrene (50.0 g) and water (500 g) in a 1 L round-bottomed flask equipped with a large magnetic stirrer. The mean diameters of these three purified latexes were assessed by scanning electron microscopy and dynamic light scattering.

The above protocol for aqueous emulsion polymerisation was repeated utilising 0.050 g rhodamine piperazine-methacrylate (1 wt % based on styrene) to prepare a fluorescently-labelled latex for fluorescence microscopy experiments.

Preparation of Pickering Emulsions via Homogenisation

7.00 ml of a 1.0 % aqueous dispersion of 230 nm PGMA$_{50}$-PS latex was homogenised with 1.00 ml of sunflower oil for 2 minutes using an IKA Ultra-Turrax T-18 homogeniser with a 10 mm dispersing tool operating at 12,000 rpm.

Preparation of Pickering Emulsions via Stirred Cell Membrane Emulsification

Membrane emulsification studies were conducted using a Micropore Technologies Ltd stirred cell (Micropore Technologies Ltd, Hatton, Derbyshire, UK). This unit uses a 24 V DC motor to drive a paddle stirrer above a stationary nickel membrane to create surface shear (see Figure 5.3). Applied voltages ranging from 4 to 15 V, the relationship between operating voltage and stirrer speed is linear and corresponds to approximate stirring rates of 500 to 1900 rpm (according to the manufacturer). The oil injection rate was controlled using a syringe pump (0.03 – 0.40 ml/min) and a total oil volume of 10 ml was injected for each experiment. Both a standard membrane and an annular ring membrane were evaluated, with the latter proving more useful. Both membranes had a 5 μm pore diameter and a mean pore pitch (spacing) of 200 μm. The aqueous phase (70 ml) comprised 0.6 to 7.0 wt % PGMA$_{50}$-PS latex with a mean particle diameter of either 130, 230 or 1100 nm, as determined by dynamic light scattering. In the studies in the previous chapter, *n*-dodecane was utilised as the oil phase. However, it was found that this oil led to undesirable swelling of the membrane gasket and injection tubing. For this reason, sunflower oil was preferred in the present work. As more sunflower oil was injected

into the cell, the number of free, non-adsorbed latex particles in solution is gradually reduced. Thus for subsequent oil injections there may be insufficient latex particles to stabilise new oil droplets, hence coalescence can be observed. In order to avoid this problem, particularly for the larger latex used in these studies, the targeted emulsion concentrations were kept relatively low ($\sim$ 13 v/v %), so that excess latex particles always remained in the aqueous phase.
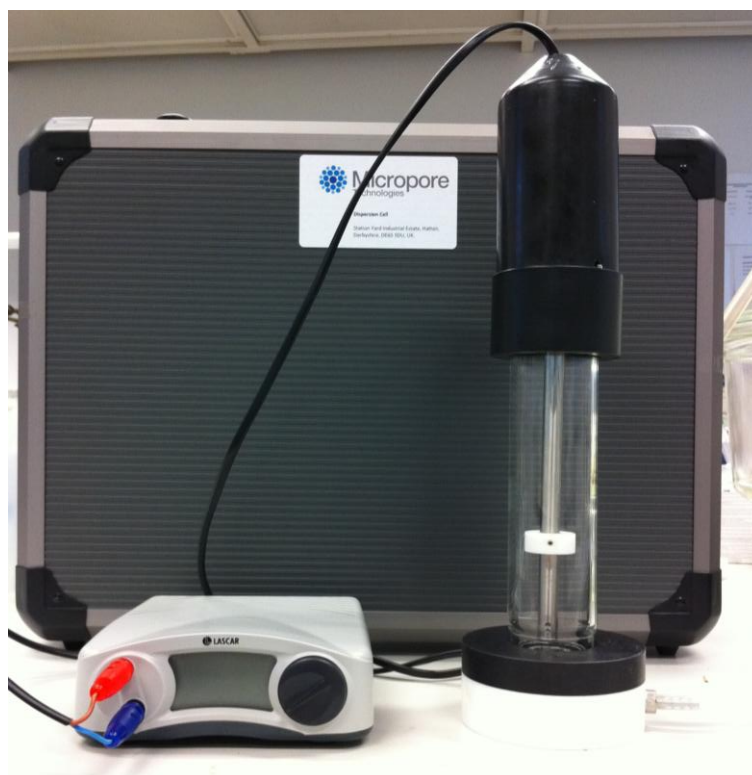
Figure 5.3. Digital photograph of the stirred-cell membrane emulsification apparatus.

Preparation of Colloidosomes via Stirred Cell Membrane Emulsification

Covalently cross-linked colloidosomes were prepared via stirred cell membrane emulsification according to the procedure above, with 4 mg/ml tolylene 2,4-diisocyanate-terminated poly(propylene glycol) [PPG-TDI] dissolved in the oil phase prior to injection.

Latex and Emulsion Characterisation

Dynamic Light Scattering (DLS)

Intensity-average hydrodynamic diameters of the three latexes were obtained by DLS using a Malvern Zetasizer NanoZS instrument at a fixed scattering angle of 173°. Aqueous dispersions of 0.01 wt % latex were analysed using disposable cuvettes and the results were averaged over three consecutive runs. The deionised water used to dilute each latex was ultra-filtered through a 0.20 μm membrane so as to remove dust.

Laser Diffraction

A Malvern Mastersizer 2000 instrument equipped with a small volume Hydro 2000SM sample dispersion unit (ca. 50 ml), a HeNe laser operating at 633 nm, and a solid-state blue laser operating at 466 nm was used to size each emulsion. The stirring rate was adjusted to 1,000 rpm in order to avoid creaming of the emulsion during analysis. After each measurement, the cell was rinsed once with ethanol, followed by three rinses with doubly-distilled water; the glass walls of the cell were carefully wiped with lens cleaning tissue to avoid cross-contamination and the laser was aligned centrally to the detector prior to data acquisition.

The mean droplet diameter was taken to be the volume mean diameter ($D_{4/3}$), which is mathematically expressed as $D_{4/3} = \Sigma D_i^4 N_i / \Sigma D_i^3 N_i$. As an indication of the droplet size distribution we report the coefficient of variation (CV) calculated from the standard deviation (σ):

$$CV(\%) = \frac{\sigma}{D_{4,3}} \times 100$$

Optical Microscopy

Optical microscopy images were recorded using a Motic DMBA300 digital biological microscope with a built in camera and Motic Images Plus 2.0 ML software.

Scanning Electron Microscopy (SEM)

SEM studies were performed using a FEI Sirion field emission scanning electron microscope using a beam current of 244 μA and a typical operating voltage of 20 kV. Colloidosome samples were washed repeatedly with ethanol to remove any traces of oil. Samples were dried onto aluminum stubs and sputter-coated with a thin layer of gold prior to examination so as to prevent sample charging.

Fluorescent Microscopy

Parallel fluorescence and brightfield microscopy was carried out using a Nikon Eclipse LV100 microscope. The fluorescence excitation and emission wavelengths were controlled by a 49004 ET - CY3 filter block (Chroma Technology Corp). Fluorescent images were captured using a high sensitivity EMCCD Andor iXon+ 897 camera (512x512 pixels). Brightfield (diascopic) images were captures using a Luminera 2.1 CCD camera.

RESULTS AND DISCUSSION

The aim of this work was to evaluate stirred cell membrane emulsification for the preparation of relatively uniform oil-in-water Pickering emulsions. A series of three poly(glycerol monomethacrylate)-stabilised polystyrene (PGMA$_{50}$-PS) latexes were utilised as emulsifiers in this study. Such latexes proved in chapter 3 to be extremely efficient Pickering emulsifiers, since the vast majority (> 99 %) are adsorbed at the surface of oil droplets, with little or no excess non-adsorbed particles remaining in the aqueous continuous phase. Due to the large scale required for these membrane emulsification experiments, new batches of PGMA$_{50}$-PS latexes were prepared for this work, thus the diameters of the particles used in this chapter differ slightly from those reported in chapters 2 and 3. Work in the previous chapters focussed on emulsions and colloidosome preparation via homogenisation using an ultra Turrax homogeniser. Although some degree of control over the mean droplet diameter was demonstrated by varying the initial latex concentration, only relatively polydisperse emulsion droplets were produced, as judged by optical microscopy and laser diffraction.[17] The coefficient of variation (CV) for emulsion droplets generated by homogenisation typically exceeds 50 %. In this chapter, four model PGMA$_{50}$-PS latexes were evaluated, with their mean diameters displayed in Table 5.1. The majority of the experiments conducted in this chapter are using the 230 nm PGMA$_{50}$-PS particles that were synthesised on a much larger scale (see entry 2, Table 5.1).

Table 5.1. Summary of the PGMA$_{50}$-PS latexes used for membrane emulsion experiments. * 1.0 wt % rhodamine piperazine methacrylate comonomer.

Entry No	Polymerisation method	DLS Diameter (nm)	PDI
1	Emulsion	130	0.05
2	Emulsion	230	0.06
3	Emulsion*	150	0.09
4	Dispersion	1100	0.04
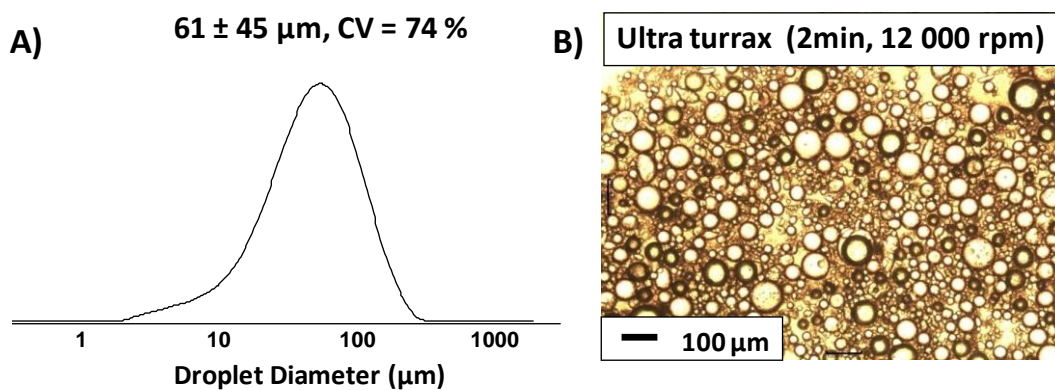
Figure 5.4. (A) A typical droplet size distribution as determined by Malvern Mastersizer for an oil-in-water emulsion prepared using 1% aqueous solution of 230 nm $PGMA_{50}$-PS latex particles (7 ml) and sunflower oil (1 ml), homogenised at 12,000 rpm for 2 mins using an Ultra Turrax homogeniser. (B) The corresponding optical microscopy image of the resulting emulsion. Note the polydispersity of the sample.

A representative emulsion droplet size distribution obtained via laser diffraction and a representative optical micrograph for a Pickering emulsion prepared using conventional homogenisation at 12,000 rpm for 2 minutes using the 230 nm $PGMA_{50}$-PS latex and sunflower oil is shown in Figure 5.4. A wide range of droplet diameters can be seen by optical microscopy and the CV in this case is 74 %, as judged by laser diffraction. Based on the recent literature,[11, 13, 18] it was anticipated that using membrane emulsification instead of homogenisation might allow significantly narrower droplet size distributions to be achieved.
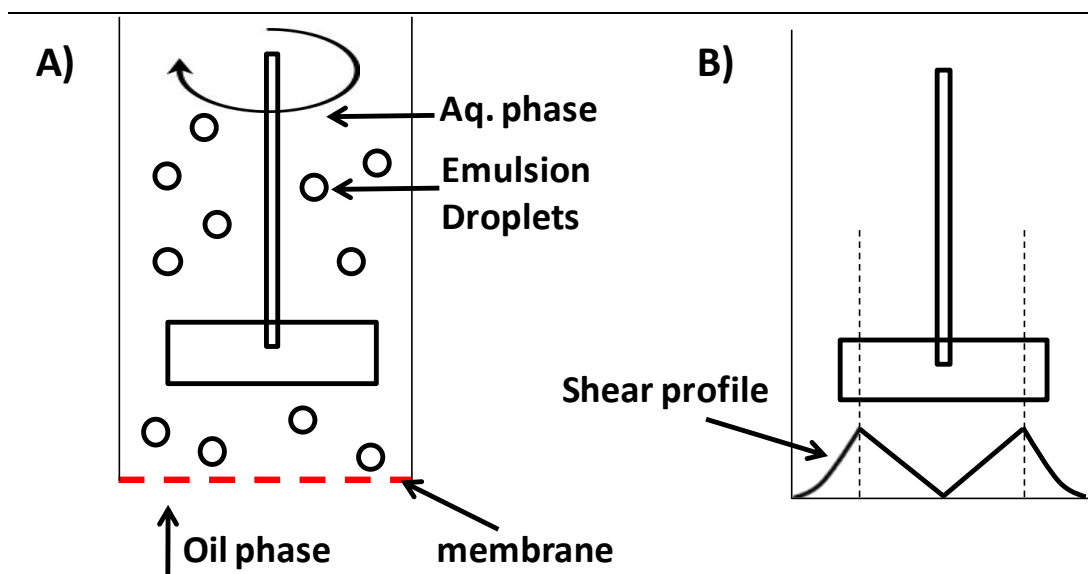
Figure 5.5. Schematic showing A) the stirred cell set up and b) the shear profile under the stirrer.

The Pickering emulsions in this work were prepared via stirred cell membrane emulsification, using a commercial dispersion cell. The cell set-up is shown in Figure 5.5A. The oil phase, in this case sunflower oil, is pumped through a flat, stationary, nickel membrane of known pore size and pore spacing, into the vessel containing the continuous aqueous phase. The droplets are broken off by the shear force created by a paddle stirrer above the stationary membrane; the shear profile underneath this blade stirrer is shown in Figure 5.5B. Two types of membrane were investigated: a standard membrane and an annular ring membrane. Both membranes had a mean pore diameter of 5 μm and a mean pore spacing of 200 μm. The standard membrane contains open pores across the entire membrane surface, whereas the annular ring membrane contains only a narrow region of open pores (see Figure 5.6). Due to the configuration of the stirred cell, there is a non-uniform shear profile beneath the paddle stirrer. Thus more uniform droplets are expected for the ring membrane as the shear on its surface will be more constant. At first sight, it seems rather surprising that the standard membrane offers any improvement in control over the droplet size distribution. Nevertheless, surfactant-stabilised sunflower-in-water emulsions of reduced polydispersity have been reported using a standard membrane (mean pore size = 20 μm).[19] In this earlier study it was suggested that, because of the non-uniform shear profile, the shear stress must attain a maximum value at some point on the membrane radius. At this point, there will be minimal pressure at the

membrane surface and hence droplet formation across the membrane in this region should be more efficient. Thus more uniform droplets can be formed using a standard membrane, since most of the droplets actually emerge from within a relatively narrow ring on the membrane surface.
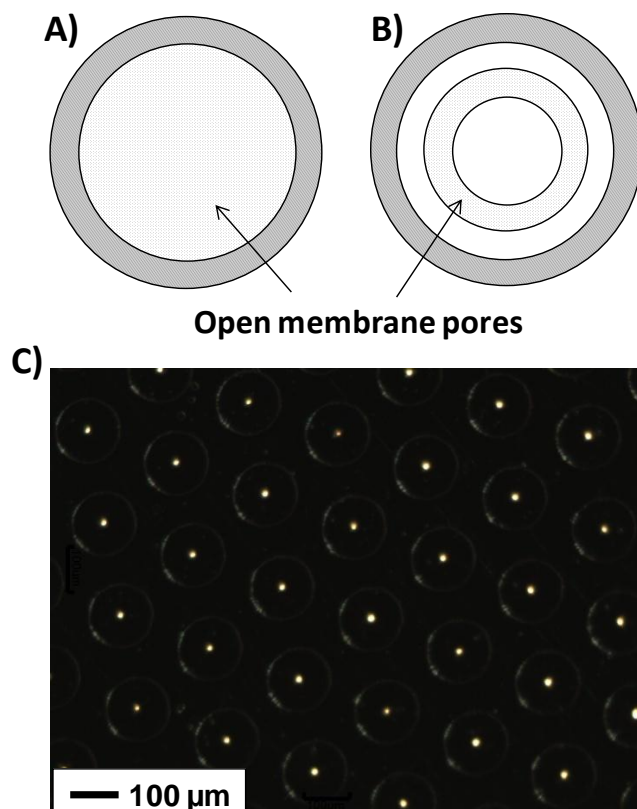
Figure 5.6. (A) The standard membrane, (B) the annular radial ring membrane and (C) an optical microscopy image showing the regular array of open 5 µm pores arranged with a pore spacing of 200 µm.

Both the standard and annular ring membranes were initially investigated for the present Pickering emulsion system. A 1.0 wt % solution of 230 nm $PGMA_{50}$-PS latex particles (70 ml) was used as the aqueous phase and the sunflower oil flux through each membrane was set at 13 L m^{-2} h^{-1} using a fixed paddle stirrer speed of 1500 rpm (12 V). Optical micrographs for the resulting Pickering emulsions are shown in Figure 5.7. In the case of the standard membrane, the size control was poor: the CV was 74 % for a mean oil droplet diameter of 171 µm. There was also some evidence for a bimodal distribution with the resulting CV showing no improvement over that of homogenisation. This disappointing result is attributed to the non-uniform shear profile discussed above. Drops can be detached by differing

shear forces, which results in a broader droplet size distribution. In contrast, an equivalent emulsion produced using the annular ring membrane, where the pores are restricted to a fixed radial distance around the membrane surface, gave much more uniform oil droplets of 44 µm diameter with a CV of only 25 %. This is a significant improvement over both the standard membrane set-up and also conventional homogenisation, with the width of the size distributions being more than halved. As a result of this observation, the annular ring membrane was used for all further emulsification studies in order to optimise the uniformity achieved over a wide range of variables.

Standard membrane   **Annular radial ring membrane**

171 ± 127 µm (CV = 74 %)   44 ± 11 µm (CV = 25 %)

100 µm   100 µm
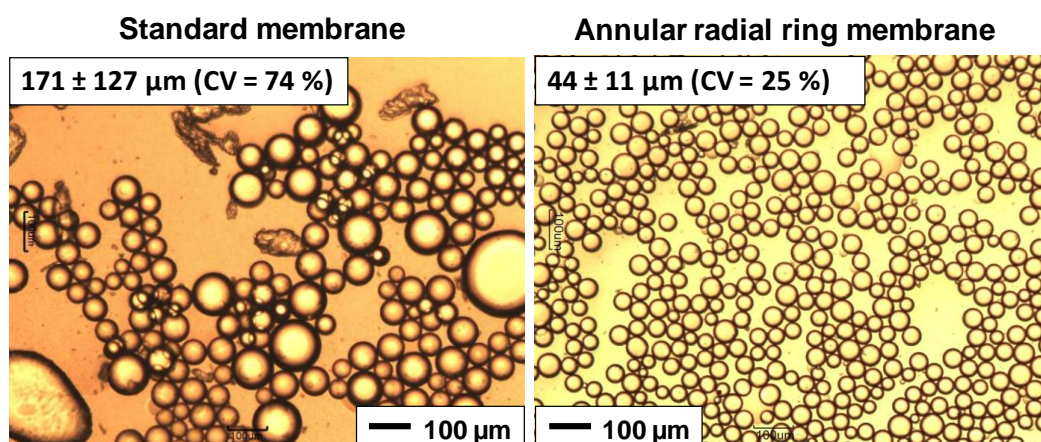
Figure 5.7. Optical microscopy images of Pickering emulsions prepared using a 1% aqueous solution of 230 nm $PGMA_{50}$-PS particles (70 ml) and sunflower oil (10 ml) at around 13 % solids using A) the standard 5 µm membrane and B) the 5 µm ring membrane. All other parameters were kept constant. The oil phase flux was 13 L m-2 h-1 and the stirrer speed was 12 V (approx 1500 rpm).

Unlike the more widely studied small molecule surfactant-stabilised emulsions, the relatively large particles used in this work should require longer times to adsorb at the droplet interface. To our knowledge there are no current literature reports on the use of this particular dispersion cell for the formation of particle-stabilised emulsions and thus the best cell operating conditions for such a Pickering emulsion were not known. Therefore the oil flux rate and paddle stirrer speed were systematically varied in order to achieve the best possible operating conditions for the production of more uniform, stable Pickering emulsions.

Firstly, the effect of the oil flux through the membrane was investigated. Previous membrane emulsification studies have shown that the droplet diameter typically increases as the oil flux through the membrane increases.[12, 18] This is because there is a fixed characteristic time required for droplet detachment at a given shear rate.[20] A higher oil flux leads to oil droplets attaining larger diameters prior to detachment. Occasionally, at very high flux rates, a sharp drop in both the mean droplet diameter and the corresponding CV is observed. This has been attributed to a phenomenon known as droplet 'push off' or a 'push to detach' mechanism.[21] This occurs when the oil flux is so great that the majority of membrane pores are active and any given droplet is influenced by adjacent droplet(s) emerging from neighbouring pore(s). In this scenario, the droplet break-off force is not limited to the shear force, but includes an extra 'push-off' force due to the close proximity of the neighbouring droplets. This causes the droplets to detach more quickly and hence explains the observed size reduction.[18] This droplet 'push-off' effect should be more pronounced for membranes with smaller pore spacing. In this study the pore spacing of the annular ring membrane is relatively large at 200 μm, so it was anticipated in this case that droplet detachment should not be influenced by a 'push-off' force. Figure 5.8 shows the effect of oil flux on the mean diameter and CV of the Pickering emulsion droplets. As expected, a greater flux results in an increase in the droplet dimensions, as indicated by the optical micrographs and the corresponding laser diffraction data shown in Figure 5.9. Oil droplets ranging from 44 to 65 μm with CV's of ≤ 27 % can be prepared at flux rates of 65 L m^{-2} h^{-1} or lower. However, a sharp increase in the CV to 51 % is observed at a flux rate of 75 L m^{-2} h^{-1} and above, indicating there is an upper limit oil flux for the formation of more uniform emulsions. Also as expected, there is no evidence for any 'push off' force being exerted over the oil flux range

investigated, which is consistent with the large pore spacing of this particular membrane. In principle, it should be possible to observe such a mechanism if the pore spacing was much smaller or the oil flux was significantly higher. However, such changes may also result in droplet coalescence if neighbouring droplets come into close contact before the latex emulsifier can confer sufficient stabilisation.
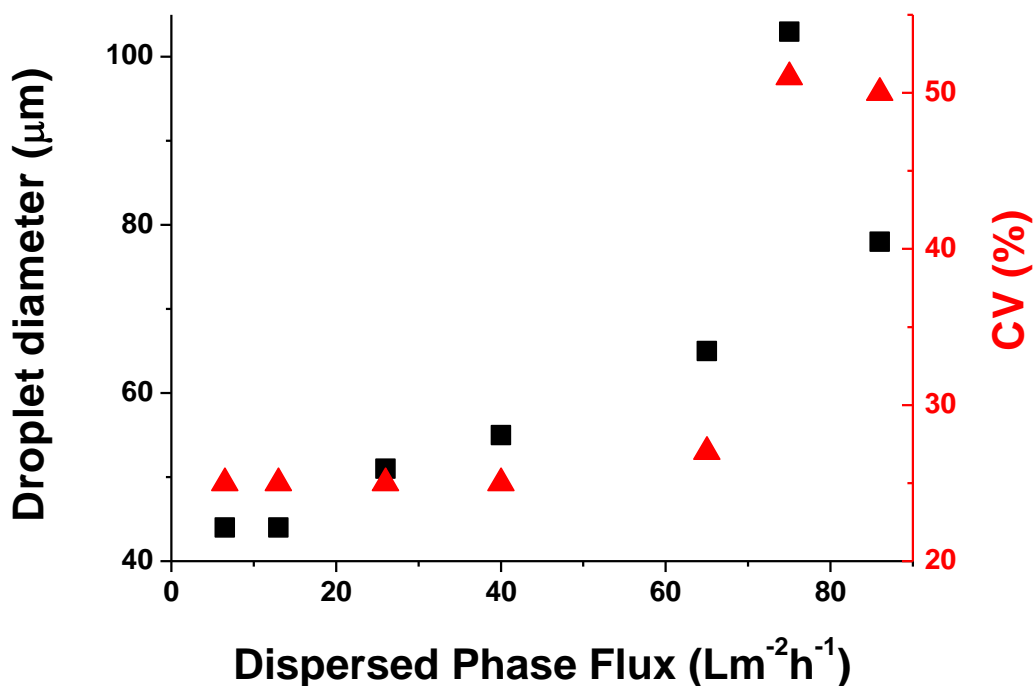
Figure 5.8. The effect of oil phase flux on the droplet diameter (squares) and coefficient of variation (triangles) for Pickering emulsions prepared using sunflower oil (total injected volume 10 ml) and 1 % aqueous solution of 230 nm PGMA50-PS particles. The stirring speed was kept constant at 12 V (1500 rpm). The membrane used was the 5 μm pore ring membrane.
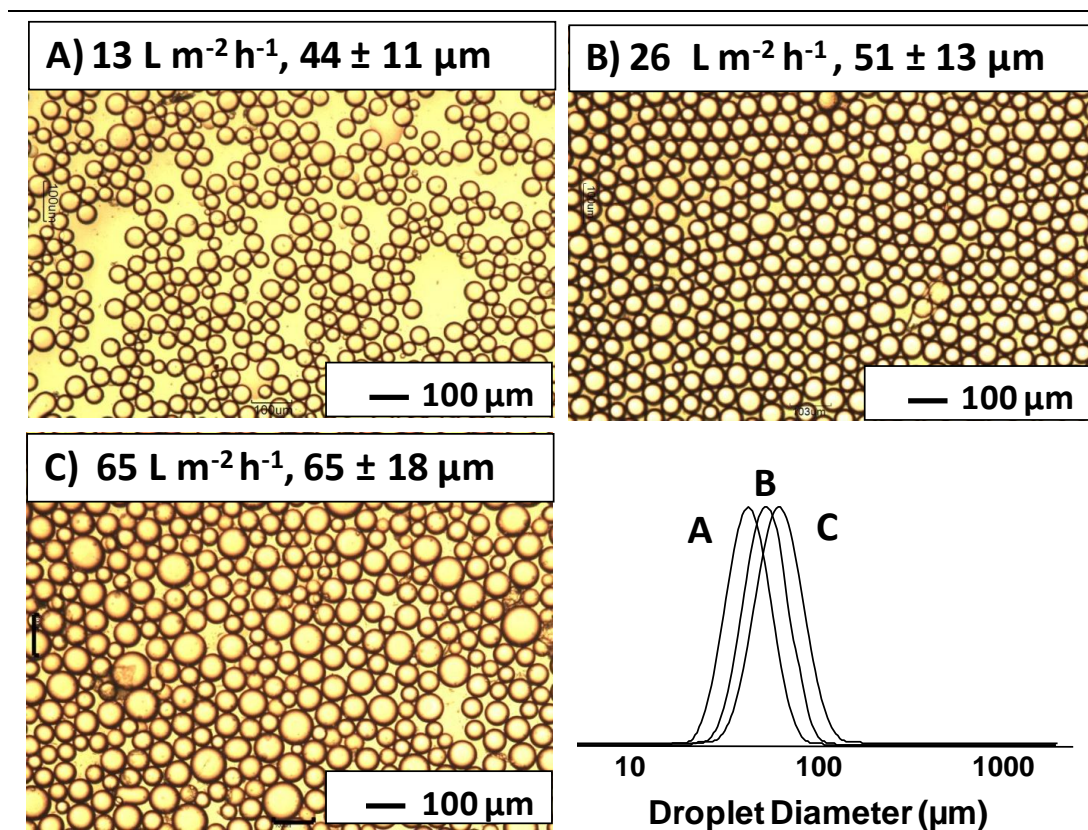
Figure 5.9. Optical microscopy images and Malvern Mastersizer data for Pickering emulsions prepared with oil phase fluxes of A) 13 L m^{-2} h^{-1}, B) 26 L m^{-2} h^{-1} and C) 65 L m^{-2} h^{-1}. Samples were prepared using sunflower oil (total injected volume 10 ml) and 1 % aqueous solution of 230 nm PGMA$_{50}$-PS particles. The stirring speed was kept constant at 12 V (1500 rpm). The membrane used was the 5 µm pore ring membrane.

The effect of surface shear was also investigated by varying the paddle stirrer speed above the membrane. Increasing the lateral shear stress should reduce the droplet diameter since detachment from the membrane should occur sooner.[12, 18] Figure 5.10A illustrates the effect of varying the stirring speed on the droplet size distribution. Initially, an increase in shear leads to the expected reduction in both the mean droplet diameter and the corresponding CV. Indeed, values as low as 25 % can be achieved for the latter parameter at a stirring speeds of approximately 1200 - 1500 rpm (10-12 V).
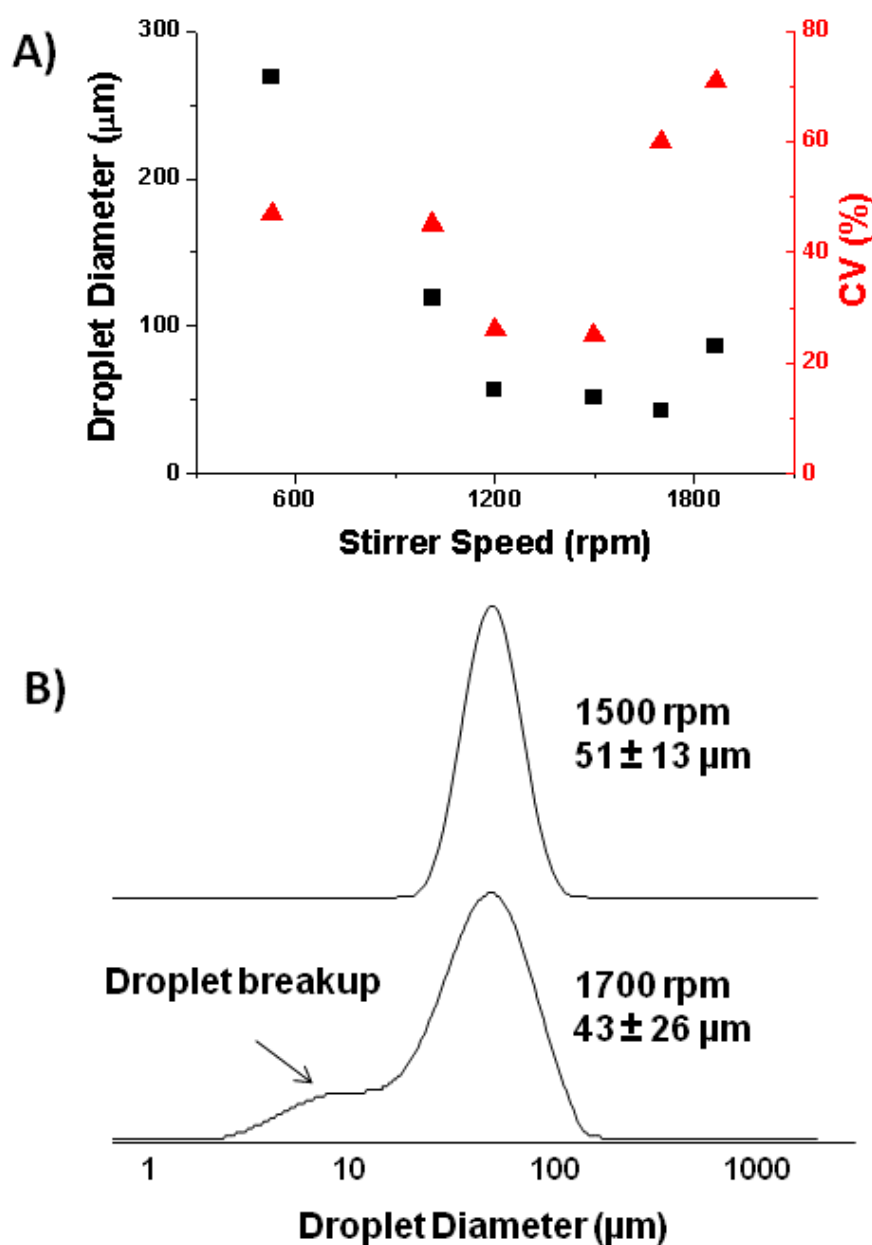
Figure 5.10. A) The effect of increasing stirring speed on the droplet diameter (squares) and CV (triangles) of Pickering emulsions prepared with the 5 μm pore ring membrane using sunflower oil (total injected volume 10 ml) and 1 % aqueous solution of 230 nm $PGMA_{50}$-PS particles. The oil phase flux was kept constant at 26 $L\ m^{-2}\ h^{-1}$. B) Droplet size distributions for Pickering emulsions prepared at 1500 and 1700 rpm, note the presence of droplet breakup for the higher shear rate.

However, on further increasing the stirring speed to 1700 the CV increases significantly to 60 %. Figure 5.10B shows the droplet size distributions as

determined by laser diffraction for the Pickering emulsions formed at 1500 and 1700 rpm. These clearly show that at the higher shear rate of 1700 rpm some smaller droplets are created within the dispersion cell, causing a significant increase in the polydispersity of the system. Figure 5.11 shows selected optical micrographs of the emulsion droplets obtained by varying the stirring speed. In the case of the higher stirring speed investigated (>1700 rpm), the relatively small droplets detected by laser diffraction studies are clearly visible. Such debris is the result of 'droplet break-up'. Droplets are initially created but then broken up by the high shear within the cell achieved by rapid stirring, inevitably leading to the presence of much smaller drops and a broadening of the droplet size distribution. The fact that the diameters of some of these droplets are smaller than the 5 μm membrane pore diameter confirms that they are the result of the break-up of larger droplets, rather than being created directly from the membrane pores. Similar results have been reported previously when using high shear rates[18, 22] and this finding highlights the need to optimise the shear forces within the dispersion cell in order to gain maximum control over the droplet size distribution.
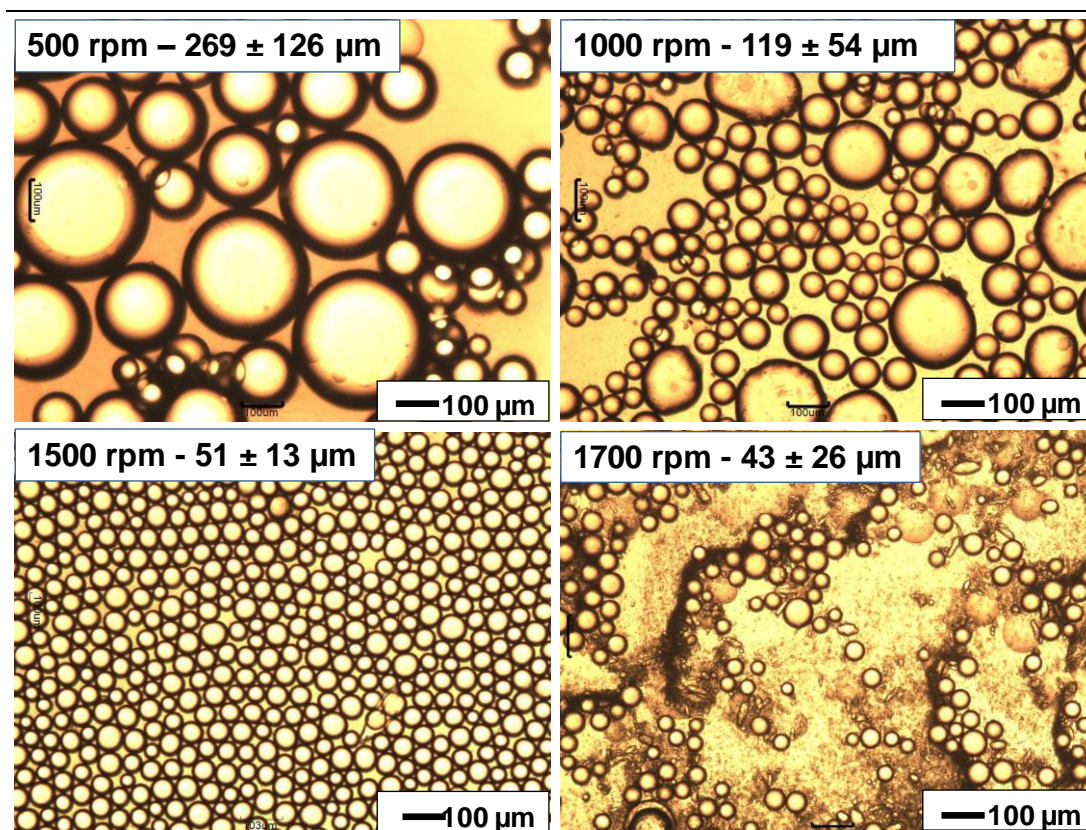
Figure 5.11. Optical microscopy images of Pickering emulsions formed from 1 % aqueous dispersion of 230 nm $PGMA_{50}$-PS particles and sunflower oil with varying stirrer speeds. The oil phase flux was kept constant at 26 L m^{-2} h^{-1} and the membrane used was the 5 μm pore ring membrane. Notice how some droplet breakup is observed at very high stirring rates (1700 rpm).

Having investigated the influence of oil phase flux and surface shear, the effect of varying the latex diameter on the droplet dimensions was explored. The Pickering emulsifier performance of $PGMA_{50}$-PS particles with mean intensity-average diameters of 130, 230 and 1100 nm was investigated. All three latexes should have essentially the same surface chemistry and therefore comparable wettabilities. Smaller particles should be able to diffuse more quickly to the newly created interface[13] and hence are more likely to be able to stabilise smaller droplets.
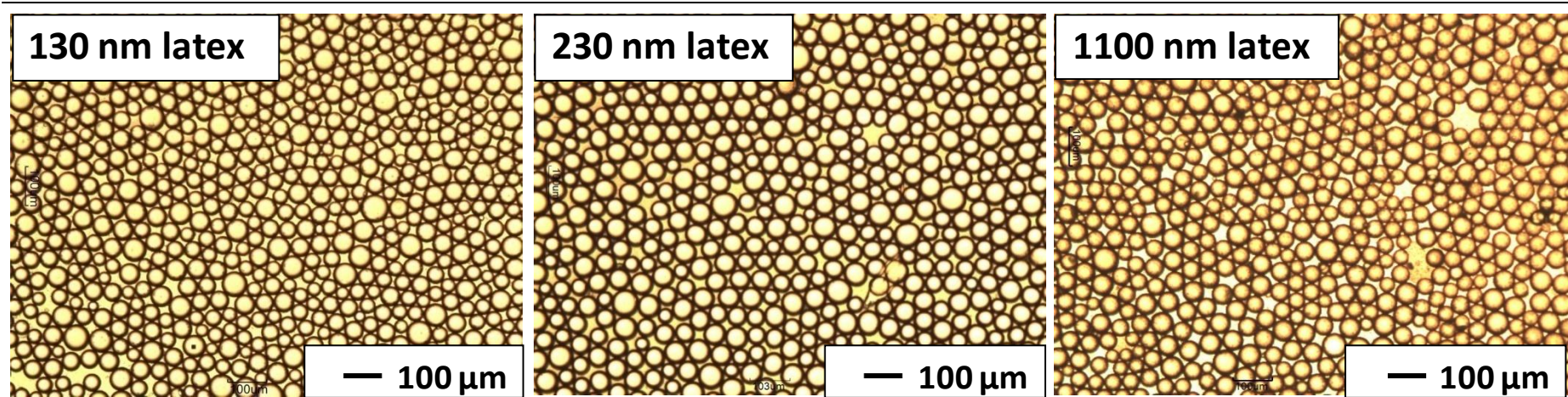
Figure 5.12. Optical microscopy images of sunflower-in-water Pickering emulsions prepared by stirred-cell membrane emulsification using aqueous solutions of latexes of varying diameters. The oil phase flux was kept constant at 26 L m^{-2} h^{-1} and the stirrer speed was 1500 rpm.

For these experiments, the stirring speed was fixed at 1500 rpm (12 V) and the flux through the annular ring membrane was held constant at 26 L m^{-2} h^{-1}. In order to keep the overall total surface area of the different latexes approximately constant, different concentrations of each latex were required for these experiments (0.6 wt % for 130 nm, 1.0 wt % for 230 nm and 7.0 wt % for the 1100 nm particles; in each case these conditions correspond to a total latex surface area of approximately 18 m^2). Optical micrographs of each emulsion produced using the three different latexes are shown in Figure 5.12. At first sight, there appears to be little size difference between the three emulsions. Indeed, the smallest (130 nm) latex produced Pickering emulsions with an average droplet diameter of 48 ± 12 µm, which is comparable to the 51 ± 13 µm diameter obtained when using the 230 nm latex. This suggests that, under the conditions investigated, oil droplet stabilisation by these two latexes is not diffusion-limited. The largest (1100 nm) latex produced droplets that initially seemed to be of similar size (~ 47 µm diameter) and uniformity to those prepared with the smaller latexes when examined by optical microscopy. However, laser diffraction studies indicated a mean droplet diameter of 67 ± 27 µm, which is significantly larger (and broader) than that suggested by optical microscopy. This indicates that there may be some flocculation or aggregation of the oil droplets in this particular emulsion. This may be due to slower latex diffusion preventing effective stabilisation of the growing oil droplets.

In order to confirm that these latex particles are adsorbed onto the oil droplets, the membrane emulsification protocol was repeated using rhodamine 6G-piperazine methacrylate-labelled PGMA$_{50}$-PS particles. The resulting emulsion was allowed to cream (by leaving to stand for a few hours at 20°C) and the underlying aqueous phase was repeatedly replaced with pure water (at least five times) in order to remove any excess non-adsorbed latex. Figure 5.13 shows the fluorescence micrograph obtained for this purified emulsion. It is clear from the micrograph that the PGMA$_{50}$-PS particles have adsorbed onto the sunflower oil droplets, as expected for a Pickering emulsion.
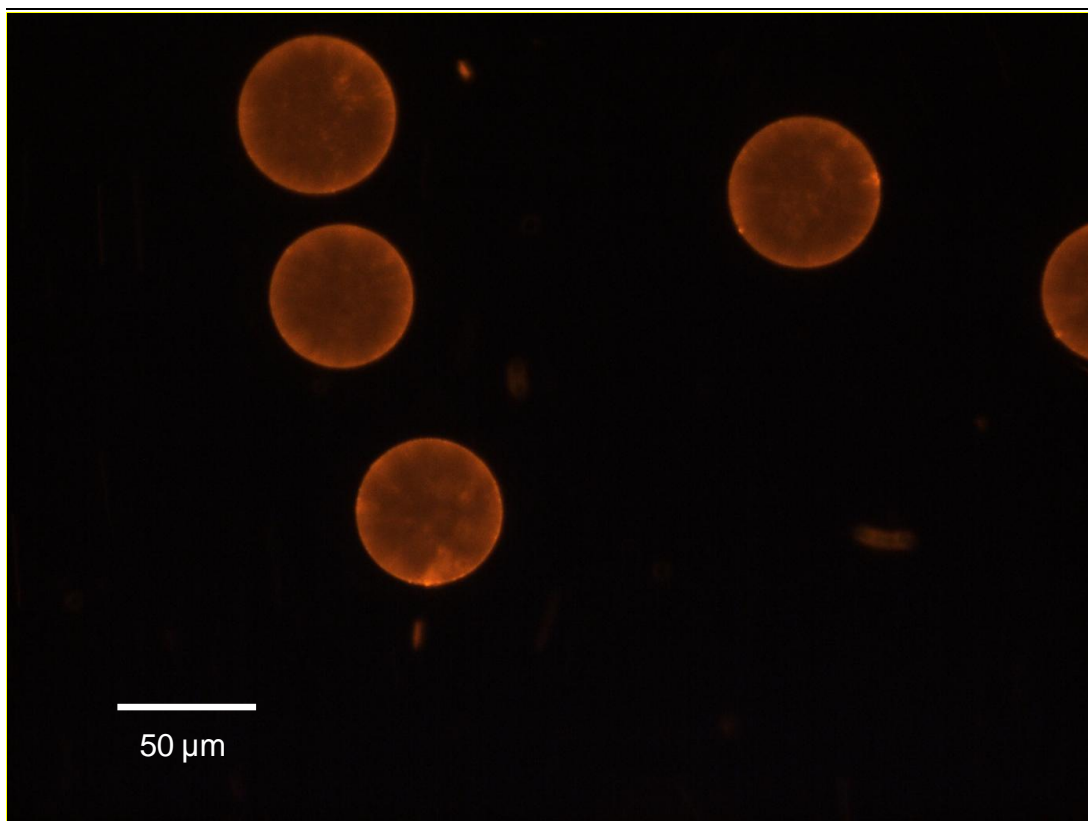
Figure 5.13. Fluorescence microscopy image of a Pickering emulsion prepared with a rhodamine 6G-piperazine methacrylate-labelled PGMA$_{50}$-PS latex (70 ml of a 1.0 w/v % aqueous dispersion) and sunflower oil (10.0 ml). The oil phase flux was 26 L m^{-2}h^{-1}and the stirrer speed was 1500 rpm.

The type of PGMA$_{50}$-PS latex used in this work has been previously utilised for the preparation of covalently cross-linked colloidosome microcapsules (see chapter 3). The hydroxy groups on the PGMA chains can be cross-linked from within the oil droplets using an oil-soluble polymeric diisocyanate, tolylene 2,4-diisocyanate-terminated poly(propylene glycol) (PPG-TDI). Such covalently cross-linked structures readily survive after removal of the oil template by washing with excess alcohol. Cross-linking from *within* the oil droplets means that colloidosomes can be prepared at high solids (50 vol %), without the risk of inter-colloidosome fusion. However, in this work these colloidosomes were prepared by conventional homogenisation and therefore had the broad droplet size distributions that are characteristic of such emulsions. Colloidosomes with significantly lower polydispersity can be prepared by stirred-cell membrane emulsification by simply dissolving the PPG-TDI cross-linker in the oil phase prior to injection (see optical

micrograph in Figure 5.14). The droplet size distribution of these colloidosomes is shown as an inset. Comparison with the equivalent Pickering emulsion size distribution (see Figure 5.9B), confirms that the presence of PPG-TDI cross-linker has little or no effect on the resulting droplet size and uniformity. Also shown in Figure 5.14 are representative scanning electron micrographs of these low polydispersity colloidosomes after washing with excess alcohol to remove the sunflower oil. The microcapsule structure is clearly preserved, and control experiments confirm that no such structures are obtained in the absence of cross-linking.

The Pickering emulsions reported herein are more uniform (with CVs as low as 25 %) compared to those prepared by Yuan *et al.*[13] using either the cross-flow or rotating membrane techniques. Furthermore, the convenient scale of the dispersion cell allows stable emulsions to be prepared using a relatively small amount of material, making it suitable for laboratory scale experiments on new or expensive stabilisers, unlike many cross-flow systems. Moreover, membranes with a wide range of pore sizes and spacings are available to enable systematic variation of the mean droplet diameter.
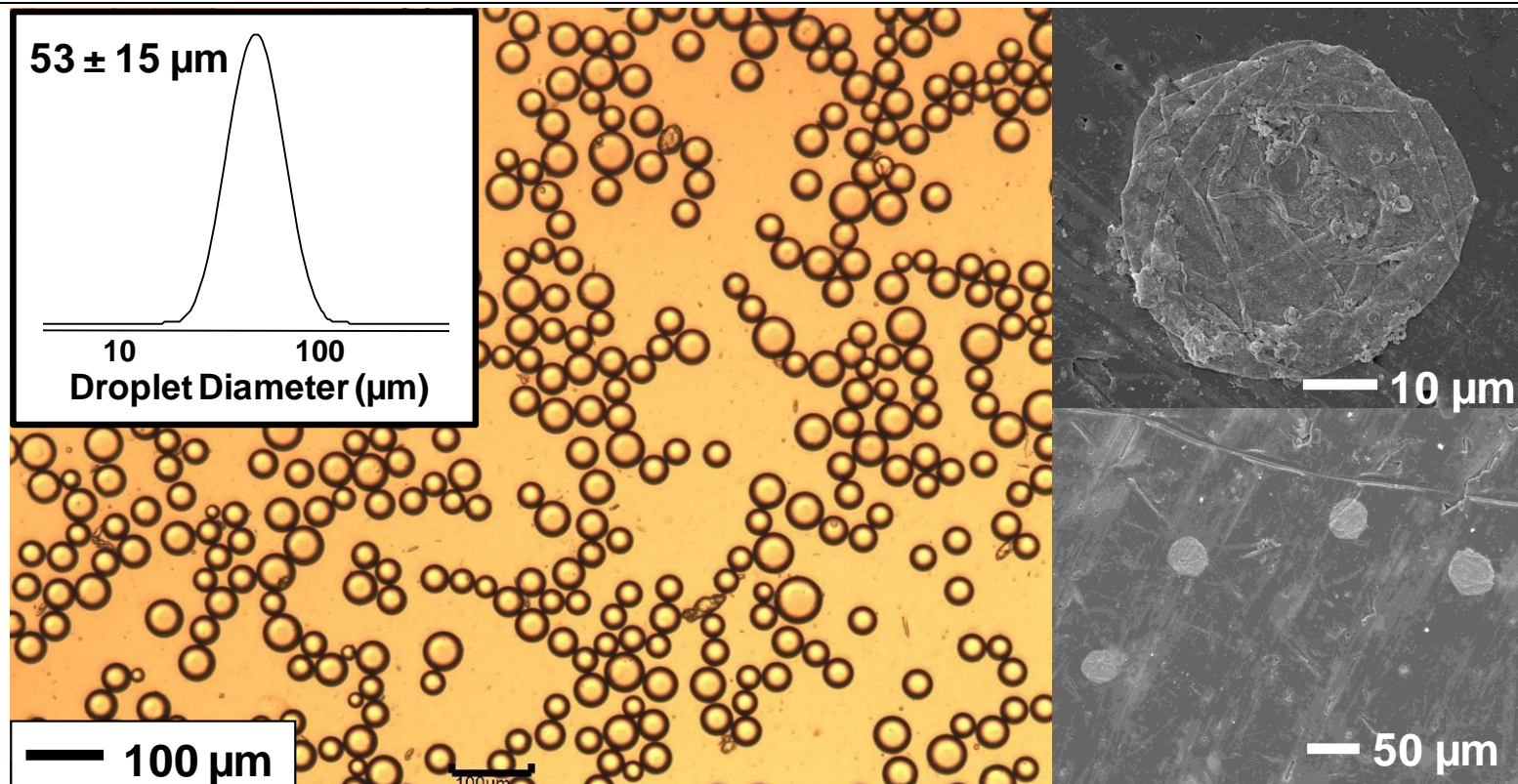
Figure 5.14. Optical microscopy image and droplet size distribution (before alcohol challenge) and scanning electron microscopy images (after the alcohol challenge) of covalently cross-linked colloidosomes prepared with the 230 nm PGMA50-PS particles, sunflower oil and PPG-TDI cross-linker. The oil phase flux was kept constant at 26 L m-2 h-1and the stirrer speed was 12 V (1500 rpm).

CONCLUSIONS

In summary, oil-in-water Pickering emulsions with relatively narrow size distributions can be conveniently prepared by stirred cell membrane emulsification using a $PGMA_{50}$-PS latex as the sole emulsifier for sunflower oil. An annular ring membrane (5 μm pore diameter and 200 μm inter-pore spacing) was preferred to the equivalent standard membrane, since the former produces significantly more uniform emulsion droplets. Droplets of 44-78 μm in diameter with CV's as low as 25 % can be prepared by changing the oil flux through the membrane. Slower oil injection rates led to smaller, more uniform droplets being produced, as expected. In this case, there is no evidence for a 'push-off' force contributing to droplet detachment, which is consistent with the relatively slow injection rates and the large pore spacing. Higher stirring rates at a constant oil flux of 26 L m^{-2} h^{-1} typically led to smaller, more monodisperse droplets. However, droplet break-up was observed at stirring speeds in excess of 1700 rpm, showing that the shear forces must be carefully balanced within the dispersion cell. Emulsion droplets with coefficients of variation as low as 25 % can be produced by careful optimisation of the oil flux and stirring rate. This is a significant improvement over the relatively large droplet size distributions achievable by conventional homogenisation, which in the case of this system has a coefficient of variation of 74 %. Moreover, the cell design requires less than 100 ml of the aqueous phase, making it well-suited for small-scale laboratory evaluation of potential new emulsifiers. Finally, the addition of a suitable oil-soluble polymeric cross-linker enables the corresponding low polydispersity colloidosomes to be prepared in situ from such Pickering emulsions.

REFERENCES

1.   Aveyard, R.; Binks, B. P.; Clint, J. H., *Adv. Colloid Interface Sci.,* **2003,** *100-102*, 503-546.

2.   Binks, B. P.; Whitby, C. P., *Langmuir,* **2004,** *20*, 1130-1137.

3.   Giermanska-Kahn, J.; Schmitt, V.; Binks, B. P.; Leal-Calderon, F., *Langmuir,* **2002,** *18*, 2515-2518.

4.   Mabille, C.; Schmitt, V.; Gorria, P.; Leal Calderon, F.; Faye, V.; Deminière, B.; Bibette, J., *Langmuir,* **1999,** *16*, 422-429.

5.   Subramaniam, A. B.; Abkarian, M.; Stone, H. A., *Nat. Mater.,* **2005,** *4*, 553-556.

6.   Xu, Q. Y.; Nakajima, M.; Binks, B. P., *Colloids and Surfaces a-Physicochemical and Engineering Aspects,* **2005,** *262*, 94-100.

7.   Nie, Z. H.; Il Park, J.; Li, W.; Bon, S. A. F.; Kumacheva, E., *J. Am. Chem. Soc.,* **2008,** *130*, 16508-16509.

8.   Shah, R. K.; Kim, J. W.; Weitz, D. A., *Langmuir,* **2010,** *26*, 1561-1565.

9.   Romanowsky, M.; Abate, A. R.; Weitz, D. A. Scale-up of microfluidic devices. WO 2010104597, 2010.

10.   Vladisavljevic, G. T.; Williams, R. A., *Adv. Colloid Interface Sci.,* **2005,** *113*, 1-20.

11.   , G. T.; Kosvintsev, S. R., *Ind. Eng. Chem. Res.,* **2010,** *49*, 3810-3817.

12.   Egidi, E.; Gasparini, G.; Holdich, R. G.; Vladisavljevic, G. T.; Kosvintsev, S. R., *J. Membr. Sci.,* **2008,** *323*, 414-420.

13.   Yuan, Q. C.; Cayre, O. J.; Manga, M.; Williams, R. A.; Biggs, S., *Soft Matter,* **2010,** *6*, 1580-1588.

14.   Thompson, K. L.; Armes, S. P.; York, D. W., *Langmuir,* **2011,** *27*, 2357-2363.

15.   Thompson, K. L.; Armes, S. P.; York, D. W.; Burdis, J. A., *Macromolecules,* **2010,** *43*, 2169-2177.

16.   Madsen, J.; Warren, N. J.; Armes, S. P.; Lewis, A. L., *Biomacromolecules,* **2011**, null-null.

17. Thompson, K. L.; Armes, S. P.; Howse, J. R.; Ebbens, S.; Ahmad, I.; Zaidi, J. H.; York, D. W.; Burdis, J. A., *Macromolecules,* **2010,** *43*, 10466-10474.

18. Stillwell, M. T.; Holdich, R. G.; Kosvintsev, S. R.; Gasparini, G.; Cumming, I. W., *Ind. Eng. Chem. Res.,* **2007,** *46*, 965-972.

19. Kosvintsev, S. R.; Gasparini, G.; Holdich, R. G.; Cumming, I. W.; Stillwell, M. T., *Ind. Eng. Chem. Res.,* **2005,** *44*, 9323-9330.

20. Xu, J. H.; Luo, G. S.; Chen, G. G.; Wang, J. D., *J. Membr. Sci.,* **2005,** *266*, 121-131.

21. Zhu, J.; Barrow, D., *J. Membr. Sci.,* **2005,** *261*, 136-144.

22. Vladisavljevic, G. T.; Williams, R. A., *J. Colloid Interface Sci.,* **2006,** *299*, 396-402.

Chapter Six

Conclusions and Future Work

CONCLUSIONS

Colloidosome microcapsules can be prepared by the covalent cross-linking of latex particles at the interface of a Pickering emulsion. Judicious design of the steric stabiliser allows latex particles to be efficiently adsorbed onto oil droplets and be locked in place using an oil-soluble cross-linker. Chapter Two focused on the synthesis of such a hydroxy-functional steric stabiliser and its use in the preparation of both polystyrene and poly(2-hydroxypropyl methacrylate) latexes.

A series of near-monodisperse poly(glycerol monomethacrylate) macromonomers were prepared by a two-step protocol. ATRP of the GMA monomer was conducted using an amide-based tertiary amine-functionalised initiator, followed by post-polymerisation quaternisation of the initiator end group using 4-vinylbenzyl chloride. This afforded a series of well-defined macromonomers with narrow molecular weight distributions (M_w/M_n < 1.33). The polymerisations were well controlled for all target DPs investigated (DP = 20 to 70) in contrast to the recently reported PMPC based macromonomers prepared by the same two-step technique.[1] These macromonomers were then used as steric stabilisers for the preparation of latex particles. Near-monodisperse micrometer-sized PGMA-PS and PGMA-PHPMA latexes were prepared via alcoholic and aqueous dispersion polymerisation respectively, with both polymerisations proceeding to high monomer conversions. In contrast, the aqueous emulsion polymerisation protocol used to prepare sub-micrometer sized PGMA-PS latexes proved to be more problematic. Conventional water-soluble initiators (AIBA, ACVA, APS etc) invariably led to polydisperse, highly flocculated latexes. In contrast an oil-soluble initiator (AIBN) produced small, uniform latex particles (z-average diameter ~ 100 nm), albeit with relatively poor/incomplete monomer conversions. The reason for the unusual influence of initiator type in these reactions is currently not fully understood and could be the focus of future work. The resulting PGMA-stabilised latexes were each characterised in terms of their particle size distributions by DLS, DCP and SEM. Furthermore, techniques such as aqueous electrophoresis and XPS confirmed that the PGMA steric stabiliser chains did indeed lie at the particle surface, as expected.

In Chapter Three the PGMA$_{50}$-PS particles prepared in Chapter Two were evaluated as particulate stabilisers for Pickering emulsions. Both the 107 nm and 1188 nm

PGMA$_{50}$-PS latexes (prepared by aqueous emulsion and alcoholic dispersion polymerisation respectively) acted as efficient Pickering emulsifiers. The emulsions were characterised by both conductivity measurements and the 'drop test' as being of the oil-in-water type. This is consistent with the particles having a contact angle (θ) at the oil/water interface below < 90 °, which was anticipated for such a hydrophilic PGMA$_{50}$ stabiliser. The particles adsorbed efficiently onto n-dodecane droplets with little or no excess particles being observed in solution for lower latex concentrations. In our experience such "model" behaviour is unusual for sterically-stabilised latexes.[2-3] Increasing the aqueous latex concentration gradually reduced the volume-average droplet diameter until a plateau value was reached, above which no further reduction in droplet size was observed and excess latex is present in solution. An average minimum droplet size of 25 µm is attained for the 107 nm PGMA$_{50}$-PS latex, while 60 µm proved to be the lower limit for droplets prepared with the 1188 nm PGMA$_{50}$-PS latex. Using these data, the packing efficiency (P) of the latex particles on the oil droplet surface can be determined. A P value of 0.85 ± 0.01 was calculated for both the 107 nm and 1188 nm latex. This high P suggests that the latex particles are very closely packed on the oil surface, which was confirmed by fluorescence microscopy in the case of the larger PGMA$_{50}$-PS latex. The same theoretical value of P is consistent with the small and large latexes having essentially the same surface chemistry and thus adsorbing onto and packing in a similar manner on the n-dodecane surface. Once it was established that these PGMA$_{50}$-PS particles indeed acted as Pickering emulsifiers, cross-linking of the hydroxy units on the latex surface was attempted, in order to 'lock in' the colloidosome superstructure. Successful cross-linking was achieved from inside the oil droplets using an oil-soluble polymeric diisocyanate (tolylene 2,4-diisocyanate-terminated poly(propylene glycol) or PPG-TDI). This protocol leads to microcapsules that show no evidence of inter-colloidosome fusion even at 50 vol % solids, and are resistant to challenges with either added surfactant or excess alcohol. Colloidosome formation takes approximately 20 mins at 20 °C and, in the case of the small 107 nm PGMA$_{50}$-PS latex, the reaction can be monitored by ^{1}H NMR spectroscopy.

These cross-linked colloidosomes generally collapse upon drying, as the links between adjacent latex particles are flexible and do not impart any structural rigidity. More robust colloidosomes that are more resistant to collapse can be prepared by

either thermal or solvent-assisted annealing. Incorporation of 20 vol % cyclohexane into the *n*-dodecane oil phase enables closure of the latex interstices within 1 h at 50 °C. Thermal annealing in the absence of cyclohexane at temperatures well below the polystyrene T_g was also possible, although at 50 °C significantly longer sintering times were required (> 4 h). It was anticipated that such annealed colloidosomes would retain encapsulated actives much more efficiently than merely cross-linked capsules.

A series of encapsulation and release experiments were conducted in Chapter Four to determine the permeability of the cross-linked colloidosomes prepared in Chapter Three. The effect of particle diameter, solvent annealing and further polymer deposition on the release of a small molecule dye (fluorescein) was investigated. However, cross-linked colloidosomes prepared with either the 107 nm or the 1188 nm PGMA$_{50}$-PS latexes offered essentially no barrier to dye release. In retrospect, this negative result was not surprising as the latex interstices in both cases are far greater than the molecular dimensions of the fluorescein dye. This observation is consistent with the results of Rosenberg *et al,*[4] who determined that, for encapsulated small molecules, the size of the particles making up the colloidosome shell has no measurable effect on the release profile. The solvent annealing protocol developed in Chapter Three was employed in an effort to close the latex interstices and hence improve the encapsulation efficiencies of the colloidosome microcapsules. Disappointingly, no such improvement was observed, with the annealed colloidosomes releasing the dye as quickly as their non-annealed precursors. This poor encapsulation performance is most likely attributed to two problems, (i) either the thermal annealing was incomplete (hampered by the large pentagonal defects within the shell) and/or (ii) the annealed polystyrene shell itself is too permeable to the small molecule dye. In order to address technical problem, a thin layer of polypyrrole was deposited onto the colloidosome exterior. This overlayer offered some improvement in terms of dye retention. The characteristic time for fluorescein release increase from 1 h for non-coated colloidosomes to 20 h for a 1.32 wt % PPy loading. However, this improved retention performance is still insufficient for most, if not all, industrial applications. During the course of this work it became readily apparent that such colloidosomes are very leaky microcapsules for small molecules. Nevertheless, they may yet offer potential for biological applications where

encapsulation of relatively large entities (cells, enzymes etc.) is desired in combination with high permeability of small molecules across the porous microcapsule wall. In this case the cross-linked stabiliser chains should act as a macromolecular "mesh" to aid retention of the relatively large encapsulated bioactive entities. In order to test this hypothesis, the second half of Chapter Four looked at the encapsulation of larger oil-dispersible particles. Bespoke sterically-stabilised polystyrene particles were prepared by alcoholic dispersion polymerisation using an oil-soluble PDEA-based stabiliser. It was found that colloidosomes could indeed efficiently encapsulate particles that are larger than the interstices between latex particles, confirming the original hypothesis that colloidosomes can offer encapsulation via a size exclusion mechanism, albeit on a larger length scale. The original motivation of this project was to find an alternative to the melamine-formaldehyde microcapsules currently used to encapsulate perfume oils in laundry products. Unfortunately, considering that perfume oils generally comprise of a complex mixture of small molecules, it is unlikely that these colloidosomes are suitable for such an application.

For delivery of specific amounts of actives, it is often desirable to have microcapsules with a uniform size distribution. To this end, Chapter Five describes the preparation of relatively low polydispersity Pickering emulsions and colloidosomes using a membrane emulsification technique. Techniques such as microfluidics can give highly monodisperse Pickering emulsion droplets with coefficients of variation below 5 %,[5] but this process remains problematic for scale up. Membrane emulsification offers a pragmatic alternative, allowing more uniform emulsions to be readily produced in much larger quantities compare to microfluidics. The PGMA$_{50}$-PS latexes prepared in Chapter Two were again used as Pickering emulsifiers, this time in conjunction with a stirred cell membrane emulsification apparatus. A hydrophilic annular nickel membrane (5 μm pore diameter and 200 μm pore spacing) allowed the generation of droplets in the region of 44-78 μm diameter. Optimisation of the oil injection rate and overhead paddle stirrer speed produced droplets with coefficients of variation (CV) as low as 25 %. This is a significant improvement in uniformity compared to conventional homogenisation techniques, where CVs range from 50 to 75 %. In addition, this affordable bench top apparatus allows membrane emulsification to be conducted on a convenient scale. Less than

100 ml of aqueous continuous phase is required per experiment, which is convenient for the preliminary examination of relatively expensive or new Pickering emulsifiers, such as the bespoke latexes utilised in this work.

FUTURE WORK

This work has shown that colloidosomes can be efficiently prepared from Pickering emulsions using sterically-stabilised latex particles and a suitable oil-soluble cross-linker. This versatile protocol can be expanded to include alternative latex stabilisers and cross-linking chemistries. Some preliminary studies haves already been conducted in the Armes group, with poly(ethylene imine) (PEI) being used as a reactive stabiliser for preparation of cationic polystyrene particles.[2] These PEI-PS particles can be cross-linked from either the aqueous or oil phases using either poly(ethylene glycol) diglycidyl ether or poly(propylene glycol) diglycidyl ether, respectively. Preliminary studies have also shown that covalent cross-linking of suitable latex cores rather than the steric stabiliser chains can also lead to successful colloidosome formation.[3] In view of the many possible options in terms of steric stabilisers, latex cores and cross-linkers, there is considerable scope to expand the covalent cross-linking approach used in this thesis. Stimulus-responsive particles could also be incorporated into the colloidosome shell to provide 'gates' that can trigger release of encapsulated actives in response to pH, temperature or ionic strength.

Successful encapsulation of relatively large oil-dispersed latex particles was demonstrated in Chapter Four. Therefore these covalently cross-linked colloidosomes offer some potential for the encapsulation of bio-entities such as enzymes or cells. In these cases the colloidosome shell acts as a macromolecular sieve and retains the active species by size exclusion. In order to examine the permeability of colloidosome shells towards such relatively large actives in more depth, further encapsulation studies should be conducted. A series of latex particles of various sizes should be prepared to probe the permeability of the colloidosome shell and hence determine the smallest particles that can be retained. Synthesis of relatively small PDEA-PS particles for encapsulation (< 200 nm diameter) was not possible via the alcoholic dispersion protocol used during this work. Addition of water to this formulation initially reduced the particle size to some extent, but further

water addition only resulted in larger more polydisperse particles, presumably because the reaction medium became too poor a solvent for the PDEA stabiliser chains. In principle, particles in the region of 50-100 nm in diameter could be prepared by RAFT alcoholic dispersion polymerisation, which has been recently optimised by the Armes group.

Although the encapsulation of latex particles has proven successful, it has become clear through the course of this thesis that colloidosomes prepared from spherical polystyrene particles cannot retain small molecules over long time scales. These findings highlight the inherent problems with microcapsule formation via the colloidosome route. Colloidosomes prepared from near-monodisperse spherical latex particles will always contain multiple pentagonal defects whose dimensions approach that of the mean latex diameter. Closing the latex interstices and pentagonal defects has proven to be a fundamental technical problem for the efficient retention of small molecules. Moreover, even in cases where complete annealing appears to have occurred,[6] complete encapsulation is still not achieved, which suggests that an annealed amorphous latex shell does not offer a sufficient barrier towards release. Therefore if encapsulation of small molecules is desired from a colloidosome microcapsule, future work should perhaps focus on non-spherical *inorganic* colloids. A non-spherical morphology should minimise packing defects, particularly if such colloids (e.g. clay platelets) form multilayers. Furthermore, crystalline inorganic shell should be much less permeable with respect to small molecule diffusion through the colloidosome. Such work is currently underway in the Armes group using a synthetic inorganic clay, Laponite.

REFERENCES

1.   Thompson, K. L.; Bannister, I.; Armes, S. P.; Lewis, A. L., *Langmuir,* **2010,** *26*, 4693-4702.

2.   Walsh, A.; Thompson, K. L.; Armes, S. P.; York, D. W., *Langmuir,* **2010,** *26*, 18039-18048.

3.   Growney, D. Synthesis and Characterisation of Novel Poly(2-tert-butylamino)ethyl Methacrylate-based Latexes: Novel pH Responsive Pickering Emulsifiers and Covalently Cross-linked Colloidosomes. *MChem Thesis,* University of Sheffield, **2011**.

4.   Rosenberg, R. T.; Dan, N. R., *J. Colloid Interface Sci.,* **2011,** *354*, 478-482.

5.   Nie, Z. H.; Il Park, J.; Li, W.; Bon, S. A. F.; Kumacheva, E., *J. Am. Chem. Soc.,* **2008,** *130*, 16508-16509.

6.   Yow, H. N.; Routh, A. F., *Langmuir,* **2009,** *25*, 159-166.